# CHAPTER ONE

# INTRODUCTION

## 1.1 Background of the Study

Paint is mostly considered as a mixture of pigment, binder, thinner and additives which when spread in a thin film, forms a solid adherent surface coating (Bandela and Puniya, 2008). There are three types of paints used in different processes of industries namely; water based paint, alkyd paint and speciality paint. Water based paints are also referred to as “latex” paint. These paint types have different components used for producing them and each component of paint also determines the characteristics of the waste generated during its manufacture and use (Körbahti and Tanyolac¸, 2009). Latex paint wastes are not hazardous and can be disposed into most sewage treatment systems or landfills. The oils and solvents in alkyd paints and speciality coatings are toxic. If released into the environment they have the potential to contaminate drinking water supplies, groundwater and can be toxic to plants and aquatic animals. Water contaminated by paints and the solvents used in cleaning painted tools can also contaminate drinking water supplies and other aspects of the environment. Vapours released from alkyd paints are toxic to humans if inhaled over a long period of time in high concentrations. These vapours have the potential to start a fire if exposed to a spark or flame and support a fire once started because they are flammable. Summarily,

paint effluents are alkaline and have high BOD, COD, heavy metals, suspended solids and coloured materials (Moshen *et al.*, 2010).

Therefore, treatment technique must be adopted in order to control pollution, since effluent generated from paint industries contains heavy metals such as zinc, lead, copper, chromium, nickel, cobalt, etc. Each heavy metal has a specific effect on the ecosystem when released at higher concentration (Rahbar *et al.*, 2006). Recently, several purification processes have emerged with the aim of treating paint effluent to meet the standard stipulated by the National Environmental Standards and Regulation Enforcement Agency of Nigeria (NESREA), since the end of the passage route of these effluent is rivers, lakes, dams, oceans, estuaries or wetlands etc. Processes of wastewater treatment are primary, secondary and tertiary.

Primary treatment involves sedimentation, and is the process by which about 30 to 50 percent of the suspended solid materials in raw wastewater are removed. The organic matter remaining after primary treatment is extracted by biological secondary treatment processes to meet effluent standards. Secondary treatment is commonly carried out using activated-sludge processes, trickling filters, or rotating biological contactors. In the activated-sludge method, wastewater is fed continuously into an aerated tank where microorganisms break down the organic matters. The resulting microbial floc (activated sludge) is settled under quiescent (calm-water) conditions in a final clarifier and returned to an aeration tank. The plant effluent is clear supernatant from secondary

settling. Trickling filters and rotating biological contactors have media to support microbial films**.** These slime growths extract organic materials from wastewater as it trickles over the surfaces. Oxygen is supplied from air moving through voids (empty spaces) in the media. Excessive biological growth washes out and is collected in a secondary clarifier. Tertiary wastewater treatment is the additional treatment that follows primary and secondary treatment processes. It is employed when primary and secondary treatment cannot accomplish all that is required. For example, phosphorus removal may be needed for wastewaters that are discharged to receiving waters that are likely to become eutrophic, or enriched with nutrients **(**Warren, Water encyclopedia).

Tertiary treatment is combination of physical and chemical methods of treatment such as, chlorination, ozonation, neutralization, coagulation, adsorption, ion exchange, flocculation and settling.

Coagulation-flocculation is one of the physicochemical methods most widely used in water treatment for purification of urban and industrial wastewater. The process is effective for removal of particles, suspended solids, and organic matter and is simple and cheap to use (Vanerkar *et al*., 2013).

Coagulants mostly known are those based on aluminium and iron. The aluminium coagulants include aluminium sulphate, aluminium chloride and sodium aluminate. The iron coagulants include ferric sulphate, ferrous sulphate, ferric chloride and ferric chloride sulphate. Other chemicals used as coagulants include hydrated lime and

magnesium carbonate, poly(aluminum chloride), poly(aluminium sulphate chloride), poly(aluminium silicate chloride) and forms of poly(aluminium chloride) with organic polymers (Alex, 2015). The problem with this inorganic and synthetic chemical is that poly(aluminium chloride) and alum add impurities, such as epichlodine, which are carcinogenic. Besides that, aluminium is regarded as a major poisoning factor in encephalopathy dialysis and one of the factors which might contribute to Alzheimer disease. Acrylamide, has neurotoxicity and strong carcinogenic effects (Syafalni *et al*., 2013). Hence, the use of natural product as coagulant came to the limelight since they are biodegradable, environmentally friendly, renewable and cheap.

This study is aimed at treating paint effluent using shells of unmodified and modified *Archachatina marginata* (land snail), *Tympanotonus fuscatus (*periwinkle) and *Mercenaria mercenari,* (hard clam) and studying the optimal process and kinetics of coagulation-floculation. Both modified and unmodified shells were used in this study to ascertain the best coagulant in the treatment of paint effluents under the same condition.

## 1.2 Statement of the problem

Paint industry is one of the fastest growing economies in Nigeria. The effluents its discharge has contributed a lot to the pollution of our environment because of toxic chemicals and heavy metals that are emanating from them (Körbahti and Tanyolac¸ 2009). These toxic chemicals and heavy metals end up in our rivers, dams, lakes and

oceans killing the aquatic lives thereby making the water unfit for drinking and domestic purposes. Conventional physicochemical methods used to treat and remove colours from paint effluent are costly and cannot be used by small scale industries to treat and remove colours from effluent hence coagulation-flocculation becomes an alternative because it is cheaper and simple to use ( Obiora-okafo and Onukwuli, 2015).

Most of the coagulants in used are synthetic and inorganic chemicals and they have been prohibited by NESREA due to environmental health challenges associated with them (Okolo *et al*., 2015).

### 1.3 Aim and Objectives of Study

The aim of this research is to treat paint effluent using biomass of *Archachina marginata* (land snail), *Tympanotonus fuscatus (*periwinkle) and *Mercenaria smercenaria* (hard clam) shells by coagulation – flocculation method. The objectives of this work are to:

1. determine some physicochemical attributes of paint effluent before treatment and after treatment.
2. prepare the unmodified and modified coagulants, characterize in terms of proximate composition and physical characteristics ( pH, $pH_{zpc}$, density, porosity, surface area, SEM, XRD, XRF and FTIR).
3. design batch experiments to treat paint effluent by the coagulation-flocculation method with a view to optimize process variables.

4. Study the kinetics of the coagulation-flocculation process.

## 1.4 Scope of the Study

This research involves collection of paint effluent and biomass of the three species of molluscs shells namely; *Archachina marginata* (land snail), *Tympanotonus fuscatus (*periwinkle) and *Mercenaria mercenaria* (hard clam). Physicochemical analysis of the untreated effluent, proximate analyses and characterization of coagulants using FTIR, SEM, XRD and XRF and by physical parameters such as surface area, pH of zero point charge, densities and porosity were carried out. Shells of unmodified and modified *Archachatina marginata* (land snail), *Tympanotonus fuscatus (*periwinkle) and *Mercenaria mercenaria* (hard clam) were used as coagulant to treat Industry paint effluent. This study also explored the optimization of coagulation-flocculation process using Response surface methodology and finally, kinetics of coagulation-flocculation process was highlighted.

## 1.5 Significance of the Study

Paint effluents discharge has caused untold health challenges to man, sometimes resulting to death. Our environment is not left out because they are poisoned by the heavy metals and toxic chemicals that are dangerous even to plants and animals. Our rivers, lakes, dams and oceans are polluted and contaminated which led to the death of fishes and water not safe for drinking or domestic purposes. The conventional coagulants like synthetic and inorganic coagulants are not recommendable since most

of them cause cancer, Alzheimer diseases and neurological disorder. Considering equally the biodegradability, simplicity, renewability, cheapness, and environmentally friendliness of organic coagulants makes this work to be of much significant.

## 1.6 Justification of the study

Coagulation- flocculation method is environmentally friendly, easy and cheap to use. The waste shells biomasses are converted to a useful product. The conventional coagulants increase the volume of the sludge after treatment and dissolve in the effluent during treatment therefore, creating another problem of pollution. This study is a part of a response to green chemistry because of the health risk associated with inorganic and synthetic chemicals.

# CHAPTER TWO

# LITERATURE REVIEW

## 2.1 Coagulation-Flocculation

All waters, especially surface waters, contain both dissolved and suspended particles. Coagulation and flocculation processes are used to separate the suspended solids from the water. The suspended particles vary considerably in source, composition charge, particle size, shape and density. Correct application of coagulation and flocculation processes and selection of the coagulants depend upon understanding the interaction between these factors. The small particles are stabilized (kept in suspension) by the action of physical forces on the particles themselves. One of the forces playing a dominant role in stabilization results from the surface charge present on the particles. Most solids suspended in water possess a negative charge and since they have the same type of surface charge, repel each other when they come closer. Therefore, they will remain in suspension rather than clump together and settle out of the water (Sawyer *et al.,* 1994). The traditional use of coagulation has been primarily for the removal of turbidity from potable water. However, recently, coagulation has been shown to be an effective process for the removal of many other contaminants that can be adsor bed by colloids such as metals, toxic organic matter, viruses, and radio nuclides (Wang *et al.,* 2005).

Coagulation is the process in which destabilization of particles occurs by the reduction of the repulsive potential of the electrical double layer. Hence the agglomeration of particles in suspension occurs (Faust and Aly, 1983).

Flocculation on the other hand is the process by which destabilized particles are brought together to form aggregates called flocs that are of a large size which can easily sediment. In this way separation of water and flocs formed is achieved (Faust and Aly, 1983). Coagulation is the phase in the overall process whereby the constituents of a given water are destabilized and flocculation is the phase whereby destabilized particles, or particles formed during destabilization are induced to collect into aggregates. These particles that are destabilized are referred to as colloids and finely divided matter (Amirtharajah and O'Melia, 1999). There are three steps to coagulation process:

1 Coagulation formation

2 Particle destabilization

3 Interparticle collision

The first two steps are usually fast and take place in a rapid mixing tank. The third step, interparticle collision is a slower process that is achieved by fluid flow and slow mixing. This is the process that causes the agglomeration of particles and it takes place in the flocculation tank as shown in Figure 2.1 (Amirtharajah and O'Melia, 1999).

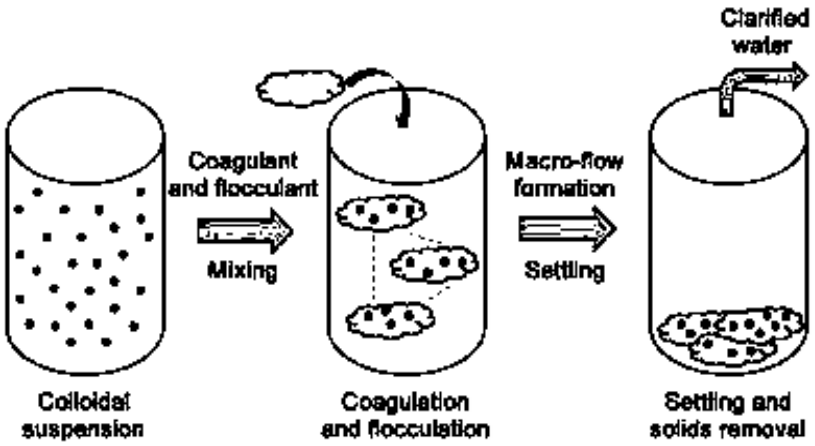


**Figure 2.1: Coagulation- flocculation process**

## 2.2 Particulates in water

There are several types of components of variable sizes found in wastewater that can be removed using coagulation-flocculation methods: molecules (<1nm), colloidal materials (1 to 1,000 nm) and suspended solids (>1µm). Molecular species may include salts, inorganic or organic compounds with variable water solubility. Colloids are also known as non settleable solids that do not dissolve in water although they are electrically charged. Still, the particles are so small that they will not settle out of the water even after several years and they cannot be removed by filtration alone (Kerri, 2002). Colloids are very small particles that exhibit light-scattering phenomena, which are a consequence of their comparable size to the wavelength of scattered light. Colloids display unique physicochemical properties, such as high surface area, high interfacial energy and high surface- to-charge ratio. They can only be seen with a high-powered

microscope. Examples include bacteria, fine clays, and silts. Colloids often cause coloured water, such as the "tea colour" of swamp water (Lee, 2014).

A colloid is composed of two phases: the dispersed phase, or the solute, and the dispersion medium, or the solvent. Both of these phases can have all three states of matter which are solid, liquid, and gas. For example, the dispersion medium may be a liquid and the dispersed phase may be a solid. This system is called a liquid sol, an example of which is the turbidity in water. The dispersion medium may be a gas and dispersed phase may be solid. This system is called a gaseous sol and examples are dust and smoke (Sincero and Sincero, 2003).

Three types of colloids are commonly encountered: hydrophilic, hydrophobic and association colloids (Manahan, 2010). Hydrophilic colloids display a strong interaction with water and may be generally regarded as solutions of very large molecules (e.g. starch, gums, proteins and bicolloids like virus and bacteria) or ions; such suspensions are less affected by the presence of salts compared with hydrophobic colloids. The affinity of the hydrophilic sols for water is due to polar functional groups that exist on their surfaces. These groups include such polar groups as $-OH$, $-COOH$, and $-NH_2$. They are, respectively, called the hydroxyl, carboxylic, and amine groups (Manahan, 2010). Hydrophobic colloids interact less favorably with water but are relatively stable due to the presence of a negative or positive charge because of electrical double layer. Thus, hydrophobic colloids, such as gold sol, silver halogenides, non hydrated metal

oxides, clay particles or petroleum droplets, can be destabilized by the addition of a salt due to compression of the electrical double layer (Bratby, 2006). Association colloids are formed by surface active agents (e.g., detergents and polymers) that possess hydrophilic (water-loving) and hydrophobic (water-hating) domains. The formation of micelles (aggregates) may occur for association colloids at a particular concentration, referred to as the critical micelle concentration. Micelles are formed by cationic, anionic or non-ionic detergents and may vary in size from one to 100nm, depending on the nature of the detergent. Inorganic minerals, organic pollutants, proteins, bacteria and microscopic plant life may exist as diverse types of colloids, as described above.

The colloidal stability of such systems plays a very important role in the quality of natural water and waste waters. Suspended solids may be visible without or with a microscope and may settle over time, such as sand and silt deposits. While it is possible to filter out suspended solids, molecular or colloidal materials cannot be efficiently removed using conventional filtration methods. Hence, the application of coagulation-flocculation methods is a versatile approach for addressing the removal of colloids and suspended solids for a range of water treatment applications (Lee, 2014). In waste water treatment, it is usually difficult to classify particular water as being either hydrophobic or hydrophilic colloids dispersion. Both types may co-exist in a particular system and furthermore, there may be a continuous transition from one state to the other, as occurs for example, during treatment. A further difficulty in classification is that at some

instance both hydrophobic and hydrophilic areas may exist on the colloids together. Although the term hydrophobic infers a definite solid boundary, there is in reality a layer of water molecules perhaps in some cases only a molecule thick, bound strongly enough to the colloids surface such that as the colloids move in water, the plane of shear is a water-water boundary, the water molecule exists as dipole with a positive end resulting from the two bonded hydrogen atom and a negative end from the two free pairs of electrons of the oxygen atoms. The result of this charge distribution is a strong dipole moment of $1.8 \times 10^{-18}$ esu. In the condition encountered in water and wastewater treatment, colloidal materials always possess a net of these two factors; the dipolarity of the water molecule and the surface charge carried by the colloids is to (i) bind the molecules to the solid-liquid interface and (ii) orient water molecules or alter the way in which molecules are arranged in the vicinity of the charged surface (Bratby, 2006).

There are three principal ways in which the surface charge may originate

1. The charge could arise from chemical reaction at the surface. Many solid surfaces contain functional groups which are readily ionized, such as OH, -COOH, -$OPO_3H_2$. For example with a bacterium, the overall charge may be visualized as resulting from ionization of functional amino and carboxyl groups. The charge of the particles with such surfaces becomes dependent on the degree of ionization (proton transfer) and consequently on the pH of the surrounding liquid. At low pH a positively charged surface prevails while at higher pH, a negatively charged

surface prevails. At some intermediate pH (the isoelectric point or the zero point of charge, $pH_{zpc}$), the charge will be zero. Surface charges can also originate by processes in which solute coordinately bond to solid surfaces.

2. Surface charge could be caused by lattice imperfection at the solid surface. For example, if in an array of solid, $SiO_2$, tetrahedral site, $Si^{4+}$ atom is replaced by an $Al^{3+}$ atom or $Fe^{2+}$ for $Al^{3+}$ in an octahedral site, results in a local charge deficit of positive charge, that is ( Al having one electron less than Si ) a negative charged framework is established. Clay is an example of such atomic substitutions. Surface charge of this type is independent of the pH of the liquid.
3. Surface charge could also be established by adsorption of ions. Adsorption of one type of ion on a surface can arise from London- Van der Waal's force and from hydrogen bonding.

## 2.3 Effect of surface charge

Surface charge influences the distribution of nearby ions in the liquid. Ions of opposite charge (counter ions) are attracted towards the surface and ions of like charge (co-ions) are repelled away from the surface ( Sincero and Sincero, 2003). This together with the mixing tendency of thermal motion and mutual ionic repulsion or attraction, leads to the formation of an electrical double layer made up of the charged surface and a neutralizing excess of counter ions over co-ions distributed in a diffuse manner in the nearby liquid. The theory of the electrical double layer deals with the distribution of

ions and hence with the magnitude of the locality of the charged surface. Electrical potential is analogous to gravitational potential but now, think of a point in an electric field. Thus in the field around a negative charge, for example another negative charge moves from points near the charge to points further away and one may say that point around the charge have a electric potential whose magnitude depends on their relative proximity to the charge. The electrical double layer can be regarded generally as consisting of two regions: an inner region which probably includes water molecules and adsorbed (hydrated) ions and a diffuse region in which ions are distributed according to the influence of electrical forces and random thermal motion (Abuzaid *et al*., 1998).

Historically, the electrical double layer was first considered of a charge surface and a diffused region of ions around the surface. This led to a model developed by Gouy and Chapman. The second development was considered in addition to the diffused region of ions, a region in which ions are adsorbed and held to the surface. This led to model developed by stern. Stern's model therefore is a modification of Gouy-Chapman model with an adsorbed layer of ions being considered.

The chemistry of coagulation and flocculation is primarily based on electricity. Electricity is the behaviour of negative and positively charged particles due to their attraction and repulsion. Like charges (two negatively charged particles or two positively charged particles) repel each other while opposite charges (a positively charged particle and a negatively charged particle) attract.

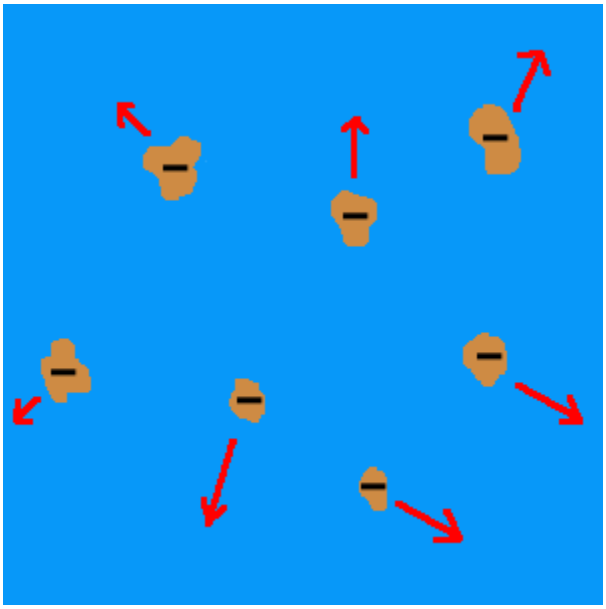

**Figure 2.2 : Negatively charged particles repel each other due to electricity.**

Most particles that dissolve in water have a negative charge, so they tend to repel each other. As a result, they stay dispersed and dissolved or colloidal in the water, as shown in Figure 2.2 (Lee, 2014).

The purpose of most coagulant chemicals is to neutralize the negative charges on the turbidity particles to prevent those particles from repelling each other. The amount of coagulant which should be added to the water will depend on the zeta potential, a measurement of the magnitude of electrical charge surrounding the colloidal particles. Zeta potential is the amount of repulsive force which keeps the particles in the water. It is also the charge at the boundary of the colloidal turbidity particle and the surrounding water. The higher the charge the more is the repulsion between the turbidity particles, less the coagulation, and vice versa. Higher zeta potential requires a higher coagulant

dose. An effective coagulation is aimed at reducing zeta potential charge to almost 0. If the zeta potential is large, then more coagulants will be needed (ADEM, 1989). Coagulants tend to be positively charged, due to their positive charge, they are attracted to the negative particles in the water, as shown in Figure 2.3

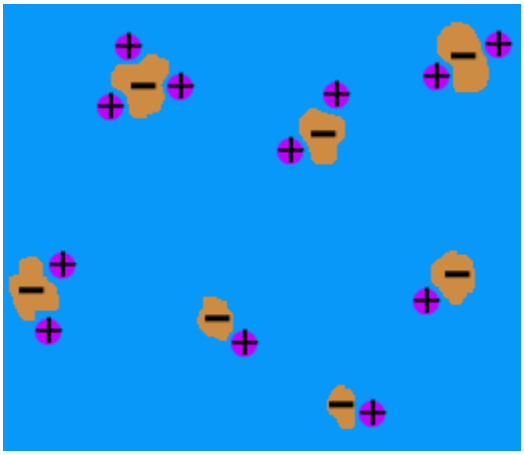

**Figure 2.3: Positively charged coagulants attracted to negatively charged particles due to electricity.**

The combination of positive and negative charges results in a neutral, or lack of charge. As a result, the particles no longer repel each other. The next force which will affect the particles is known as Van der Waal's forces. Van der Waal's force is referred to as the tendency of particles in nature to attract each other weakly if they have no charge.

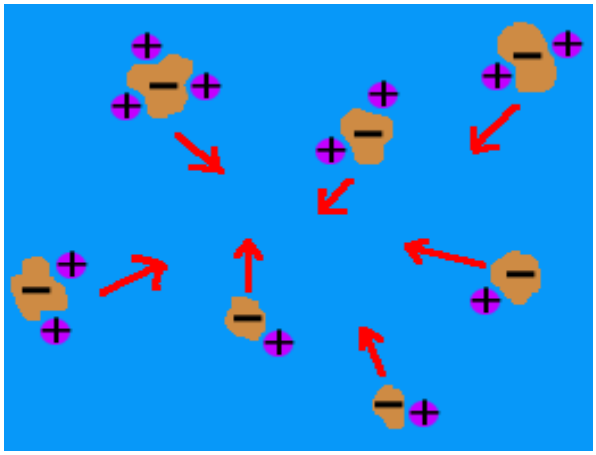

**Figure 2.4: Neutrally charged particles attract due to van der Waal's forces.**

Once the particles in water are not repelling each other, van der Waal's forces make the particles drift toward each other and join together into a group. When enough particles have joined together, they become floc and will settle out of the water as shown in Figure 2.4 (Kerri, 2002).

## 2.4 Types of Coagulants

Coagulant chemicals are of two main types - primary coagulants and coagulant aids. Primary coagulants are metal coagulants and polymeric coagulants.

### 2.4.1 Metal Coagulants

The commonly used metal coagulant fall into two general categories: those based on aluminium and those based on iron. The aluminium coagulants include aluminium sulphate, aluminium chloride, polyaluminium chloride and sodium aluminate. The iron coagulants include ferric chloride, ferric sulphate and ferrous sulphate.

### 2.4.1.1 Aluminum sulphate, $Al_2(SO_4)_3.14H_2O$

Aluminium sulphate probably the most widely used coagulant is manufactured from digestion of bauxite or aluminium ores with sulphuric acid. The quantities of bauxites used are just over the stoichiometric amounts needed to combine with the acid so that in the product no free acid is present. Evaporation of water in the process results in the dry product having the approximate formula $Al_2(SO_4)_3.14H_2O$ with an aluminium oxide ($Al_2O_3$) content ranging from 141-181 (m/m). Dry aluminium sulphate may be supplied as stabs, kibbled and screened or kibbled and ground. These are the reactions of the aluminium sulphate with common alkaline reagent (Bratby, 2006)

$$Al_2(SO_4)_3\,(H_2O)_{14} + 6OH^- \rightarrow 2Al(OH)_3 + 3SO_4^{2-} + 14H_2O \qquad 2.1$$

$$Al_2(SO_4)_3\,(H_2O)_{14} + 3Ca(HCO_3)_2 \rightarrow 2Al(OH)_3 + 3CaSO_4 + 6CO_2 + 14H_2O \qquad 2.2$$

$$Al_2(SO_4)_3\,(H_2O)_{14} + 6NaHCO_3 \rightarrow 2Al(OH)_3 + 3Na_2SO_4 + 6CO_2 + 14H_2O \qquad 2.3$$

### 2.4.1.2 Aluminium Chloride – $AlCl_3.6H_2O$

Aluminum Chloride is normally supplied in solution form containing 20% $Al_2O_3$ with a pH and density of approximately 2.5 and 1300 $kgm^{-3}$ respectvely. It has been widely used for sludge conditioning and has often been described as a good general purpose conditioner.

### 2.4.1.3 Polyaluminium Chloride, $(Al(OH)_{1.5}(SO_4)_{0.125}Cl_{1.25})n$

This coagulant is a relatively new product developed in Japan. It is partially hydrolysed aluminium chloride incorporating a small amount of sulphate. The result obtained with the coagualnt are equivalent to using aluminium sulphate in conjuction with a polyelectrolyte. Polyaluminium chloride is supplied inform of liquid with the equivalent of 10% $Al_2O_3$. Diluted solution of concentrated 0.4-3% show evidence of slow hydrolysis (Bratby, 2006).

### 2.4.1.4 Sodium Aluminate $NaAlO_2$

Sodium aluminate differs from alum in that it is alkaline rather than acidic in its reactions but generally with alum to obtain some special result. For example, in the coagulation of highly coloured water, alum (plus acid usually) is added to the water to coagulate the colour at its low pH, this however, results in undesirable concentrations of soluble aluminium compounds, alkaline sodium aluminate is then added, also lime if reqiured to increase the pH at least 6.0 which causes the soluble aluminium to precipate out in a secondary settling basin.

The reaction of $NaAlO_2$ with $Al_2(SO_4)_3$ $(H_2O)_{14}$ and with free $CO_2$ produce insoluble aluminum compound ( Bratby, 2006) viz

$$6NaAlO_2 + Al_2(SO_4)_3\,(H_2O)_{14} \rightarrow 8Al(OH)_3 + 3Na_2SO_4 + 2H_2O \qquad 2.4$$

$2NaAlO_2 + CO_2 + 3H_2O \rightarrow Na_2CO_3 + 2Al(OH)_3$ 2.5

$NaAlO_2$ is purchased either as solids or solution.

### 2.4.1.5 Ferric sulphate, $Fe_2(SO_4)_3.8H_2O$

This is available in solid or liquid form. In solid form the material is grannular and free flowing with the following typical specification 72/75% m/m $Fe_2(SO_4)_3$ and 20/21% m/m in $Fe^{3+}$. All ferric coagulant are used over a wide range of pH 4.0 to 11.0. Ferric sulphate is particularly useful for colour removal at low pH values and also at high pH values where it is used for iron and high and manganese removal and in the softening process. For the latter uses the insoloubility of the ferric hydroxide at high pH values makes the iron coagulants in general prefereable to alum. The chemical rections with alkali are shown below (Bratby, 2006):

$Fe_2(SO_4)_3 + 3Ca(HCO_3)_2 \rightarrow 2Fe(OH)_3 + 3CaSO_4 + 6CO_2$ 2.6

$Fe_2(SO_4)_3 + 6NaHCO_3 \rightarrow 2Fe(OH)_3 + 3Na_2SO_4 + 6CO_2$ 2.7

$Fe_2(SO_4)_3 + 6NaOH \rightarrow 2Fe(OH)_3 + 3Na_2SO_4$ 2.8

### 2.4.1.6 Ferrous sulphate, $FeSO_4.7H_2O$

Also known as copperas (although the latter term is becoming obsolete) ferrous sulphate is avaliable either as crystal or granules containing 20% Fe, both of which are readily soluble in water. Ferrous sulphate reacts with neutral alkalinity or added

alkalinity to form ferrous hydroxide, $Fe(OH)_2$ but since ferrous hydroxide is relatively soluble, it must be oxidized to ferric hydroxide in order to be useful. The important reactions for ferrous sulphate are (Bratby, 2006):

$$FeSO_4(H_2O)_7 + Ca(OH)_2 \rightarrow Fe(OH)_2 + CaSO_4 + 7H_2O \quad 2.9$$

$$4Fe(OH)_2 + O_2 + 2H_2O \rightarrow 4Fe(OH)_3 \quad 2.10$$

Ferrous sulphate and lime find their greatest use at high pH values: for example, the lime soda softening process and in iron and magnanese removal.

### 2.4.1.7 Chlorinated ferrous sulphate

When chlorine is used to oxidize the ferrous hydroxide obtained from ferrous sulphate, the process is known as the chlorinated copperas treatment. In contrast to the high pH values required for the oxidization by oxgyen. Chlorine will react over a wide pH range. In practice ferrous sulphate and chlorine are fed separately and are generally mixed just prior to entry into the coagulation system. The reaction with chlorine produces ferric sulphate and ferric chloride and each mg/L of ferrous sulphate theoretically requires 0.13 mg/L of chlorine, although an excess of chlorine is generally added to ensure complete reaction and to provide chlorine for distinfection purposes. The reaction is as follows (Bratby, 2006):

$$6FeSO_4(H_2O)_7 + 3Cl_2 \rightarrow 2Fe_2(SO_4)_3 + 2FeCl_3 + 7H_2 \quad 2.11$$

Caogulation with copperas ( or Ferrous sulphate) is especially useful where pre-chlorination is required. It has further advantage over ferrous sulphate in that coagultion may be obtained over a wide range of pH values 4.0 to 11.0.

### 2.4.1.8 Ferric chloride, $FeCl_3$

Ferric chloride is available commercially in the liquid, crystal or anhydrous forms. The liquid and crystal forms are very corrosive and must be handled in similar fashion to hydrochloric acid. Because ferric chloride is very hygroscopic, drums must remain sealed until needed and that entire contents must be dissolved at one time, the reactions of ferric chloride with natural or added alkalinity may be written as follows (Bratby, 2006).

$$2FeCl_3 + 3Ca(HCO_3)_2 \rightarrow 2Fe(OH)_3 + 3CaCl_2 + 6CO_2 \quad 2.12$$

$$2FeCl_3 + 3Ca(OH)_2 \rightarrow 2Fe(OH)_3 + 3CaCl_2 \quad 2.13$$

### 2.4.2 Polyelectrolyte or Polymer coagulants

Polymers or polyelectrolyte consist of simple monomers that are polymerized into high-molecular-weight substances with molecular weights varying from 104 to 106 Daltons (Crittenden *et al*., 2005). The term polyelectrolyte as used here refers to a large variety of natural or synthetic, water soluble, macro-molecular compound has the ability to destabilize or enhance flocculation of the constituents of a body of water. Strictly

speaking the term polymeric flocculants is more appropriate as a general description, polyelectrolyte being perhaps better reserved for those carrying ionized groups. However because of its widespread usage, the term polyelectrolyte will be taken as including those polymeric flocculants which are essentially non-ionic.

A polymer molecule may be described as series of repeating chemical unit held together by covalent bonds. If the chemical unit are of the same molecular structure the compound is termed homopolymer. However, if the molecule is formed from more than one type of repeating chemical unit, it is termed copolymer. The individual repeating units are called monomers and the molecular weight of the polymer molecule is the sum of the molecular weight of the individual monomers. The total number of monomers units is referred to as the degree of polymerization. Polyelectrolytes are special classes of polymers containing certain functional groups along the polymer back bone which may be ionizable. If present, when the ionizable groups dissociate, the polymer molecule becomes charged either positively or negatively, depending on the specific functional groups present, and are thus referred to as cationic or anionic polyelectrolyte. Polyelectrolytes that possess both positively and negatively charged sites are referred to as amphoteric whereas those that possess no ionizable functional groups are termed non ionic polyelectrolyes. All polyelectrolytes are typically hydrophilic colloids. They have molecular weight generally in the range of $10^4$ and $10^7$ and are soluble in water due to hydration of functional groups. Polyelectrolyes are effective in enhancing the rate of

orthokinetics flocculation when added to a system already destabilized with metal coagulants as shown below (Polasek and Mutl, 2002)

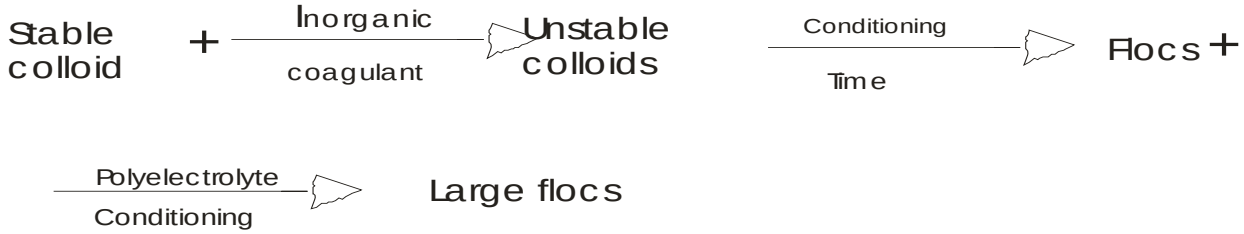


Polyelectrolytes may also be effectively applied as primary coagulants as shown below

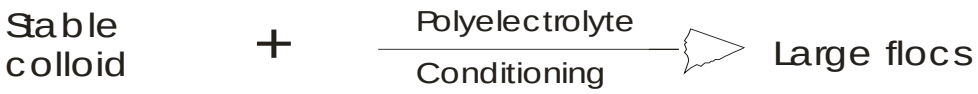


Furthermore, there are instances where polyelectrolyte is effective in precipitating substances dissolved in solution. From the above comments, it is appreciated that the destabilization mechanism operative with polyelectrolyte is complex and cannot be collectively ascribed to one particular phenomena. For a given system, there may be a dominance of charge effects, or adsorption or chemical reaction at the functional groups. The predominance or relatively combination of each phenomenon depends on the characteristics of the system and of the added polyelectrolyte (Theodoro *et al.*, 2013). Polyelectrolytes are of two classes namely; natural and synthetic. The polysaccharides, mainly starch and its constituents, different types of gums, alginic acid, cellulose and its derivatives, dextran, glycogen etc. are among the natural polymers used. Polyacrylamide (PAM) and poly (ethylene oxide)(PEO) are non-ionic.

The majority of the cationic groups of polyelectrolytes are derived by introducing quaternary ammonium groups onto the polymer backbone, although polymers containing sulphonium and phosphonium groups are used to a limited extent. The most commonly used cationic polyelectrolytes are poly (diallyldimethyl ammonium chloride) (polyDADMAC). In the anionic group of polyelectrolytes, mainly two types of polymers are used; one type is polymer containing carboxyl functional groups and the other containing sulphonic acid groups. A representative of the former is poly(acrylic acid and its derivatives, of the latter poly(styrene sulphonic acid) (PSSA) (Witold *et al.,* 2009).

### 2.5.2.1 Nonionic Polyelectroltye

These polymers are called nonionic; even though slight hydrolysis of the amide groups gives them an anionic nature (with an anionicity of less than 1%). Nonionic polymers containing less than 1% of anionic groups may be obtained under special polymerization conditions. Their main characteristics are:

- Molecular weight: between1.5 and 15 million
- Viscosity at 5 g/L: between 8 and 200 cps.

They are used for the treatment of potable water, the treatment of waste process water, municipal sewage and treatment of ores (SNF FLOERGER)

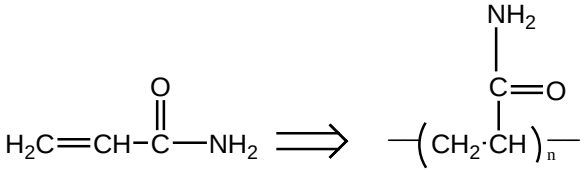

Acrylamide Polyacrylamide

### 2.4.2.2 Anionic polyelectrolyes

Anionic flocculants are obtained either by hydrolysis of the amide groups on a polyacrylamide chain or by copolymerization of the polyacrylamide with a carboxylic or sulphonic acid salt. The most commonly used is acrylic acid:

The anionicity of these copolymers can vary between 0% and 100% depending on the ratio of the monomers involved. The main characteristics of the copolymers are:

I. Molecular weight: 3to 30 million
II. Viscosity at 5 g/L: between 200 and 2800 cps.

They are also used as thickeners in the petroleum, textile, cosmetic and other industries. Another example of anionic polyelectrolyte is activated silica (O'Melia *et al*., 1999).

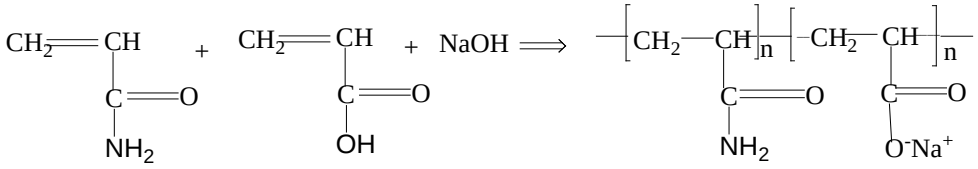

Acrylamide Acrylic acid Na acrylate- acrylamide

#### 2.4.2.2.1 Activated silica as anionic polyelectrolyte

Activated silica is probably the first polyelectrolyte to be used widely in water clarification. In preparing activated silica (which is an anionic polyelectrolyte) commercial sodium silicate solutions (pH approximately 12) in concentration in excess of $2x10^{-3}M$ are neutralize with acid reagent (eg sulphric acid, chlorine, aluminum sulphate or sodium bicarbonate) to a pH less than 9. A disadvantage with this chemical is that with carelessness in the method of preparation (concentration of reagent, mixing, degree of neutralization, aging etc) silica gel may form. For this reason, the usage of activated silica often leads to blockages in pumps and feed pipes and may give rise to reduce filter runs (Robinson, 2001).

#### 2.4.2.3 Cationic polyelectrolyte

Cationic flocculants are mainly derived from the copolymerization of acrylamide with dimethylaminoethylacrylate (DMAEA) in quaternized form. A first reaction of DMAEA with methylchloride allows it to be converted into a quaternary ammonium salt in the form of chloromethylated DMAEA(DMAEA-MeCl): The copolymerization of DMAEA-MeCl with acrylamide produces the cationic polymer

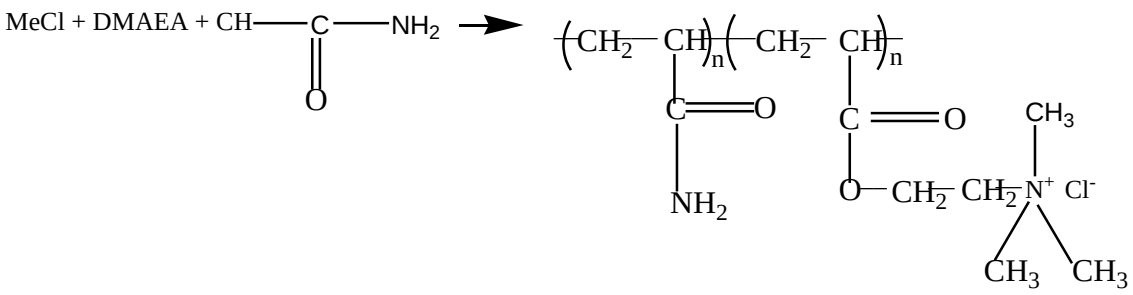


The cationic charge of the copolymer is determined by the ratio of each monomer and may vary between 0 and 100%. The ester group of the copolymer is very sensitive to the pH above 6.

Hydrolysis of the polymer reduces its efficiency by creating amphoteric polymers and the anionic polymers. It is therefore essential to prepare these polymers at a pH of about 5.5, even though the flocculation is carried out at a higher pH. However, during flocculation, the floc may be converted by chemical modification of the polymer when the contact times are long, for example during settling (Ram and Sahu, 2013).

The main characteristics of the products obtained are: Molecular weight: 3 to10 million, Viscosity at 5g/L: 100 to1700cps.

### 2.4.2.4 Amphoteric polymers

Amphoteric polymers exhibit both cationic and anionic behaviour, for example acrylamide-acrylicacid-DMAEA-MeClorDADMAC-acrylicacid. The strength and the relative number of sites of opposite ionic nature may vary.

### 2.4.3 Natural polyelectrolytes

Polyelectrolytes, although a comparatively recent term, have long been used as flocculants. Sankrit literature mention the use of crushed nuts of the Nirmel tree, *Strychnos potatorum* as a means of clarifying water, their action is most likely due to the presence of an organic water soluble polymer. Today, there are several such naturally derived substances used as polyelectrolyte. Most of them have polysaccharide skeleton with anionic property due to presence of carboxyl groups and their molecular weight up 105. An advantage of natural polyelectrolytes, especially for use in potable water treatment is that they are virtually toxic free (Duan and Gregory, 2003). Examples are Guar gum, starches, tannins, sodium alginate, chitin, chitosan and sodium carboxymethyl cellulose.

#### 2.4.3.1 Guar gums

It is neutral (non ionic) polysaccharides relatively un affected by pH and ionic strength. The structure comprises of a chain of D-mannose with a D-galactoseside chain on approximately every alternate mannose unit, has a molecular weight of the order of 220,000. As a result of its wide range properties, guar gum is the most extensively used gum, both in food and industrial applications. They are subject to enzymatic degradation of citric or oxalic acid. Guar gum has been used in uranium processing. In the mining industry guar gum is used as floating agent, they form stabilizer, filtration

and water treating agent. In textile industry, it is used as a sizing agent and as a thickner for dyestuff ( Tripathy and Ranjan De, 2006).

### 2.4.3.2 Starches

Starches isolated from different sources are all used to some degree as polyelectrolyte, but some work better with certain substrate than others. It has been reported that the amylose fraction of starch is superior to amylopectin or native starch in red polyelectrolyte. Examples of starches are processed polymers based on potato. They are non-ionic, cationic or anionic depending on the processing. The cationic types have quaternary group substituent and the anionic type carboxylic substitutions. Dosage efficiency and dispersibility of starch polyelectrolyte are improved by introduction of cationic and anionic substituent (Tripathy and Ranjan De, 2006).

### 2.4.3.3 Tannins

Complex polysaccharides tannin derivatives that have been used extensively in potable, waste water and industrial effluent treatment applications. They are generally most effective under acidic condition. Care must be taken on storage as they are subject to degradation reaction if left for long periods (Bratby, 2006).

### 2.4.3.4 Sodium aliginate

This is non toxic polyelectrolyte (widely used as a food additive) which is extracted from brown seaweed. The commercial product contains sodium and calcium carbonates (Bratby, 2006).

### 2.4.3.5 Chitin derivatives and chitosan

Chitin is water insoluble high molecular weight polymer of 2-acetamide-2-deoxy-D-glycopyranosyl unit linked through β(1-4)- D-bonds. This may be converted to chitosan by partial or complete deacetylation. In the protonated form, this cationic polyelectrolyte is water soluble with a number of potential commercial uses including polyelectrolyte and drug delivery (Tripathy and Ranjan De, 2006).

### 2.4.3.6 Sodium carboxymethy cellulose

This is water soluble gum produced from alkali cellulose (alkali salt of poly β-D-glucose) and monochloroacetic acid with degree of substitution in the range of 0.4-1.5. Unlike many derived from natural product, it is relatively resistant to biological and hydrolytic degradation (Tripathy and Ranjan De, 2006).

## 2.5 Coagulant Aids

Coagulant aids add density to slow-settling flocs and add toughness to the flocs so that they will not break up during the mixing and settling processes. Nearly all coagulant aids are very expensive, so care must be taken to use the proper amount of these chemicals. In many cases, coagulant aids are not required during the normal operation of the treatment plant, but are used during emergency treatment of water which has not been adequately treated in the flocculation and sedimentation basin (Arcadio and Gregoria, 2003; Harendra *et al.*, 2011). A couple of coagulant aids are considered below.

### 2.5.1 Lime

Lime is a coagulant aid used to increase the alkalinity of the water. The increase in alkalinity results in an increase in ions (electrically charged particles) in the water, some of which are positively charged. These positively charged particles attract the colloidal particles in the water, forming floc.

### 2.5.2 Bentonite

Bentonite is a type of clay used as a weighting agent in water that is high in colour and low in turbidity and mineral content. This type of water usually would not form floc large enough to settle out of the water. The bentonite joins with the small floc, making the floc heavier and thus making it settle more quickly.

## 2.6 Mechanism of destabilization of Polyelectrolyte

There is no single mechanism of destabilization by polyelectrolytes which may be considered applicable in all instances. However, it is possible to set down two principal mechanisms which in some instances may be operative conjointly, whereas in others the predominance of one over the others is fairly simple to indentify. In some case, the two phenomena may operate in opposition. The two mechanism are based on (1) bridging the model, where polyelectrolyte segment are adsorbed on the surface of the adjacent colloid thereby binding them together and (11) a model whereby ionic polyelectrolytes, bearing a charge of opposite sign to the suspended material, are adsorbed and thereby reducing the potential energy of repulsion between adjacent colloids. With (1) it is seen that (11) may support the action, or oppose it, depending on whether there is strong electrostatic attraction between the polyelectrolyte and colloid surface. With (11), it is appreciated that if (1) contributes to destabilization, it will always support the action of the other. The two mechanism described above are referred to as bridging mechanism and electrostatic patch mechanism respectively (Bratby, 2006).

### 2.6.1 Bridging mechanism

The bridging mechanisms of destabilization by polyelectrolytes have been an accepted phenomenon for some time. The principal basis for acceptance lies in the ability of charged polyelectrolyte to destabilize particles bearing the same charge. Furthermore,

direct evidence is available whereby electron micrographs have identified polyelectrolyte bridges between particles. Stages in the bridging mechanism of polyelectrolytes in suspension are

1 Dispersion of polyelectrolyte in the suspension
2 compression or settling down of the adsorbed polyelectrolyte
3 Adsorption at the solid-liquid interface
4 Collision of adjacent polyelectrolyte coated particles to form bridges and thereby increasing larger flocs.

### 2.6.1.1 Dispersion in the suspension

Polyelectrolytes have high molecular weight, because of this; they tend to exhibit high viscosity and low diffusion rates when in solution. The adsorption of polyelectrolytes to particle surface is essentially irreversible, for adsorption to occur evenly on all particles it is important that the polyelectrolyte throughout the suspension is as quick and efficiently as possible. This is accomplished during the rapid mixing stage where a short vigorous mixing environment is required to effect dispersion in the shortest possible time (Bratby, 2006)

### 2.6.1.2 Adsorption at the solid-liquid interface

After step (1), where polyelectrolyte has diffused to the solid-liquid interface, adsorption of initial one functional group will occur while the rest of the chain is for a

while momentarily free and extends into the solution. As time proceeds, due to continuous Brownian movement, the chain becomes successfully attached at more point along its length until eventually there are no dangling ends extending into the solution phase. The mechanism of adsorption of polyelectrolyte segments to a solid surface depends on both the chemical characteristics of the polyelectrolyte and the adsorbent surface. For example adsorption could be due to cation exchange, as reported in the adsorption of polyelectrolyte on clay particles, electrostatic linkages, hydrogen bonding or ionic bonding (Bratby, 2006). In the case of polyelectrolytes and particles of like sign, adsorption may be strongly dependent on ionic strength. For example, for the case of hydrolyzed polyacrylamide and negatively charged kaolinite clay surfaces, adsorption has been found to be strongly dependent on calcium ion concentration. In general, with calcium ions a critical concentration of approximately $10^{-3}$ M is often found which correspond to hardness in excess of 100 mg/L as $CaCO_{3.}$ In some cases, the presence of cation $Ca^{2+}$ may have the effect of complexing with polyelectrolyte functional group thereby aiding adsorption of negative particles by anionic polymers by a certain bridge effect.

Ionic strength may influence adsorption by two effects; (1) reduce repulsion between similarly charged particle surface and polyelectrolyte segment, thus permitting more polyelectrolyte chain to be accommodated on particle surface, (ii) reduce the size of

the polyelectrolyte coil thus permitting more polyelectrolyte chains to be accomodated on the particle surface.

Adsorption is effectively irreversible although the energy of adsorption at any particular site may be low and under normal circumstances may indicate a probability of desorption, the chance of desorption occurring simultaneously at a number of site is low. Although under condition of destabilization with polyelectrolyte, desorption of the whole chain from the particle surface does not occur, displacement may be induced by, for example, suitably adjusting pH conditions or adding a sufficiently high concentration of surface competitor, such as sodium tripolyphosphate (Bratby, 2006).

#### 2.6.1.3 Compression of adsorbed chain

The probability of a successful bridge forming between two adjacent particles depends on the configuration of the adsorbed polyelectrolyte at the surface. A progressive greater number of polyelectrolyte segments will become adsorbed on the particle surface and consequently, the polyelectrolyte chain will become compressed to the surface. The polyelectrolyte layer requires a finite time to become compressed and initially will consist of long loops. It is during this initial period, where loops are longest and extend further into the solution that bridging is most effective. With extensive adsorption of segments to the surface, the polyelectrolyte chain progressively assumes a flatter configuration until the extent of double layer repulsion exceeds the size of the loops. The effect is particularly pronounced for dilute colloidal suspension where a statistically longer time is available for compression of polyelectrolyte loops. A

possible solution is to add polyelectrolyte in stages thus ensuring that large loops are retained for period sufficient for bridging to occur. The configuration of the adsorbed polyelectrolyte depend upon the size of the polyelectrolyte (molecular weight); its structure; flexibility; charge density (% hydrolysis); interaction energy between polyelectrolyte and particle surface; chemical nature and physical spacing of the adsorption sites on the particle surface and competition between polyelectrolyte and other adsorbing molecules in solution.

As regard molecular weight, in general where the bridging mechanism is predominant, an increase in chain length gives rise to an increase in the optimum polyelectrolyte/solid ratio. This is because longer chain does not lie flat on the surface as shorter chains and therefore, individual chain does not occupy many adsorption sites. Therefore, bridging is more efficient with polyelectrolyte of higher molecular weight since loops will tend to extend further into solution. This is evident from the fact that with appropriate systems, for a given applied electrolyte concentration, the higher the molecular weight the higher is the efficiency of destabilization (assessed in term of size of flocs, settling rates, and filterability and so on).

Flexibility of polyelectrolyte segments influences the size of the pendant loops: a relatively inflexible polyelectrolyte chain will tend to be attached by a few segments and the loops will tend to be longer than for a relatively flexible chain.

Considering percentage of hydrolysis (or charge density) the higher the charge density the greater is the repulsion between adjacent segments and the more extended is the polyelectrolyte chain for a given molecular weight. The more extended the polyelectrolyte, the further should the pendant loops extend into solution and the more effective should be the bridging mechanism. However, unlike molecular weight where there is upper limit to the charge density, beyond which electrostatic repulsion (in the case of polyelectrolyte and solid surface of similar charge characteristics) will effectively retard adsorption.

An ionic strength consideration to a certain extent reduces the range of inter-particle repulsion (after polyelectrolyte adsorption). Increasing ionic strength reduces the range of inter-particles repulsion (after polyelectrolyte adsorption) so that particles will have a statistically high opportunity of approaching close enough together for bridging to take place before extensive compression of polyelectrolyte segments occurs. However, on the other hand, the greater the ionic strength, the less extended is the polyelectrolyte chain and the shorter is the range of extension of polyelectrolyte loops (Brathy, 2006).

#### 2.6.1.4 Bridging formation

After adsorption has taken place as described in the preceding factors; polyelectrolyte loop extending into solution from the particle surface will further become adsorbed onto adjacent particles thus forming a number of bridges. The strength of the flocs thus formed depends on the number of bridges formed, which in turn is dependent on the

number of loops available. The number of loops available for mutual adsorption between extensive compressions has taken place and the loops are within the bounds of the respective double layer, and are dependent on a number of factors related to both the suspension and the added polyelectrolyte. A crucial important factor during bridging is the availability of adsorption sites on particles to accommodate polyelectrolyte loops from neighboring particles, such availability depends on the concentration of polyelectrolyte added: if an excess of polyelectrolyte is added, too many adsorption sites per particles will be occupied and bridge formation is prevented; the particle effectively become re-stabilized (Bratby, 2006).

### 2.6.2 The electrostatic patch mechanism

For the case of non-ionic and anionic polyelectrolytes applied to a negatively charged colloidal dispersion, a destabilization mechanism described by the bridging model adequately accounts for the phenomena taking place. Indeed in many cases, it would be difficult to account for the phenomena by a mechanism other than bridging. However, for the case of charged polyelectrolytes applied to dispersion with particle carrying surface charges of opposite sign, the bridging model is often inadequate. Such systems include cationic polyelectrolytes applied to a negative colloidal dispersion and anionic polyelectrolyte applied destabilize with metal coagulants. i.e as flocculant aids to particle metal hydrolysis product aggregates, which may be positively charged.

It is seen that the electrostatic patch model as described above bears a resemblance to the electrical double colloid destability, where the adsorption of counter-ions in the stern layer brings about a reduction in the potential energy of repulsion between particle. For bridging mechanism to be effective, destabilization would need to be virtually complete within the time required for loops to be compressed and be ineffective for bridging. This would be greatly influenced by the collision frequency of particles and therefore is directly related to particle concentration. At high particle concentrations a given particle will collide with many others while polyelectrolyte loops are still in a relatively extended state.

## 2.7 Advantages of Polyelectrolyte

The advantages of polyelectrolyte are as follows:

I. During clarification, the volume of sludge produced can be reduced by 50 to 90%.
II. The resulting sludge is more easily dewatered and contains less water.
III. Polymeric coagulants do not affect pH. Therefore, the need for an alkaline chemical such as lime, caustic, or soda ash is reduced or eliminated.
IV. Polymeric coagulants do not add to the total dissolved solids concentration.
V. Soluble iron or aluminum carryover in the clarifier effluent can result from inorganic coagulant use. By using polymeric coagulants, this problem can be reduced or eliminated (Robinson, 2001).

## 2.8 Factors affecting Coagulation-Flocculation

1. Dosage**:** The concentration of coagulant required for coagulation is to be proportional to the concentration of an organic matter present in solution, and it was stated that before turbidity can be removed, the coagulant must be added in sufficient amounts to destabilize the organic matter. Apparently, these substances react with the coagulants before the coagulants can destabilize clay suspensions. Coagulant dosage decreases with decrease pH because more carboxylic groups become prorogated and do not interact with coagulant. There is no reliable formula to determine the effective dosage. However, a jar test is the most reliable method to determine both the effective type of coagulant and their proper dosage (Kawamura, 1996; Bolto and Gregory, 2007). Proper coagulation is essential for good clarification and filtration performance and for the control of pathogens and disinfection by-products. Improper coagulation can cause high residual coagulant in treated water and post-treatment precipitation of particles causing turbidity, deposition and coatings of pipes in the distribution system. Care must be exercised in coagulant addition, since over-addition could result in reversal of surface charge and result in inter-particle repulsion.
2. pH: Alkalinity refers to the acid- neutralizing capacity of water, and is a general indication of water's buffering capacity. Alkalinity and pH are related; high alkalinity waters have high pH. Metal coagulants are acidic, and coagulant

addition consumes alkalinity. For low alkalinity waters, coagulant addition may consume all the available alkalinity, depressing the pH to values too low for effective treatment. High alkalinity waters (highly buffered) may require elevated coagulant additions to depress the pH to values favourable for coagulation. Alum and ferric chloride are more acidic than PACls, and therefore, result in greater alkalinity consumption after addition. For Poly(aluminium chloride) PACl, alkalinity consumption is related to basicity. At higher basicity PACl will consume less alkalinity than low or medium basicity ones. The pH at which coagulation occurs is the most important parameter for proper coagulation performance, as it affects the; surface charge of colloids, charge of natural organic matter functional group, charge of the dissolved-phase coagulant species, Surface charge of floc particles and coagulant solubility (Pernitsky, 2003). If pH is lowered to improve coagulation and organic removal, it is typically necessary to raise pH in the final effluent from the plant to provide less corrosive finished water.

3. The pH may be adjusted at one or more points for the treatment, including rapid mixing, pre-filtration and post-filtration. In case of enhanced coagulation, it is recommended to readjust the pH after the filtration process as compared to pre-filtration. This is because some animate matter may be adsorbed onto the floc that may be carried-over from the clarification process, and any pre-filtration pH adjustment may then result in “release” of that biological matter, which could

pass through the filters and contribute to subsequent DPB formation (Sahu and Chaudhari, 2013).

4. Temperature: Low temperature affects coagulation and flocculation processes by altering coagulant solubility, increasing water viscosity, and retarding the kinetics of hydrolysis reactions and particle flocculation. At higher coagulant doses, the addition of flocculation or filter aids, longer flocculation times, and lower flotation, sedimentation, and/or filtration rates are often required to produce low turbidity treated water. Thus, higher coagulant dosages and additional flocculation time are required at a low temperature. Low water temperatures decrease the rates of coagulant dissolution, precipitation, cell enmeshment and floc formation, especially when alum is used (O'Connor and Brazos, 1990). Warm water often causes an increased level of algae and other organic matter in raw water. Temperature also significantly affects turbidity and particle counts during coagulation (Braul *et al.,* 2001). However, dissolved organic carbon (DOC) and colour removal are not sensitive to temperature. The negative effect of temperature tends to be greatest with dilute suspensions (Sahu and Chaudhari, 2013). Summarily, the higher the temperature, the faster the reaction, and the more effective is the coagulation. Winter temperature will slow down the reaction rate, which can be helped by an extended detention time.
5. Mixing and Time: Proper mixing and detention times are very important to coagulation. Quick mixing of the coagulant will ensure rapid hydrolysis of the

coagulant, contact between the sols and the suspended solids will retard the development of large flocs which are inactive in destabilizing the dispersion and removing of a pollutant. The parameter expressing mixing intensity is called the velocity gradient or G-value ($s^{-1}$). Recommended G- value for rapid mixing is minimally $1500s^{-1}$. Mixing intensity and time has the significant effect on the mechanisms (e.g. sweep coagulation, sedimentation) involved in the following process of coagulation (Chichuan *et al*., 2002). Higher velocity causes the shearing or breaking of floc particles and lower velocity will let them settle in the flocculation basins. Velocity around 1 ft/sec in the flocculation basins should be maintained.

6. Intense mixing may disrupt polyelectrolyte bridges and give rise to desorption and or re-arrangement of loose chain on the particle surface. The mixing should not be too violent nor too long a period. The addition of dilute polyelectrolyte solution is clearly of advantage.
7. Zeta potential: Zeta potential is the charge at the boundary of the colloidal turbidity particle and the surrounding water. The higher the charge the more is the repulsion between the turbidity particles, the high is the coagulation, and vice versa. Higher zeta potential requires the higher coagulant dose. An effective coagulation is aimed at reducing zeta potential charge to almost 0.

## 2.9 Mollusc shells

The mollusc shell is typically a calcareous exoskeleton which encloses supports and protects the soft parts of an animal. The phylum Mollusc includes snails, clams, tusk shells, and several other classes. All of the shells above are inhabited by molluscs -- invertebrate animals with an unsegmented body, that generally consists of a head, foot, visceral mass, and hanging flaps of the body wall that constitute the mantle. Zoologists group them in the phylum Mollusc. They mostly live in the sea or fresh water and use gills for respiration, although terrestrial and some freshwater snails breathe by a rudimentary lung. Molluscs have no internal supporting skeleton; instead, the shell usually serves to protect the body against the outside world. It is a product of secretion by the mantle, and it is deposited in several separate layers. Different types of molecules make up each layer, and depending on the type of secretion, the shell can be thickened, hardened, enlarged, or if necessary repaired by the overlapping mantle. The molluscs might well be considered the ultimate examples of "morphing," both in regard to details of their body plan and details of the shell, itself. Nevertheless, the basic body plan is one of front-to-back bilateral symmetry, with well defined nerve ganglia, gills, a blood circulatory system, as well as digestive, reproductive, and excretory organs. Hundreds of soluble and insoluble proteins, control shell formation. They are secreted into the extrapallial space by the mantle. The mantle edge secrets a shell which has two components. The organic constituent is mainly made up of

polysaccharides and glycoprotiens. This organic framework controls the formation of calcium carbonate. Insoluble proteins tend to be thought of as playing a more important/major role in crystallization control (Belcher *et al.,* 1996). The organic matrix of shells tends to consist of β-chitin and silk fibroin. Perlucin encourages carbonate deposition, and is found at the interface of the chitinous and aragonitic layer in some shells. An acidic shell matrix appears to be essential to shell formation, in the cephalopods at least; the matrix in the non-mineralized *squid gladius*is basic (Gotliv *et al.,* 2003). The formation of a shell in molluscs appears to be related to the secretion of ammonia, which originates from urea. The presence of an ammonium ion raises the pH of the extra pallial fluid, favouring the deposition of calcium carbonate. This mechanism has been proposed not only for molluscs, but also for other unrelated mineralizing lineages. The calcium carbonate layers in a shell are generally of two types: an outer, chalk-like prismatic layer and an inner pearly, lamellar or nacreous layer (Sudo, *et al.*, 1997). The layers usually incorporate a substance called conchiolin, often in order to help bind the calcium carbonate crystals together. Conchiolin is composed largely of quinone-tanned proteins.

## 2.10 *Archachatina marginata*

Plate 2.1 is the shell of *Archachatina marginata*. The common name is the giant West African snail or banana rasp snail; in Eastern part of Nigeria it is called 'ejula'. It is a species of air-breathing tropical and snail, a terrestrial pulmonate gastropod mollusk

in the family of Achatinidae. They can grow up to 20 cm long, and live up to 10 year and attain sexual maturity at 9–10 months under laboratory conditions. The snail has a bulbous protoconch that is large and broad, with a white or bluish-white columella, parietal wall and outer lip. The shell, when magnified, has the appearance of a woven texture. It can be found in West Africa countries like Nigeria, Angola, Benin, Cameroon, Congo, The Democratic Republic of the; Côte d'Ivoire; Equatorial Guinea (Equatorial Guinea (mainland)); Gabon; Gambia; Ghana; Guinea; Guinea-Bissau; Liberia; SenegalSierra Leone; Togo (Wikipedia)


**Plate 2.1: The shell of *Archachatina marginata***

## 2.11*Tympanotonos fuscatus*

Plate 2.2 is *the shell of Tympanotonos fuscatus.* It is called West African Mud Creeper, Eastern part of Nigeria called it ‘Isam’. It is a species of snail living in brackish water, a

gastropod mollusk in the family of Potamididae. Shells of *Tympanotonos fuscatus* can reach a size of about 35–100 millimetres . This species is found along the coasts of Nigeria, Angola, Benin, Cameroon, Congo, the Democratic Republic of the; Côte d'Ivoire; Equatorial Guinea (Equatorial Guinea (mainland); Gabon, Gambia, Ghana, Guinea, Guinea-Bissau, Liberia, Senegal, Sierra Leone, Togo (*Tympanotonus Fuscatus* Wikipedia)

**Plate 2.2: The shell of *Tympanotonos fuscatus***

## 2.12 *Mercenaria mercenaria*

Scientific classification

Kingdom: Animalia

Phylum: Mollusc

Class: Bivalvia

Order: Veneroida

Family: Veneridae

Genus: Mercenaria

Species: M. mercenaria

Binomial name

*Mercenaria mercenaria*


**Plate 2.3 The shell of *Mercenaria mercenaria***

Plate 2.3 is shell of *Mercenaria mercenaria*, the hard clam also known as quahog (or quahaug), round clam, or hard-shell (or hard-shelled) clam, is an edible marine bivalve mollusc that is native to the eastern shores of North America and Central America, from Prince Edward Island to the Yucatán Peninsula. It can also be found in Nigeria. Older literature sources may use the systematic name *Venus mercenaria*; this species is in the family Veneridae, the venus clams. Hard clams can be found in coastal lagoons and estuaries from about 12-30‰ but most large populations occur at >15%. They grow from 10-30 °C, but most growth occurs from 18-25 °C; below

5°C, clams become dormant. Clams burrow from just below the surface to about 15 cm in all sediment types, near oyster reefs, and in sea grass beds, but prefer sediments that are a mixture of sand and mud with some coarse material. They range from the intertidal zone to 15 m (Kraeuter and Castagna, 2001).

## 2.13 Chitin

Chitin $(C_8H_{13}O_5N)_n$ is a long-chain polymer of an N-acetylglucosamine, a derivative of glucose, and is found in many places throughout the natural world. It is a characteristic component of the cell walls of fungi, the exoskeletons of arthropods such as crustaceans (e.g., crabs, lobsters and shrimps) and insects, the radulae of molluscs, and the beaks and internal shells of cephalopods, including squid and octopuses and on the scales and other soft tissues of fish and amphibians. The structure of chitin is comparable to the polysaccharide cellulose, forming crystalline nanofibrils or whiskers. In terms of function, it may be compared to the protein keratin (Pradip *et al.*, 2004)

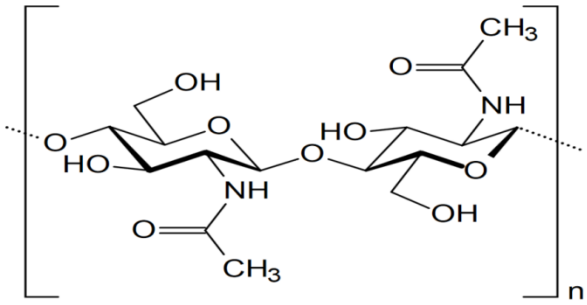


**Structure of Chitin**

Chitin is also modified polysaccharide that contains nitrogen; it is synthesized from units of N-acetylglucosamine (2-(acetylamino)-2-deoxy-D-glucose). These units form covalent β-1,4 linkages (similar to the linkages between glucose units forming cellulose). Therefore, chitin may be described as cellulose with one hydroxyl group on each monomer replaced with an acetyl amine group. This allows for increased hydrogen bonding between adjacent polymers, giving the chitin-polymer matrix more strength. In its pure, unmodified form, chitin is translucent, pliable, resilient, and quite tough. In most arthropods, however, it is often modified, occurring largely as a component of composite materials, such as in sclerotin, a tanned proteinaceous matrix, which forms much of the exoskeleton of insects. Combined with calcium carbonate, as in the shells of crustaceans and molluscs, chitin produces a much stronger composite. This composite material is much harder and stiffer than pure chitin, and is tougher and less brittle than pure calcium carbonate. Another difference between pure and composite forms can be seen by comparing the flexible body wall of a caterpillar (mainly chitin) to the stiff, light elytron of a beetle (containing a large proportion of sclerotin) (Dutta *et al*., 2002).

## 2.14 Chitosan

Chitosan is a linear polysaccharide composed of randomly distributed β-(1-4)-linked D-glucosamine (deacetylated unit) and N-acetyl-D-glucosamine (acetylated unit). It is made by treating the chitin shells of shrimp and other crustaceans with an alkaline

substance, like sodium hydroxide and HCl. Chitosan has a number of commercial and possible biomedical uses. It can be used in agriculture as a seed treatment and biopesticide, helping plants to fight off fungal infections. In wine making it can be used as a fining agent, also helping to prevent spoilage. In industry, it can be used in a self-healing polyurethane paint coating. In medicine, it may be useful in bandages to reduce bleeding and as an antibacterial agent; it can also be used to help deliver drugs through the skin. More controversially, chitosan has been asserted to have use in limiting fat absorption, which would make it useful for dieting, but there is evidence against this. Other uses of chitosan that have been researched include use as a soluble dietary fibre (Shukla, 2013).

Chitosan is produced commercially by deacetylation of chitin, which is the structural element in the exoskeleton of crustaceans (such as crabs and shrimp) and cell walls of fungi. The degree of deacetylation (%DD) can be determined by NMR spectroscopy, and the %DD in commercial chitosans ranges from 60 to 100%. On average, the molecular weight of commercially produced chitosan is between 3800 and 20,000 Daltons. A common method for the synthesis of chitosan is the deacetylation of chitin using sodium hydroxide in excess as a reagent and water as a solvent. The reaction occurs in two stages under first-order kinetic control. Activation energy for the first step is higher than the second; its value is an estimated 48.76 kJ/mol at 25-120$^{o}$C. This reaction pathway, when allowed to go to completion (complete deacetylation) yields up

to 98% product (Ahlafi *et al.*, 2013). The amino group in chitosan has a pKa value of ~6.5, which leads to a protonation in acidic to neutral solution with a charge density dependent on pH and the %DA-value. This makes chitosan water-soluble and a bioadhesive which readily binds to negatively charged surfaces (Lim *et al*., 2015) such as mucosal membranes. Chitosan enhances the transport of polar drugs across epithelial surfaces, and is biocompatible and biodegradable. It is not approved by FDA for drug delivery though; purified quantities of chitosans are available for biomedical applications.

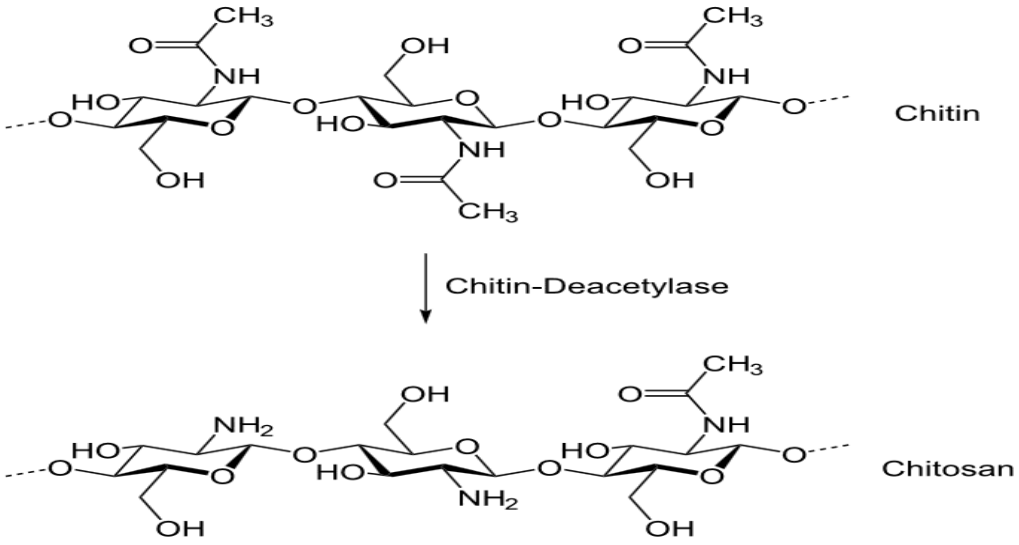


**Partial deacetylation of Chitin**

Chitosan and its derivatives, such as trimethylchitosan (where the amino group has been trimethylated), have been used in nonviral gene delivery. Trimethylchitosan, or quaternised chitosan, has been shown to transfect breast cancer cells, with increased degree of trimethylation increasing the cytotoxicity; at approximately 50%

trimethylation, the derivative is the most efficient at gene delivery. Oligomeric derivatives (3-6 kDa) are relatively nontoxic and have good gene delivery properties (Kean *et al*., 2005).

### 2.15 Related literature on some natural Coagulants

Menkiti *et al*., (2016) treated paint effluent using *Tympanotonos fuscatus (TF),* in the work titled Post-treatment sludge analyses and purification of paint effluent by Coagulation-flocculation method. Influence of pH, dosage and settling time on treatment efficiency on the removal of turbidity from paint effluent was studied. Scanning electron microscopic, Fourier transform infra red, x-ray diffraction and differential scanning calorimetric/thermogravimetric analyses were carried out to investigate, respectively, the surface morphology, functional group, crystalline/lattice structure and thermal stability of TF and settled sludge after treatment. The results obtained showed that paint effluent was optimally treated at 2 g/L TF dosage, pH 5 and 97 % efficiency. Results indicated that TF could be an efficient treatment agent for paint effluent at the conditions of the experiment.

The ability of a coagulant prepared from snail shell (SS) to carry out removal of suspended solid (TSS) in a fibre-cement plant effluent has been evaluated by Ani *et al*., (2010) at bench scale using a standard jar test apparatus operated at room temperature in their work titled Coagulation-flocculation performance of snail shell biomass for waste water purification . In order to verify the results obtained from the study, alum

was used in the control experiment. The effects of variation of coagulant dosage and flocculation reaction kinetics at the pH of the wastewater were also investigated. The optimum coagulant dosage for turbidity removal was found to range between 400 and 500 mg/l at the end of 30 minutes of coagulation. The highest values of coagulation rate constant, k recorded were $4.5x10^{-3}$ and $7.6x10^{-3}$ l /mg. min for SS and alum at dosage of 400 mg/L. From the results it was suggested that SS is an efficient coagulation agent and a potential alterative for the treatment of waste water at the conditions of the experiment.

A comparative study on Coagulation-flocculation kinetics of pharmaceutical Industrial effluent by *Achatina maginata* and aluminum sulphate (AMSC) has been reported by Ugonabo *et al*., (2013). *Achatina maginata* and aluminum sulphate were used to remove total suspended and dissolved particles (TSDP) from the effluent sample. The experiments were carried using standard nephelometric jar test method. Microkinetic data generated were fitted to specific models to evaluate interaction effects of coagulation factors (effluent medium pH, coagulant dosage, and settling time) on the treatment efficiency. Results obtained indicated that the best performance for AMSC are at pH of 13, dosage of 0.2 X $10^{-3}$ kg/$m^3$ and settling time of 2400 sec while for alum is at pH of 10 and dosage of 0.1 x $10^{-3}$ kg/$m^3$ and settling time of 2400 sec. The optimum value recorded for both coag-flocculation activities is 93.26% removal efficiency of TSDP at rate constant of 1.34E – 04 $m^3$/kg.s for alum. It can be concluded

that AMSC is a good alternative for alum having achieved good performance even better in some cases for all pH and dosages studied.

Ugonabo *et al*., (2012) studied the Kinetics and coagulation performance of snail shell biomass in pharmaceutical effluent and evaluated coagulation performance using a bio-coagulant (snail shell derived coagulant) at varying; time, dosage, pH and at room temperature. A conventional standard Jar test apparatus was employed for the tests, while the bio-coagulant denoted as SSC (snail shell coagulant) was produced following standard method. Coagulation kinetics data obtained were fitted into relevant model equations for the determination of coag-flocculation functional parameters. , reaction order, rate constant, dosage and pH, recorded maximum values at 7.25 s, 2.3 x $10^{-4}$ $m^3$/kg.s, 0.1 x $10^{-3}$ kg/$m^3$ and 13, respectively. The system achieved maximum efficiency of 90.82% in alkaline effluent medium. The results obtained affirmed that SSC is a good alternative natural resource for the removal of TDSP from pharmaceutical effluent.

*Moringa oleifera*, *Cicer arietinum*, and *Dolichos lablab* were used as locally available natural coagulants to reduce turbidity of synthetic water by Asrafuzzaman *et al*., (2011) in the work titled Reduction of turbidity of water using locally available natural coagulant. The tests were carried out, using artificial turbid water with conventional jar test apparatus. Optimum mixing intensity and duration were determined. After dosing, water-soluble extracts of *Moringa oleifera*, *Cicer arietinum*, and *Dolichos lablab*

reduced turbidity to 5.9, 3.9, and 11.1 NTU, respectively, from 100 NTU and 5, 3.3, and 9.5, NTU, respectively, after dosing and filtration. Highest turbidity reduction efficiency (95.89%) was found with *Cicer arietinum*.

Coagulation and flocculation treatment of fibre-cement effluent has been studied in respect of pH and dosage variation at room temperature using snail shell biomass as a precursor to coagulant by Ani *et al*., (2011) in the paper titled Coagulation-flocculation performance of snail shell biomass for waste water purification. Coagulation kinetics parameters such as order of reaction, α, and rate constant, k. were determined. Coagulation performance was measured in nephelometric jar test while coagulant preparation was based on work reported by Fernandez-Kim. Maximum parameter values were recorded at k of 4.5 x $10^{-3}$ L/mg.min, α of 2 and total solid of 2028 mg/l. Parameters obtained lie within acceptable range while it can be concluded that the coagulation performance of snail shell biomass is adequate to be use as biocoagulant.

Sludge characterization and treatment of produced water (PW) using *Tympanotonos fuscatus* coagulant has been studied by Menkiti and Ezemagu, (2015). Coagulation-flocculation method was used to investigate the effects of pH, dosage and settling time on the treatment efficiency. *Tympanotonos fuscatus* and post treatment settled sludge were subjected to FTIR, XRD, SEM, thermogravimetric/differential scanning calorimetric and elemental analyses. Optimal treatment efficiency of 91.5% was

obtained at 1 g/L and pH 2. It was concluded that *Tympanotonos fuscatus* was thermally stable and has potential for application as an effective bio-coagulant.

The performance of using dragon fruit foliage as coagulant was investigated by Shafad *et al*., (2013) in his paper titled, A preliminary study on dragon fruit foliage as natural coagulant for water treatment. Parameters affecting the coagulant performance such as drying temperature, pH, dosage, initial turbidity, and sedimentation time were studied using standard jar test method. From the study, the optimum drying temperature found for dragon fruit foliage was 50˚C, the optimum pH was 7 and the final pH was relatively unaffected by the coagulant added. The optimum dosage for 100 NTU, 200 NTU and 400 NTU found were 5 mg/L, 10 mg/L and 20 mg/L respectively. The sedimentation time found was very fast where 10 min was considered to be enough. The performance of dragon fruit foliage in turbidity removal was comparable to commercial alum and the optimum dosage for dragon fruit foliage was 1.5 times lower than alum. Combining dragon fruit foliage and alum showed better performance in turbidity removal. Hence, it can be concluded that dragon fruit foliage has a high potential as a natural coagulant for application in water treatment.

New bacterial exopolysaccharides isolated from *Bacillus licheniformis*, *B. insolitus* and *B. alvei*, were used as natural coagulants during coagulation-flocculation process by Raed *et al*. (2015). Efficiency of extracted bacterial exopolysaccharides was examined through removal ability of bacterial indicators and some physicochemical parameters of

River Nile water samples. Bacterial exopolysaccharides showed great removal percent when used as sole coagulant materials. Addition of alum to bacterial exopolysaccharides enhances removal efficiency.

Hendrawati *et al*., (2016) studied the effect of *Moringa oleifera* seed as natural coagulant to replace synthetic coagulant in their work titled The Use of Moringa Oleifera Seed Powder as Coagulant to Improve the Quality of Wastewater and Ground Water. The findings showed that Moringa. *oleifera* reduced 98.6% turbidity, 10.8 % of its conductivity, and 11.7% of its BOD and metal contents (Cd, Cr, Mn) in waste water. When applied to ground water, *M. oleifera* removed the turbidity of ground water as much as 97.5%, while conductivity and BOD are 53.4 % and 18%, respectively.

Mohammed *et al.*, (2013) studied the Application of natural Clays and Aluminium chloride for Waste water treatment". The experiments were designed in Completely Randomized Design (CRD) in three replicates using jar test apparatus for coagulation-flocculation process. The efficiency was calculated by evaluating turbidity, COD, and colour removal. The removal efficiency of PAC and its combined use with Shendi and Singa for turbidity was 96.2%, 94.8%, and 95.7%, for COD was 70.7%, 63.2%, and 61.1% and for colour removal was 82.1%, 78.1% and 80.7% respectively. While the efficiency of sole use of Shendi and Singa for turbidity was 59.2% and 27.9%, COD was 26.3% and 28.1% and colour was 26.3% and 10.3% respectively.

Yusuf *et al*., (2015) studied the Assessment of Coagulation efficiency of Okra seed extract for surface water treatment and evaluated the treatment efficiency of natural coagulant obtained from okra seed (okra seed extract). The coagulation ability of the coagulant was assessed by the use of standard jar test experiment involving two water samples (obtained from River Rima and Goronyo Dam of Sokoto) with various coagulant doses. The coagulation capacity of the okra seed extract was measured on the basis of turbidity removal. It was found from the results that okra seed coagulant was effective in removing the turbidity of surface water because the turbidities of the water samples considered were removed effectively at an optimum dose of 300 mg/L of the seed extract with optimum pH of about 7.0 from 745 NTU to 11 NTU for sample 1 and from 580 NTU to 5 NTU for sample 2. It was also discovered that the coagulant could be used to, effectively remove the turbidity of the samples with initial turbidity of about 580 NTU to WHO standard limit of 5 NTU. Therefore, it was concluded that Okra seed extract is a very effective coagulant in water treatment.

Luis *et al.,* (2013) studied the use of the polysaccharides contained in seeds of two fruits of *Annona diversifolia* and *Annona. muricata* using coagulation-flocculation method.. The results they obtained showed that *A. diversifolia*, removed 37.6% COD and 2mL sludge/L at 50ml. On the other hand, *A. muricata* removed 35% of the COD, with a dose of 100 mg/L and 5 mL sludge/L.

An evaluation of five extracts from cladode of *Opuntia Ficus Indica* (OFI), extracted by different solvents at high temperature was investigated by Belbahloul *et al.,* (2014) in the work titled Low technology water treatment: Investigation of the performance of Cactus extracts as a natural flocculant for flocculation of local clay suspensions. Experiments were conducted to determine optimum conditions for treating the turbid water loaded by clays from lakes in Morocco. The turbidity removal efficiency for two extracts was greater than 95% and can achieve 99% at optimal conditions of dosage and pH.

Pamila *et al.,* (2015) used five different powdered coagulants obtained from drumstick seeds, tamarind seeds, neem seeds, banana peel and sweet to treat surface water and compared against commercial coagulants like Alum and Lime in the work, Influence of Homemade Coagulant on the characteristics of surface water treatment: Experimental study. The best coagulant performance was found by comparing the optimum coagulant dosage, settling time, rate of settling, removal efficiency, clarity and cost. The results obtained followed this order Neem seed > banana peel > *Moringa olifera* > sweet potato > tamarind seed. Applications of these natural coagulants were recommended for rural people who rely on low quality water sources.

Soap and detergent industrial waste water has been treated by using polymeric Chitosan extracted from crustacean shells for the reduction of chemical oxygen demand and color using coagulation-flocculation process by Anteneh and Sahu, (2014), in the

work they titled Natural coagulant for the treatment of food Industry waste water. Their results showed that at pH 7 mass loading 50 mm and 150 rpm have capability to reduce the 83% of chemical oxygen demand as well as 90 % of colour. The scanning electron microscope shows that it has jelly structure which is better than other coagulant.

Ahmadi *et al*., (2016) studied the use of *Descurainia sophia L*.as a potential source of natural coagulant for the treatment of dye-containing wastewater in the paper Use of *Descurainia sophia L* as a natural Coagulant for the treatment of dye containing waste water. Response surface methodology (RSM) based on a three-variable, three-level Box–Behnken design (BBD) was used to analyze the decolourization of a model textile wastewater containing neutral red dye. The effect of three parameters including contact time, pH, and the coagulant dose on the colour removal was investigated. A second-order polynomial equation could accurately model the process with a $R^2$ of 0.96. The pH was found to be the most significant parameter affecting the colour removal. High colour (90.2%) removal efficiency was obtained at the optimal conditions of 6.5 min, pH 5.6, and 102.6 mg/L of coagulant.

Beltran-Heredia *et al.,* (2011) in the work “Textile wastewater purification through natural Coagulant” evaluated new coagulant obtained through polymerization of *Acacia mearnsii* de Wild tannin extract for the removal of two dangerous dye pollutants: Alizarin Violet 3R and Palatine Fast Black WAN. This coagulant was lab-synthesized according to the etherification of tannins with glycidyl trimethyl ammonium chloride

and formaldehyde and its performance in dye removal in terms of efficiency was high. A reasonably low coagulant dosage (ca.50 $mgL^{-1}$) reaches high capacity levels at 0.8 for Alizarin Violet 3R and 1.6 for Palatine Fast Black WAN mg dye $mg^{-1}$of coagulant while pH and temperature were not extremely affecting variables. The systems coagulant dyes were successfully modeled by applying the Langmuir hypothesis. q and b parameters were obtained with an adjusted correlation factor ($r^2$) above 0.8.

Thakur and Choubey, (2014) examined the coagulant characteristics of the tannins obtained from *Acacia catechu* as a primary coagulant in the work titled the Use of Tannin based natural coagulants for water treatment: An alternative to inorganic chemicals. The powdered material extract obtained from bark of *acacia catechu* was used to test coagulant rate and dose. The turbidity and other physico-chemicals of surface water sample were measured before and after the jar-test by using portable instruments. Turbidity meter was used to measure turbidity, while digital pH meter was used to measure pH. Total suspended solids were analyzed using gravimetric method. The experiments were carried out with coagulant dosage of 1.0, 2.0, 3.0, 4.0 and 5.0 mL with the intervals of 1mL in each raw water sample. The results showed that *acacia catechu* powder can remove turbidity up to 91% at the optimal dosage of 3.0 ml/L. On the other hand, the powder of *acacia catechu* can remove total dissolve solids by 57.3% but not other parameters.

The potentiality of *Cactus opuntia* (*Ficus-indica*), as a coagulant for the treatment of simulated industrial water-based paint wastewater in terms of colour, chemical oxygen demand (COD) and turbidity has been investigated by Vishali and Karthikeyan, (2014) in their work An eco-friendly alternative coagulant in the treatment of paint effluent. The coagulation ability was assessed for 1litre of effluent using the standard jar test apparatus by varying the operational variables like eluent type (water, NaCl and $BaCl_2$), eluent concentration n (1–5 N), coagulant dosage (1–6 g), coagulant volume (20–100 mL), initial pH (5–11) and initial effluent concentration (3100, 4224, 5650, 6258 and 7693 mg/L named as sample number 1–5, respectively). The results were maximum when 100 mL of 3 g of *C. opuntia*, eluted using 3 N NaCl as a coagulant to treat a litre of effluent. The favourable pH to run the treatment was confirmed as the actual pH of the sample (7.2–7.8). It was found that the removal efficiency increased as the pollution load swelled. The FTIR study revealed the presence of various functional groups, which are responsible for the coagulation process. The obtained results were compared with conventional coagulant ferric chloride. The results acknowledged that *Cactus opuntia* (*ficus-indica*) a natural, eco-friendly coagulant, could be a strong alternative to the conventional coagulant in the treatment of water-based paint wastewater.

The coagulation potential of alginate extracted from brown algae, *Sargassum* sp. for the removal of Congo red dye from aqueous solution has been identified by Vijayaraghavan and Shanthakumar, (2015) in the work on Performance study on algal alginate as

natural coagulant for the removal of Congo red dye. The yield of alginate extraction was found to be 40.8%. The extracted alginate was characterized by Fourier transform infrared spectroscopy and Scanning electron microscopy techniques. The effect of initial pH (4–6), alginate dose (10–60 mg/L), calcium dose (1–6 g/L), and initial dye concentration (50–250 mg/L) on dye removal were also investigated. It was inferred from the study that the maximum removal of dye (96%) was achieved with increasing alginate and calcium dose for increasing dye concentration, at pH 4.

Billuri *et al*., (2015) investigated the use of natural cationic polymers (chitosan and cationic starches with varying degrees of substitution) and the synthetic cationic polymer (poly(diallyldimethylammonium chloride) [pDADMAC]) to flocculate *Chlorella protothecoides* and *Nannochloropsis salina.* Algae surface charge and flocculation efficiency were examined in response to variable pH, coagulant dosage, cell concentration, and salinity. Overall effectiveness of coagulation, flocculation, and sedimentation is referred to as flocculation efficiency and is determined by measuring the percentage decrease in optical density of the microalgae suspensions. Cationic starch with a degree of substitution (DS) of 0.5 and chitosan neutralized the charge on *C. protothecoides* at lower dosages compared with pDADMAC, *C. protothecoides* flocculation efficiencies >95% were achieved with dense cultures (1g/L algae dry weight) at cationic starch (DS 0.5) and chitosan dosages of 0.02 g/g algae dry weight. Zeta potential measurements indicated that complete charge neutralization was not

necessary for maximum flocculation. Of the polymers tested, zeta potential analysis indicated that only chitosan was sensitive to pH. Maximum flocculation efficiency of *N. salina* was achieved through chitosan precipitation and subsequent sweep floc at pH 8.0. However, cationic starch (DS 0.5) and pDADMAC optimum doses were lower than that required for *N. salina* flocculation with chitosan.

Altaher *et al*., (2016) evaluated the use of the *Corchorus Olitorius* L. (COL), a leaf vegetable grown in Africa and the Middle East, as a novel coagulant aid.COL has important advantages over other coagulant aids. It is an agricultural waste that is widely produced and does not require further chemical treatment. Tests were carried out to evaluate the optimal dosages and conditions required to achieve optimum removal of both turbidity and humic acid. Based on the results of jar test, COL is an efficient coagulation aid. It has the ability to reduce both the primary coagulant dose from 600 mg $L^{-1}$ to 300 mg $L^{-1}$ and the residual turbidity from 5.63 to 0.26 NTU. This novel coagulant aid also reduced the total organic carbon (TOC) concentration to zero level. It also increased the rate of flocculation.

Kazi and Virupakshi, (2013) used *Cicer arietinum, Moringa oleifera*, and *Cactus* as locally available natural coagulants to reduce turbidity and COD of tannery wastewater. The tests were carried out using tannery wastewater with conventional jar test apparatus. Optimum dosage and optimum pH were determined. The optimum dosage of *Cicer arietinum, Moringa oleifera,* and *Cactus* were found as 0.1, 0.3 and

0.2gm/500mL respectively. The optimum pH value with *Cicer arietinum*, *Moringa oleifera*, and *Cactus* were found to be 5.5, 4.5 and 5.5, respectively. In case of *Cicer arietinum, Moringa oleifera*, and *Cactus* maximum reduction in turbidity were found to be 81.20%, 82.02% and 78.54%, and maximum reduction in COD were found to be 90%, 83.33% and 75%, respectively. Among the natural coagulants used in this study maximum turbidity reduction of 82.02% and COD reduction of 90% was found with *Moringa oleifera* and *Cicer aretinum*, respectively.

Fretias *et al*., (2015) in the work titled Optimization of coagulation-flocculation process for treatment of industrial textile wastewater using okra (*A. esculentus*) mucilage as natural coagulant conducted the coagulant activity of okra mucilage (*Abelmoschus esculentus*) as natural coagulant and their efficiency was compared to chloride ferric (chemical agent) in CF of textile wastewater. Optimization assays were carried out by the standard jar test method. The effect of pH, coagulant dosage and mucilage dosage on the percent removal of chemical oxygen demand (COD), turbidity and colour were analyzed. A high removal of colour (93.57%), turbidity (97.24%), COD (85.69%) was obtained using a low amount of the okra mucilage; 3.20 mg $L^{-1}$, 88.0 mg $L^{-1}$ $Fe^{3+}$ at pH 6.0. The amount of $Fe^{3+}$ can be reduced up to 72.5% (from 3.20 to 88.0 mg $L^{-1}$) and can increase the COD removal about 35.74% with addition of okra mucilage. The mucilage of residual okra has coagulant activity in the textile wastewater treatment and showed to be an available, biodegradable and non-toxic coagulant.

Chi and Cheng, (2006) studied the Use of Chitosan as a coagulant to treat waste water from milk processing plant". Chitosan is a natural material, the sludge cake from the coagulation after dehydrated could be used directly as feed supplement, therefore not only saving the spent on waste disposal but also recycling useful material. The result shows that the optimal result was reached under the condition of pH 7 with the coagulant dosage of 25 mg/L.

Nnaji *et al*., (2013) in their work "Modelling the Coag-flocculation kinetics of cashew nut testa tannins in an Industrial effluent" demonstrated the coagulant behaviour of tannins of *Anacardium occidentale* (CANTETA) testa for the removal of suspended solids from a fibre cement industrial effluent. A series of flocculation experiments were conducted to examine the optimal concentration of the coagulation together with the pH of the effluent needed to obtain the best results. The results showed that CANTETA have significant properties particularly at lower doses and in alkaline medium. Optimum efficiency of TSS removal was 84% with 100 mg/L (CANTETA) at initial effluent pH of 12. The kinetic of coagulation process suitably fits the second order kinetic model.

Ani *et al*., (2012) studied the use of the Turbidmetry in the coagulation performance of *Detarium microcarpum* (DM) in a fibre cement effluent (FCE) at room temperature. Analysis of variance (ANOVA) and Duncan new multiple range test (DNMRT) statistics were used to determine statistical difference of the coagulation performance of DM at various dosages and varying FCE pH. However, varying FCE pH between 4 and

12 using the same coagulant dosage had significant difference on the coagulation performance of DM.

**2.16 Response Surface Methodology (RSM)**

Response surface methodology (RSM) is an optimization approach commonly used in Industrial process control and engineering where the goal is to find levels of input variables that optimize a particular response (Bingol *et al.*, 2010). The responses and the corresponding factor are modelled and optimized using the RSM. RSM is also atechnique consisting of (a) designing of experiments to provide adequate and reliable measurements of the response, (b) developing a mathematical model having the best fit to the data obtained from the experimental design and (c) determining the optimal value of the independent variables that produces maximum or minimum value of the response. It is a designed regression analysis meant to predict the value of a dependent variable based on the controlled values of the independent variables and for seeking the optimum conditions for a multivariable system efficiently (Jabasingh and Pavithra, 2010; Kaushik and Malik, 2011; Fakhi, 2013).

In response surface methodology, the second order polynomial equation is mostly developed to fit the experimental data and also to determine the relevant model terms. The second order polynomial equation is

$$Y = \beta_O + \sum_{i=1}^{K} \beta_i x_i + \sum_{i=1}^{k} \beta_{ii} x_i^2 + \sum_{1 \le i \le j}^{k} \beta_{ij} x_i x_j + \varepsilon \qquad 2.0$$

Where Y represent the predicted response that is the coagulation flocculation efficiency of the (%),$\beta_{O,}$ the constant coefficient, $\beta_{i\ ,}$ the ith linear coefficient of the imput factor, $x_i$, $\beta_{ii}$ the ith quadratic coefficient of the imput factor, $x_i$, $\beta_{ij,}$ the different interaction coefficients between input factor $x_i$, and $x_j$ ( i =1-3, j = 1-3 and i/=j) and ε, the error of the model. The equation expresses the relationship between the predicted response and independent variables in coded values.

## 2.17 Working Principle of Ultraviolet Visible Spectrophotometer

The instrument used in monitoring the colour removal from paint effluent is ultraviolet-visible spectroscopy. It measures the intensity of light passing through a sample (I), and compares it to the intensity of light before it passes through the sample ($I_o$). The ratio$\frac{\boldsymbol{I}}{\boldsymbol{I_o}}$is called the "transmittance", and is usually expressed as a percentage (%T). The absorbance, A, is based on the transmittance:

$$\boldsymbol{A = -log\left(\frac{T\%}{100\%}\right)} \qquad \textbf{2.14}$$

The UV-visible spectrophotometer can also be configured to measure reflectance. In this case, the spectrophotometer measures the intensity of light reflected from a sample (I), and compares it to the intensity of light reflected from a reference material ($I_o$) (such as a white tile). The ratio $I / I_o$ are called the "reflectance", and are usually expressed as

a percentage (%R). UV/ Visible radiations are made up of the following components as shown in Figure 2.5

1. Sources (UV and visible)
2. Wavelength selector (monochromator)
3. Sample containers
4. Detector
5. Signal processor and readout

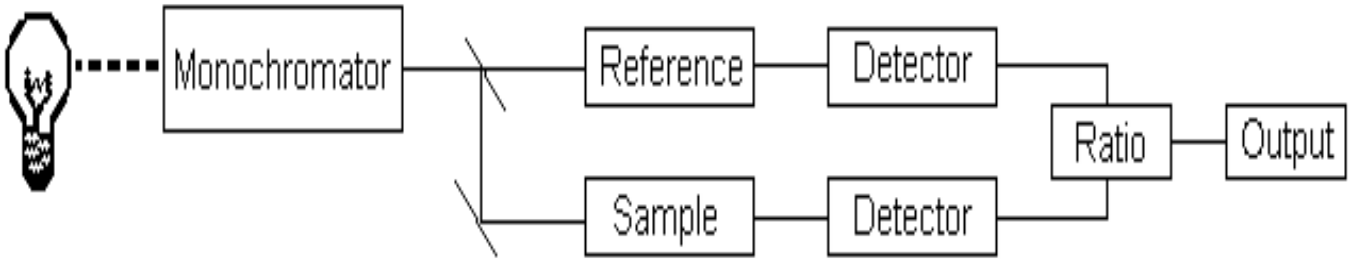


**Figure 2.5: UV/VIS compartments**

### 2.17.1 Sources of UV radiation

It is important that the power of the radiation source does not change abruptly over its wavelength range. The electrical excitation of deuterium or hydrogen at low pressure produces a continuous UV spectrum. The mechanism for this involves formation of an excited molecular species, which breaks up to give two atomic species and an ultraviolet photon. This can be shown as;

$D_2$ + electrical energy -> $D_2^*$ -> D' + D" + hv

Both deuterium and hydrogen lamps emit radiation in the range 160 - 375 nm. Quartz windows must be used in these lamps, and quartz cuvettes must be used, because glass absorbs radiation of wavelengths less than 350 nm.

### 2.17.2 Sources of visible radiation

The tungsten filament lamp is commonly employed as a source of visible light. This type of lamp is used in the wavelength range of 350 - 2500 nm. The energy emitted by a tungsten filament lamp is proportional to the fourth power of the operating voltage. This means that for the energy output to be stable, the voltage to the lamp must be very stable indeed. Electronic voltage regulators or constant-voltage transformers are used to ensure this stability.

Tungsten/halogen lamps contain a small amount of iodine in a quartz "envelope" which also contains the tungsten filament. The iodine reacts with gaseous tungsten, formed by sublimation, producing the volatile compound $WI_2$. When molecules of $WI_2$ hit the filament they decompose, re-depositing tungsten back on the filament. The lifetime of a tungsten/halogen lamp is approximately double that of an ordinary tungsten filament lamp. Tungsten/halogen lamps are very efficient, and their output extends well into the ultra-violet. They are used in many modern spectrophotometers.

### 2.17.3 Wavelength selector (monochromator*)*

All monochromators contain the following component parts;

1. An entrance slit
2. A collimating lens
3. A dispersing device (usually a prism or a grating)
4. A focusing lens
5. An exit slit

Polychromatic radiation (radiation of more than one wavelength) enters the monochromatic through the entrance slit. The beam is collimated, and then strikes the dispersing element at an angle. The beam is split into its component wavelengths by the grating or prism. By moving the dispersing element or the exit slit, radiation of only a particular wavelength leaves the monochromator through the exit slit.

### 2.17.4 Cuvettes

The containers for the sample and reference solution must be transparent to the radiation which will pass through them. Quartz or fused silica cuvettes are required for spectroscopy in the UV region. These cells are also transparent in the visible region. Silicate glasses can be used for the manufacture of cuvettes for use between 350 and 2000 nm.

### 2.17.5 Detectors

The photomultiplier tube is a commonly used detector in UV-Vis spectroscopy. It consists of a photoemissive cathode (a cathode which emits electrons when struck by photons of radiation), several dynodes (which emit several electrons for each electron striking them) and an anode.

A photon of radiation entering the tube strikes the cathode, causing the emission of several electrons. These electrons are accelerated towards the first dynode (which is 90V more positive than the cathode). The electrons strike the first dynode, causing the emission of several electrons for each incident electron. These electrons are then accelerated towards the second dynode, to produce more electrons which are accelerated towards dynode three and so on. Eventually, the electrons are collected at the anode. By this time, each original photon has produced $10^6$ - $10^7$ electrons. The resulting current is amplified and measured.

Photomultipliers are very sensitive to UV and visible radiation. They have fast response times. Intense light damages photomultipliers; they are limited to measuring low power radiation ( Prabhakar and Dubinskii, 2002).

### 2.18 Scanning Electron Microscope

Scanning electron microscope (SEM) is a type of electron microscope that produces images of a sample by scanning it with a focused beam of electrons. The electrons

interact with atoms in the sample, producing various signals that contain information about the sample's surface topography and composition. The electron beam is generally scanned in a raster scan pattern, and the beam's position is combined with the detected signal to produce an image. SEM can achieve resolution better than 1 nanometer. Specimens can be observed in high vacuum, in low vacuum, in wet conditions (in environmental SEM), and at a wide range of cryogenic or elevated temperatures. As the name suggests, SEMs use an electron beam instead of a beam of light, which is directed towards the specimen under examination. An electron gun, located at the top of the device, shoots out a beam of highly concentrated electrons. There are two main types of electron guns used by SEMs. The first, thermionic guns, heat a filament until electrons stream away. Field emission guns, the other popular choice, rip electrons away from their atoms by generating a strong electrical field. The microscope is composed of a series of lenses within a vacuum chamber. These lenses direct the electrons towards the specimen in order to maximize efficiency. The more electrons that are used the more powerful the magnification. The SEM usually requires a vacuum chamber to function, as the electron beam; it must not be obstructed as it passes through the body of the microscope. Small particles could deflect the electrons onto the specimen itself, obscuring the results. When a specimen is hit with a beam of the electrons known as the incident beam, it emits X-rays and three kinds of electrons: primary backscattered electrons, secondary electrons and Auger electrons. The SEM uses primary backscatter electrons and secondary electrons. An electron recorder picks up the rebounding

electrons and records their imprint. This information is translated onto a screen which allows three-dimensional images to be represented clearly. One of the SEM's greatest advantages is its ability to reproduce textual information in a consistent and coherent manner (McMullan, 2006).

### 2.19 X-Ray Diffraction (XRD)

X-rays are electromagnetic radiation. They have enough energy to cause ionization. When high energy electrons strike an anode in a sealed vacuum, x-rays are generated. Anodes are often made of copper, iron or molybdenum. Figure 2.6 shows the schematic of XRD and components of XRD are (a) X-ray source (b) Device for restricting wavelength range “goniometer” (c) Sample holder (d) Radiation detector (e) Signal processor and readout. The working principle is as follows;

a) A continuous beam of X-rays is incident on the crystal.
b) The diffracted radiation is very intense in certain directions – These directions correspond to constructive interference from waves reflected from the layers of the crystal.
c) The beam reflected from the lower surface travels farther than the one reflected from the upper surface
d) If the path difference equals some integral multiple of the wavelength, constructive interference occurs.

e) The diffraction pattern is detected by photographic film

Bragg's Law gives the conditions for constructive interference as $\lambda = 2dSin\Theta$ where $\lambda$ is the wavelength of x-rays, and moving electrons, protons and neutrons, d is the spacing between the planes in the atomic lattice, and $\theta$ is the angle between the incident ray and the scattering planes (Scintag Inc, 1999)

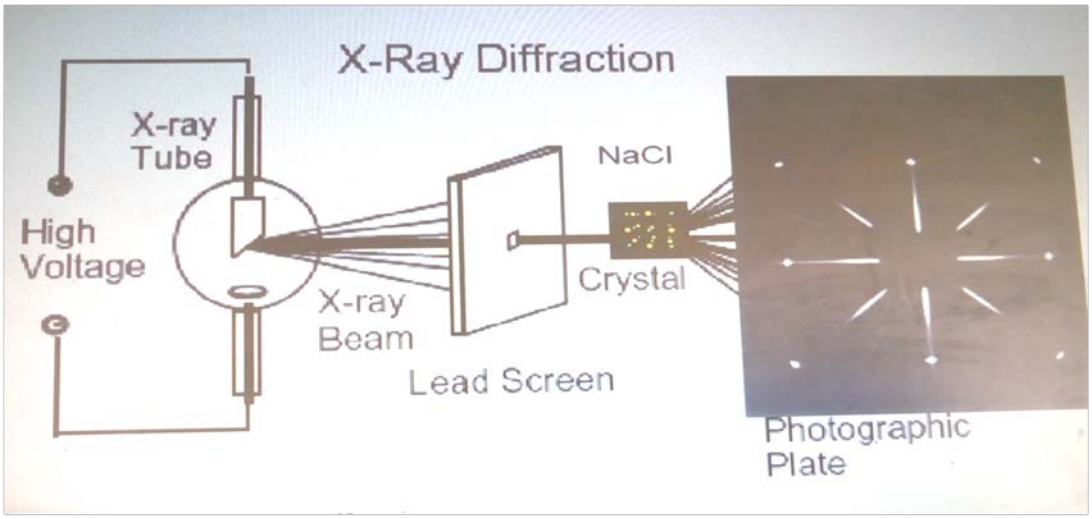


**Figure 2.6: A schematic of XRD**

Applications of XRD are;

I. Determination of Crystal structure
II. Phase identification / transition
III. Grain size / micro-strain
IV. Texture/stress( i.e.polymer , fiber )
V. Determination of thin film composition

VI. Industry Identification of archeological materials

## 2.20 Fourier Transform Infra-Red (FTIR) Spectrometer

Fourier transform infrared spectroscopy (FTIR) is a technique which is used to obtain an infrared spectrum of absorption or emission of a solid, liquid or gas. An FTIR spectrometer simultaneously collects high spectral resolution data over a wide spectral range. This confers a significant advantage over a dispersive spectrometer which measures intensity over a narrow range of wavelengths at a time. A common FTIR spectrometer consists of a source, interferometer, sample compartment, detector, amplifier, A/D convertor, and a computer as shown in Figure 2.7. The source generates radiation which passes the sample through the interferometer and reaches the detector. Then the signal is amplified and converted to digital signal by the amplifier and analog-to-digital converter, respectively. Eventually, the signal is transferred to a computer in which Fourier transform is carried out. This device shines a beam containing many frequencies of light at once, and measures how much of that beam is absorbed by the sample. Next, the beam is modified to contain a different combination of frequencies, giving a second data point. This process is repeated many times. Afterwards, a

computer takes all these data and works backwards to infer what the absorption is at each wavelength.

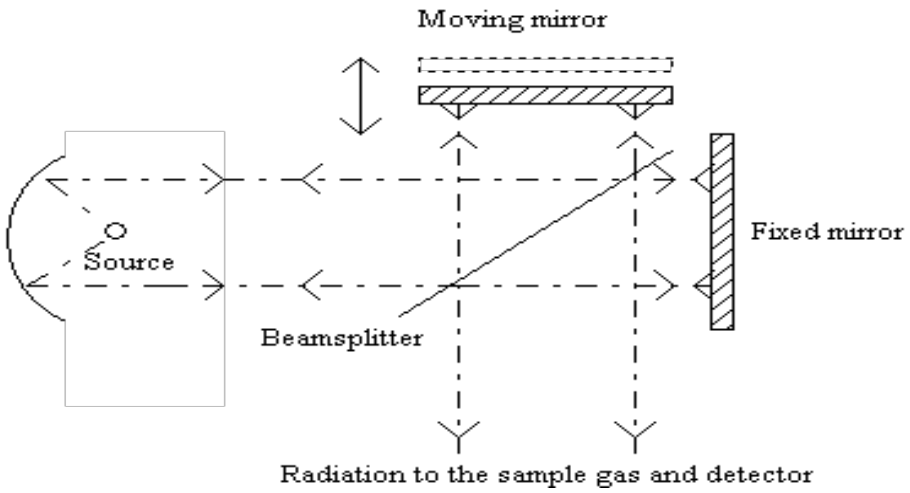


**Figure 2.7 A schematic of FTIR**

The beam described above is generated by starting with a broadband light source-one containing the full spectrum of wavelengths to be measured. The light shines into a Michelson interferometer-a certain configuration of mirrors, one of which is moved by a motor. As this mirror moves, each wavelength of light in the beam is periodically blocked, transmitted, by the interferometer, due to wave interference. Different wavelengths are modulated at different rates, so that at each moment, the beam coming out of the interferometer has a different spectrum. As mentioned, computer processing is required to turn the raw data (light absorption for each mirror position) into the desired result (light absorption for each wavelength). The processing required turns out to be a common algorithm called the Fourier transform (hence the name, Fourier

transform spectroscopy). The raw data is sometimes called an interferogram" (Griffiths and de Hasseth, 2007).

## 2.21Theoretical consideration of coagulation-flocculation Kinetics

The kinetics of Brownian coagulation of mono-dispersed particles at the early stage can be described as in equation (2.1) (Ani *et al.*, 2012),

$$-\frac{dC}{dt} = kC^{\alpha} \qquad 2.15$$

Where C is the concentration of the effluent k = coagulation rate constant, α = order of reaction.

If α=1 equation 2.1 becomes

$$\frac{dC}{dt} = -kC \qquad 2.16$$

Rearranging equation 2.16 and integrating with the limit gives

$$\int_{C_0}^{C_t} \frac{dC}{C} = -k \int_0^t dt \qquad 2.17$$

Solving equation 2.17 gives

$$InC_t = InC_0 - kt \qquad 2.18$$

If α becomes 2 equation 2.15 will be

$$\frac{dC}{dt} = -kC^2 \quad 2.19$$

Also rearranging equation 2.5 and integrating within limit gives

$$\int_{C_0}^{C_t} \frac{dC}{C^2} = -k \int_0^t dt \Rightarrow \frac{1}{C_0} - \frac{1}{C_t} = -kt \Rightarrow \frac{1}{C_t} = \frac{1}{C_0} + kt \quad 2.19b$$

Solving equation 2.19b gives us the coagulation-flocculation half life or period obtained by the following:

At $t_{1/2}$ $[C]_t = ½[C]_0$ substituting this in eq. 2.19b and evaluating it we have

$$t_{1/2} = \frac{1}{K[C]_0} \quad 2.19c$$

Where $C_t$ is the concentration of effluent at time t, $C_0$ is the initial concentration of the effluent at time 0, t is the time and k is αth order coagulation constant. The rate constant is a product of collision efficiency, Ɛ and the Smoluchowaski rate constant of rapid coagulation, $k_R$ (Abel *et al*., 1994)

$$k = \text{Ɛ}k_R \quad 2.20$$

The repulsive colloidal forces and hydrodynamic (viscous) interactions (D) affect the rate at which suspended particles coagulate. The rapid coagulation rate constant is given by (Ani *et al*., 2012)

$$k_R = \frac{4K_BT}{3\eta_0} \quad 2.21$$

Where $K_B$ is the Boltzman constant, T is the absolute temperature and $\eta_o$ is the viscosity of the fluid. Combining equation (2.20) and (2.21) give the following expression

$$k = \frac{4\varepsilon k_B T}{3\eta_o} \quad 2.22$$

It has been shown that Brownian diffusion coefficient (D) has the following expression (Menkiti and Onukwuli, 2011)

$$D = \frac{K_B T}{6\pi\eta_o r} \quad 2.23$$

Making $\eta_o$ the subject of formula in equation (2.23) gives equation (2.24) for the effluent viscosity

$$\eta_o = {K_B T}/{6\pi D r} \quad 2.24$$

Comparing equation (2.22) and (2.24) gives a expression for the collision efficiency as

$$\varepsilon = \frac{k}{8\pi D r} \quad 2.25$$

Combining equation (2.20) and (2.25) give an expression for the Smoluchowski constant

$$k_R = 8\pi r D \quad 2.26$$

An expression for Brownian diffusion coefficient has been shown to be (Menkiti and Onukwuli, 2011)

$$D = \frac{K_B T}{\beta_{BR}} \qquad 2.27$$

The expression for friction factor can be obtained by comparing equation (2.23) and (2.27) to give

$$\beta_{BR} = 6\pi\eta_o r \qquad 2.28$$

The relationship between friction factor ($\beta_{BR}$) and $\alpha th$ order coagulation constant (K) is given below in 2.29 (Menkiti and Onukwuli, 2011)

$$\beta_{BR} = 2k \qquad 2.29$$

Comparing equation (2.28) and (2.29), therefore gives the following

$$\eta_o = \frac{k}{3\pi r} \qquad 2.30$$

Where $\eta_o$ the viscosity of the effluent and r is is the particle radius. As an approximation, the particles radius can be replaced with the radius of the coagulation-flocculation (obtained from sieve measurement) to give the following expression

$$\eta_o^{Nn} = \frac{k}{3\pi r^{Nn}} \qquad 2.31$$

Substituting equation (2.31) into equation (2.21) give the Smoluchwoski-Nnaji constant for rapid coagulation (Nnaji *et al.*, 2013)

$$k_R^{Nn} = \frac{4K_BT}{3\eta_o^{Nn}} \qquad 2.32$$

Subsequently, the Smoluchowski rate constant can be replace by the Smoluchowski-Nnaji rate constant in equation (2.20) to give an expression for collision efficiency (Nnaji *et al*., 2013)

$$\varepsilon^{Nn} = \frac{K}{K_R^{Nn}} \qquad 2.33$$

# CHAPTER THREE

# MATERIALS AND METHODS

## 3.1 Materials

### 3.1.1 Samples collection

The shells of *Archachatina marginata*, (land snail), *Tympanotonus fuscatus, (*periwinkle)and *Mercenaria mercenaria*, (hard clam) were collected from Ochanja Market at Onitsha, Anambra State. Paint industry effluent was obtained from Hall Mark Paint Industry MCC, Onitsha. These shells were identified by Dr. T.C. Mogbo of Zoology Department, Nnamdi Azikwe University, Awka.

### 3.1.2 Chemicals

Sodium hydroxide, Sodium thiosulphate, Hydrochloric acid, Combined reagent, Buffer solution, 1% starch solution, Phenolphthalein indicator, EDTA, SolochromeBlack-T-indicator, Phenol disulphonic acid, Distilled water,Barium chloride, Ammonium solution, Silver nitrate, Manganoussulphate, Potassium dichromate, Ammonium persulphate, Bromocresol, Salicylic acid, Sulphuric acid, Alkaline Iodide Azide, Selenium powder. All the chemicals listed above were of analytical grade and sourced from Bridge Head Market, Onitsha.

## 3.2 Apparatus

Beakers, crucible, density bottle, measuring cylinder, oven filter papers, pipette, burette, conical flasks, stirring rod, magnetic stirrer model Search tech. 78HW-1, UV/Vis spectrophotometer model Apel PD-3000UV, FTIR spectrometer model Agilent tech. Cary 630, XRD spectrometer, XRF spectrometer, SEM model Phenom prox MVE016477830, digital weighing balance Ohaus model CP 413, electrical conductivity meter Model DDS-307, Turbidimeter Lab. Tech. model 038, pH meter Hanna model HI991300, digital weighing balance model Cp 413, max-4100g and Viscometer model NDJ-55.

## 3.3 Methods

### 3.3.1 Preparation of the shells materials

The shells of the *Archachatina marginata* AM, (land snail), *Tympanotonus fuscatus TF, (*periwinkle) and *Mercenaria mercenaria* MM were washed with water to remove all the dirt and sand. They were dried for two weeks under sunshine and ground into particles sizes and sieved; 1.18 µm for MM, AM and TF respectively.

## 3.4 Determination of the pH of the coagulants

For each coagulant, 1.0 g was soaked in 50 mL of distilled water in separate beakers stirred for 24 hrs, filtered and the final pH was measured (Dawolu and Akpomie, 2014).

### 3.5 Specific Surface Area

Exactly 0.5 g of each coagulant was acidified with 0.1M HCl to a pH of 3.0-3.5 in beakers. The volume was made up to 50 mL of distilled water after addition of 10g of NaCl. The titration was carried out with standard 0.1 M NaOH in a thermostatic bath at 298 $K \pm 0.5$ to pH 4.0, then to pH 9.0. The volume (V) required to raised the pH from 4-9 was noted and the surface area computed using equation. 3.1 (Unabonah *et al*., 2008).

$$S(m^2/g) = 32V - 25 \qquad 3.1$$

### 3.6 pH of Zero point charge ($pH_{zpc}$)

A 50mL of 0.01 M KCl were prepared and added into a series of glass bottles with corks. The pH values of the solution were adjusted to the range 2 and 12 at interval of 0.5 using either 0.01 M HCl or 0.01 M NaOH. The pH of initial solution was measured; 0.15 g of each sample was added to the bottles. The set ups were shaken for 48hrs and the pH values measured (Unabonah *et al*., 2009).

### 3.7 Determination of densities.

#### 3.7.1 Bulk density

A measuring cylinder was weighed and recorded as $w_1$, MM coagulant was put into it and the weight of a sample was taken as $w_2$, total weight = $w_1 + w_2$ and volume of the

sample of the measuring cylinder was noted as $v_o$. Therefore bulk density is $w_1 + w_2/v_o$ (Dada *et al*., 2012; ANL, 2016). This was repeated for all the coagulants.

### 3.7.2 True density

Eureka measuring cylinder was used in this measurement. A known mass of the MM coagulant was put in measuring cylinders and known volume of distilled water was added to it. The volume of water displaced is noted as $V_1$ obtained from initial volume of water added – final volume in the cylinder after displacement of water (WHO, 2012). . The experiment was repeated to obtain the true densities of other coagulants.

$$True\ density = \frac{mass\ of\ the\ sample}{V_1} \qquad 3.2$$

And same procedure was repeated using other coagulants.

### 3.7.3 Tap density

A known mass of MM coagulant was put in a measuring cylinder and tapped until a constant volume was obtained and recorded as $V_{tap}$ (WHO, 2012). The experiment was repeated with other coagulants to obtain their tap densities.

$$Tap\ density = \frac{mass\ of\ the\ sample}{V_{tap}} \qquad 3.3$$

The following can be calculated from the densities as follows:

$$porosity = 1 - \frac{D_{tap}}{D_{true}}\ x100 \quad 3.4$$

where $D_{tap}$ and $D_{true}$ are the tap density and the true density.

$$Hausner\ ratio\ (HR) = \frac{D_{tap}}{D_{bulk}}, \quad 3.5$$

$$Carr's\ index(CI) = \frac{D_{tap} - D_{bulk}}{D_{tap}} \times 100 \quad 3.6$$

### 3.8 Modification of the coagulants

For each coagulant, 150 g were weighed into different beakers. It was demineralised by adding 100 mL of 2 M HCl and heated for 2 hrs in a water bath at 60$^{o}$C, filtered and rinsed with distilled water, deproteinized with 50 mL of 2 M NaOH and heated again for 16hrs at 70$^{o}$C, filtered and rinsed with distilled water. Thereafter, kept in solution containing chloroform, methanol and water (ratio of 1:2:4) for 1hr for further decolourization, finally dried at 60$^{o}$C (Kaya *et al*., 2014).

### 3.8 Coagulation-Flocculation procedure

Coagulation-Flocculation experiment was studied using three factors; effect of settling time from 10 mins - 30 mins, pH from 2-10 and effect of dosage from 100 mg/L-500 mg/L. 100 mg of each coagulant was weighed into 250mL beakers and 100 mL of desired pH effluent was added into them. Desired pH was obtained by using 2M HCl and 2M NaOH. For example the pH of the effluent was made to be at pH 2 using 2 M

HCl solutions. The content of the beaker was stirred for 2 minutes of rapid mixing (120 rpm) and 20 mins of slow mixing (10 rpm) with a magnetic stirrer, and then left undisturbed for 20 mins. It was filtered and the filtrate was subjected to colour removal analysis using UV/VIS spectrophotometer. The maximum absorbance of wavelength ($\lambda_{max}$) used for paint Industry effluent was 619 nm. The procedure was repeated using design matrix of Reponse surface methodology by Box Behnken, in Table 3.2. Finally, all the filtrates were mixed together and physicochemical analysis conducted on them to determine the level of treatment with each coagulant.

### 3.10 Coagulation-flocculation kinetics experiment

The coagulation-flocculation experiment was carried out using varying dosages of 100 mg/L, 200mg/L, 300 mg/L, 400 mg/L, 500 mg/L and time of 5 mins-30 mins at constant pH obtained from optimization that is pH of 2 for MM, AM and TF coagulants While for modified coagulants pH of 6, 2 and 6 for MMM, MAM and MTF respectively, all at room temperature. The results obtained were fitted into $1^{st}$ order and $2^{nd}$ order reaction kinetics, followed by calculations of the kinetics parameters.

### 3.9 Response Surface Methodology

The Design Expert 10 (State-Ease, Inc., Minneapolis, MN, USA) software was used for regression and graphical analyses of the data obtained. The three level box-Behnken experimental designs with categorical factor was employed to optimize the coagulation-

flocculation efficiency of the three samples of snail shells namely *Archachatina marginata* (land snail), *Tympanotonus fuscatus (*periwinkle) and *Mercenaria mercenaria (*hard clam).

**Table 3.1 Levels and range of variables tested in $2^3$Box behnken design (BBD)**

| Factor | Low level (-1) | Medium level (0) | High level (+1) |
|---|---|---|---|
| Dosage (A) | 100 mg/L | 300 mg/L | 500 mg/L |
| pH (B) | 2 | 6 | 10 |
| Time (C) | 10 mins | 20 mins | 30 mins |

**Table 3.2 Design Matrix of Box Behnken of 17 runs experiment**

| Runs | Factor 1 Dosage(A) (mg/L) | Factor 2 pH (B) | Factor 3 Time(C) (mins) | MM Response(%) | AM Response (%) | TF Response (%) | MMM Response(%) | MAM Response(%) | MTF Response(%) |
|---|---|---|---|---|---|---|---|---|---|
| 1 | 100.00 | 10.00 | 20.00 | | | | | | |
| 2 | 500.00 | 6.00 | 30.00 | | | | | | |
| 3 | 300.00 | 10.00 | 10.00 | | | | | | |
| 4 | 100.00 | 2.00 | 20.00 | | | | | | |
| 5 | 500.00 | 10.00 | 20.00 | | | | | | |
| 6 | 300.00 | 6.00 | 20.00 | | | | | | |
| 7 | 500.00 | 2.00 | 30.00 | | | | | | |
| 8 | 100.00 | 6.00 | 10.00 | | | | | | |
| 9 | 100.00 | 6.00 | 30.00 | | | | | | |
| 10 | 300.00 | 2.00 | 30.00 | | | | | | |
| 11 | 300.00 | 6.00 | 20.00 | | | | | | |
| 12 | 300.00 | 2.00 | 10.00 | | | | | | |
| 13 | 300.00 | 6.00 | 20.00 | | | | | | |
| 14 | 300.00 | 6.00 | 20.00 | | | | | | |
| 15 | 300.00 | 10.00 | 30.00 | | | | | | |
| 16 | 500.00 | 6.00 | 10.00 | | | | | | |
| 17 | 300.00 | 6.00 | 20.00 | | | | | | |

The design was composed of three levels (low, medium, and high) obtained by coding of the variables and this was done according to the following

equation:$x_i = \frac{X_i - X_0}{\Delta X_i}$ 3.7

here $x_i$ is the dimensionless value of an independent variable, $x_i$ is the real value of an independent variable, $x_0$ is the real value of an independent variable at the center point, and $\Delta x_i$ is the step change of the real value of the variable i corresponding to a variation of a unit for the dimensionless value of the variable i. The number of experiments (N) needed for the development of Box–behnken matrix is defined as N =2k(k-1) + r, where (k) is the factor number and (r) is the replicate number of the central point. The totals of 17 runs were carried out to optimize the chosen variables such as, dosage, pH and settling time. The three independent variables were denoted as A, B and C respectively. The range and the level used in this experiment are listed in Table 3.1 while Table 3.2 is the designed matrix of Box behnken.

### 3.10 Determination of Alkalinity

A 50 mL burette was rinsed severally with 0.02 N HCl, and was filled with it. Exactly 100 mL of the effluent to be was measured into a 250 mL Erlenmeyer flask. It was titrated to a bromocresol green (pH = 4.5) end point (Ademoroti, 1996)..

Alkalinity is expressed in terms of milligrams of calcium carbonate per liter.

$$Alkalinity = \frac{mL\ HCl\ tritrant\ x\ normality\ of\ HCl\ x\ 50000}{mL\ of water\ sample} \quad 3.8$$

### 3.12 Biochemical Oxygen Demand Determination by Winkler method

#### 3.12.1 Dissolved oxygen

The stopper was carefully removed from the effluent bottle and added into 1mL manganous sulphate solution followed by 1 mL alkaline - iodide -azide solution. When introducing various reagents into the full bottle of sample, the tips of the pipette was wiped below the surface of the liquid. The stopper was carefully replaced after each addition so as to avoid inclusion of air bubbles. The content was thoroughly mixed by inversion and rotation until clear supernatant water was obtained. 1 mL of concentrated sulphuric acids was added with the tip of the pipette below the level of solution and again the stopper was replaced. Mixing was enhanced by rotation until the precipitation completely dissolved. A 100 mL of the solution was taken into a 250 mL of conical flask and immediately titrated it against standard sodium thiosulphate (0.025 mol/L) using freshly prepared starch solution as the indicator and it was added when solution becomes pale yellow). The titration was repeated.

$$D.O = \frac{mole\ of\ titrant\ x\ normality\ of\ \ the\ titrant\ x\ 8000}{mL\ of the\ sample\ used} \qquad 3.9$$

The general equation for the determination of a BOD value is:

BOD (mg/L) = $D_1 - D_2$

Where $D_1$ =initial DO of the sample, $D_2$ = final DO of the sample after 5 days, and P = decimal volumetric fraction of sample used.

If 100 mL of effluent are diluted to 300 mL, then P= 0.33. Note that if no dilution was necessary, P = 1.0 and the BOD is determined by $D_1 - D_2$ (Ademoroti, 1996).

### 3.13 Determination of Chemical Oxygen Demand

A 15 mL of the effluent was added into a 250mL beaker, 2.5mL standard 5% $K_2Cr_2O_7$ digestion reagent was added slowly and 3.5mL of concentrated sulphuric acid reagent was introduced through side of the tubes. It was corked and shaken to obtain a homogenous mixture, after was transferred into a water bath. Distilled water was added to make the volume to 50 mL. Finally, it was titrated with 0.05 M ferrous ammonium sulphate solution (FAS) (Morsh Salt)

$$COD\ in\ mg/L\ = \frac{A-Bx8000}{mL\ sample} \qquad 3.10$$

A = Titre of the blank, B = Titre of the sample, M = Molarity of the FAS (0.05M)

**3.14 Determination of Phosphate**

Exactly 100 mL of the homogenized and filtered effluent was pipette into a conical flask. The same volume of distilled water (serving as control) was also pipette into another conical flask. A 1 mL of 18 M $H_2SO_4$ and 0.89 g of ammonium persulphate were added to both conical flasks and gently boiled for 1 ½ hrs, keeping the volume of 25-50 $cm^3$ with distilled water. It was then cooled; one drop of phenolphthalein indicator was added and after neutralized to a faint pink colour with 2M NaOH solution. The pink colour was discharged by drop wise addition of 2 M HCl, and the solution made up to 100 mL with distilled water. For the colorimetric analysis, 20 mL of the effluent was pipette into test tubes, 10 mL of the combined reagent added, shaken and left to stand for 10 mins before reading the absorbance at 690 nm on a

spectrophotometer, using 20 mL of distilled water plus 1mL of the reagent as reference (APHA, 1998).

### 3.14.1 Method for Calibration

Standard phosphate solution: Exactly 219.5 mg of dried potassium hydrogen phosphate was dissolved in distilled water and made up to 1000 mL, where 1 mL is 50.0 μg. of phosphate. 10 mL of the stock solution was made up to 1000 mL to give 1 mL is to 0.05 mg. Standards of strength ranging from 0 (blank) to 0.05 mg/L at intervals of 0.01 mg was prepared by diluting the stock with distilled water (APHA, 1998).

$$Conc.ofsample = \frac{Abs\ of\ sample\ x\ conc\ of\ standard}{Abs\ of\ std} \quad 3.11$$

### 3.15 Determination of Chloride

A 100 mL of the clear effluent was pipette into an Erlenmeyer flask and the pH adjusted to 7-10 with either $H_2SO_4$ or NaOH solution. Then 1mL of $K_2Cr_2O_7$ indicator solution was added and titrated with standard solution of $AgNO_3$ in a permanent reddish brown colouration. The $AgNO_3$ titrant was standardized and a reagent blank established. A blank of 0.2-0.3mL is always used for the method (APHA, 1998).

Chloride Conc. = Titre value (x) x 10 = mg/L 3.12

### 3.16 Determination of Sulphate

A 250 mL of the effluent was evaporated to dryness on a dish. The residue was moisten with a few drop of concentration HCl and 30 mL distilled water was added. This was boiled and then filtered. The dish was rinsed and the filter paper washed with several

portions of distilled water and both filtrate and washings added together. This was heated to boiling and then 10 mL of 10% $BaCl_2$ solution was added, drop by drop with constant stirring. The mixture was digested for about 30 minutes, filtered and the filter paper washed with warm distilled water. It was then ignited, cooled and weighed in an already weighed crucible (APHA, 1998).

mg/L $SO_4^{2-}$ = mg $BaSO_4$ x 411.5 mLof effluent sample 3.13

**3.17 Determination of Nitrate**

Nitrate was determined using PD303 UV spectrophotometer (APHA,1998).

Exactly 50 mL of the effluent was pipetted into a porcelain dish and evaporated to dryness on a hot water bath. A 2 mL of phenol disulphonic acid was added to dissolve the residue by constant stirring with a glass rod. Concentrated solution of sodium hydroxide and distilled water was added with stirring to make it alkaline. This was filtered into a Nesslers tube and made up to 50 mL with distilled water, the absorbance was read at 410 nm using a spectrophotometer after the development of colour. The standard graph was plotted by taking concentration along X – axis and the spectrophotometeric readings (absorbance) along Y-axis. The value of nitrate was found by comparing absorbance of sample with the standard curve and expressed in mg/L.

$$Conc.ofnitrate = \frac{Abs\ of\ sample\ x\ conc.\ of\ std}{Abs\ of\ std} \quad 3.14$$

### 3.18 Determination of Total solids

Total solids is the term applied to the material residue left in the vessel after evaporation of the water sample and its subsequent drying in an oven at a temperature of 103-105$^{o}$C. Total solids include total suspended solids and total dissolved solids (APHA, 1998).

A 100 mL of the effluent was measured into a pre-weighed dish and evaporated to dryness at 103$^{o}$C on a steam bath. The evaporated sample was dried in an oven for about an hour at 105$^{o}$C, cooled in a desiccator and recorded for constant weight.

### 3.19 Determination of Total suspended Solids

Total suspended solid was determined by subtracting the result of total dissolved solids from total solid.

Total solids (TS) – Total dissolved solids (TDS) = Total Suspended solids (TSS).

### 3.20 Total Hardness using titration Method

A 50 mL of effluent was put into a beaker**;** 1 mL of 50% buffer solution of $NH_3$ was added**.** Exactly 3 drops of solocrome black tea indicator was also added and stirred properly. The mixture was titrated with 0.01 EDTA solutions until the colour changed from wine red to pure blue with no bluish tinge remaining.

$$Total\ hardness\ =\ (mg/CaCO_3)\ \ =\ \frac{Volume\ of\ titrate\ x\ 1000}{Volume\ of\ sample} \qquad 3.15$$

### 3.21 Determination of Total Dissolved Solids

Total dissolved solid was determined using APHA 2510A, model TDS 139 tester (APHA; 1998) .The fibre filter disc was prepared by placing its wrinkled side up, in the filtration apparatus. Vacuum was applied and the disc washed with three successive 20 mL washings of distilled water. Continuous suction was then applied to remove all traces of water. A clean evaporating dish was heated to 180 ± 2$^{o}$C in an oven for 1 hr, Cooled and stored in a desiccator until needed. It was weighed immediately before use. An effluent volume was chosen to yield between 2.5 and 200 mg dried residue. A 50 mL of well mixed sample was filtered through the glass-fibre filter; it was washed with three successive 10 mL volumes of distilled water, allowing complete draining between washings. Suction was continually applied for about 3 mins after filtration is complete. Filtrate was transferred to a weighed evaporating dish and evaporated to dryness on a steam bath. The evaporating dish was finally dried for at least 1hr in an oven at 180 ± 2$^{o}$C, cooled in a desiccator and weighed.

$$TDS = \frac{(A-B)x103mg/L}{sample\ volume\ in\ mL} \qquad 3.16$$

Where A = weight of dish + solids (mg), B = weight of dish before use (mg)

### 3.22 Determination of pH

pH was measured by Electrometric Method using Laboratory pH Meter, Hanna model HI991300.The electrode was rinsed with distilled water and blot dry. After, it was rinsed in a small beaker with a portion of the effluent. Sufficient amount of the effluent

was poured into a small beaker to allow the tips of the electrodes to be immersed to a depth of about 2 cm. The electrode was at least 1cm away from the sides and bottom of the beaker. The temperature adjustment dial was adjusted accordingly. The pH meter was turn on and the pH of sample recorded.

### 3.23 Determination of Electrical Conductivity

Analysis was carried out according to APHA 2510 B guideline, Model DDS-307 (APHA, 1998). The conductivity cell was rinsed with at least three portions of the effluent. The temperature of the effluent was then adjusted to 20 ± 0.1$^{o}$C.The conductivity cell containing the electrodes was immersed in sufficient volume of the effluent. The conductivity meter was turned on and the conductivity of the effluent recorded.

### 3.24 Determination of Carbohydrate

(Differential method) 100 – (%Protein + %Moisture + %Ash + %Fat + %Fibre) 3.17

### 3.25 Determination of Ash content

Empty platinum crucible was washed, dried and the weight noted. Exactly 2 g of coagulant was weighed into the platinum crucible and placed in a muffle furnace at 500$^{o}$C for 3 hours. The samples was cooled in desiccators after burning and weighed.

Calculations: $\% \, Ash \, content = \frac{W_3 - W_1}{W_2 - W_1} x \frac{100}{1}$ 3.18

Where

$W_1$ = weight of empty platinum crucible

$W_2$ = weight of platinum crucible and sample before burning

$W_3$ = weight of platinum and ash.

**3.26 Determination of Crude fat (Soxhlet Fat Extraction Method)**

A 250 mL clean boiling flask was dried in an oven at $110^0$C for about 30 minutes. It was transferred into a dessicator and allowed to cool**.** The boiling flask was filled with 300 mL of petroleum ether (boiling point 40 - $60^0$C) and 100 g of the MM coagulant**.** The extraction thimble was plug lightly with cotton wool**.** It was refluxed for about 6 hours with a sohlex extractor and the thimble was removed with care to allow petroleum ether to be collected in the top container of the set-up and drained into a container for re-use. The boiling flask that is free of petroleum ether was removed and dried at $110^0$C for 1hour. Finally, it was transferred from the oven into desiccator and allowed to cool and weighed. The experiment was repeated with other coagulants.

**3.27 Determination of Crude Proteins**

Principle: The method is the digestion of sample with hot concentrated sulphuric acid in the presence of a metallic catalyst. Organic nitrogen in the sample is reduced to ammonia. This is retained in the solution as ammonium sulphate. The solution is made alkaline, and then distilled to release the ammonia. The ammonia is trapped in dilute acid and then titrated (AOAC, 1984). Exactly 0.5 g of MM coagulant was weighed into a 30 mL kjehdal flask gently to prevent the sample from touching the walls of the side of flask and then the flask were stoppered, shake and 0.5 g of the kjedahl catalyst

mixture was added. The mixture was heated cautiously in a digestion rack under fire until a clear solution appeared. The clear solution was allowed to stand for 30 minutes in order to cool. After cooling, 100 mL of distilled water was added to avoid caking and then 50 mL was transferred to the kjedahl distillation apparatus. A 100 mL receiver flask containing 5 mL of 2% boric acid and indicator mixture containing 5 drops of Bromocresol blue and 1 drop of methlene blue was placed under a condenser of the distillation apparatus so that the tap was 20 cm inside the solution. A 5 mL of 40% sodium hydroxide was added to the digested sample in the apparatus and distilled immediately until 50 drops gets into the receiver flask, after which it was titrated to pink colour using 0.01 N hydrochloric acid. The procedure was repeated using other coagulants.

$$\%\ Nitrogen\ =\ Titre\ value\ x\ 0.01\ x\ 14\ x\ 4 \qquad 3.19$$

$$\%\ Protein\ =\ \%\ Nitrogen\ x\ 6.25 \qquad 3.20$$

**3.28 Determination of Moisture content**

A petri-dish was washed and dried in the oven and 2 g of MM coagulant was weighed into petri dish. The weight of the petri dish and sample was noted before drying as $W_1$. The petridish and sample were put in the oven and heated at $100^0$C for 1 hr the result noted. The content of the petridish was again heated for another 1 hr until a steady result is obtained and the weight was noted. The drying procedure was continued until a constant weight was obtained noted as $W_2$. This procedure was repeated using other coagulants.

$$\%\ moisture\ content = \frac{W_1 - W_2}{Weight\ of\ sample} x \frac{100}{1} \quad 3.21$$

Where $W_1$ = weight of petridish and sample before drying.

$W_2$ is weight of petridish and sample after drying.

**3.29 Determination of Crude Fibre**

A 2 g portion of MM coagulant was de-fatted with petroleum ether. It was boiled under reflux for 30 minutes with 200 mL of 1 M of $H_2SO_4$. The solution was filtered using linen or several layers of cheese cloth on a fluted funnel, then washed with boiling water until the washing was no longer acidic. The residue was transferred to a beaker and boiled for 30 minutes with 200 mL of a solution containing 1.25 g of carbonate free NaOH per 100 mL. Final residue was filtered through a thin but close pad of washed and ignited asbestos in a Gooch crucible, dried in an electric oven and weighed, incinerated, cooled and weighed again. The loss in weight after incineration x 100 is the weight of the crude fibre.

$$\%\ Crude\ fibre\ = \frac{weight\ of\ fibre\ x100}{Weight\ of\ sample} \quad 3.22$$

# CHAPTER FOUR

# RESULTS AND DISCUSSION

## 4.1 Physical characteristics of unmodified coagulants

Table 4.1 shows the physical properties of the unmodified coagulants of *Mercenaria mercenaria* (MM), *Archachatina marginata (AM)* and *Tympanotonus fuscatus, (TF)*. The parameters listed in the Table 4.1 are good indicators of flowability rate. Good flow of powder helps to avoid the extensive costs and time involved in unloading powders that will not flow out of storage containers as well as help to achieve the best formulation and improve the quality and consistency of the product (Mahmud, 2013).

**Table 4.1: Physical properties of the MM, AM and TF coagulants**

| **Parameters** | **MM coagulant** | **AM coagulant** | **TF coagulant** |
|---|---|---|---|
| Bulk density $g/cm^3$ | 1.516 | 1.056 | 1.627 |
| Tap density $g/cm^3$ | 1.724 | 1.192 | 1.786 |
| True density $g/cm^3$ | 3.125 | 2.782 | 4.383 |
| Carr's Index | 12.065 | 11.409 | 8.903 |
| Porosity (%) | 44.832 | 57.153 | 59.252 |
| Hausner ratio | 1.137 | 1.129 | 1.098 |
| Surface area $(m^2/g)$ | 55.000 | 58.000 | 151.000 |
| pH | 7.39 | 7.70 | 7.84 |

**Table 4.2 Standard values for relationship between Carr's index, Hausner ratio and flowability**

| Carr's index | Flow character | Hausner ratio |
|---|---|---|
| <10 | Excellent | 1.00-1.11 |
| 11-15 | Good | 1.12-1.18 |
| 16-20 | Fair | 1.19-1.25 |
| 21-25 | Passable | 1.26-1.34 |
| 26-31 | Poor | 1.35-1.45 |
| 32-37 | Very poor | 1.46-1.59 |
| >38 | Very very poor | >60 |

**Copley,2008)**

They also measure the powder's ability to settle and permit an assessment of the relative importance of interparticulate interactions. In a free-flowing powder, such interactions are less significant, and the bulk and tap densities would be closer in value. For poorer flowing materials, there are frequently greater interparticle interactions and a greater difference between the bulk and tap densities will be observed ((Mahmud, 2013). As can be inferred from the Table 4.1 the bulk and tap densities of the coagulant are closer in values, for MM coagulant the difference between the bulk and tap density is (0.208), AM (0.136) and TF (0.159) respectively showing that they can settle at the bottom of the container very easily. These differences also reflected in the Compressibility Index or Carr's index/Hausner Ratio (De Campos and Ferreira, 2013). Table 4.2 is the standard values for relationship between Carr's index, Hausner ratio and flowability, comparing Table 4.1 and 4.2 it can be observed that all the coagulants have good flowability since all the parameters calculated such as

bulk and tap densities, Carr's index and Hausner ratio were all within the standard value of a material having a good flow character. Porosity result of the three coagulants are 44.832, 57.153, 59.252% for MM, AM, and TF respectively. Porosity measures the void (i.e. "empty") spaces in a material. Increase in the number of pores enhances coagulation. Surface area of the coagulant increases in the same manner as porosity in the three coagulants with MM having surface area of 55.000 $cm^2/g$, AM 58.000 $cm^2/g$ and TF 151.000 $cm^2/g$. Again decrease in particle size increases the contact area between the particles, thereby decreasing the cohesive forces and the Carr's index hence good flow rate and the colloid particles has more chances of attaching themselves on the coagulant. (Ganesan *et al*., 2008).

**4.2 Result of physical characteristics of the modified coagulants**

Table 4.3 is the Physical parameters of modified coagulants. The bulk and tapped densities of MMM coagulant are 1.185 $g/cm^3$ and 1.333 $g/cm^3$, for MAM coagulant 1.085 $g/cm^3$ and 1.176 $g/cm^3$, while for MTF 1.261 $g/cm^3$ and 1.381 $g/cm^3$ respectively. Comparing result of Table 4.3 with Table 4.2, it can be deduced that the modified *Merceneria merceneria* (MMM) has the least flow character with Carr's index of 11.02 and Hausner ratio of 1.125, this is followed by modified *Archachantina marginata* (MAM) with the Carr's index of 10.289 and Hausner ratio of 1.114, and the greatest

among all in terms of flow character is modified *Tympanotous fuscatus (*MTF) having Carr's index of 8.689 and Hausner ratio of 1.095.

**Table 4.3: Physical parameters of modified coagulants**

| **Parameters** | **MMM coagulant** | **MAM coagulant** | **MTF coagulant** |
|---|---|---|---|
| Bulk density $g/cm^3$ | 1.185 | 1.055 | 1.261 |
| Tapped density $g/cm^3$ | 1.333 | 1.176 | 1.381 |
| True density $g/cm^3$ | 3.667 | 5.000 | 6.667 |
| Carr's Index | 11.102 | 10.289 | 8.689 |
| Porosity (%) | 63.648 | 76.480 | 79.286 |
| Hausner ratio | 1.125 | 1.114 | 1.095 |
| Surface area $(m^2/g)$ | 64.000 | 83.000 | 163.000 |
| pH | 8.250 | 7.070 | 8.480 |

This shows that these modified coagulants have excellent flowabilty and settle ability that is required in this study. There is an improvement in the surface area and the porosities of the three modified coagulants. The porosity and surface area increase in this order, MMM (63.648% and 64.000 $m^3/g$) < MAM (76.480% and 83.000 $m^3/g$) < MTF (79.286% and 163.000 $m^3/g$). Increase in the number of pores and surface area enhances coagulation (Ganesan *et al*., 2008).

**Table 4.4: Proximate composition of the unmodified coagulants**

| Parameters | MM coagulant | AM coagulant | TF coagulant |
|---|---|---|---|
| Fat (%) | 7.692 | 5.847 | 8.637 |
| Crude protein (%) | 2.800 | 2.100 | 3.500 |
| Crude fibre (%) | 15.680 | 15.200 | 5.900 |
| Carbohydrate (%) | 52.171 | 52.756 | 54.017 |
| Ash content (%) | 20.960 | 23.700 | 27.498 |
| Moisture content (%) | 0.697 | 0.397 | 0.448 |

### 4.3 Proximate analysis of unmodified coagulants

Table 4.4 is the proximate composition of the three coagulants. It could be inferred from the Table that these coagulants contained low moisture content in order of MM(0.697%)<TF(0.448%)<AM(0.397%). The moisture content of any sample is an index of its water activity and is used as a measure of stability and susceptibility to microbial contamination (Ajayi, *et al*., 2014). High amount of moisture in a sample makes them vulnerable to microbial attack, hence spoilage. Therefore, these coagulants have high shelf life and can be stored for a long time. Ash content of the three coagulants increases in order of MM(20.960%)<AM(23.700%)<TF(27.498%). Ash content measures mineral content of a material, the higher the ash content, the higher the minerals found in that material (Ajiboye, 2013). The ash content is also an indication of the presence of carbon compounds and inorganic components in the form

of salts and oxides (Usman, 2006) in material. Percentage of carbohydrate decreases in order of TF (54.017)>AM(52.756)>MM(52.171), while % of crude fibre MM(15.680)>AM(15.200)>TF(5.9). Again the three coagulants contain highest percentage of carbohydrate followed by crude fibre, fats and the least is protein. This result agrees fairly well with the work of Jatto *et al*., (2010) on proximate analysis of the land snail shells, where he found that *Archachatina marginata (AM)* shell analyzed contained highest percentage of carbohydrate > Ash content >fibre>protein.

**Table 4.5: Proximate composition of the modified coagulants**

| **Parameters** | **MMM coagulant** | **MAM coagulant** | **MTF coagulant** |
|---|---|---|---|
| Fat (%) | 2.794 | 3.099 | 7.631 |
| Crude protein (%) | 2.100 | 1.400 | 2.100 |
| Crude fibre (%) | 4.650 | 12.800 | 6.770 |
| Carbohydrate (%) | 64.666 | 63.389 | 58.899 |
| Ash content (%) | 24.240 | 18.300 | 23.350 |
| Moisture content (%) | 1.550 | 1.111 | 1.250 |

### 4.4: Proximate analysis of the modified coagulants (chitosan)

Table 4.5 depicts the proximate composition of the modified coagulants. It could be depicted from the Table that these modified coagulants contained low fat, protein and crude fibre compared with the unmodified coagulants in Table 4.4 while there is a general increase in carbohydrate, ash and moisture content of the modified coagulant. The increasing order in which they contained carbohydrate is MTF(58.899%)<

MAM(63.389%) <MMM(64.666%). For fibre content, MAM(4.650%) < MTF(6.770%) < MMM(12.800%), for Ash content MMM(24.240%)>MTF(23.350%)>MAM(18.300). In % fat this trend MTF>MAM>MMM is observed. Crude protein follows this trend MAM>MMM=MAM. This behaviour may be attributed to the acidification and alkalinization of these coagulations which increases both the $H^+$ and $OH^-$ ions in the coagulants and also partial deacetylation of the Chitin.

**4.5 Result of pH of zero charge of the unmodified coagulants**

Figures 4.1a-c show the result of point of zero charge (pzc) which is the pH at which a coagulant surface has net neutral charge. It is the value obtained at the intersection of the initial pH (x-axis) with the pH initial –pH final = 0 line (y-axis). In Figures 4.1a-c, it can be observed that $pH_{pzc}$ of MM, AM and TF are 7.800, 7.600 and 7.480 respectively. At pH below this pzc the coagulant surface will have positive charge surface and anion can attach on it while at pH above this pzc, it will have a negative charge surface and cation can attach on it (Dong-su, 2003, Ria, 2013).

(a)

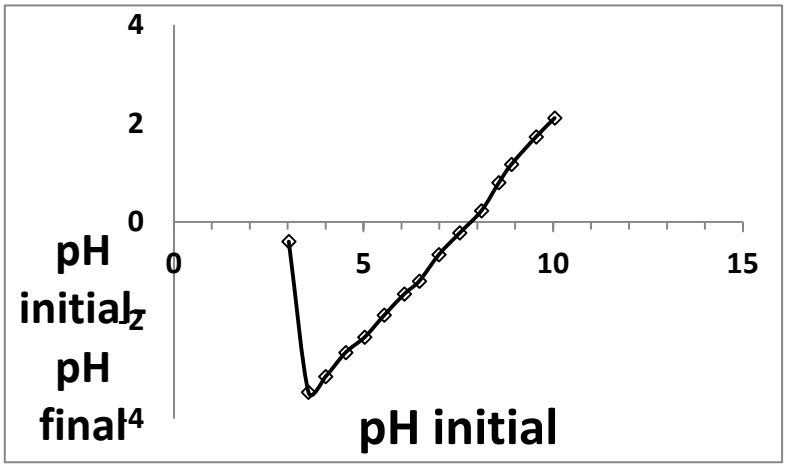

(b)

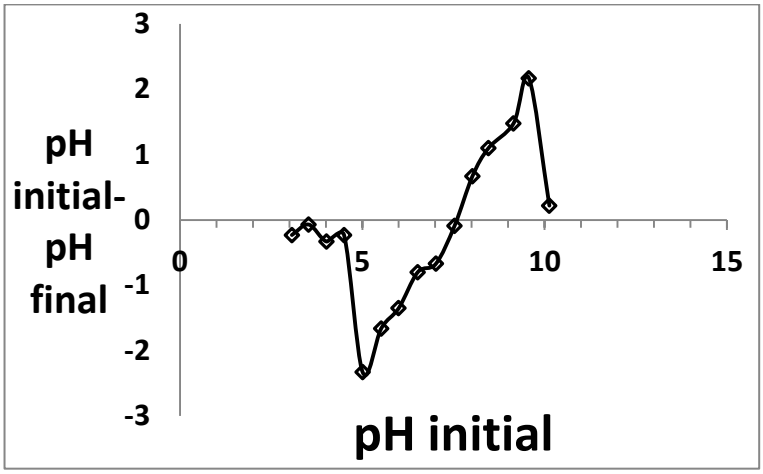


( c)

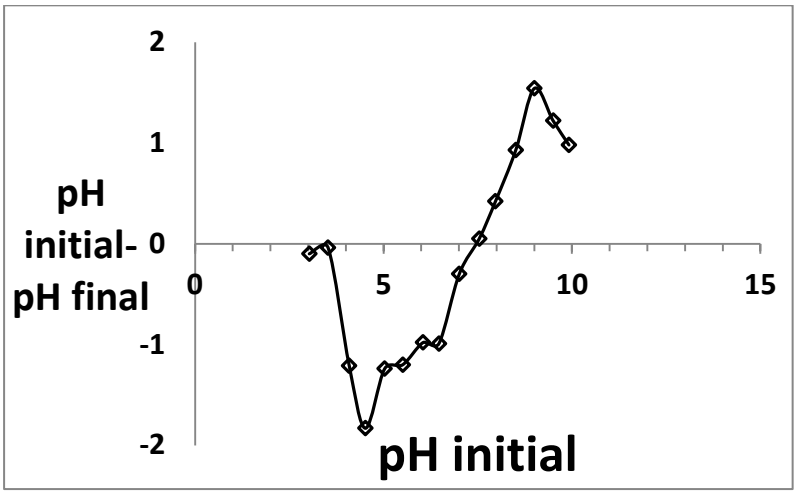


**Figure 4.1: Point of zero charge for (a) MM, (b) AM and (c) TF**

## 4.6 pH of zero point charge (pHzpc) of modified coagulants

Figures 4.2a-c are the result of zero point charge. In Figures 4.2a-c, it can be observed that $pH_{pzc}$ of MMM, MAM and MTF are 7.700, 7.800 and 7.900 respectively. This means that at pH below this pzc, the coagulant surface will have positive charge and anion can attach on it while at pH above this pzc, these coagulants surface will have a negative charge and cation can attach on it (Dong-su, 2003, Ria, 3013).

(a)

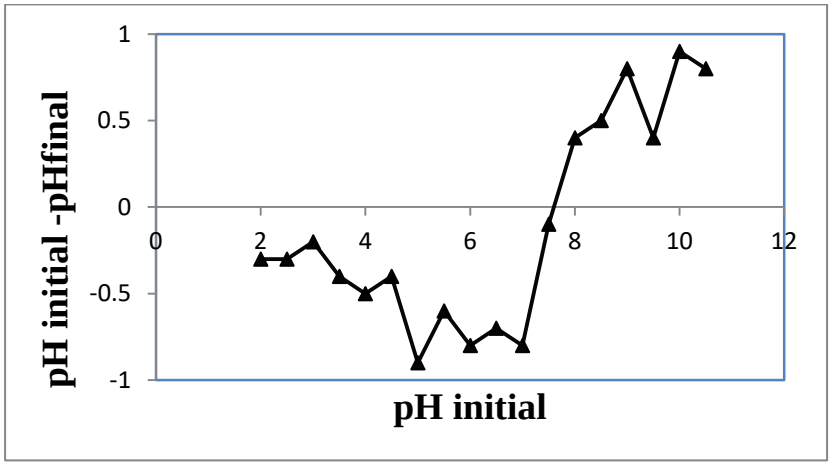


**Figure 4.2a: Point of zero charge of MMM coagulant**

(b)

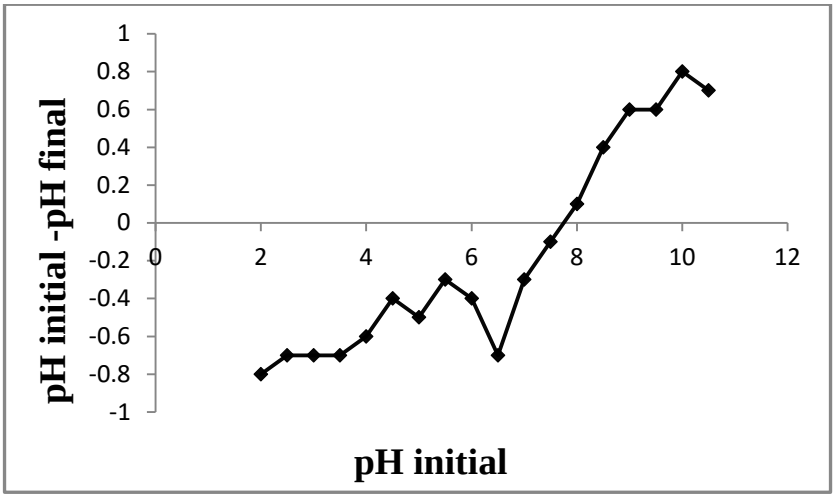


**Figure 4.2b: Point of zero charge of MAM coagulant**

(c)

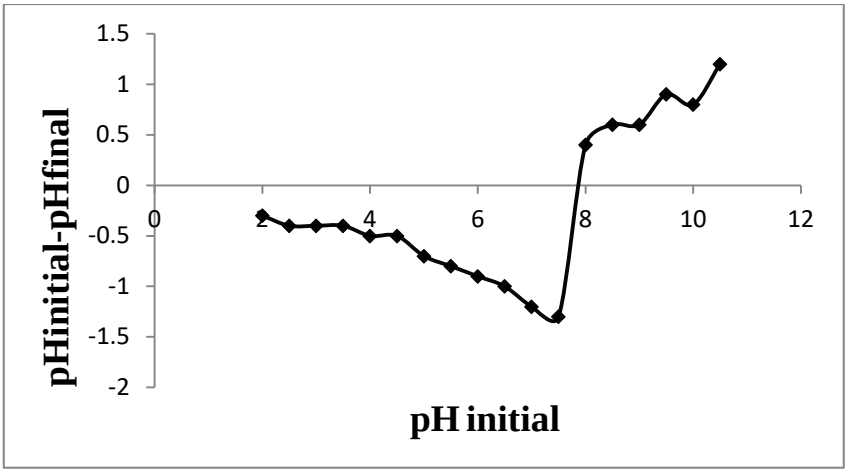


s

**Figure 4.2c: Point of zero charge of MTF coagulant**

**Table 4.6: Physicochemical analyses of the effluent**

| Parameters | Untreated effluent | Treated with MM | Treated with AM | Treated with TF | WHO (STD) | NESREA(STD) |
|---|---|---|---|---|---|---|
| pH | 8.65 | 8.25 | 8.13 | 8.04 | 6.5- 8.5 | 5-9 |
| Alkalinity (mg/L) | 3900 | 862.5 | 568.5 | 453.5 | 200 | - |
| Total hardness (mg/L) | 720 | 1420 | 1110 | 1800 | 70 | - |
| Chloride (mg/L) | 2770 | 640 | 600 | 490 | 250 | 750 |
| Sulphate (mg/L) | 67.07 | 508 | 496 | 450.59 | 250 | 750 |
| Phosphate (mg/L) | 0.272 | 0.169 | 0.55 | 0.658 | - | - |
| Nitrate (mg/L) | 3.29 | 1.30 | 2.72 | 1.687 | 10 | 10 |
| TSS (%) | 2.1 | 0.004 | 0.003 | 0.002 | 30 | 35 |
| TDS (%) | 0.42 | 0.179 | 0.788 | 0.132 | NS | <1200 |
| COD (mg/L) | 720 | 56 | 58.6 | 69.3 | NS | 80 |
| BOD (mg/L) | 534 | 222 | 32 | 35 | 40 | 40 |
| Conductivity (μS/cm) | 22.4 | 15.64 | 15.89 | 16.04 | - | 400 |
| Turbidity (NTU) | 834 | 345 | 234 | 153 | - | 5 |

( NESREA STD.) From Environmental protection act 2002; WHO (STD) from Onuegbu et al., 2013)

## 4.7 Physicochemical analyses of the untreated and treated paint effluent with unmodified coagulants

Table 4.6 shows the result of the physicochemical analyses of the paint industry effluent. In this Table, pH value of the untreated effluent 8.65 is slightly above the permissible limit of World Health Organization (WHO) and within the limit of National Environmental Standards and Regulations Enforcement agency of Nigeria (NESREA). After treating this paint effluent, it was discovered that the values of the pH with MM, AM and TF coagulants were 8.25, 8.12 and 8.04 and they were all within the

permissible limit of both WHO and NESREA. Alkalinity (3900 mg/L) of the untreated paint effluent is above the WHO permissible limit. After treatment there was a reduction in the alkalinity values of this paint effluent with various coagulants for MM (862.5 mg/L), AM (568.5 mg/L), and TF (553.5 mg/L) but not within the acceptable limit of WHO. Total hardness (720 mg/L) of the untreated effluent is above WHO guide standard. Total hardness measures the mineral content in an effluent that is irreversible by boiling. It is also equivalent to the total calcium and magnesium hardness. It could be observed that after treatment, the values of the total hardness with various coagulants were very high this is because these coagulants contained mainly calcium and it reacted with the effluent thus increasing the total hardness of this treated effluent. Chloride (2770 mg/L) of the untreated paint effluent is above the WHO and NESREA standard. It can be inferred from the Table that there was a reduction in the values of this Chloride after treating with MM(640 mg/L), AM(600 mg/L) and TF(490 mg/L) coagulants and is within the NESREA acceptable standard. COD (720 mg/L) of the untreated effluent is above the NESREA standard for effluent disposal. The COD test gives a measure of the non-biodegradable organic materials present (Siyanbola *et al*., 2011) also determines the amount of oxygen required by both potassium dichromate and concentrated sulphuric acid to breakdown both organic and inorganic matters. There was appreciable decrease in the values of the COD after treating with MM(56 mg/L), AM (58.6 mg/L) and TF(69.3 mg/L) respectively and they were all within the permissible limit of effluent discharge. BOD (534 mg/L) of the

untreated paint effluent is above the limit permitted by WHO and NESREA. Biological Oxygen demand (BOD) measures the oxygen required by microorganisms in breaking down organic matter (Osobamiro and Atewolara-Odule, 2015). The presence of organic compounds such as nitro cellulose used as thickener, alkyd resins and acrylic /styrene co-polymer used as dispersants and binders accounts for high BOD of paint effluent. (Onuegbu *et al*., 2013). After treatment, the values of BOD treated with AM(32 mg/L) and TF(35 mg/L) coagulants decreased to acceptable limit of effluent discharge while that of the MM (222 mg/L) decreased but not within the acceptable limit. Sulphate (67.07 mg/L), Nitrate (3.29 mg/L), Phosphate (0.272 mg/L), TSS (2.1%) and TDS (0.42%) of the untreated effluent are within the acceptable limit of WHO and NESREA. As can be deduced from Table 4.6, after treating with various coagulants the values of Sulphate, Nitrate, phosphate, TSS and TDS decreased and were within the acceptable range of effluent discharge. Conductivity is an indicator of salinity and total salt of the effluent (Osobamisro and Atewolara-odule, 2015). Conductivity of the untreated effluent 22.4 μS/cm is observed to be within NESREA limit. The values of the conductivity after treating with MM( 15.64 μS/cm), AM(15.89 μS/cm) and TF(16.04 μS/cm) coagulants were found to decrease though still within the acceptable range of effluent disposal. Turbidity level of this untreated effluent is found to be 834 NTU which is far above the WHO standard for effluent discharge on the environment. High turbidity levels are often associated with higher levels of disease-causing micro organisms such as viruses, parasites and some bacteria. These organisms can cause

symptoms such as nausea, cramps, diarrhea and associated headaches. Water-borne infectious disease caused by viruses, bacteria, protozoa and other micro organisms is associated with outbreaks and background rates of disease in developed and developing countries worldwide (Patale and Pandya, 2012). Turbidity values of the treated effluent were reduced in MM(345 NTU), AM(234 NTU) and TF(153 NTU) respectively but not within the acceptable limit.

**Table 4.7: Physicochemical analyses of both untreated and treated paint effluent with modified coagulants**

| Parameters | Untreated effluent | Treated with MMM | Treated with MAM | Treated with MTF | WHO (STD) | NESREA (STD) |
|---|---|---|---|---|---|---|
| pH | 8.65 | 8.35 | 8.42 | 7.400 | 6.5- 8.5 | 5-9 |
| Alkalinity (mg/L) | 3900 | 452 | 252.5 | 201 | 200 | - |
| Total hardness (mg/L) | 720 | 740 | 1020 | 960 | 70 | - |
| Chloride (mg/L) | 2770 | 456 | 478 | 345 | 250 | 750 |
| Sulphate (mg/L) | 67.07 | 236 | 23.87 | 35.80 | 250 | 750 |
| Phosphate (mg/L) | 0.272 | 0.239 | 0.244 | 0.615 | - | - |
| Nitrate (mg/L) | 3.29 | 2.450 | 9.72 | 1.064 | 10 | 10 |
| TSS (%) | 2.1 | 0.756 | 1.095 | 0.396 | 30 | 35 |
| TDS (%) | 0.42 | 0.346 | 0.02 | 0.400 | NS | <1200 |
| COD (mg/L) | 720 | 90.00 | 76.00 | 53.32 | NS | 80 |
| BOD (mg/L) | 534 | 37.00 | 12.00 | 39.00 | 40 | 40 |
| Conductivity (μS/cm) | 22.4 | 5.89 | 3.77 | 2.76 | - | 400 |
| Turbidity (NTU) | 834 | 313 | 212 | 134 | - | 5 |

( NESREA STD.) From Environmental protection act 2002; WHO (STD) from Onuegbu et al., 2013)

## 4.8 Physicochemical analyses of untreated and treated paint effluent with modified coagulants

Table 4.7 shows the result of the physicochemical analyses of both untreated and treated paint effluent with modified coagulants. In this Table, pH value of the untreated effluent 8.65 is above the permissible limit of World Health Organization (WHO) and within the limit of National Environmental Standards and Regulations Enforcement agency of Nigeria (NESREA).

After treating this paint effluent, it was discovered that the values of the pH with MMM, MAM and MTF coagulants were 8.35, 8.42 and 7.40 and they were all within the permissible limit of both WHO and NESREA. After treatment there was a reduction in the alkalinity values of this paint effluent with various coagulants for MMM (452.5 mg/L), MAM (252.5 mg/L), and MTF (201 mg/L) against (3900 mg/L) of the untreated effluent but not within the acceptable limit of WHO. It could be observed that after treatment that the values of the total hardness with various coagulants MMM (740 mg/L), MAM(1020 mg/L) and MTF(960 mg/L) were very high compared to the untreated (720 mg/L) this is because this coagulants contained mainly calcium and it reacted with the effluent thus increasing the total hardness of this treated effluent. It can be seen from the Table that there was a reduction in the values of this Chloride after treating with MMM(456 mg/L), MAM(478 mg/L) and MTF(345 mg/L) coagulants against (2770 mg/L) of the untreated and they were within the NESREA acceptable standard. COD (720 mg/L) of the untreated effluent is above the NESREA standard for effluent discharge. There was a decrease in the values of the COD after treating with MMM(90 mg/L), MAM (76 mg/L) and MTF(53.32 mg/L) respectively and they were

all within the permissible limit of effluent discharge except the one of MMM coagulants. After treatment, the values of BOD treated with MMM(37 mg/L), MAM(12 mg/L) and MTF(39 mg/L) coagulants decreased to acceptable limit of effluent disposal. Sulphate (67.07 mg/L), Nitrate (3.29 mg/L), Phosphate (0.272 mg/L), TSS (2.1%) and TDS (0.42%) of the untreated effluent are within the acceptable limit of WHO and NESREA. The same Table 4.7 showed that after treating with various modified coagulants, the values of Sulphate, Nitrate, phosphate, TSS and TDS decreased and were within the acceptable range of effluent discharge. Conductivity of untreated effluent (22.4 μS/cm) is observed to be within NESREA limit. The values of the conductivity after treating with MMM (5.89 μS/cm), MAM(3.77 μS/cm) and MTF(2.76 μS/cm) coagulants were found to decrease though still within the acceptable range of effluent disposal. Turbidity level of this untreated effluent is found to be 834 NTU which is above the WHO standard for effluent discharge on the environment. Turbidity values of the treated effluent were reduced in MMM(313NTU), MAM(212NTU) and MTF(134 NTU) respectively but not within the acceptable limit.

**4.9 SEM Results of MM, AM and TF coagulants**

The surface condition and the existence of particles on the coagulants after treatment are confirmed by the SEM images before and after treatment result in Figures 4.3a to b 4.4a to b and 4.5a to b. Figures 4.3a to b, 4.4a to b and 4.5a to b show images of a single and magnified irregular-shaped particle surrounded with dark field void. Void is

a pore of active site which any particle can attach to. After treatment of the paint effluent with coagulants the sludge that came out of it was equally analyzed result in Figures 4.6a-c, as magnified SEM. The Figures demonstrated good pictures of the particles that were trapped into the pores closing all the voids seen in Figures 4.3a to b, 4.4a to b and 4.5a to b, meaning that there were changes in the surface morphology of the coagulants when particles of the colloids attached themselves to them. From the results of SEM, it can be concluded that a greater number of particles where trapped in MM, AM and TF sludge in Figures 4.6a-c comparing with Figures 4.3a to b, 4.4a to b, and 4.5a to b because of the large pores and surface area seen there. The SEM results also confirmed the result of porosity and surface area of the coagulants that was obtained in Table 4.1 with the TF showing the highest value of porosity and surface area followed by AM and MM.

(a)

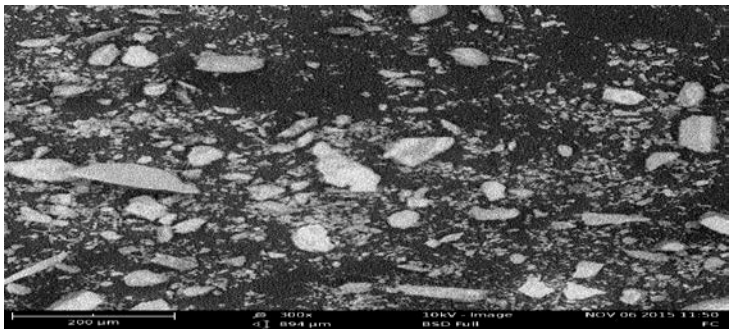

(b)

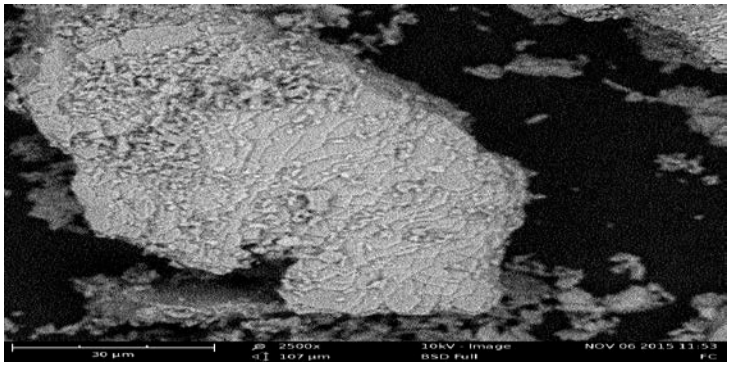


**Figure 4.3a,b: SEM images of MM before treatment (a) single (b) magnified**

**(a)**

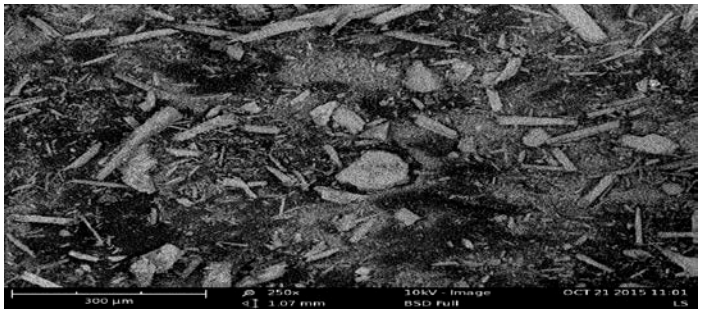


**(b)**

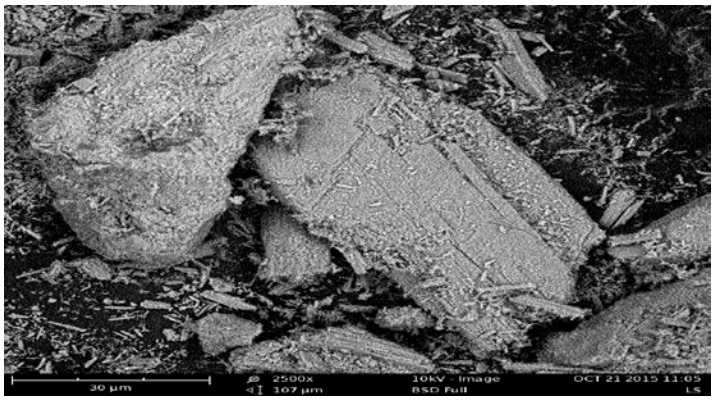


**Figure 4.4: SEM images of AM before treatment (a) single (b) magnified**

**(a)**

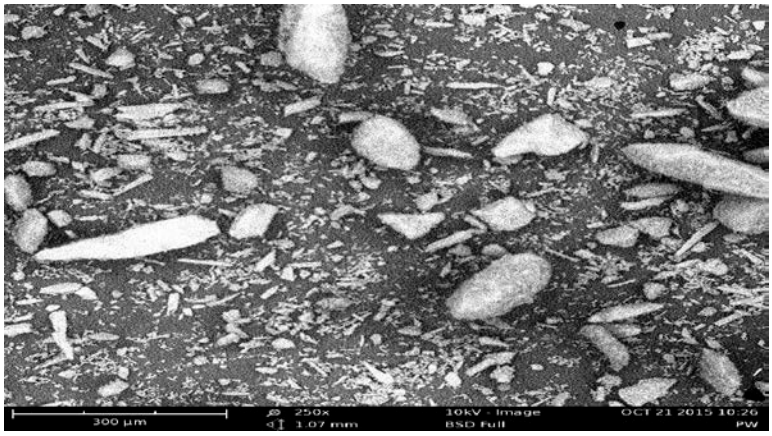


**(b)**

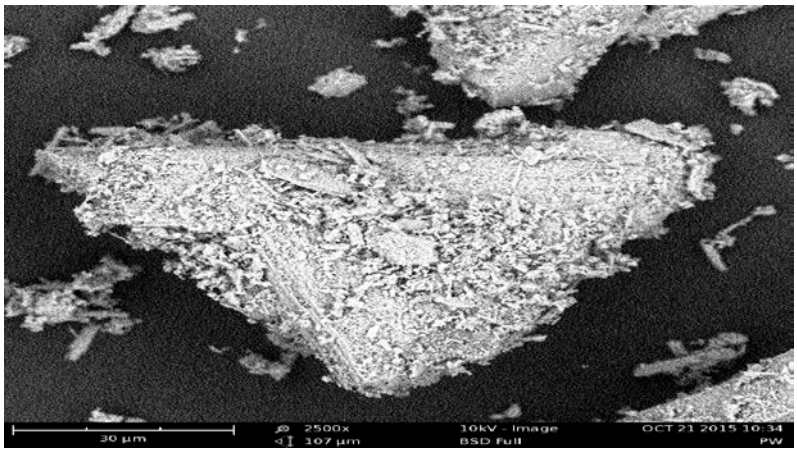


**Figure 4.5: SEM images of TF before treatment (a) single (b) magnified**

(b)

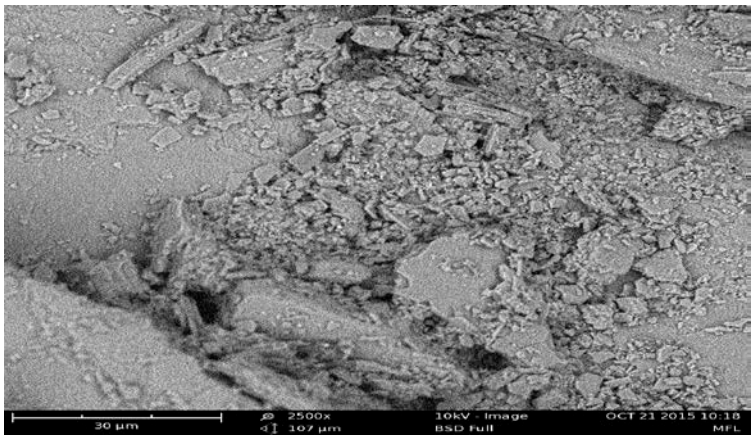


(b)

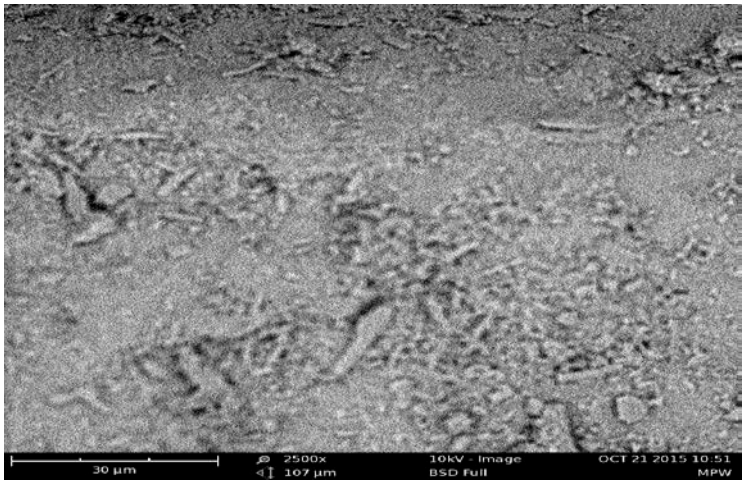


(c)

**Figure 4.6: SEM images of sludge (a) MM, (b) AM, and (c) TF**

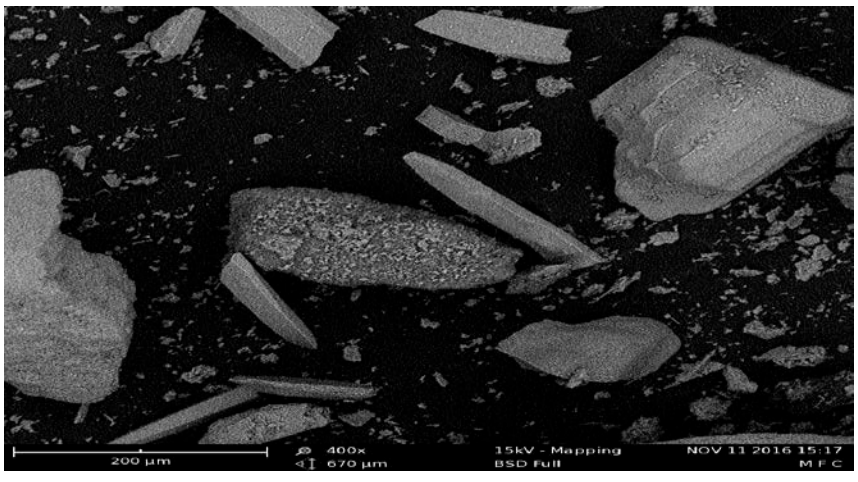


**(a)**

(b) 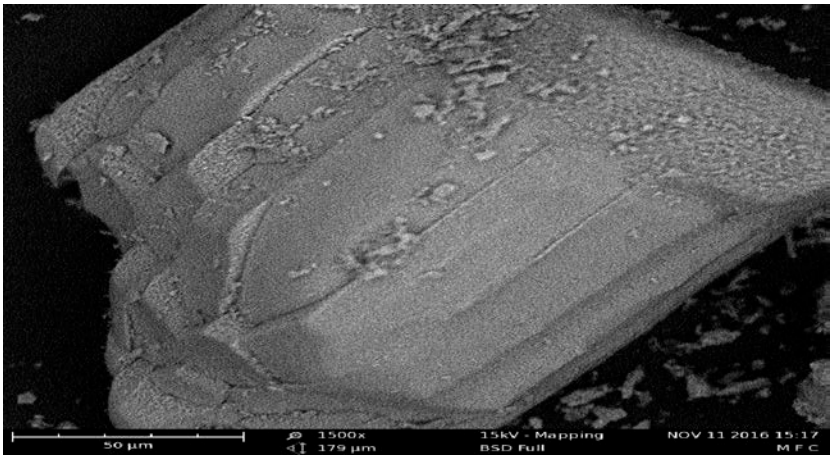


**Figure 4.7: SEM images of MMM coagulant before treatment (a) single (b) magnified**

(a) 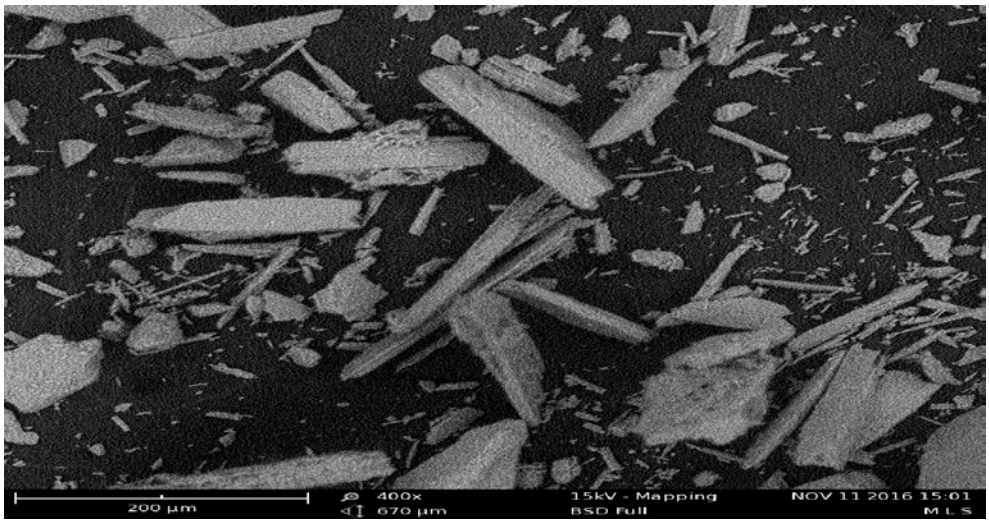


(b) 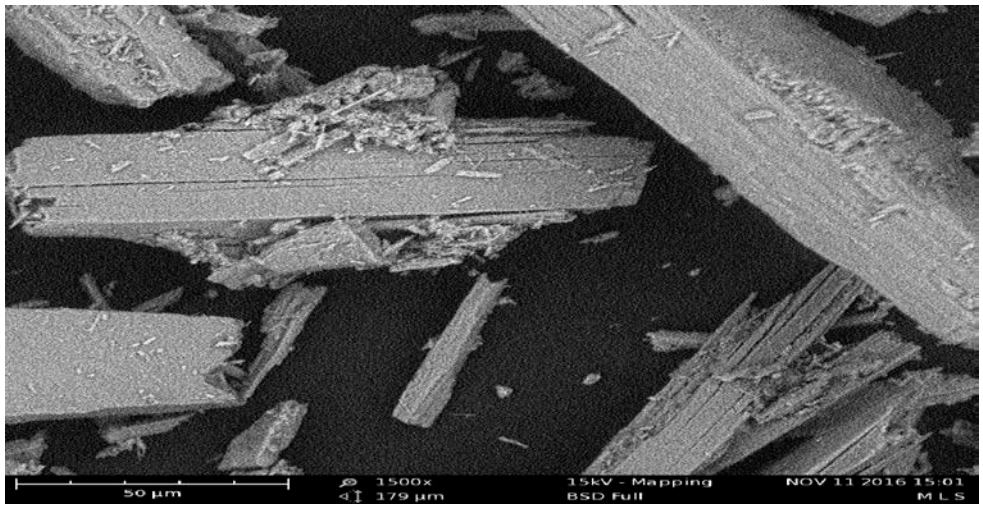

**Figure 4.8: SEM images of MAM coagulant before treatment (a) single (b) magnified**

**(a)**

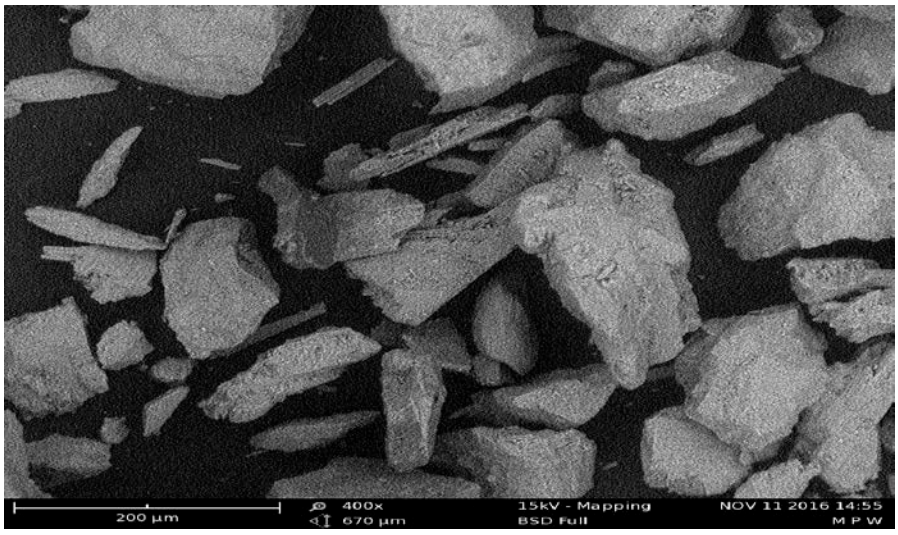


**(b)**

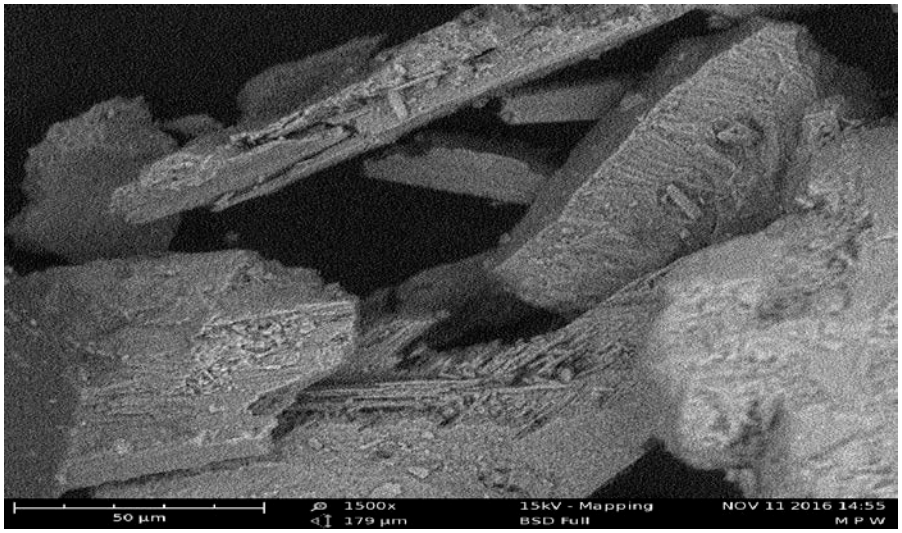


**Figure 4.9: SEM images of MTF coagulant before treatment (a) single (b) magnified**

(a)


**(b)**

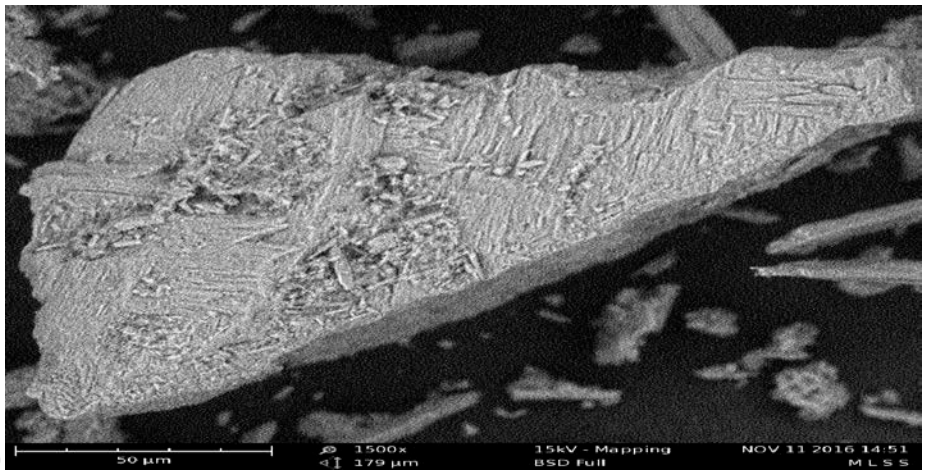


(c)

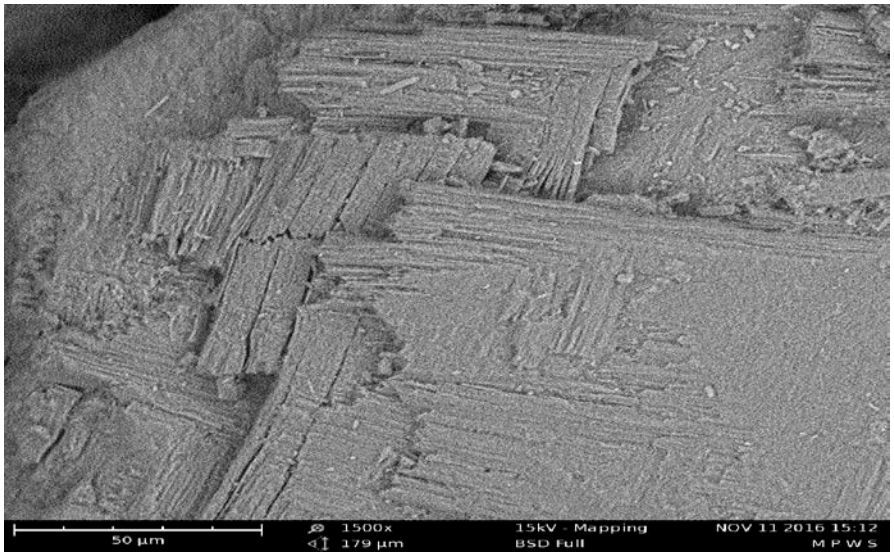


**Figure 4.10: SEM images of sludges (a) MMM, MAM, and (c) MTF**

## 4.10 SEM results of MMM, MAM and MTF coagulants

Figures 4.7a to b, 4.8a to b and 4.9a to b show images of a single and magnified irregular-shaped particle surrounded with dark field void. After treatment of the paint effluent with coagulants, the sludge that came out of it was analyzed, the result in Figures 4.10a-c, as magnified SEM. Comparing Figures 4.7a & b, 4.8a to b and 4.9a & b, to Figures 4.3a to b, 4.4a to b and 4.5a to b, it can be deduced that there is much pores in these modified than unmodified coagulants. The Figures in 4.10a-c demonstrated a good picture of the particles that were trapped into the pores closing some of the voids seen in Figures 4.7a to b - 4.9a to b, making them to look like a cemented object. This means that, there were changes in the surface morphology of the coagulants when particles of the colloids attached themselves to them. From the SEM results, MTF seems to have attracted a greater number of colloid particles followed by MAM and least is with MMM coagulant.

## 4.11 XRD pattern of the unmodified coagulants

XRD analyze the crystallinity of a compound. The XRD patterns of the three unmodified coagulants are shown in Figures 4.11a-c. From these XRD results (Figure 4.11a-c), It could be observed that the peaks are broadened because they have weak diffraction and overlap with each other, which indicates poor crystallinity of MM, AM and TF coagulants. These broad peaks appeared in different 2Ɵ in all the coagulants. Therefore, MM, AM, and TF coagulants are amorphous because of the broadening of

peaks observed in all the XRD patterns as the intense peaks would give a crystalline structure (Shangkun *et al*., 2012; Harish and Renu, 2013).

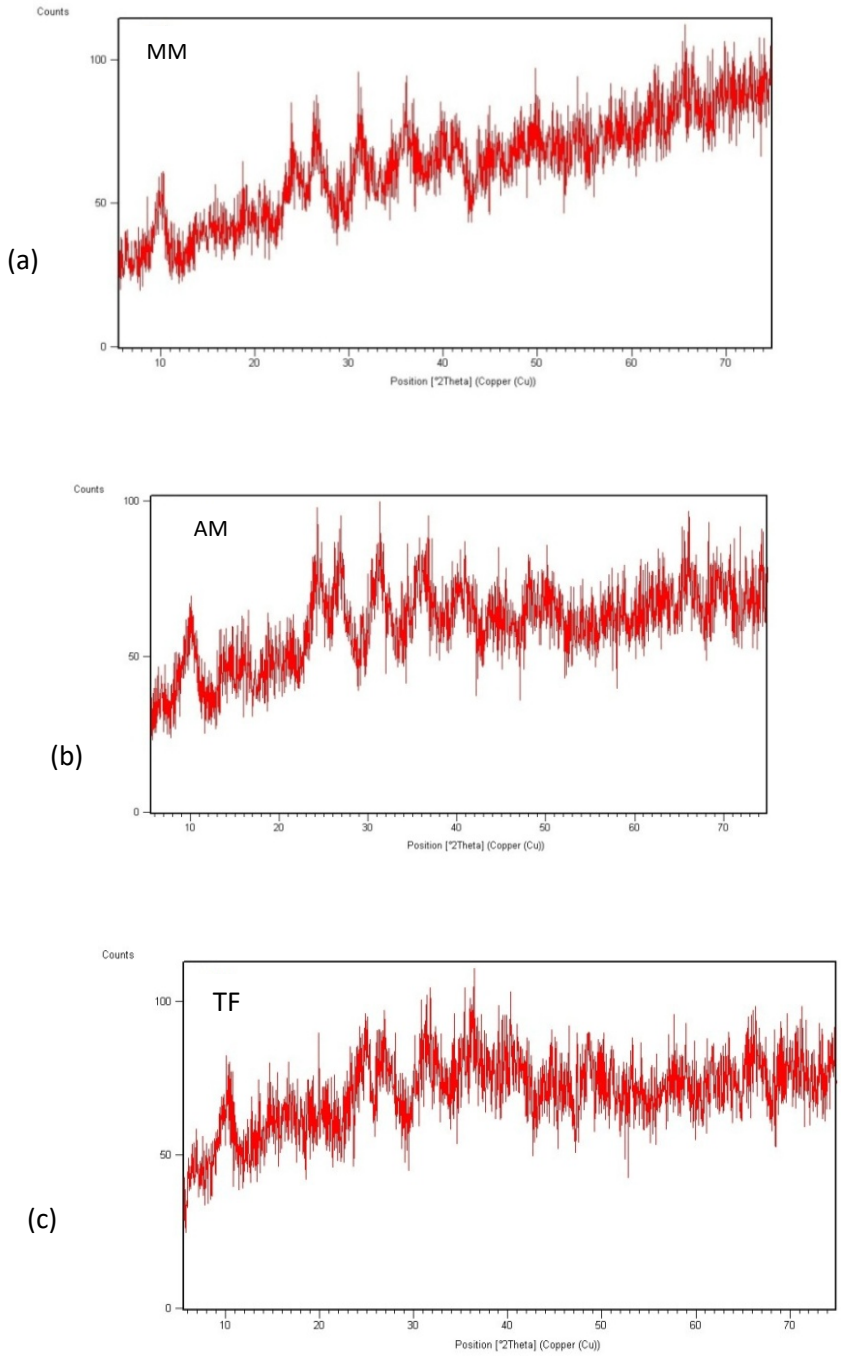


**Figure 4.11: XRD pattern of (a) MM, (b) AM and (c) TF coagulants**

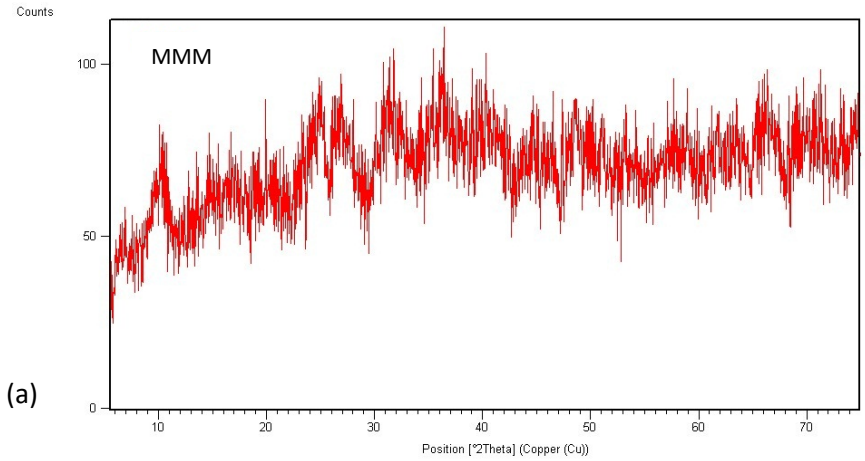


(a)

**Figure 4.12a: XRD pattern of MMM coagulant**

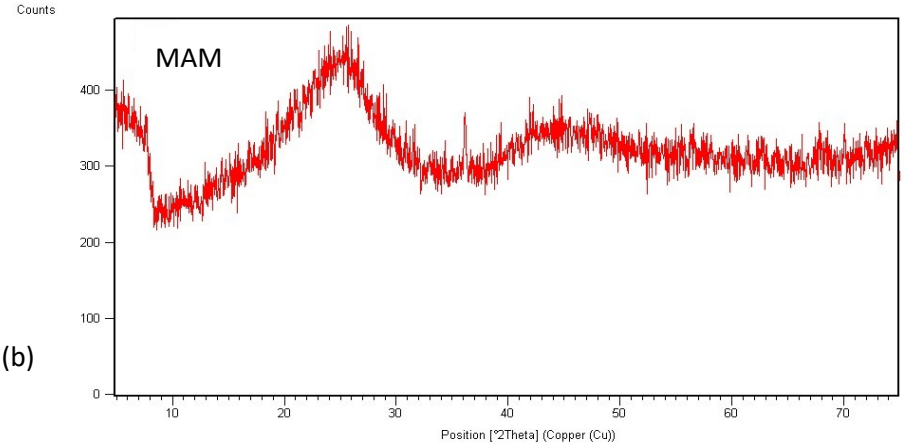


(b)

**Figure 4.12b: XRD pattern of MAM coagulant**

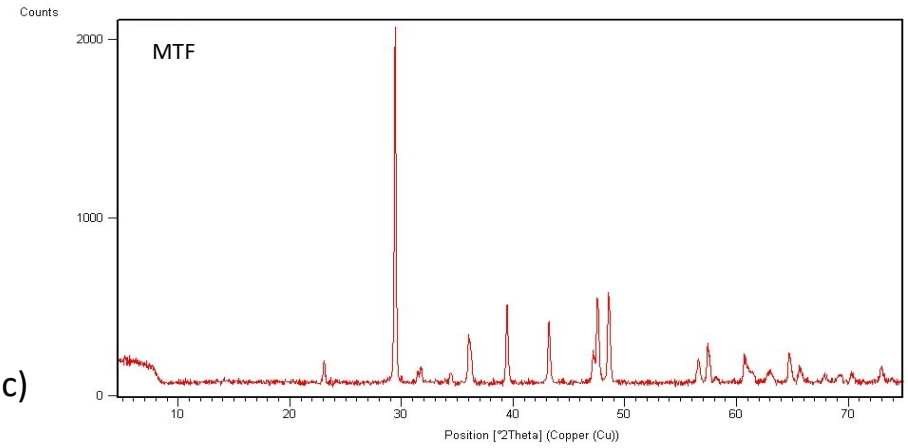


(c)

**Figure 4.12c: XRD pattern of MTF coagulant**

## 4.12 XRD pattern of MMM, MAM and MTF

The XRD patterns of the modified three coagulants are shown in Figures 4.20a-c. Figures 4.12a and 4.12b depict that MMM and MAM have amorphous structure because of the broadening of peaks observed in their XRD patterns at all the 2 theta angles, while MTF (Figure 4.12c) has primitive crystalline structure because of the presence of intense peaks seen at 2 theta 23º, 29 º, 36 º, 38.5 º and 43.2º in the XRD result. Intense peaks means that the lattice are well ordered, that is crystalline while broadening of the peaks shows amorphous structure (Shangkun *et al*., 2012; Harish and Renu, 2013; Pinhua *et al*., 2015). Crystalline structure is caused by small subset of crystallite in the powder that had a plane oriented exactly parallel to the reference plane (Menkiti *et al*., 2016).

**Table 4.8: Elemental composition of the unmodified coagulants from XRF**

| Element | MM (%) | AM (%) | TF(%) |
|---|---|---|---|
| S | 0.133 | 0 | 0.148 |
| K | 0 | 0.144 | 0.107 |
| Ca | 99.135 | 99.451 | 99.067 |
| Ti | 0.028 | 0.019 | 0.020 |
| Mn | 0.243 | 0.029 | 0.078 |
| Fe | 0.171 | 0.034 | 0.195 |
| Co | 0.007 | 0.006 | 0.009 |
| Ni | 0 | 0 | 0.009 |
| Zn | 0.004 | 0.001 | 0.005 |
| Sr | 0.152 | 0.254 | 0.289 |
| Zr | 0.001 | 0.001 | 0.002 |
| Pd | 0 | 0 | 0.002 |
| Sb | 0.003 | 0.003 | 0.003 |
| Te | 0.015 | 0.010 | 0.013 |
| Cs | 0.014 | 0.010 | 0.012 |
| Ba | 0.092 | 0.034 | 0.039 |
| Au | 0 | 0.001 | 0 |
| Hg | 0.002 | 0.002 | 0.002 |
| Th | 0.001 | 0.001 | 0.001 |
| Total | 100 | 100 | 100 |

## 4.13 XRF result of the three unmodified coagulants

Table 4.8 is the XRF result of these coagulants. XRF was used to obtain the elemental composition of these coagulants (Appendix 1-3). Inspection of the Table shows that AM coagulant contained highest amount of calcium 99.451%, follow by MM 99.135% and the least is TF coagulant 99.067%. This depicts that the shells of these coagulants contain mostly calcium. This result is in agreement with (Meredith *et al*., 2007; Edokpayi *et al*., 2015 and Kolawole *et al*., 2017) on XRF of AM and MM respectively. In MM coagulant, elements such as Fe, Sr, S, Mn, Ti, Te, Ba, Cs, Co, Hg, Th, Sb, Zr, Zn, appeared in trace quantities while K, Ni, Pd, Au were absent. In AM coagulant, Fe, Sr, Mn, Ti, Te, Ba, Cs, Co, Hg, Th, Sb, Zr, Zn, appeared in small quantity while Ni, Pd and S were absent. Moreover, in TF coagulant, Fe, Sr, Mn, Ti, Te, Ba, Cs, Co, Hg, Th,

Sb, Zr, Zn, S, Pd, Ni appeared in small amount while Au was absent. This elemental composition justified the percentage ash content obtained in Table 4.4 where TF had the highest % Ash content followed AM the least was MM coagulant.

**Table 4.9: XRF result of modified coagulants**

| Elements | MMM(%) | MAM(%) | MTF(%) |
|---|---|---|---|
| S | 6.105 | 0 | 0 |
| K | 0 | 0.138 | 0.152 |
| Ca | 92.762 | 99.509 | 99.162 |
| Sc | 0.158 | 0 | 0 |
| Ti | 0 | 0.024 | 0.0185 |
| Mn | 0.279 | 0.020 | 0.0663 |
| Fe | 0.190 | 0.022 | 0.123 |
| Co | 0.010 | 0.006 | 0.0117 |
| Ni | 0.010 | 0.006 | 0.0083 |
| Zn | 0.005 | 0.001 | 0.0018 |
| Sr | 0.226 | 0.215 | 0.352 |
| Zr | 0.004 | 0.001 | 0.0015 |
| Pd | 0.003 | 0 | 0 |
| Ag | 0.002 | 0 | 0 |
| Cd | 0.003 | 0 | 0 |
| Sn | 0.007 | 0 | 0.0024 |
| Sb | 0.014 | 0 | 0.0041 |
| Te | 0.042 | 0.012 | 0.0199 |
| Cs | 0.028 | 0.009 | 0.0170 |
| Ba | 0.149 | 0.035 | 0.0537 |
| Au | 0 | 0 | 0.0012 |
| Hg | 0 | 0.001 | 0.0025 |
| Th | 0.001 | 0.001 | 0.0015 |
| Total | 100 | 100 | 100 |

## 4.14 XRF results of the modified coagulants

XRF is used to obtain the elemental composition of these coagulants. Table 4.9 shows the result of XRF of the modified coagulants. Inspection of the Table shows that MAM coagulant contained highest amount of calcium 99.505%, followed by MTF 99.162%

and the least is MMM 92.762%. This shows that after modification of these coagulants, there is an increase in the amount of calcium in them except in MMM, while other elements appeared in minor amount. This result agrees fairly well with the work of Edokpayi in his research on XRF of some land snail shells, where modified MAM shells contained a high percentage of calcium (Edokpayi *et al*., 2015). From the same Table the % of Sulphur has been found to increase in MMM coagulant than in unmodified ones in Table 4.8. Closely inspection of the Table shows that in MMM coagulant, elements such as Mn, Fe, Co, Zn, Sr, Zr, Sc, Ag, Cd, Sn, Sb, Te, Cs, Ba, and Th were present in small amount while K, Ti, Hg, and Au were absent and new element such as Sc, Cd, Ag and Sn were added. In MAM coagulant elements such as K, Mn, Fe, Co, Zn, Sr, Te, Cs, Ba, Au and Th were present in little quantity, while S, Sc, pd, Ag, Cd, Sn, Sb, and Au were absent. MTF coagulant contained the following elements in small amount; Mn, Fe, Co, Zn, Sr, Zr, Sn, Sb, Te, Cs, Ba, and Th while S, Sc, Pd, Ag, and Cd, were absent and new element such as Sn was added. This again confirmed the result of % Ash content obtained in Table 4.5.

**Table 4.10a: FTIR result of the three unmodified coagulants**

| Spectral bands in $cm^{-1}$ | | | Assignment |
|---|---|---|---|
| **MM coagulant** | **AM coagulant** | **TF coagulant** | |
| 3895.37 and 2930.93 | 3895.37 and 2930.93 | 2908.00 | O-H stretch |
| 3428.58 | 3432.44 | 3385.78 | N-H symmetric and asymmetric stretch |
| 1628.94 | 1632.80 | 1637.62 | N-H bend |
| 1442.8 | - | - | C-H bend |
| 1041.60 | 1255.7 and 1042.56 | 1055.10 | C-O stretch |

**Table 4.10b: FTIR result of the sludge of the unmodified coagulants**

| Spectral bands in $cm^{-1}$ | | | Assignment |
|---|---|---|---|
| **MM sludge** | **AM Sludge** | **TF sludge** | |
| 3770.96 and 2939.61 | 3965.78, 2972.8 and 2528.76 | 3869.33, and 3470.06 | O-H stretch |
| 3421.83 | 3431.48 | - | N-H symmetric and asymmetric stretch |
| - | - | 1377.22 | $–CH_3C$-H bend |
| 2281.87 | 2108.27 | - | C≡C stretch |
| 1641.48$cm^{-1}$ | 1647.26 | - | N-H bend |
| 1424.48 | 1423.51 | - | C-H bend |
| 1241.23 and 1048.48 | 1028.16 | 1089.82 and 1047.26 | C-O stretch |

## 4.15 FTIR results of the unmodified coagulants

FTIR spectra of MM, AM and TF coagulants before treatment with the effluent are presented in Table 4.10a. In Table 4.10a for MM coagulant (see appendix 4), absorption bands at 3895.37 and 2930.93 $cm^{-1}$ denote O-H stretching. This depicts the

presence of alcohol group, supporting the presence of carbohydrate in MM coagulant. 3428.58 $cm^{-1}$ was assigned N-H symmetric and asymmetric stretch. 1628.94 $cm^{-1}$ denotes N-H bend. Peak at 1442.8 $cm^{-1}$ indicates the presence of C-H bending, 1041.60 $cm^{-1}$ signifies C-O stretching. For AM coagulant (appendix 5) absorption at 3895.37$cm^{-1}$ and 2930.93 $cm^{-1}$ indicates O-H stretching from alcohol group. Spectra band at 3432.44 $cm^{-1}$was assigned to N-H symmetric and asymmetric stretch, 1632.80 $cm^{-1}$ denote N-H bending. Peaks at 1255.7 $cm^{-1}$ and 1042.56 $cm^{-1}$ characterize C-O stretching. In TF coagulant (see appendix 6), it can be inferred that absorption band at 3385.78 $cm^{-1}$denotes N-H symmetric and asymmetric stretch, peak at 2908.0 $cm^{-1}$ signifies O-H stretching, 1637.62 $cm^{-1}$ indicates N-H bend, peak at 1055.10 $cm^{-1}$ is C-O stretching vibration. Table 4.10b shows the FTIR results of the MM, AM, and TF sludge (after using them to treat paint Industry effluent). In MM sludge (see appendix 7), the peaks at 3770.96 $cm^{-1}$and 2939.61 $cm^{-1}$ are O-H stretching vibration, 3421.83 $cm^{-1}$ is N-H symmetric and asymmetric stretch. Absorption band at 2281.87 denotes C≡C stretches, 1641.48$cm^{-1}$ shows N-H bend, the peaks at 1424.48 $cm^{-1}$ is C-H bend, 1241.23 $cm^{-1}$ and 1048.48 $cm^{-1}$ denote C-O stretch. For AM Sludge (see appendix 8), absorption bands at 3965.78 $cm^{-1}$, 2972.8 $cm^{1}$ and 2528.76 $cm^{-1}$ are O-H stretch, 3431.48 $cm^{-1}$ is N-H symmetric and asymmetric stretch, 2108.27 $cm^{-1}$ is C≡C stretch, 1647.26 $cm^{-1}$ is N-H bend, 1423.51 $cm^{-1}$is C-H bend and 1028.16 $cm^{-1}$ is C-O stretch. In TF sludge see (appendix 9), the peaks at 3869.33 $cm^{-1}$, and 3470.06 $cm^{-1}$ depict O-H stretch, 1377.22 $cm^{-1}$ indicates $–CH_3C$-H bend. The peaks at 1089.82 and 1047.26 $cm^{-1}$

characterize C-O stretch. The Table also depicts that some bands were shifted upward and downward, while some were removed and added, this is as a result of the interaction of these functional groups of the coagulants and the effluent. This shows clearly that the three coagulants removed impurities from the paint effluent after treatment. This result also agrees fairly well with the report elsewhere (Menkiti *et al.*, 2016). Metals generally give absorption bands in fingerprint region below 1000 $cm^{-1}$ arising from inter-atomic vibrations (Harish and Renu, 2013). Therefore, all these coagulants gave absorption bands below 1000 $cm^{-1}$ and metals absorptions are suspected. This is also evident in XRF results in Table 4.8.

**4. 16: FTIR results of the modified coagulants**

The FTIR spectra of MMM, MAM and MTF coagulants before treatment with effluent is presented in Table 4.11a. From the Table, the FTIR result of MMM coagulant (see also appendix 10), absorption band at 3746.0 $cm^{-1}$, 3671.4 $cm^{-1}$ and 3518.6 $cm^{-1}$ depict O-H stretch from alcohol group, supporting the presence of carbohydrate in MMM coagulant. The band observed at 3399.3 $cm^{-1}$ can be attributed to N-H stretch from amine group, this also support the presence of protein in the coagulant. The bands at1872.6, 1822.7, and 1787.1 $cm^{-1}$ was assigned to C=O stretching vibration, 1621.4 $cm^{-1}$ is N-H bend. Peak at 1453.7 $cm^{-1}$ denotes C-H bending. Peak at 1110.7 $cm^{-1}$ indicates

**Table 4.11a: FTIR result of the modified coagulants**

| Spectral bands in $cm^{-1}$ | | | Assignment |
|---|---|---|---|
| **MMM coagulant** | **MAM coagulant** | **MTF coagulant** | |
| 3746.0, 3671.4 and 3518.6 | 3526.1 and 2509.8 | 2519.7 | O-H stretch |
| 3399.3 | 3389.5 and 3205.5 | - | N-H symmetric and asymmetric stretch |
| 1872.6, 1822.7, and 1787.1 | 1669.7 and 1304.6 | 1785.4 | C=O stretch |
| 1621.4 | 1617.7 | 1651.2cm | N-H bend |
| 1453.7 | I476.0, 1427.6, and 2840.2 | 2098.5, 1986.7 and 1446.2 | C-H bend |
| - | - | 2202.9 and 2288.6 | C≡C stretch |
| 1110.7 | 1181.6, 1151.7, 1073.5 and 1042.56 | - | C-O stretch |
| - | 1385.6 | - | $CH_3C$- H bend |

**Table 4.11b: FTIR result of the sludge**

| Spectral bands in $cm^{-1}$ | | | Assignment |
|---|---|---|---|
| **MMM sludge** | **MAM Sludge** | **MTF sludge** | |
| 3753.4 and 3652.8 | - | 2519.7 | O-H stretch |
| 3447.8 | - | - | N-H symmetric and asymmetric stretch |
| 1781.7 | 1785.4 | 1785.4 | C=O stretch |
| 2109.7 and 2299.8 | 2109.7 | 2161.9$cm^{-1}$ and 2109.7 | C≡C stretch |
| - | 1647.26 | - | N-H |
| 1476.0 and 1994.1 | 1461.1 and 1982.9 | 1446.2 | C-H bend |
| 1148.0 and 1080.0 | 1080 | 1089.82 and 1047.2 | C-O stretch |
| - | - | 1651.2 | C=C stretch |

the presence of C-O stretch. This result is similar with the result obtained elsewhere (Menkiti *et al*., 2016). For MAM coagulant in the same Table 4.11a (appendix 11),

absorption band at 3526.1cm$^{-1}$ and 2509.8 cm$^{-1}$ indicate O-H stretch, absorption band at 3389.5 cm$^{-1}$ and 3205.5 cm$^{-1}$depict N-H stretch. Peak observed at 2840.2 cm$^{-1}$, 1476.0 and 1427.6 cm$^{-1}$ denotes C-H bending vibration, 1669.7 cm$^{-1}$ and 1304.6 cm$^{-1}$ are C=O stretch, 1617.7 cm$^{-1}$ is N-H bend. 1385.6 cm$^{-1}$ denote $CH_3$C-H bend. Peak at 1181.6, 1151.7, 1073.5 and 1042.56 cm$^{-1}$ characterize C-O stretching.

In MTF coagulant from the same Table (see also appendix 12), It is seen that absorption band at 2519.7 cm$^{-1}$ signifies O-H stretching from carboxylic acid, 2098.5, and 1986.7 cm$^{-1}$ indicate C-H bend, peak at 1785.4 cm$^{-1}$ is C=O stretch, 1651.2 cm$^{-1}$ is N-H stretch from amine group while peak at 1446.2 cm$^{-1}$ was assigned to C-H bend. Table 4.11b gives the FTIR result of the MMM, MAM and MTF sludge (after using them to treat paint industry effluent). Table 4.19b shows the result of sludge after treatment with modified coagulants. In MMM sludge (see also appendix 13); the peaks at 3753.4 cm$^{-1}$and 3652.8 cm$^{-1}$ denote O-H stretch, 3447.8 cm$^{-1}$ is N-H bend, $^{-1.}$ 1781.7 cm$^{-1}$ is C=O stretch, 1476.0 cm$^{-1}$ and 1994.1 cm$^{-1}$ were assigned C-H bend, absorption band at 2109.7 and 2299.8 cm$^{-1}$ were assign to C≡C stretch , 1148.0 and 1080.0 cm$^{-1}$ depict C-O stretch. For MAM sludge (appendix 14), absorption band at 2109.7 cm$^{-1}$ is C≡C stretch, 1982.9 cm$^{-1}$ is C-H bending, 1785.4 cm$^{-1}$ is C=O stretch, 1461.1 cm$^{-1}$ is C-H bending, 1080 cm$^{-1}$ is C-O stretch. In MTF sludge (appendix 15), peak at 2519.7 cm$^{-1}$ is O-H stretching, 2161.9 cm$^{-1}$ and 2109.7 cm$^{-1}$ is C≡C stretch, 1785.4 cm$^{-1}$ is C=O stretch, 1651.2 cm$^{-1}$ was assigned to C=C stretch, absorption band at 1446.2 cm$^{-1}$ is C-H. Visual review of the results in Tables 4.11a and Tables 4.10a clearly

demonstrated that C=O functional group was added to all the modified coagulants. The results also show that some bands were shifted upward and downward, while some were added and removed. This is as a result of the interaction of the particles of the paint effluent and that of the coagulants (functional groups). This means that the three modified coagulants removed pollutants from the paint effluent after treatment. Metals generally give absorption bands in fingerprint region below 1000 $cm^{-1}$ arising from inter-atomic vibrations (Harish and Renu, 2013). Closely inspection of the Appendix 10-15, one will note that all these modified coagulants and their sludge gave absorption bands below 1000 $cm^{-1}$ and metals absorptions are suspected. This is also evident in XRF results in Table 4.9.

## 4.17 Result of Colour removal efficiency with unmodified coagulants by Coagulation-flocculation method using Response surface methodology (RSM) by BBD design

Table 4.12 is Box-Behnken (BBD) experimental design matrix with % colour removal efficiency of the three coagulants together with the corresponding responses from each coagulant.

**Table 4.12: Box-Behnken experimental design matrix with % colour removal efficiency of the three coagulants as responses**

| Run | Factor 1 Dosage(A) (mg/L) | Factor 2 pH (B) | Factor 3 Time (c) (mins) | MM Efficiency of Colour removal (%) | AM Efficiency of Colour removal (%) | TF Efficiency of Colour removal (%) |
|---|---|---|---|---|---|---|
| 1 | 100.00 | 10.00 | 20.00 | 46.17 | 68.38 | 88.77 |
| 2 | 500.00 | 6.00 | 30.00 | 47.66 | 60.04 | 68.87 |
| 3 | 300.00 | 10.00 | 10.00 | 44.29 | 71.04 | 81.71 |
| 4 | 100.00 | 2.00 | 20.00 | 76.55 | 36.00 | 79.11 |
| 5 | 500.00 | 10.00 | 20.00 | 38.52 | 78.31 | 79.10 |
| 6 | 300.00 | 6.00 | 20.00 | 50.82 | 53.19 | 74.10 |
| 7 | 500.00 | 2.00 | 20.00 | 64.69 | 46.13 | 48.93 |
| 8 | 100.00 | 6.00 | 10.00 | 59.94 | 47.93 | 75.31 |
| 9 | 100.00 | 6.00 | 30.00 | 55.95 | 50.00 | 76.32 |
| 10 | 300.00 | 2.00 | 30.00 | 67.82 | 42.50 | 53.32 |
| 11 | 300.00 | 6.00 | 20.00 | 51.13 | 52.97 | 74.12 |
| 12 | 300.00 | 2.00 | 10.00 | 71.24 | 40.93 | 50.11 |
| 13 | 300.00 | 6.00 | 20.00 | 50.18 | 53.01 | 74.35 |
| 14 | 300.00 | 6.00 | 20.00 | 50.56 | 53.10 | 74.12 |
| 15 | 300.00 | 10.00 | 30.00 | 40.73 | 75.17 | 85.77 |
| 16 | 500.00 | 6.00 | 10.00 | 50.77 | 56.73 | 68.87 |
| 17 | 300.00 | 6.00 | 20.00 | 51.01 | 53.05 | 74.99 |

Visual inspection of the Table showed that the maximum colour removal efficiency by the three coagulants is found to be < 90%. The result in Table 4.12 was evaluated by multiple regression analysis and second order polynomial equation fitted between the responses represented by colour removal efficiency (*Y*) and the input variable of dosage (*A)*, pH (*B)* and time (C*)*. The empirical models in terms of coded factors for coagulation-flocculation of MM, AM and TF gave a quadratic equation.

**Table 4.13a : ANOVA for Response Surface Quadratic model for MM coagulant**

| Source | Sum of Squares | df | Mean Square | F Value | p-value Prob > F | |
|---|---|---|---|---|---|---|
| Model | 1805.88 | 9 | 200.65 | 627.15 | < 0.0001 | Significant |
| A-Dosage | 176.71 | 1 | 176.71 | 552.32 | < 0.0001 | |
| B-pH | 1502.64 | 1 | 1502.64 | 4696.60 | < 0.0001 | |
| C-Time | 19.22 | 1 | 19.22 | 60.07 | 0.0001 | |
| AB | 4.54 | 1 | 4.54 | 14.20 | 0.0070 | |
| AC | 0.61 | 1 | 0.61 | 1.89 | 0.2114 | |
| BC | 0.18 | 1 | 0.18 | 0.58 | 0.4720 | |
| $A^2$ | 9.09 | 1 | 9.09 | 28.42 | 0.0011 | |
| $B^2$ | 79.04 | 1 | 79.04 | 247.04 | < 0.0001 | |
| $C^2$ | 6.81 | 1 | 6.81 | 21.29 | 0.0024 | |
| Residual | 2.24 | 7 | 0.32 | | | |
| Lack of Fit | 1.84 | 3 | 0.61 | 6.10 | 0.0566 | not significant |
| Pure Error | 0.40 | 4 | 0.10 | | | |
| Corr. Total | 1808.12 | 16 | | | | |
| R- square | | 0.9986 | | | | |
| Adj. R-square | | 0.9972 | | | | |
| Pred.R-square | | 0.9834 | | | | |
| Adeq.precision | | 84.850 | | | | |

**Table 4.13b: ANOVA for Response Surface Quadratic model for AM coagulant**

| Source | Sum of Squares | df | Mean Square | F Value | p-value Prob > F | |
|---|---|---|---|---|---|---|
| Model | 2303.23 | 9 | 255.91 | 3178.77 | < 0.0001 | Significant |
| A-Dosage | 190.84 | 1 | 190.84 | 2370.43 | < 0.0001 | |
| B-pH | 2027.16 | 1 | 2027.16 | 25179.76 | < 0.0001 | |
| C-Time | 15.83 | 1 | 15.83 | 196.65 | < 0.0001 | |
| AB | 9.120E-003 | 1 | 9.120E-003 | 0.11 | 0.7463 | |
| AC | 0.49 | 1 | 0.49 | 6.14 | 0.0424 | |
| BC | 1.64 | 1 | 1.64 | 20.32 | 0.0028 | |
| $A^2$ | 0.21 | 1 | 0.21 | 2.62 | 0.1494 | |
| $B^2$ | 64.63 | 1 | 64.63 | 802.81 | < 0.0001 | |
| $C^2$ | 0.78 | 1 | 0.78 | 9.75 | 0.0168 | |
| Residual | 0.56 | 7 | 0.081 | | | |
| Lack of Fit | 0.53 | 3 | 0.18 | 24.65 | 0.0049 | Significant |
| Pure Error | 0.029 | 4 | 7.231E-003 | | | |
| Cor Total | 2303.80 | 16 | | | | |
| R-square | 0.9998 | | | | | |
| Adj.R-square | 0.9994 | | | | | |
| Pred.R-square | 0.9963 | | | | | |
| Adeq.Precision | 191.184 | | | | | |

**Table 4.13c: ANOVA for Response Surface Quadratic model for TF coagulant**

| Source | Sum of Squares | df | Mean Square | F Value | p-value Prob > F | |
|---|---|---|---|---|---|---|
| Model | 2208.86 | 9 | 245.43 | 136.00 | < 0.0001 | significant |
| A-Dosage | 12.27 | 1 | 12.27 | 6.80 | 0.0350 | |
| B-pH | 1569.88 | 1 | 1569.88 | 869.92 | < 0.0001 | |
| C-Time | 35.36 | 1 | 35.36 | 19.60 | 0.0031 | |
| AB | 23.03 | 1 | 23.03 | 12.76 | 0.0091 | |
| AC | 2.27 | 1 | 2.27 | 1.26 | 0.2995 | |
| BC | 2.89 | 1 | 2.89 | 1.60 | 0.2459 | |
| $A^2$ | 283.34 | 1 | 283.34 | 157.01 | < 0.0001 | |
| $B^2$ | 248.43 | 1 | 248.43 | 137.66 | < 0.0001 | |
| $C^2$ | 0.19 | 1 | 0.19 | 0.10 | 0.7567 | |
| Residual | 12.63 | 7 | 1.80 | | | |
| Lack of Fit | 12.06 | 3 | 4.02 | 28.11 | 0.0038 | Significant |
| Pure Error | 0.57 | 4 | 0.14 | | | |
| Corr.Total | 2221.45 | 16 | | | | |
| R-square | 0.9943 | | | | | |
| Adj.R-square | 0.9870 | | | | | |
| Pred R-Squared | 0.9127 | | | | | |
| Adeq Precision | 41.756 | | | | | |

The statistical significance of the quadratic model was evaluated by the analysis of variance (ANOVA), as presented in Tables 4.13a-4.13c, The quadratic equation obtained from the ANOVA is given in equation 4.1 (MM), 4.2 (AM) and 4.3(TF) respectively for the three coagulants.

$$Y = +50.67 - 4.70A - 13.71B - 1.55C + 1.07AC + 0.39AB + 0.22BC + 1.47A^2 + 4.33B^2 + 1.27C^2 \quad 4.1$$

$$Y = +53.06 + 4.88A - 15.92B + 1.41C - 0.048AB + 0.35AC - 0.64BC + 0.22A^2 + 3.92B^2 + 0.43C^2 \quad 4.2$$

$$Y = +74.33 + 1.24A - 14.01B + 2.10C + 2.40AB - 0.75AC - 0.85BC - 8.20A^2 - 7.66B^2 - 0.21C^2 \quad 4.3$$

In order to develop the regression model that is statistically significant, the insignificant terms in equation 4.1 - 4.3 were eliminated. The term with *p* values more than 0.05 are insignificant (Table 4.13a-c) and hence removed to obtain the regression model equation 4.4- 4.6. Positive sign in front of equations 4.4-4.6 indicate synergistic effect of the factors, whereas negative sign indicates antagonistic factor effect (Obiora-Okafo and Onukwuli, 2015).

$$Y_{MM} = +50.67 + 4.70A - 13.71B - 1.55C + 0.39AB + 1.47A^2 + 4.33B^2 + 1.27C^2 \quad 4.4$$

$$Y_{AM} = +53.06 + 4.88A - 15.92B + 1.41C + 0.35AC - 0.64BC + 3.92B^2 + 0.43C^2 \quad 4.5$$

$$Y_{Tf} = +74.33 + 1.24A - 1.24B + 2.103C + 2.40AB - 8.20A^2 - 7.66B^2 \quad 4.6$$

The adequacy and significance of the model was further justified through Analysis of variance (ANOVA). Tables 4.13a-c show the ANOVA for Response surface quadratic model for MM, AM and TF coagulants. In Tables 4.13a-c, the degrees of freedom (dF), sum of squares (SS) and mean squares (MS) Fischer's (F) test and probability (P) values are calculated. The MS value of a model term is obtained by dividing SS over dF. (Prasad *et al.*, 2012). F-value is the ratio of mean square for the individual term to the mean square for the residual (Ria *et al*., 2013). Model terms were evaluated by the P-value (probability) with 95% confidence level. The P-values were used to estimate whether F was large enough to indicate statistical significance and also to check the significance of each coefficient. The P-values lower than 0.05 indicated that the model

and model terms were statistically significant (Fakhri, 2014). From the Table the F-values of 627.15, 3178.77 and 136.00 for MM, AM and TF respectively shows that the model is significant according to the P value which was less than 0.05. In addition the model exhibited insignificant lack of fit for MM while significant lack of fit for AM and MM. The lack of fit test measures the failure of the model to represent data in experimental domain at points that are not included in the regression (Obiora-Okafor and Onukwuli, 2015). Significant lack of fit could occur due to noise or some important variables were left out of the experiment, then it is possible that the portion of the variability in the data not explained by the model also called residual could be large. Therefore, what measures the overall performance of a model is $R^2$, which is referred to as coefficient of determination. When predicted $R^2$ and adjusted $R^2$ differ dramatically, there is a good chance that non-significant terms have been included in the model (Thuy and Lim, 2011). The Predicted R-Squared of the three coagulants studied were 0.9713, 0.9963 and 0.9127 for MM, AM and TF respectively, and they all in reasonable agreement with the "Adj R-Squared" of 0.9972, 0.9994 and 0.9870, i.e. their difference is less than 0.2. "Adeq Precision" measures the signal to noise ratio. A ratio greater than 4 is desirable. The ratios obtained from all the three coagulants indicated an adequate signal. A high $R^2$ value closer to 1, is desirable and ensures a satisfactory adjustment of the quadratic model to the experimental data. For a model to be reliable; the response should be predicted with a reasonable accuracy when compared with the experimental

data. Figures 4.13-4.15 compare experimental (actual) colour removal efficiencies (%) with the predicted values obtained from the models. The Figures indicated good agreement between the experimental and predicted values in the three coagulants. The observed points on these plots revealed that the actual values are distributed relatively near to the straight line in most cases, indicating that the regression model is able to predict these removal efficiencies. A close relationship between predicted and experimental data indicates a good fit.

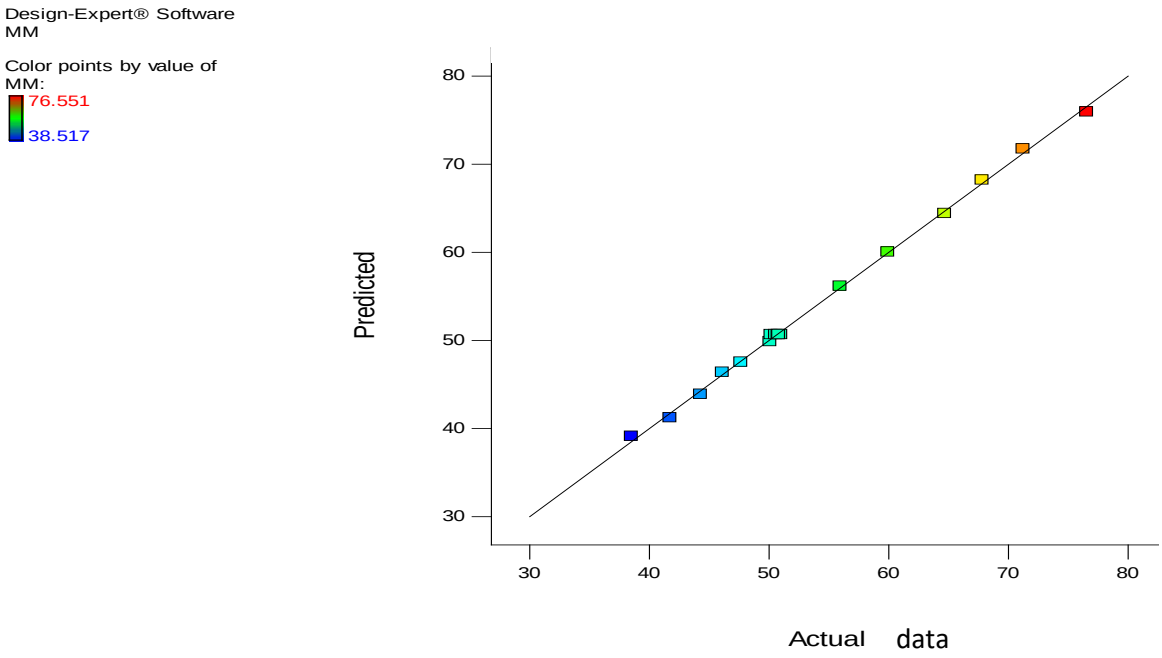


**Figure 4.13: A plot of Predicted versus Actual data for MM coagulant**

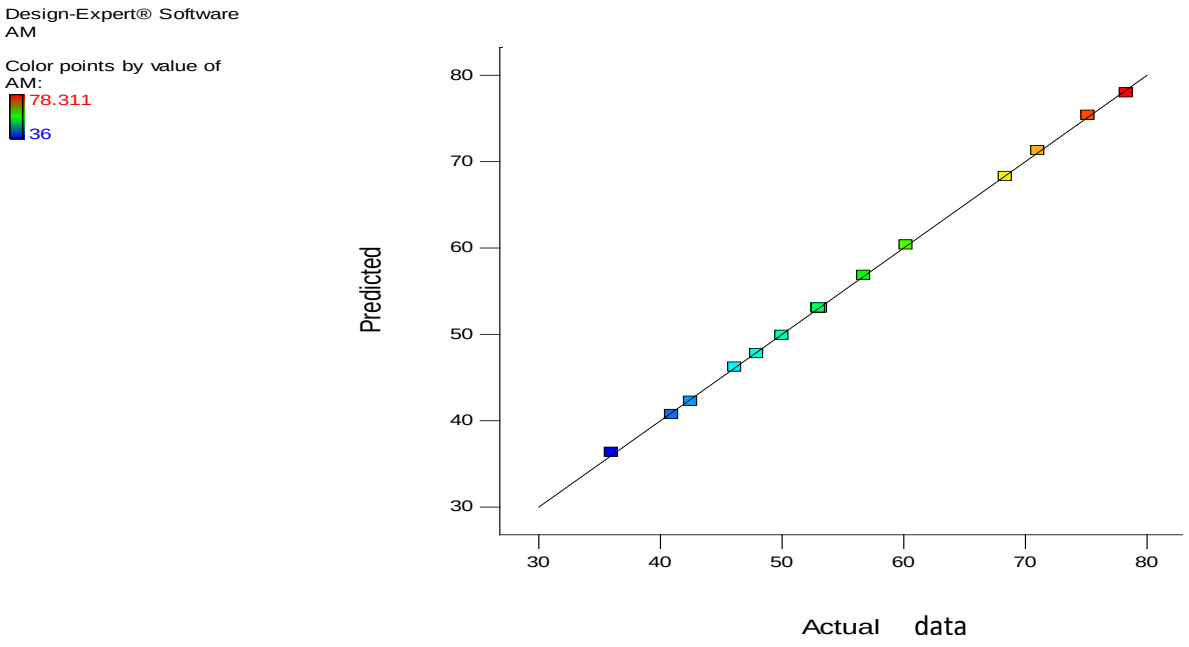


**Figure 4.14: A plot of Predicted versus Actual data for AM coagulant**

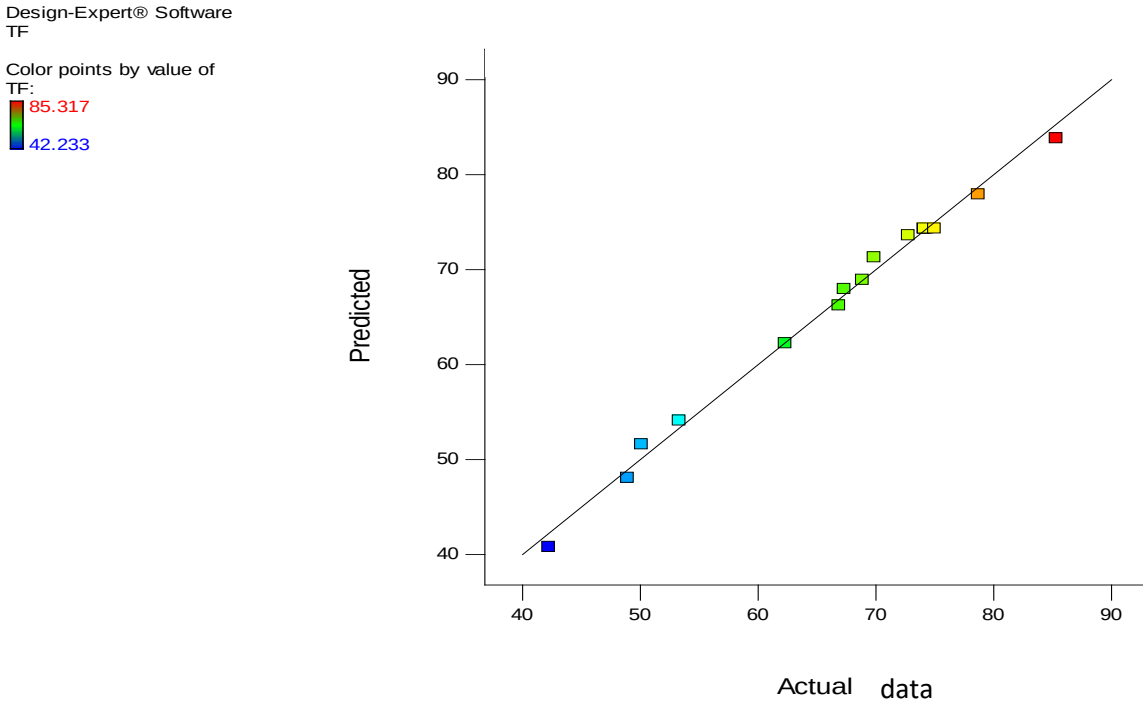


**Figure 4.15: A plot of predicted versus Actual data for TF coagulant**

## 4.18 Effect of interactive variables for unmodified coagulants (dosage, pH and time

To comprehend the impact of each variable, 3D surface plot were plotted for the estimated responses, which were the base of second order polynomial function given as Figure 4.16a-c, 4.17a-c and 4.18a-c. Here one factor was kept constant and two factors were varied. The response surface plots indicate that the maximum colour removal efficiencies are located inside the design boundary.

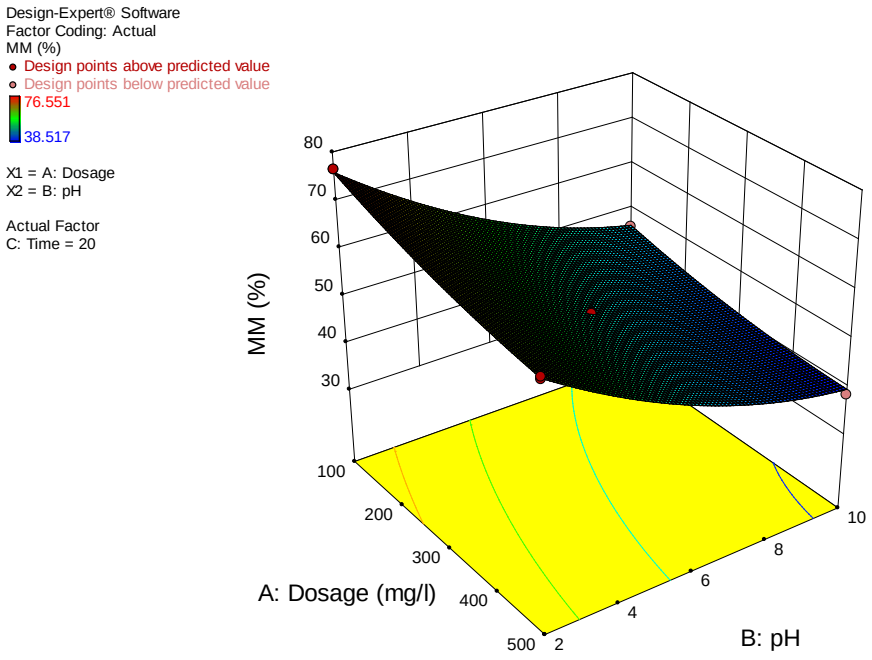


(a)

(b)

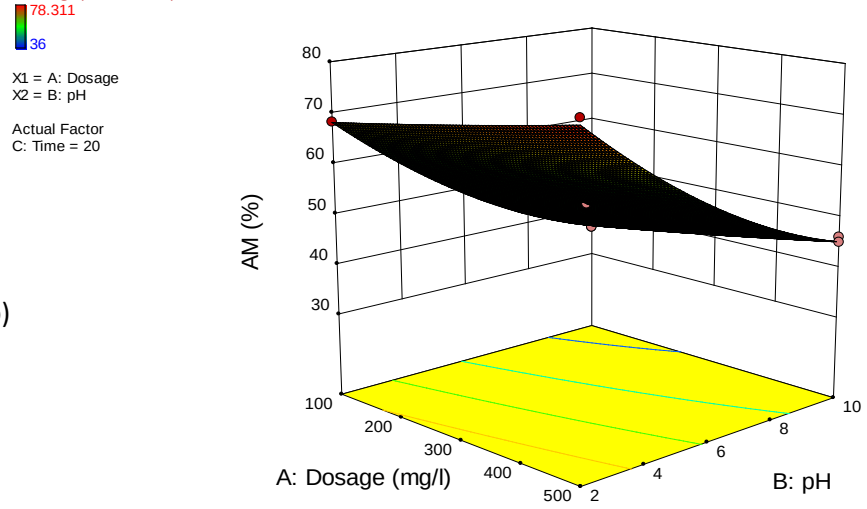


(c)

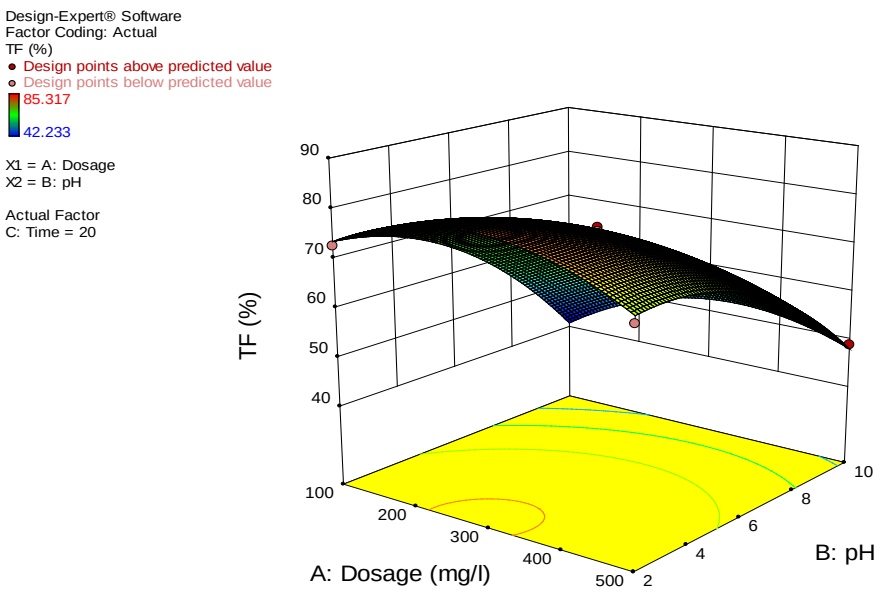


**Figure 4.16: 3D Surface of interactive effect between Dosage and pH at time of 20 minutes for (a) MM, (b) AM and (c) TF coagulants**

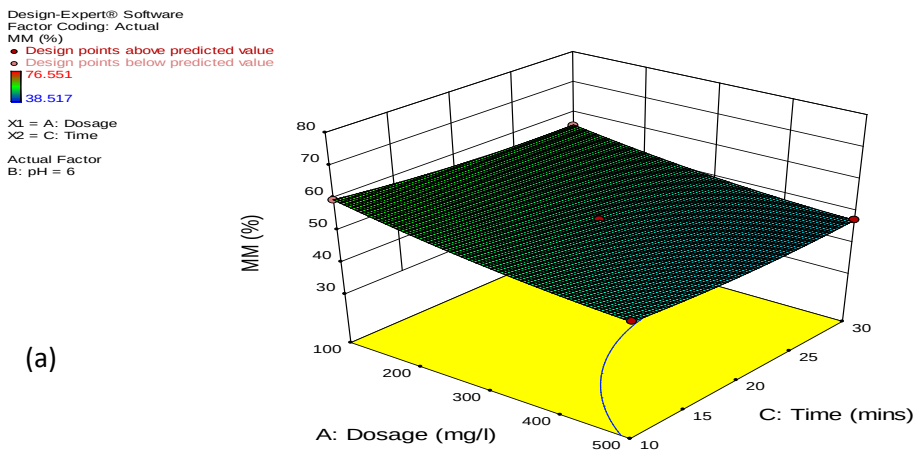


(a)

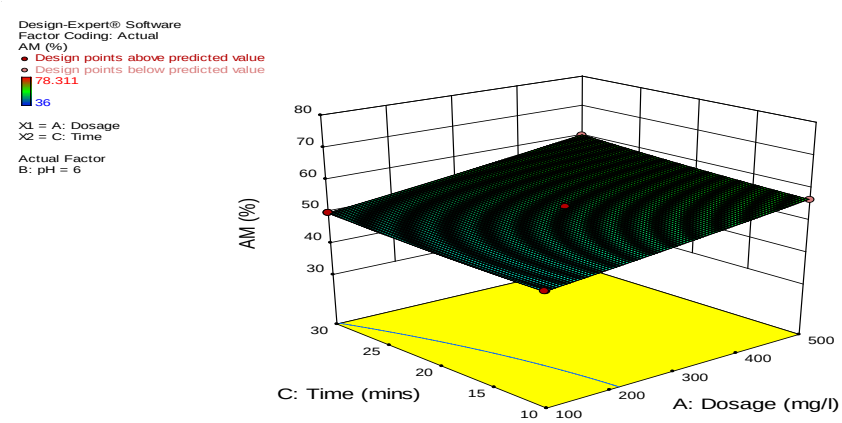


(b)

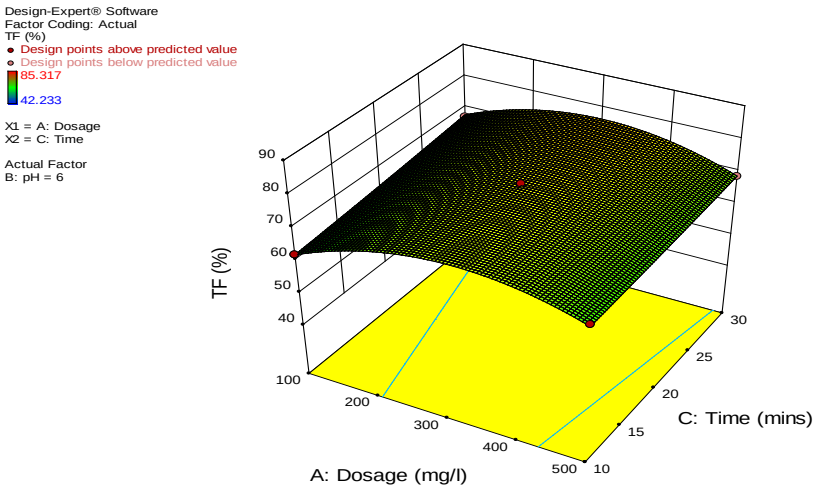


(c)

**Figure 4.17: 3D Surface of interactive effect between dosage and time at pH of 6 of (a) MM, (b) AM and (c) TF**

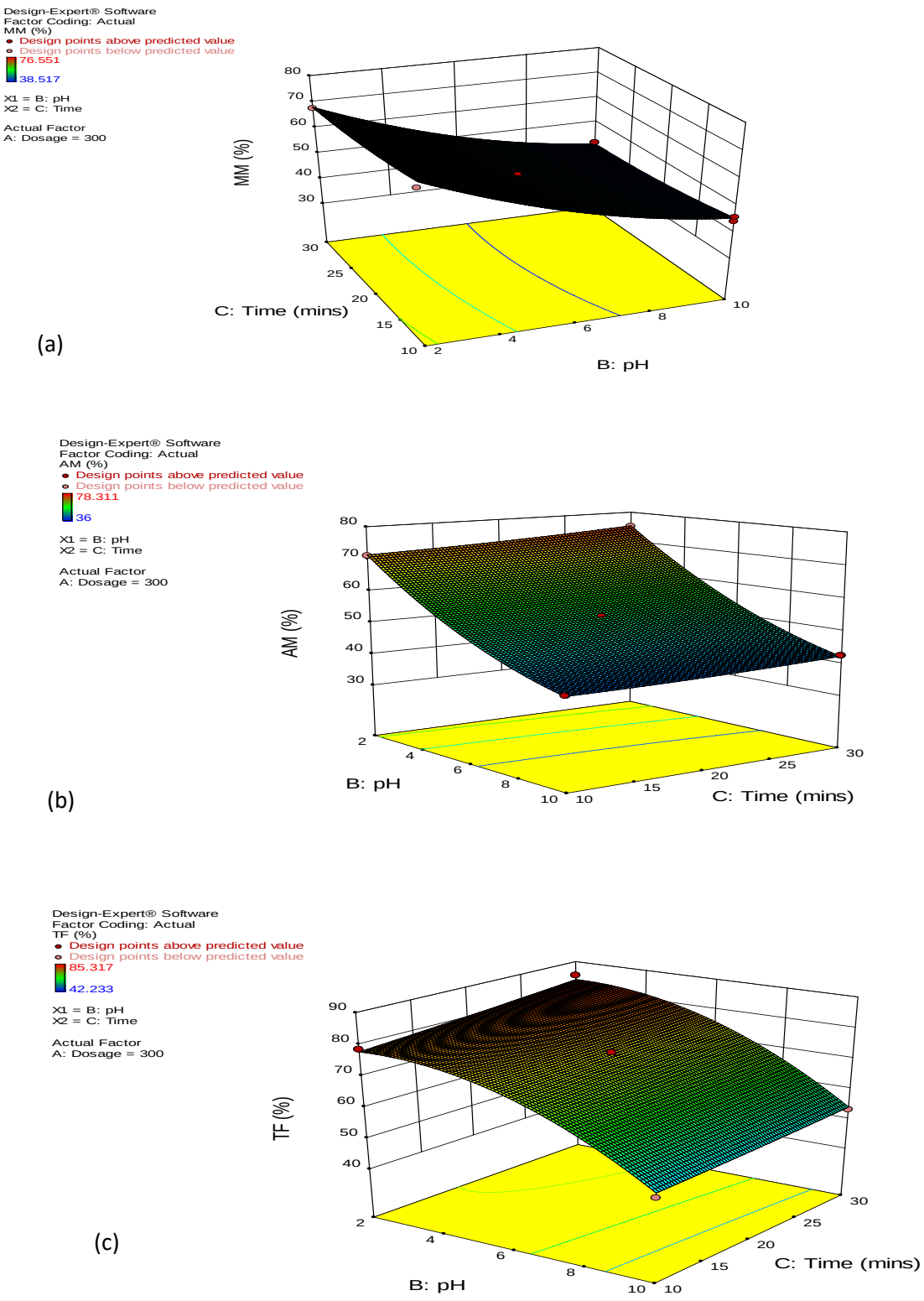


**Figure 4.18: 3D Surface of interactive effect of pH and time at dosage of 300 mg/L of (a) MM, (b) AM and (c) TF coagulants**

Figure 4.16a-c is 3D Surface of interactive effect between Dosage and pH at constant time of 20minutes for **(**a) MM, (b) AM and (c) TF coagulants. It can be inferred from the Figures that the colour removal efficiencies of the three coagulants increase as the pH of the solution decrease from pH 10-2. This behaviour can be explain on the basis of zero point charge of the coagulant ($pH_{zpc}$) which was found to be 7.800, 7.600 and 7.480 for MM, AM and TF respectively. Coagulant surface will have a positive charge when the solution pH is less than $pH_{zpc}$ (Mourabet *et al.*, 2013). In the solution with $pH_{zpc}$>pH, coagulant surface becomes positively charged and this will enhance coagulation of the colloid particles which are negatively charged making them to form floc due to increase in the force of attraction which lead to charge neutralization hence, easily removed during filtration. This mechanism will result to an increase in the colour removal efficiency. while in a solution with $pH_{zpc}$<pH, coagulant surface will have a negative charge therefore, a decrease in the colour removal efficiency as the pH increases from 2 to10 because of the repulsion of negatively charge ions (Mourabet *et al.*, 2013). Dosage in the same plots varied according to the coagulant.

In MM coagulant (Figure 4.16a), effect of the dosage on the colour removal efficiency increases as the dosage decreases from 500 mg/L to 100 mg/L, this is as a result of the decrease in the surface area of the coagulant (Rai *et al*., 2013) which led to re-stabilization of particles when the dosage increased above 100 mg/L. The highest response for colour removal efficiency lies at 76.50% at dosage of 100 mg/L and 34.40% at pH of 2. The highest response for colour removal efficiency of AM

coagulant at constant time of 20mins (Figure 4.16b) is 68.70% at dosage of 100 mg/L and 49.80% at pH 2. For TF coagulant (Figure 4.16c), it is 73.50% at dosage of 300 mg/L and 51.00% at pH of 2; this is because below this dosage there is no enough coagulant for destabilization and once exceeded this dosage there is bound to be re-stabilization of particles because of excess of dosage (Menkiti *et al*., 2016).

Figures 4.17 a-c are 3D Surface of interactive effect of dosage and time at pH of 6 for (a) MM, (b) AM and (c) TF. Visual inspection of the plots in Figures 4.17a-c disclose that time is another important variable that affect the colour removal efficiency. A general increase in time from 10-30 minutes promoted the removal efficiency of the colour from the effluent that is the time for destabilization of the colloid and formation of the floc (Survanka *et al.*, 2015; Okolo *et al*., 2015). The maximum response for colour removal efficiency of MM coagulant (Figure 4.17a) at constant pH of 6 is 60.00% at dosage of 100 mg/L and 40.00% at time of 30mins. For AM coagulant (Figure 4.17b), it is 49.00% at dosage of 500 mg/L and 50.00% at time of 30 mins. While for TF coagulant (Figure 4.17c), the highest colour removal efficiency is recorded at 61.00% at dosage of 150 mg/L and 60.00% at time of 30 minutes.

The same time increment was observed in the Figures 4.18a-c on the effect of the pH and time variables at middle level dosage of 300 mg/L on the colour removal efficiency. It was discovered that the colour removal efficiency of MM coagulants (Figure 4.18a) is 68.00% at time of 30 mins and 33.00% at pH 2. In AM coagulant

(Figure 4.18b), it is 70.00% at pH 2, and 28.00% at time of 30minute and finally in TF coagulant (Figure 4.18c), it is noted at 78.00% at pH 2 and 44.00% at time of 30minutes respectively. This results has similarity with the work of Okolo *et al*. (2015) and Menkiti *et al*., (2016) where they obtained optimum pH at 3 and 5, low dosage and high settling time respectively.

**Table 4.14: Box-Behnken experimental design matrix with % colour removal efficiency of the three modifiedcoagulants as responses**

| Run | Factor 1 Dosage(A) (mg/l) | Factor 2 pH (B) | Factor 3 Time (C) (mins) | MMM Colour Removal Efficiency(%) | MAM Colour Removal Efficiency(%) | MTF Colour Removal Efficiency(%) |
|---|---|---|---|---|---|---|
| 1 | 100.00 | 2.00 | 20.00 | 47.61 | 50.48 | 59.65 |
| 2 | 500.00 | 2.00 | 20.00 | 65.69 | 73.57 | 86.07 |
| 3 | 100.00 | 10.00 | 20.00 | 56.99 | 37.69 | 51.99 |
| 4 | 500.00 | 10.00 | 20.00 | 75.35 | 65.90 | 72.06 |
| 5 | 100.00 | 6.00 | 10.00 | 54.79 | 41.45 | 55.99 |
| 6 | 500.00 | 6.00 | 10.00 | 72.47 | 61.75 | 81.58 |
| 7 | 100.00 | 6.00 | 30.00 | 58.77 | 45.77 | 62.99 |
| 8 | 500.00 | 6.00 | 30.00 | 76.45 | 78.57 | 92.01 |
| 9 | 300.00 | 2.00 | 10.00 | 57.87 | 68.98 | 71.61 |
| 10 | 300.00 | 10.00 | 10.00 | 68.12 | 78.35 | 79.45 |
| 11 | 300.00 | 2.00 | 30.00 | 64.23 | 52.97 | 74.12 |
| 12 | 300.00 | 10.00 | 30.00 | 74.34 | 66.32 | 70.68 |
| 13 | 300.00 | 6.00 | 20.00 | 84.23 | 70.99 | 80.67 |
| 14 | 300.00 | 6.00 | 20.00 | 84.76 | 71.00 | 80.45 |
| 15 | 300.00 | 6.00 | 20.00 | 84.88 | 70.57 | 80.45 |
| 16 | 300.00 | 6.00 | 20.00 | 84.23 | 70.64 | 80.87 |
| 17 | 300.00 | 6.00 | 20.00 | 84.74 | 71.27 | 80.57 |

## 4.19 Result of Colour removal efficiency of the modified coagulants by Coagulation-flocculation method using Response surface methodology (RSM) design

Table 4.14 is Box-Behnken experimental design matrix with % efficiency of colour removal of the three coagulants as responses. The results in Table 4.20 were evaluated by multiple regression analysis and second order polynomial equation fitted between the responses represented by Colour removal efficiency (*Y*) and the input variable of Dosage (*A)*, pH (*B)* and Time (C*)*. The empirical models in terms of coded factors for coagulation-flocculation of MMM, MAM and MTF gave a quadratic equation.

**Table 4.15a: ANOVA for Response Surface Quadratic model for MMM coagulant**

| Source | Sum of Squares | df | Mean Square | F Value | p-value Prob > F | |
|---|---|---|---|---|---|---|
| Model | 2382.39 | 9 | 264.71 | 543.14 | < 0.0001 | significant |
| A-Dosage | 644.62 | 1 | 644.62 | 1322.64 | < 0.0001 | |
| B-pH | 193.94 | 1 | 193.94 | 397.93 | < 0.0001 | |
| C-Time | 52.70 | 1 | 52.70 | 108.13 | < 0.0001 | |
| AB | 0.020 | 1 | 0.020 | 0.040 | 0.8468 | |
| AC | 1.000E-006 | 1 | 1.000E-006 | 2.052E-006 | 0.9989 | |
| BC | 4.543E-003 | 1 | 4.543E-003 | 9.321E-003 | 0.9258 | |
| $A^2$ | 590.66 | 1 | 590.66 | 1211.94 | < 0.0001 | |
| $B^2$ | 539.34 | 1 | 539.34 | 1106.62 | < 0.0001 | |
| $C^2$ | 212.66 | 1 | 212.66 | 436.34 | < 0.0001 | |
| Residual | 3.41 | 7 | 0.49 | | | |
| Lack of Fit | 3.02 | 3 | 1.01 | 10.38 | 0.0234 | Significant |
| Pure Error | 0.39 | 4 | 0.097 | | | |
| Cor Total | 2385.80 | 16 | | | | |
| R-Squared | 0.9943 | | | | | |
| Adj R-Squared | 0.9870 | | | | | |
| Pred R-Squared | 0.9127 | | | | | |
| Adeq Precision | 41.756 | | | | | |

## Table 4.15b: ANOVA for Response Surface Quadratic model for MAM coagulant

| Source | Sum of Squares | df | Mean Square | F Value | p-value Prob > F | |
|---|---|---|---|---|---|---|
| Model | 2533.85 | 9 | 281.54 | 499.98 | < 0.0001 | Significant |
| A-Dosage | 1362.47 | 1 | 1362.47 | 2419.60 | < 0.0001 | |
| B-pH | 228.22 | 1 | 228.22 | 405.30 | < 0.0001 | |
| C-Time | 181.21 | 1 | 181.21 | 321.82 | < 0.0001 | |
| AB | 6.56 | 1 | 6.56 | 11.65 | 0.0112 | |
| AC | 39.06 | 1 | 39.06 | 69.37 | < 0.0001 | |
| BC | 0.80 | 1 | 0.80 | 1.42 | 0.2716 | |
| $A^2$ | 675.18 | 1 | 675.18 | 1199.04 | < 0.0001 | |
| $B^2$ | 8.81 | 1 | 8.81 | 15.64 | 0.0055 | |
| $C^2$ | 9.08 | 1 | 9.08 | 16.13 | 0.0051 | |
| Residual | 3.94 | 7 | 0.56 | | | |
| Lack of Fit | 3.01 | 3 | 1.00 | 4.30 | 0.0964 | not significant |
| Pure Error | 0.93 | 4 | 0.23 | | | |
| Cor Total | 2537.79 | 16 | | | | |
| R-Squared | 0.9984 | | | | | |
| Adj R-Squared | 0.9964 | | | | | |
| Pred R-Squared | 0.9805 | | | | | |
| Adeq Precision | 71.959 | | | | | |

**Table 4.15c: ANOVA for Response Surface Quadratic model for MTF coagulant**

| Source | Sum of Squares | df | Mean Square | F Value | p-value Prob > F | |
|---|---|---|---|---|---|---|
| Model | 2183.40 | 9 | 242.60 | 163.00 | < 0.0001 | Significant |
| A-Dosage | 1277.37 | 1 | 1277.37 | 858.26 | < 0.0001 | |
| B-pH | 249.46 | 1 | 249.46 | 167.61 | < 0.0001 | |
| C-Time | 185.88 | 1 | 185.88 | 124.89 | < 0.0001 | |
| AB | 10.05 | 1 | 10.05 | 6.75 | 0.0355 | |
| AC | 2.94 | 1 | 2.94 | 1.98 | 0.2026 | |
| BC | 7.41 | 1 | 7.41 | 4.98 | 0.0608 | |
| $A^2$ | 100.35 | 1 | 100.35 | 67.42 | < 0.0001 | |
| $B^2$ | 285.74 | 1 | 285.74 | 191.99 | < 0.0001 | |
| $C^2$ | 27.16 | 1 | 27.16 | 18.25 | 0.0037 | |
| Residual | 10.42 | 7 | 1.49 | | | |
| Lack of Fit | 10.19 | 3 | 3.40 | 58.96 | 0.0009 | Significant |
| Pure Error | 0.23 | 4 | 0.058 | | | |
| Cor Total | 2193.82 | 16 | | | | |
| R-Squared | 0.9953 | | | | | |
| Adj R-Squared | 0.9891 | | | | | |
| Pred R-Squared | 0.9255 | | | | | |
| Adeq Precision | 43.441 | | | | | |

The statistical significance of the quadratic model was evaluated by the Analysis of variance (ANOVA), as presented in Tables 4.15a, 4.15b, 4.15c. The term with *p* values more than 0.05 are insignificant while <0.05 is significant. From Table 4.15a-c the regression model of quadratic equation that fit the data is statistical significant because it Probability value (P-values) is <0.0001 for all the coagulant. This means that the model is significant at 95% confidence level by the Fisher's test (F). F-values obtained from the model are 543.14, 499.98 and 163.00 for MMM, MAM and MTF respectively.

The quadratic equation obtained from the ANOVA is given in equation 4.7 (MMM), 4.8 (MAM) and 4.9(MTF) respectively for the three coagulants.

$$Y = +84.57 + 8.98A + 4.92B + 2.57C + 0.07AB - 5.000E - 004AC - 0.034BC - 11.82A^2 - 11.32B^2 - 7.11C^2 \quad 4.7$$

$$Y = +71.02 + 13.05A - 5.34B + 4.76C + 1.28AB + 3.13AC - 0.45BC - 12.66A^2 - 1.45B^2 - 1.47C^2 \quad 4.8$$

$$Y = +80.56 + 12.61A - 5.58B + 4.82C - 1.59AB + 0.86AC + 1.36BC - 4.88A^2 - 8.24B^2 - 2.54C^2 \quad 4.9$$

For a regression model that is statistically significant to be developed, the insignificant terms in equation 4.6 to 4.9 is eliminated. The term with *p* values more than 0.05 are insignificant (Table 4.15a-c) and hence removed to obtain the regression model equation 4.10 to 4.12. Therefore, in Table 4.15a (MMM coagulant) the significant terms are A, B, C, $A^2$, $B^2$, and $C^2$ while the insignificant terms are AB, AC and BC. These insignificant terms are removed from the quadratic model equation 4.7 and the equation 4.10 is generated. This same thing is applicable in Table 4.15b (for MAM coagulant) , the significant terms are A, B, C,AB, AC, and $A^2$, while the insignificant model terms are BC, $B^2$, and $C^2$. These insignificant terms are removed from equation 4.8 and equation 4.11 is obtained. In Table 4.15c (for MTF coagulant), the significant terms are A, B, C, AB, $A^2$, $B^2$ and $C^2$, while the insignificant terms are AB, and BC and equation 4.9 is reduced to equation 4.12. Positive sign in front of equations 4.10 -4.12 indicate

synergistic effect of the factors, whereas negative sign indicates antagonistic factor effect (Obiora-Okafor and Onukwuli, 2015).

$$Y_{MMM} = +84.57 + 8.98A + 4.92B + 2.57C - 11.82A^2 - 11.32B^2 - 7.11C^2 \quad 4.10$$

$$Y_{MAM} = +71.02 + 13.05A - 5.34B + 4.76C + 1.28AB + 3.13AC - 12.66A^2 \quad 4.11$$

$$Y_{MTF} = +80.56 + 12.61A - 5.58B + 4.82C - 1.59AB - 4.88A^2 - 8.24B^2 - 2.54C^2 \quad 4.12$$

In the same Tables 4.15a-c, the model exhibited significant lack of fit for MMM and MTF while insignificant lack of fit for MAM. Lack of fit test measures the failure of the model to represent data in experimental domain at points that are not included in the regression (Obiora-Okafor and Onukwuli, 2015). If a model is significant and shows insignificant lack of fit, it does not mean that the model is a good one. Significant lack of fit may occur due to noise or some important variables were left out of the experiment, then it is possible that the portion of the variability in the data not explained by the model also called residual could be large. Therefore, what measures the overall performance of a model is $R^2$. When predicted $R^2$ and adjusted $R^2$ differ dramatically, there is a good chance that non-significant terms have been included in the model (Thuy and Lim, 2011). The Predicted $R^2$ of the three coagulants studied is 0.9127, 0.9805 and 0.9255 for MMM, MAM and MTF respectively, and they are in reasonable agreement with the adjusted $R^2$ of 0.9870, 0.9964 and 0.9891 for MMM, MAM, and MTF respectively i.e. their difference is less than 0.2. Adequate Precision measures the signal to noise ratio. A ratio greater than 4 is desirable. The ratio obtained from all three

coagulants proved an adequate signal. A high $R^2$ value close to 1 is desirable and ensures a satisfactory adjustment of the quadratic model to the experimental data. A reliable model should also be able to predict response with a reasonable accuracy when compared with the experimental data. Figures 4.19a-c are the plots of Predicted versus Actual data for MMM, MAM and MTF coagulants. It compares experimental colour removal efficiencies (%) with the predicted values obtained from the models. The Figures indicated good agreement between the experimental and predicted values in the three coagulants. The observed points on these plots revealed that the actual values are distributed relatively near to the straight line in most cases, indicating that the regression model is able to predict these removal efficiencies. A close relationship between predicted and experimental data indicates a good fit.

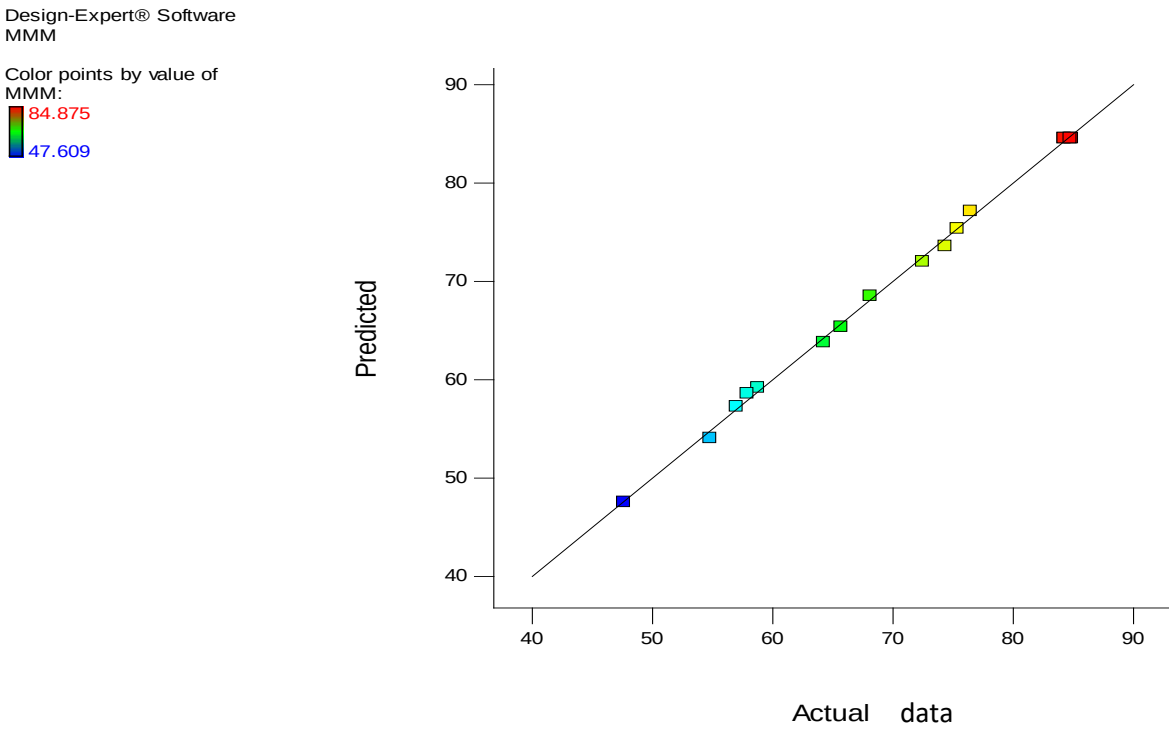


**Figure 4.19a: A plot of Predicted versus Actual data for MMM coagulant**

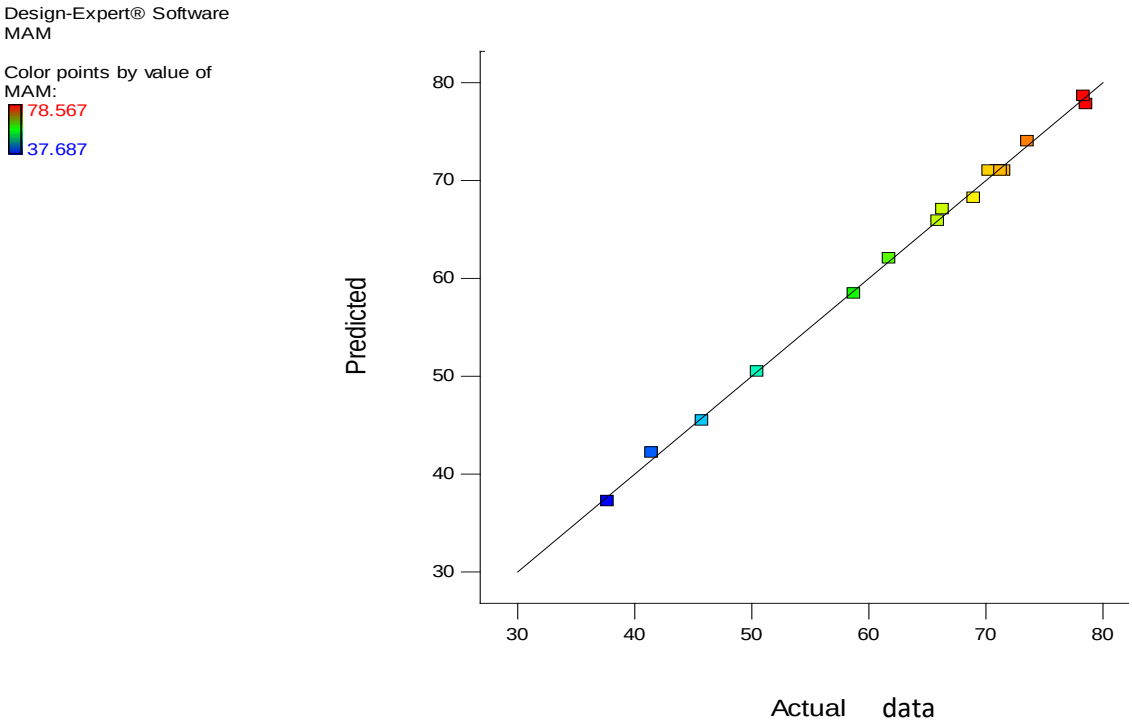


**Figure 4.19b: A plot of Predicted versus Actual data for MAM coagulant**

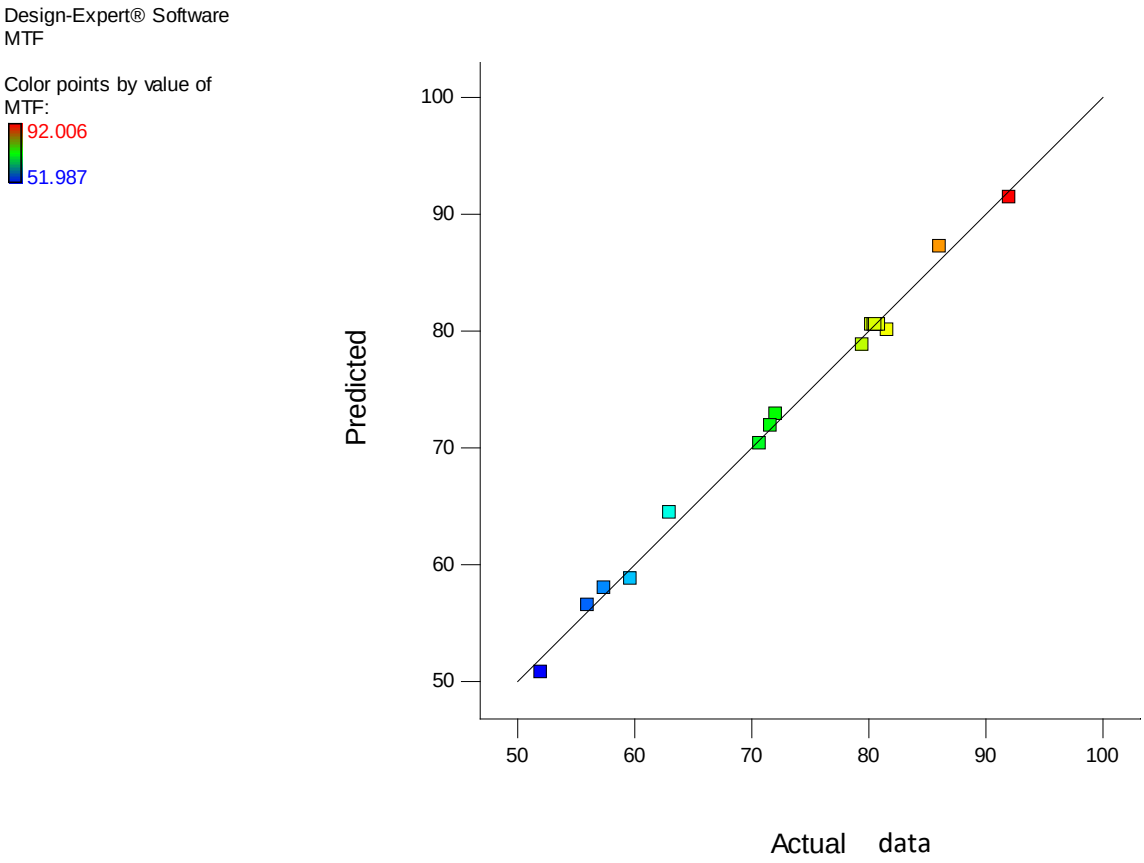


**Figure 4.19c: A plot of Predicted versus Actual data for MTF coagulant**

## 4. 20 Effect of interactive variables (dosage, pH and time) of modified coagulants

The response surface plots shows that the maximum colour removal efficiencies are located inside the design boundary. To understand the impact of each variable, 3D surface plot were plotted for the estimated responses, which were the foundation of second order polynomial function.

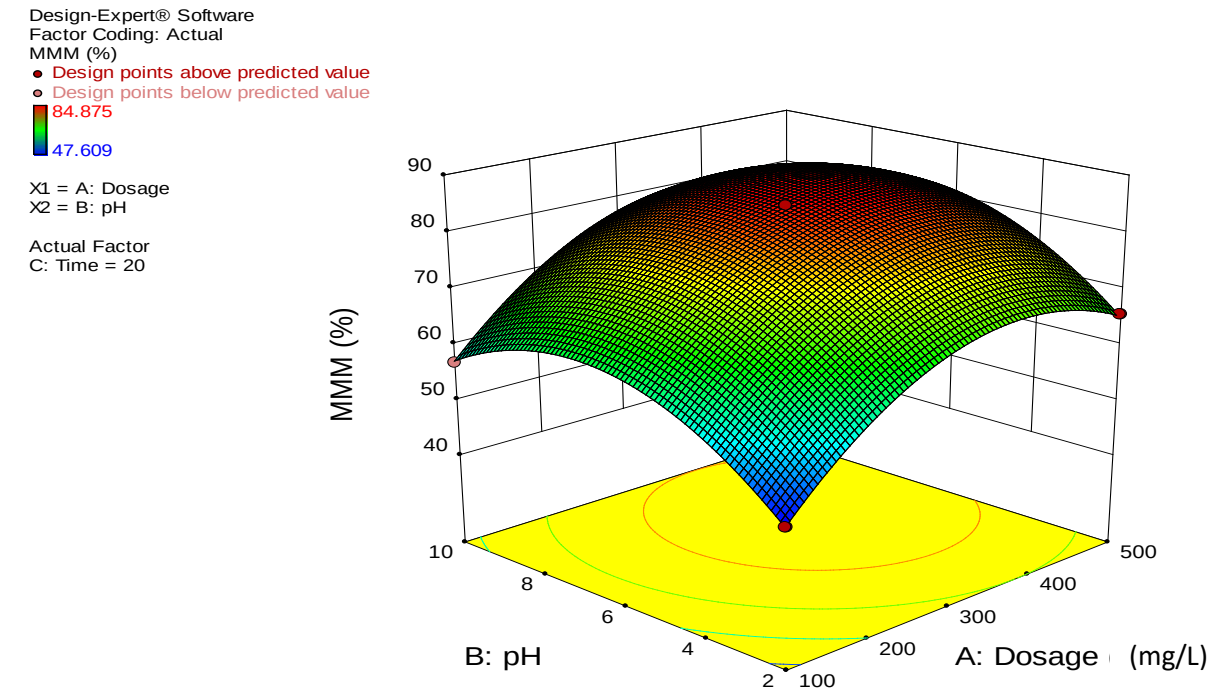
Design-Expert® Software
Factor Coding: Actual
MMM (%)
Design points above predicted value
Design points below predicted value
84.875
47.609
X1 = A: Dosage
X2 = B: pH
Actual Factor
C: Time = 20
MMM (%)
90
80
70
60
50
40
10
8
6
4
2
B: pH
100
200
300
400
500
A: Dosage (mg/L)

(a)

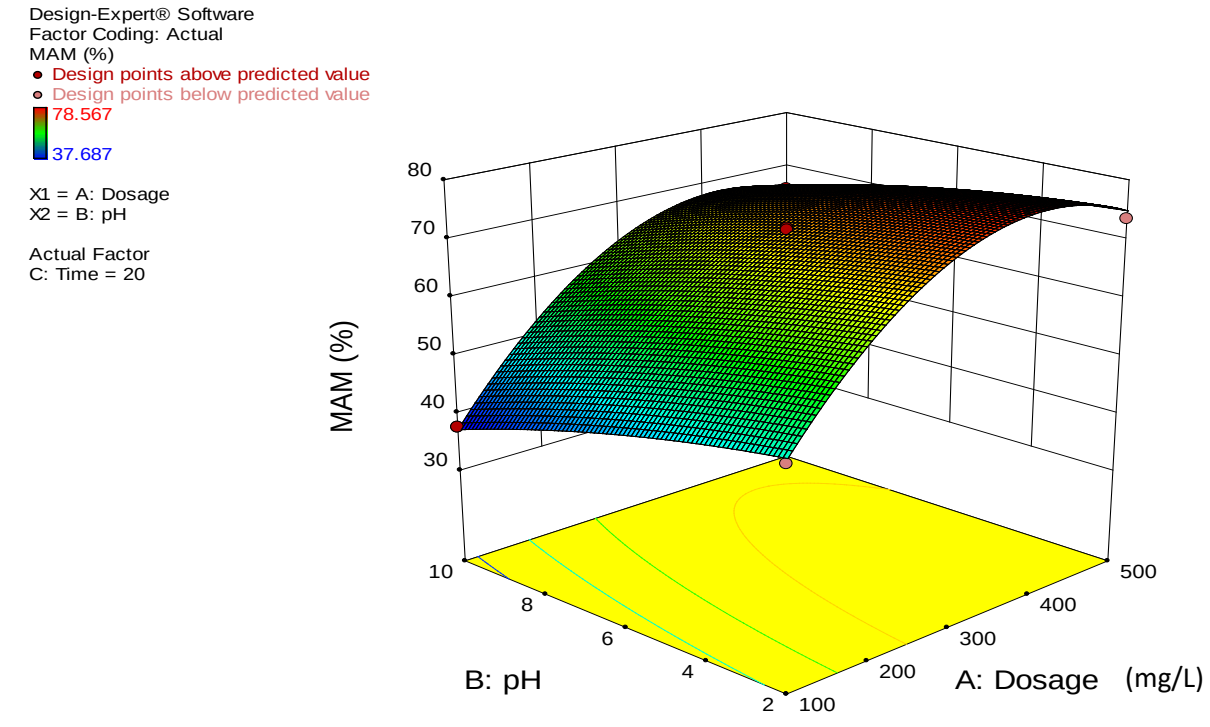
Design-Expert® Software
Factor Coding: Actual
MAM (%)
Design points above predicted value
Design points below predicted value
78.567
37.687
X1 = A: Dosage
X2 = B: pH
Actual Factor
C: Time = 20
MAM (%)
80
70
60
50
40
30
10
8
6
4
2
B: pH
100
200
300
400
500
A: Dosage (mg/L)

(b)

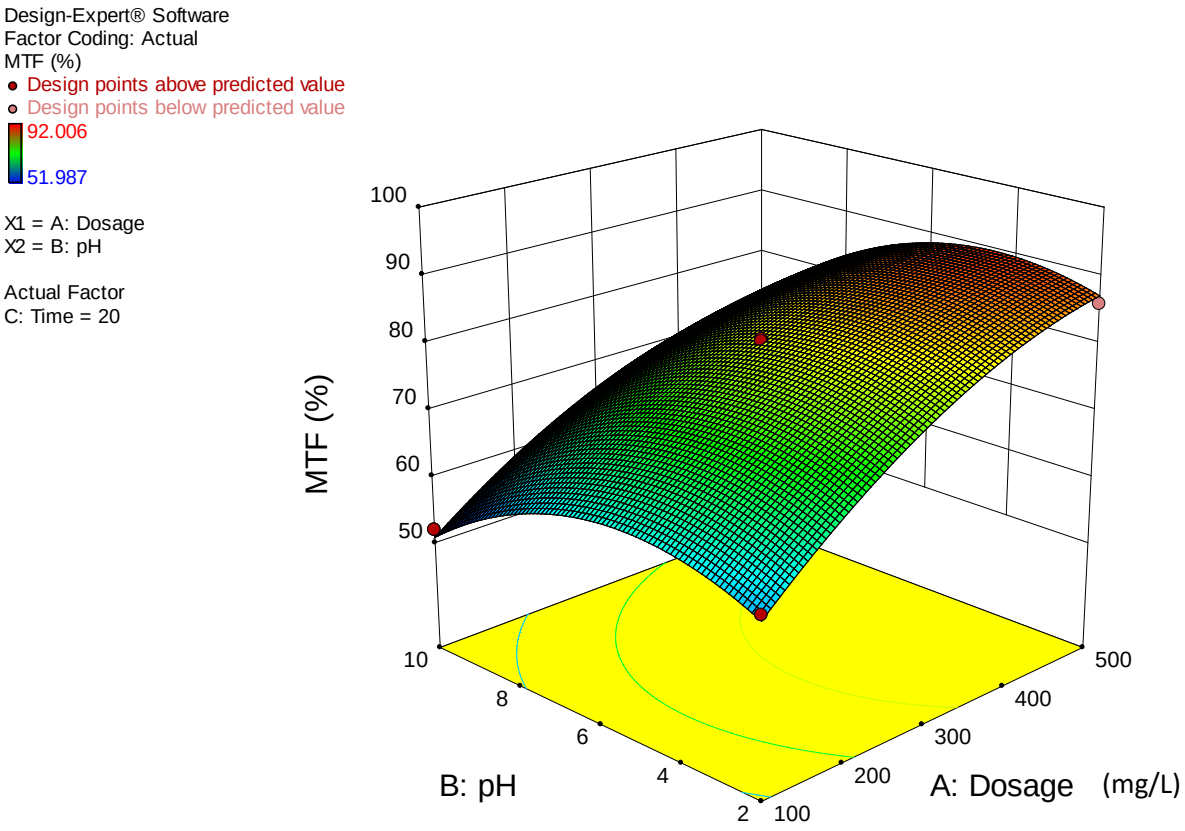


(c)

**Figure 4.20a-c: 3D Surface of interactive effect between Dosage and pH at middle level time of 20 minutes for (a) MMM, (b) MAM and (c) MTF coagulants**

Figures 4.20a-c show the surface plot of effect of dosage and pH at middle level time of 20 minutes. It can be seen from the Figures 4.20a that the colour removal efficiencies of the coagulant increases as the pH of the solution increased from pH 2 to 8. The maximum colour removal efficiency is 60% obtained at pH of 8. There was decrease in colour removal efficiency at pH 10 because of charge reversal. This can be explain on the basis of interparticle bridging mechanism by compression of adsorbed chain, where negative charges compressed and form a long loop that finally sediment

and filtered off (Roussy and Van Vooren 2008; Nharingo and Moyo 2015). Dosage in the same plots increases in the colour removal efficiency from 100 mg/l to 500 mg/l this is because of the large surface area (Mourabet *et al.,* 2013). Figures 4.20b and 4.20c demonstrated a different trend with pH. Careful examination of the Figures show that colour removal efficiency increases with decrease in pH from 10 to 2.This can be explain by pH of zero point charge of the coagulant ($pH_{zpc}$) which were found to be 7.800 and 7.900 for MAM and MTF respectively. Coagulant surface will have a positive charge when the solution pH is less than $pH_{zpc}$. In the solution with $pH_{zpc}$>pH, coagulant surface becomes positively charged, this will enhance coagulation of the colloid particles which are negatively charged making them to form floc due to increase in the force of attraction hence easily removed during filtration (Mourabet *et al*., 2013). Effect of the dosage on the colour removal efficiency increases as the dosage increases from 100 mg/L to 500 mg/L, in both MAM and MTF coagulants, this is as a result of increase in the surface area of the coagulant (Rai *et al*., 2013). The colour removal efficiency of MMM coagulant with dosage at the middle level of time 20 mins is 65.00% at dosage of 400 mg/L. For MAM coagulant it is 74.00% at dosage of 400 mg/L. While for MTF coagulant, it is 86.00% at dosage of 500 mg/L. A similar trend is observed in the work of Abdullah and Ahmad, (2016) where white Popinac seed was use to treat turbidity in River water, the turbidity removal was found to be 76% as the dosage increase to 50 mg/L.

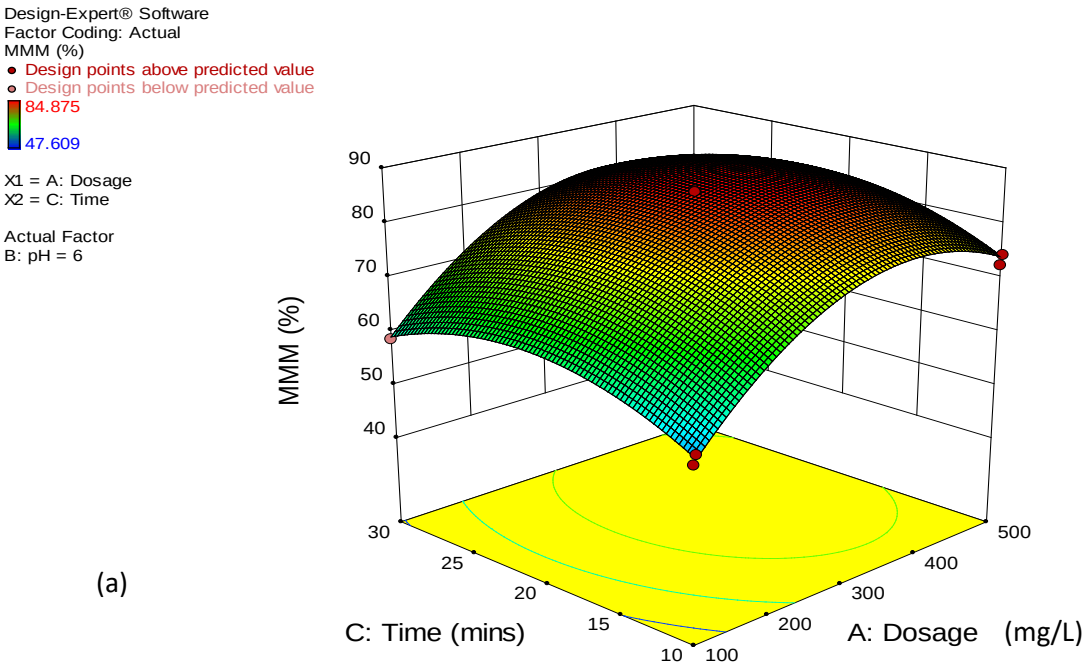
Design-Expert® Software
Factor Coding: Actual
MMM (%)
Design points above predicted value
Design points below predicted value
84.875
47.609
X1 = A: Dosage
X2 = C: Time
Actual Factor
B: pH = 6
MMM (%)
90
80
70
60
50
40
30
25
20
15
10
C: Time (mins)
100
200
300
400
500
A: Dosage (mg/L)

(a)

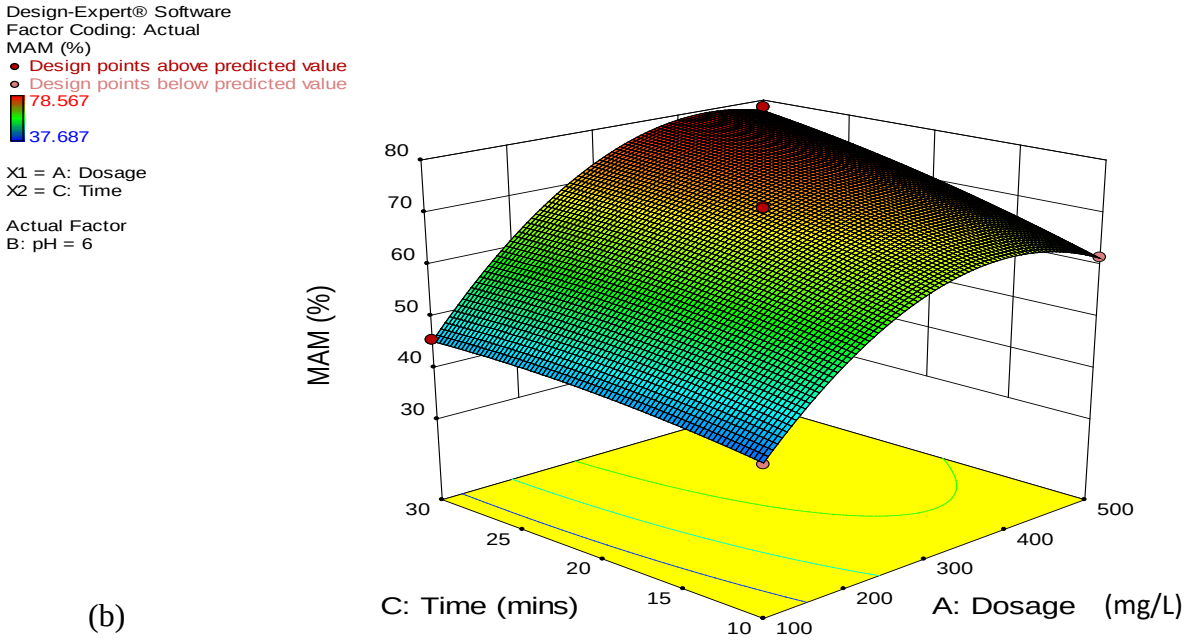
Design-Expert® Software
Factor Coding: Actual
MAM (%)
Design points above predicted value
Design points below predicted value
78.567
37.687
X1 = A: Dosage
X2 = C: Time
Actual Factor
B: pH = 6
MAM (%)
80
70
60
50
40
30
30
25
20
15
10
C: Time (mins)
100
200
300
400
500
A: Dosage (mg/L)

(b)

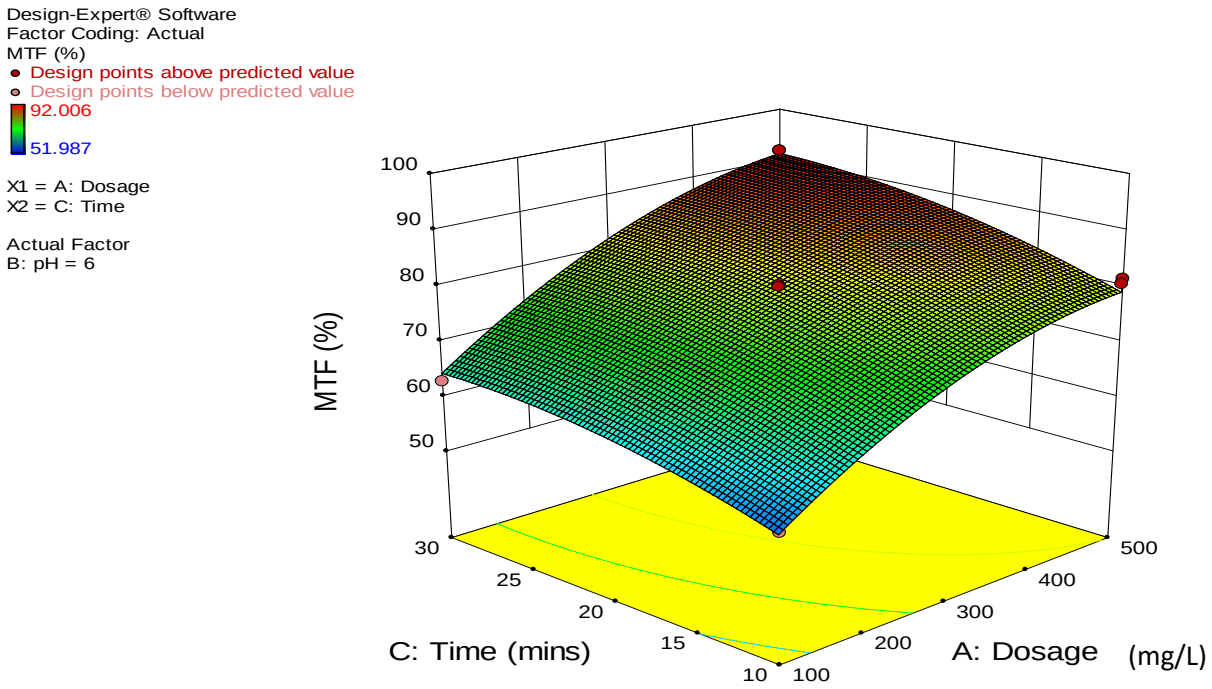


(c)

**Figure 4.21: 3D Surface of interactive effect of dosage and time at middle level pH of 6 for (a) MMM, (b) MAM and (c) MTF coagulants**

Figures 4.21a-c are the 3D Surface of interactive effect between Dosage and time at middle level pH of 6 for (a) MMM, (b) MAM and (c) MTF coagulants. From the plots in Figures 4.21a-c it can be deduce that time is another important variable that affect the colour removal efficiency. A general increase in time from 10-30 minutes promoted the removal efficiency of the colour from the effluent that is the time for destabilization of the colloid and formation of the floc (Survanka *et al*., 2015; Okolo *et al*., 2015). The maximum response for colour removal efficiency of MMM coagulants, (Figure 4.21a) at middle level pH of 6 are 72.00% at dosage of 500 mg/L and 56.00% at time of 30 mins. For MAM coagulant (Figure 4.21b) the highest response at the constant pH of 6 is 62.00% at dosage of 500 mg/L and 45.00% at the time of 30 mins. For MTF

coagulant (Figure 4.21c), it is 80.00% at dosage of 500 mg/L and 63.00% at the time of 30 minutes. Similar trend of time increment was observed in the Figure 4.22a-c on the effect of the pH and time variables at middle level dosage of 300 mg/L on the colour removal efficiency. It was discovered that the colour removal efficiency of MMM, MAM and MTF coagulants at the constant dosage of 300 mg/L were 68.00% at pH 8 and 63.00% at the time of 30 minutes, 59.00% at pH 2 and 79.00% at the time of 30 minute and finally 58.00% at pH of 2 and 80.00% at the time of 30minutes respectively.

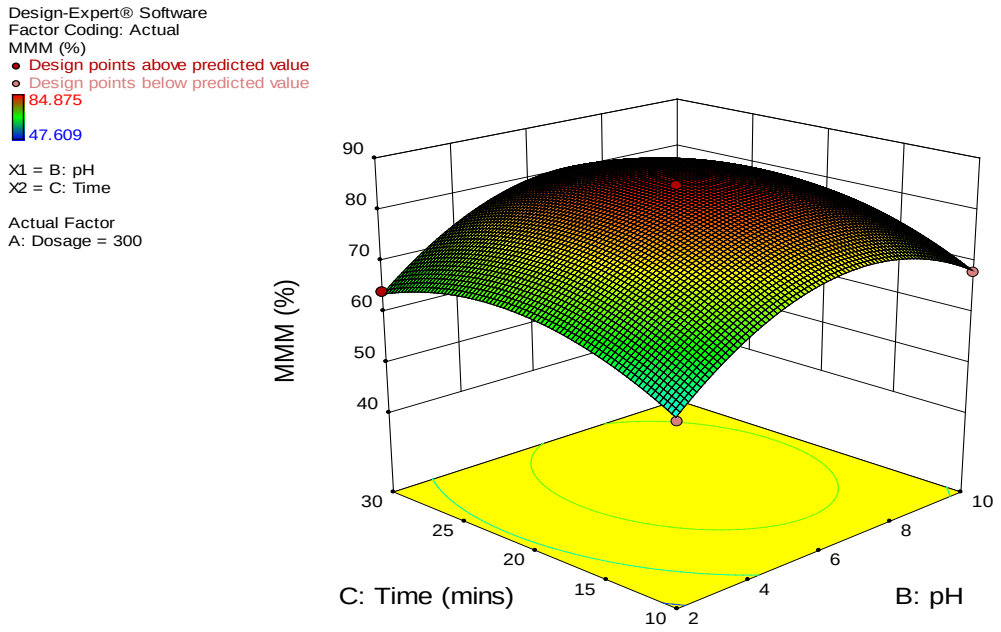


(a)

(b)

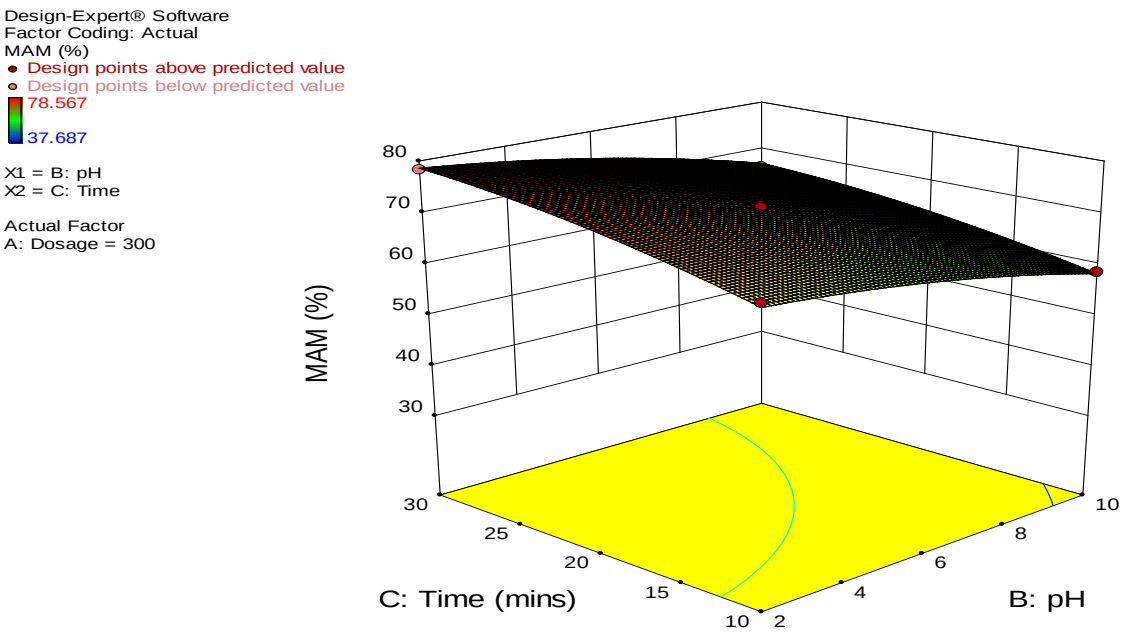


(c)

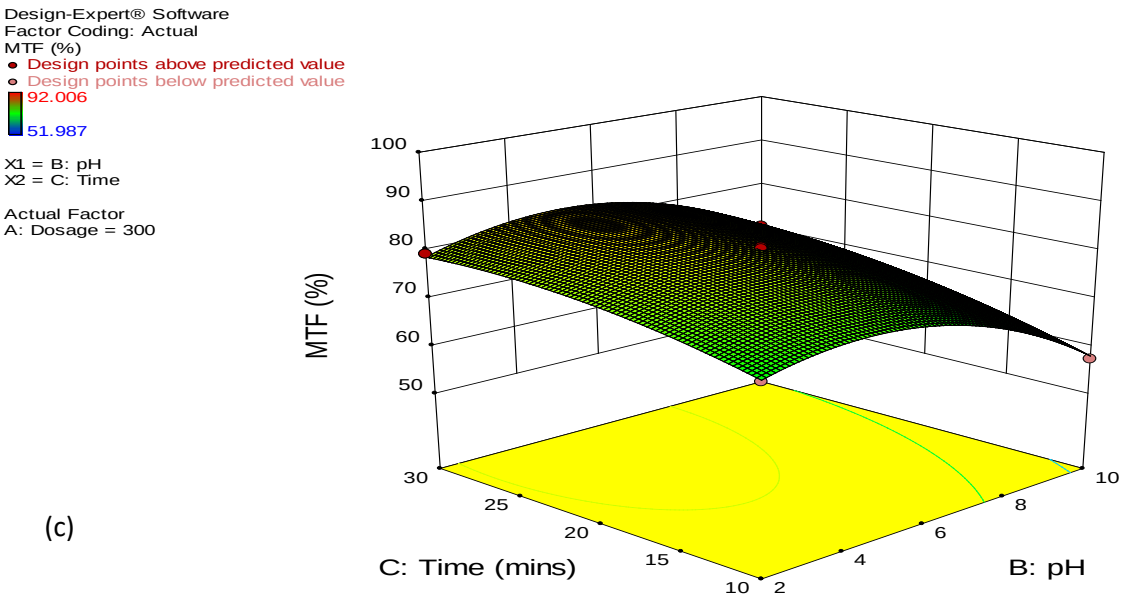


**Figure 4.22: 3D Surface of interactive effect of pH and time at middle level dosage of 300 mg/L for (a) MMM, (b) MAM and (c) MTF coagulants**

## Table 4.16: Optimal solution of colour removal efficiency of MM coagulant

| Number | Dosage(mg/L) | pH | Time(mins) | %MM | Std Error | Desirability |
|---|---|---|---|---|---|---|
| 1 | 204.915 | 9.556 | 25.919 | 43.554 | 0.361 | 1.000 |
| 2 | 100.000 | 10.000 | 20.000 | 46.397 | 0.490 | 1.000 |
| 3 | 300.000 | 6.000 | 20.000 | 50.666 | 0.253 | 1.000 |
| 4 | 300.000 | 10.000 | 10.000 | 43.900 | 0.490 | 1.000 |
| 5 | 500.000 | 2.000 | 20.000 | 64.408 | 0.490 | 1.000 |
| 6 | 100.000 | 6.000 | 10.000 | 60.046 | 0.490 | 1.000 |
| 7 | 500.000 | 10.000 | 20.000 | 39.129 | 0.490 | 1.000 |
| 8 | 100.000 | 2.000 | 20.000 | 75.939 | 0.490 | 1.000 |
| 9 | 300.000 | 2.000 | 10.000 | 71.741 | 0.490 | 1.000 |
| 10 | 300.000 | 10.000 | 30.000 | 41.230 | 0.490 | 1.000 |
| 11 | 300.000 | 2.000 | 30.000 | 68.211 | 0.490 | 1.000 |
| 12 | 100.000 | 6.000 | 30.000 | 56.168 | 0.490 | 1.000 |
| 13 | 500.000 | 6.000 | 30.000 | 47.547 | 0.490 | 1.000 |
| 14 | 121.885 | 6.751 | 22.283 | 53.062 | 0.310 | 1.000 |
| 15 | 461.570 | 7.678 | 25.088 | 42.950 | 0.318 | 1.000 |
| 16 | 118.982 | 7.227 | 11.402 | 54.549 | 0.414 | 1.000 |
| 17 | 106.329 | 7.981 | 14.958 | 51.600 | 0.379 | 1.000 |
| 18 | 400.310 | 7.371 | 15.119 | 45.603 | 0.261 | 1.000 |
| 19 | 377.885 | 9.829 | 21.496 | 40.157 | 0.339 | 1.000 |
| 20 | 123.368 | 7.422 | 29.838 | 50.748 | 0.456 | 1.000 |

## Table 4.17: Optimal solution of colour removal efficiency of AM coagulant

| Number | Dosage(mg/L) | pH | Time(mins) | AM (%) | Std Error | Desirability |
|---|---|---|---|---|---|---|
| 1 | 232.402 | 6.380 | 27.787 | 51.176 | 0.143 | 1.000 |
| 2 | 300.000 | 6.000 | 20.000 | 53.061 | 0.127 | 1.000 |
| 3 | 100.000 | 10.000 | 20.000 | 36.353 | 0.246 | 1.000 |
| 4 | 500.000 | 6.000 | 30.000 | 60.359 | 0.246 | 1.000 |
| 5 | 300.000 | 2.000 | 10.000 | 71.283 | 0.246 | 1.000 |
| 6 | 100.000 | 2.000 | 20.000 | 68.285 | 0.246 | 1.000 |
| 7 | 500.000 | 10.000 | 20.000 | 46.217 | 0.246 | 1.000 |
| 8 | 500.000 | 2.000 | 20.000 | 77.958 | 0.246 | 1.000 |
| 9 | 100.000 | 6.000 | 10.000 | 47.778 | 0.246 | 1.000 |
| 10 | 300.000 | 10.000 | 10.000 | 40.725 | 0.246 | 1.000 |
| 11 | 100.000 | 6.000 | 30.000 | 49.888 | 0.246 | 1.000 |
| 12 | 300.000 | 2.000 | 30.000 | 75.376 | 0.246 | 1.000 |
| 13 | 500.000 | 6.000 | 10.000 | 56.843 | 0.246 | 1.000 |
| 14 | 280.242 | 3.870 | 11.528 | 61.031 | 0.159 | 1.000 |
| 15 | 177.035 | 2.328 | 23.319 | 68.722 | 0.181 | 1.000 |
| 16 | 114.417 | 7.854 | 26.857 | 42.907 | 0.196 | 1.000 |
| 17 | 357.827 | 7.730 | 20.782 | 48.444 | 0.125 | 1.000 |
| 18 | 301.617 | 9.691 | 22.005 | 41.930 | 0.159 | 1.000 |
| 19 | 316.287 | 9.955 | 27.637 | 42.420 | 0.205 | 1.000 |
| 20 | 200.583 | 4.511 | 21.352 | 57.372 | 0.126 | 1.000 |

**Table 4.18: Optimal solution of colour removal efficiency of TF coagulant**

| Number | Dosage(mg/L) | pH | Time(mins) | %TF | Std Error | Desirability |
|---|---|---|---|---|---|---|
| 1 | 315.147 | 6.972 | 24.786 | 71.495 | 0.593 | 1.000 |
| 2 | 100.000 | 2.000 | 20.000 | 73.619 | 1.163 | 1.000 |
| 3 | 300.000 | 6.000 | 20.000 | 74.335 | 0.601 | 1.000 |
| 4 | 100.000 | 6.000 | 10.000 | 62.249 | 1.163 | 1.000 |
| 5 | 100.000 | 6.000 | 30.000 | 67.959 | 1.163 | 1.000 |
| 6 | 300.000 | 10.000 | 30.000 | 54.108 | 1.163 | 1.000 |
| 7 | 300.000 | 2.000 | 30.000 | 83.826 | 1.163 | 1.000 |
| 8 | 300.000 | 2.000 | 10.000 | 77.920 | 1.163 | 1.000 |
| 9 | 500.000 | 6.000 | 30.000 | 68.931 | 1.163 | 1.000 |
| 10 | 500.000 | 10.000 | 20.000 | 48.080 | 1.163 | 1.000 |
| 11 | 500.000 | 2.000 | 20.000 | 71.298 | 1.163 | 1.000 |
| 12 | 300.000 | 10.000 | 10.000 | 51.604 | 1.163 | 1.000 |
| 13 | 126.667 | 9.467 | 21.333 | 47.660 | 0.937 | 1.000 |
| 14 | 305.486 | 3.833 | 15.570 | 78.577 | 0.610 | 1.000 |
| 15 | 360.159 | 8.397 | 24.230 | 63.862 | 0.628 | 1.000 |
| 16 | 446.325 | 2.794 | 24.298 | 76.735 | 0.848 | 1.000 |
| 17 | 347.088 | 5.651 | 26.272 | 76.624 | 0.614 | 1.000 |
| 18 | 475.002 | 3.285 | 24.812 | 74.704 | 0.887 | 1.000 |
| 19 | 268.274 | 4.329 | 20.379 | 78.699 | 0.591 | 1.000 |
| 20 | 247.505 | 6.920 | 17.093 | 69.076 | 0.587 | 1.000 |

## 4.21 Optimization of coagulation-flocculation process for unmodified coagulants

Numerical optimization is applied from BBD design to obtain a desirable value and optimum process parameters to achieve highest treatment performance for colour removal efficiency of the three coagulants used for each input factors and response can be selected. Equations 4.4, 4.5 and 4.6 were solved for the best solutions such that the responses ($Y_{MM,}$ $Y_{AM}$, $Y_{TF}$) are maximized within the design space. Tables 4.16 to 4.18 are the optimal solutions of colour removal efficiency of MM, AM and TF coagulants.

The Tables also indicate the solution to the equation of our model which has been solved by BBD design and suggested several optimum colour removal efficiency of the coagulants. In Table 4.16 the maximum colour removal efficiency of MM coagulant is 75.939% at dosage of 100 mg/L, pH of 2 and time of 20 minutes. Table 4.17 gives the same optimal solution of AM coagulant for colour removal efficiency of 77.958% at dosage of 500 mg/L, pH of 2 and time of 20 mins. Again Table 4.18 shows the maximum colour removal efficiency of 83.826% at dosage of 300 mg/L, time of 30 mins and pH of 2 for TF coagulant. This is as a result of increase in surface area and porosities of these coagulants as recorded in Table 4.1. Therefore, the order of optimum colour removal efficiency of the three coagulants studied is MM<AM<TF. The SEM and FTIR results of TF also confirmed that TF is the best coagulant out of these three.

**Table 4.19: Optimal solution of colour removal efficiency of MMM coagulant**

| Number | Dosage (mg/L) | pH | Time(mins) | MMM | Std Err(MMM) | Desirability |
|---|---|---|---|---|---|---|
| 1 | 167.289 | 4.438 | 20.833 | 69.934 | 0.329 | 1.000 |
| 2 | 500.000 | 6.000 | 10.000 | 72.029 | 0.605 | 1.000 |
| 3 | 100.000 | 6.000 | 30.000 | 59.209 | 0.605 | 1.000 |
| 4 | 300.000 | 10.000 | 30.000 | 73.601 | 0.605 | 1.000 |
| 5 | 500.000 | 2.000 | 20.000 | 65.390 | 0.605 | 1.000 |
| 6 | 100.000 | 2.000 | 20.000 | 47.577 | 0.605 | 1.000 |
| 7 | 300.000 | 10.000 | 10.000 | 68.535 | 0.605 | 1.000 |
| 8 | 500.000 | 6.000 | 30.000 | 77.161 | 0.605 | 1.000 |
| 9 | 100.000 | 10.000 | 20.000 | 57.285 | 0.605 | 1.000 |
| 10 | 300.000 | 2.000 | 30.000 | 63.822 | 0.605 | 1.000 |
| 11 | 300.000 | 2.000 | 10.000 | 58.621 | 0.605 | 1.000 |
| 12 | 100.000 | 6.000 | 10.000 | 54.075 | 0.605 | 1.000 |
| 13 | 500.000 | 10.000 | 20.000 | 75.378 | 0.605 | 1.000 |
| 14 | 369.207 | 6.061 | 14.146 | 82.393 | 0.317 | 1.000 |
| 15 | 138.062 | 2.707 | 28.976 | 54.463 | 0.603 | 1.000 |
| 16 | 431.899 | 3.061 | 22.622 | 75.768 | 0.385 | 1.000 |
| 17 | 160.711 | 9.965 | 19.147 | 66.016 | 0.486 | 1.000 |
| 18 | 354.689 | 8.212 | 11.060 | 77.452 | 0.419 | 1.000 |
| 19 | 116.269 | 3.708 | 21.867 | 60.062 | 0.428 | 1.000 |
| 20 | 325.662 | 5.843 | 29.840 | 80.960 | 0.415 | 1.000 |

**Table 4.20: Optimal solution of colour removal efficiency of MAM coagulant**

| Number | Dosage(mg/L) | pH | Time(mins) | MAM | Std Err(MAM) | Desirability |
|---|---|---|---|---|---|---|
| 1 | 325.514 | 4.308 | 17.014 | 72.679 | 0.329 | 1.000 |
| 2 | 300.000 | 6.000 | 20.000 | 71.017 | 0.336 | 1.000 |
| 3 | 300.000 | 2.000 | 30.000 | 78.650 | 0.650 | 1.000 |
| 4 | 100.000 | 6.000 | 10.000 | 42.200 | 0.650 | 1.000 |
| 5 | 100.000 | 2.000 | 20.000 | 50.479 | 0.650 | 1.000 |
| 6 | 100.000 | 6.000 | 30.000 | 45.469 | 0.650 | 1.000 |
| 7 | 300.000 | 10.000 | 10.000 | 58.449 | 0.650 | 1.000 |
| 8 | 300.000 | 10.000 | 30.000 | 67.072 | 0.650 | 1.000 |
| 9 | 500.000 | 10.000 | 20.000 | 65.897 | 0.650 | 1.000 |
| 10 | 500.000 | 6.000 | 30.000 | 77.820 | 0.650 | 1.000 |
| 11 | 500.000 | 2.000 | 20.000 | 74.018 | 0.650 | 1.000 |
| 12 | 500.000 | 6.000 | 10.000 | 62.051 | 0.650 | 1.000 |
| 13 | 100.000 | 10.000 | 20.000 | 37.236 | 0.650 | 1.000 |
| 14 | 243.876 | 9.248 | 28.083 | 62.661 | 0.487 | 1.000 |
| 15 | 411.409 | 4.803 | 15.111 | 72.018 | 0.351 | 1.000 |
| 16 | 194.838 | 5.674 | 15.391 | 59.369 | 0.340 | 1.000 |
| 17 | 415.954 | 9.737 | 12.824 | 63.596 | 0.555 | 1.000 |
| 18 | 449.474 | 3.469 | 28.822 | 81.258 | 0.553 | 1.000 |
| 19 | 389.908 | 2.561 | 14.143 | 73.013 | 0.461 | 1.000 |
| 20 | 399.720 | 2.181 | 29.922 | 82.793 | 0.667 | 1.000 |

**Table 4.21: Optimal solution of colour removal efficiency of MTF coagulant**

| Number | Dosage(mg/L) | pH | Time(mins) | MTF | StdErr(MTF) | Desirability |
|---|---|---|---|---|---|---|
| 1 | 339.611 | 7.609 | 28.533 | 82.043 | 0.665 | 1.000 |
| 2 | 500.000 | 10.000 | 20.000 | 72.907 | 1.057 | 1.000 |
| 3 | 300.000 | 6.000 | 20.000 | 80.561 | 0.546 | 1.000 |
| 4 | 500.000 | 6.000 | 30.000 | 91.453 | 1.057 | 1.000 |
| 5 | 300.000 | 2.000 | 30.000 | 78.826 | 1.057 | 1.000 |
| 6 | 500.000 | 2.000 | 20.000 | 87.246 | 1.057 | 1.000 |
| 7 | 100.000 | 10.000 | 20.000 | 50.806 | 1.057 | 1.000 |
| 8 | 100.000 | 6.000 | 10.000 | 56.540 | 1.057 | 1.000 |
| 9 | 300.000 | 10.000 | 30.000 | 70.381 | 1.057 | 1.000 |
| 10 | 100.000 | 2.000 | 20.000 | 58.804 | 1.057 | 1.000 |
| 11 | 100.000 | 6.000 | 30.000 | 64.466 | 1.057 | 1.000 |
| 12 | 300.000 | 10.000 | 10.000 | 58.017 | 1.057 | 1.000 |
| 13 | 300.000 | 2.000 | 10.000 | 71.908 | 1.057 | 1.000 |
| 14 | 146.602 | 5.773 | 12.583 | 63.791 | 0.714 | 1.000 |
| 15 | 225.087 | 7.053 | 17.054 | 71.606 | 0.534 | 1.000 |
| 16 | 186.826 | 9.972 | 26.288 | 61.642 | 0.906 | 1.000 |
| 17 | 213.127 | 9.796 | 25.450 | 64.459 | 0.799 | 1.000 |
| 18 | 327.702 | 8.792 | 28.613 | 77.339 | 0.752 | 1.000 |
| 19 | 366.833 | 4.138 | 27.333 | 87.213 | 0.626 | 1.000 |
| 20 | 245.513 | 4.146 | 15.650 | 75.172 | 0.547 | 1.000 |

## 4.22 Optimization of coagulation-flocculation process using modified ccoagulants

Equations 4.10, 4.11 and 4.12 were solved for the best solutions such that the responses ($Y_{MMM,}$ $Y_{MAM}$, $Y_{MTF}$) are maximized within the design space.. Tables 4.19 - 4.21 is the

solution to the equation of our model which has been solved by BBD design and suggested several optimum colour removal efficiency of the coagulants. Table 4.19 is the optimal solution of colour removal efficiency of MMM coagulant. From that Table the maximum colour removal efficiency of MMM coagulant is 82.393% at dosage of 369.207 mg/L, pH of 6 and time of 14.146 mins. This value of dosage is desirable because further increase in the dosage will lead to charge reversal and re-stabilization of the colloid particles thereby reducing the colour removal efficiency as can be observed in the Table 4.19. Table 4.20 gives the same optimal solution of MAM coagulant for colour removal efficiency of 82.793% at dosage of 399.72 mg/L, pH of 2.181 and time of 29.922 mins. Moreover, Table 4.21 shows the optimal colour removal efficiency of 91.453% at dosage of 500.000 mg/L, time of 30 mins and pH of 6 for MTF coagulant. Therefore, the order of optimum colour removal efficiency of the modified coagulants studied is MMM<MAM<MTF. The high performance of MTF in the colour removal efficiency can be attributed to it Porosity and surface area. The SEM results of MTF coagulant also confirmed that MTF is the best coagulant out of all the coagulants studied in this work.

### 4.23 Coagulation-flocculation kinetics of unmodified coagulants in the treatment of paint industrial effluent

Coagulation-flocculation kinetics experiment was performed at optimal pH 2, for MM, AM and TF coagulants respectively and the result in (appendix 19, 20, Table 4.11b-d). The first order and second order rate equations were used to test the experimental data

in (appendices 19, 20, Tables 4.11b-d). A solution to the first and second order equations has been described in equations 2.18 and 2.19b. Plots of equation 2.18 and 2.19b are shown in Figures 4.23a-c and 4.24a-c. Figures 4.23a-c show the plot of In $C_t$ against time which are the first order kinetics for (a) MM (b) AM and (c) TF coagulants, while Figures 4.24a-c are plot of $1/C_t$ versus time which are the second order reaction of (a) MM (b) AM and (c) TF coagulants.

(a)

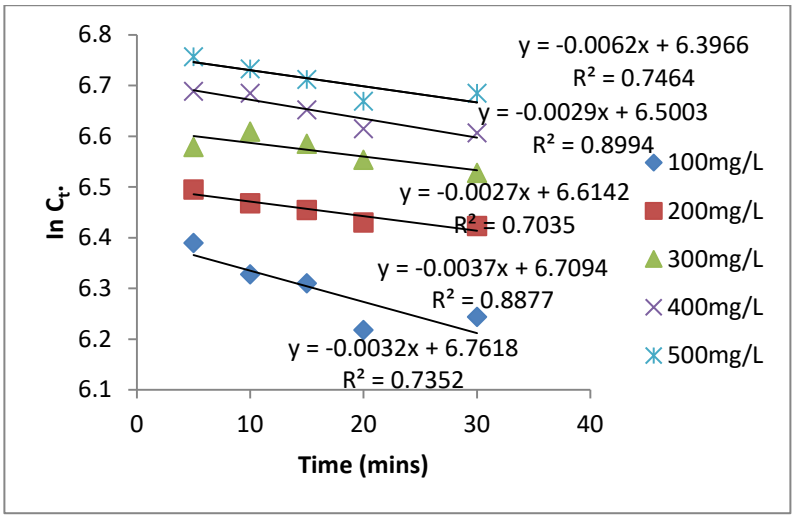


**Figure 4.23a: First order reaction of MM coagulant**

(b)

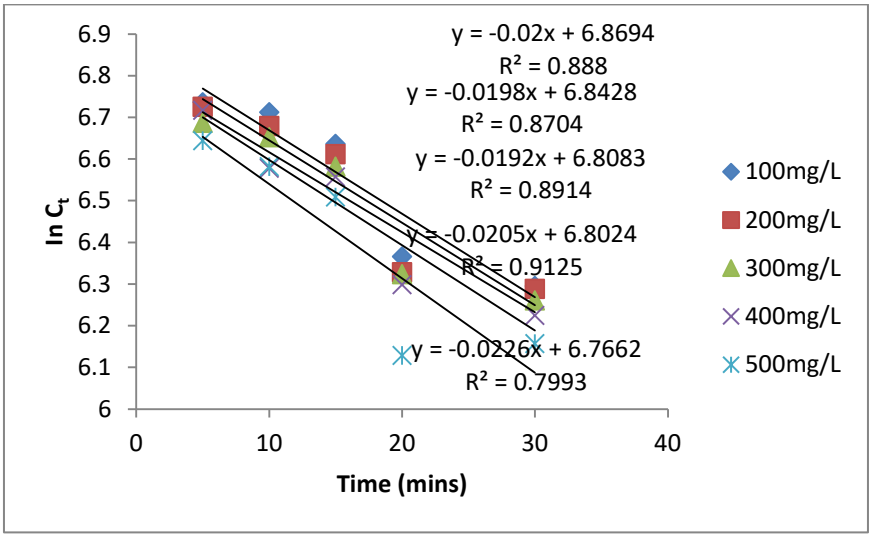


**Figure 4.23b: First order reaction of AM coagulant**

(c)

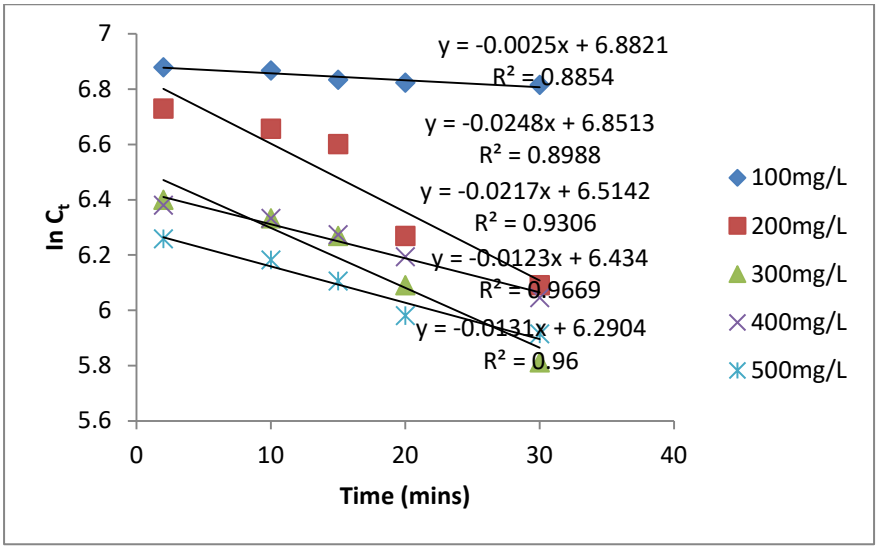


**Figure 4.23c: First order reaction of TF coagulant**

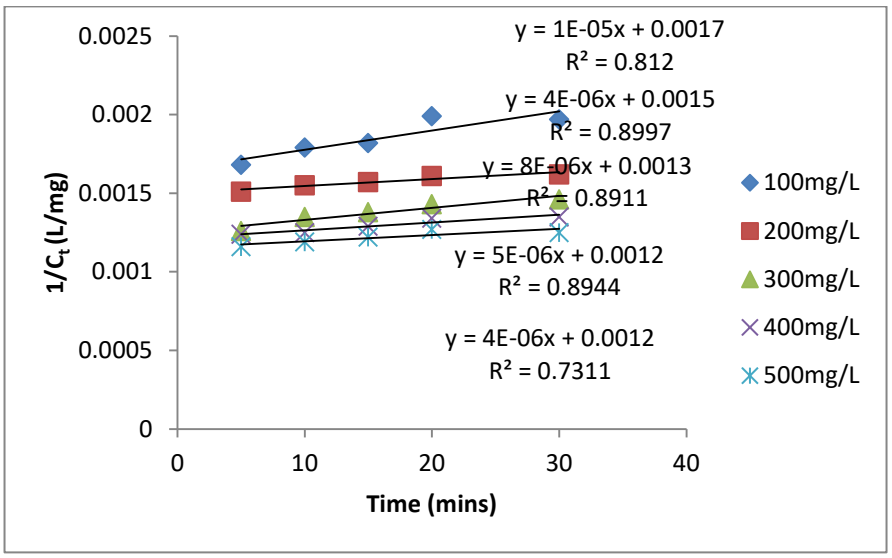


(a)

**Figure 4.24a: Second order reaction of MM coagulant**

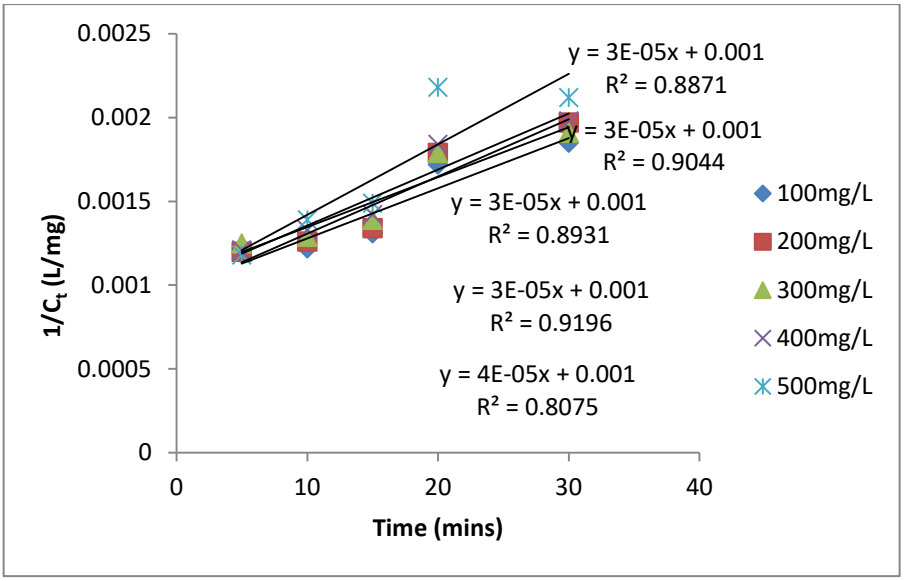


(b)

**Figure 4.24b: Second order reaction of AM coagulant**

(c)

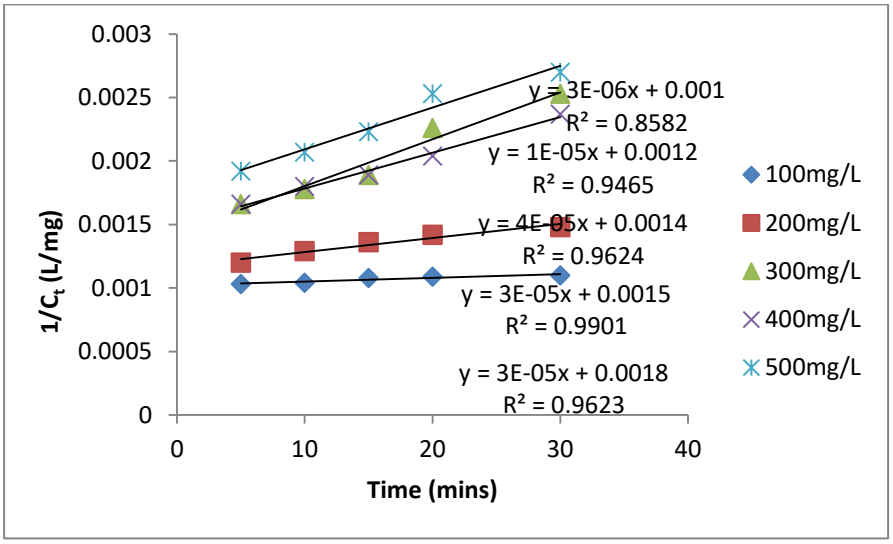


**Figure 4.24c: Second order reaction of TF coagulant**

Inspection of the kinetics plots disclosed that second order reaction fitted better considering the coefficient of determination ($R^2$) which shows the extent of linearity of a graph. High values of $R^2$ suggest great level of linearity, accuracy of the fit of a graph and effectiveness of equation 2.19b in describing the coagulation-flocculation processes (Ani *et al.*, 2012; Okolo *et al.*, 2015). Similar results had been obtained in the works reported (Ani *et al.*, 2010; Ani *et al.*, 2012 and Nnaji *et al.*, 2013). With the kinetics of coagulation-flocculation fitting second order reaction better, it means that the rate of reaction increases as the square of the concentration. The reaction mechanism between the colloid particles of the paint effluent (P) and coagulants (M, A, and T for MM, AM and TF respectively) forming complex of colloid particles and coagulant can be summarized in these equations (4.13-4.15), where $k_2$ is the rate constant;

For MM coagulant: $P + M \xrightarrow[\text{slow}]{k_2} PM$ 4.13

For AM coagulant: $P + A \xrightarrow[\text{slow}]{k_2} PA$ 4.14

For TF coagulant: $P + T \xrightarrow[\text{slow}]{k_2} PT$ 4.15

From the above mechanism a second order rate law expression can be written as equations (4.16-4.18)

$$\text{Rate} = k_2[P][M] \quad 4.16$$

$$\text{Rate} = k_2[P][A] \quad 4.17$$

$$\text{Rate} = k_2[P][T] \quad 4.18$$

Therefore, it can be concluded that the rate of these reactions is dependent function of k and concentration of both the colloid particles of paint effluent and coagulant.

**Table 4.22: Functional parameter for second order kinetics at pH 2 and varying dosages for MM coagulant**

| **Parameter** | **100 mg/L** | **200 mg/L** | **300 mg/L** | **400 mg/L** | **500 mg/L** |
|---|---|---|---|---|---|
| $R^2$ | 0.812 | 0.899 | 0.891 | 0.894 | 0.731 |
| k($Lmg^{-1}min^{-1}$) | $1.0x10^{-5}$ | $4.0x10^{-6}$ | $8.0x10^{-6}$ | $5.0x10^{-6}$ | $4.0x10^{-6}$ |
| $\beta_{BR}$ ($(Lmg^{-1}min^{-1})$ | $2.0x10^{-5}$ | $8.0x10^{-6}$ | $1.6.0x10^{-5}$ | $1.0.0x10^{-5}$ | $8.0x10^{-6}$ |
| $k_R^{Nn}$($L/min^{-1}$) | $2.2x10^{-18}$ | $5.5x10^{-18}$ | $8.3x10^{-18}$ | $1.3x10^{-17}$ | $1.66x10^{-17}$ |
| $\varepsilon^{Nn}$ ($mg^{-1}$) | $4.5x10^{12}$ | $7.2x10^{11}$ | $9.6x10^{11}$ | $3.8x10^{11}$ | $2.4x10^{11}$ |
| $t_{1/2}$(mins) | 95.238 | 238.095 | 119.048 | 190.476 | 238.095 |

**Table 4.23: Functional parameter for Second order kinetics at pH 2 and varying dosages for AM coagulant**

| Parameter | 100 mg/L | 200 mg/L | 300 mg/L | 400 mg/L | 500 mg/L |
|---|---|---|---|---|---|
| $R^2$ | 0.887 | 0.904 | 0.893 | 0.919 | 0.778 |
| k($Lmg^{-1}min^{-1}$) | $3.0x10^{-5}$ | $3.0x10^{-5}$ | $3.0x10^{-5}$ | $3.0x10^{-5}$ | $4.0x10^{-5}$ |
| $\beta_{BR}$($Lmg^{-1}min^{-1}$) | $6.0x10^{-5}$ | $6.0x10^{-5}$ | $6.0x10^{-5}$ | $6.0x10^{-5}$ | $8.0x10^{-5}$ |
| $k_R^{Nn}$ ($L/min^{-1}$) | $7.2x10^{-19}$ | $7.2x10^{-19}$ | $7.2x10^{-19}$ | $7.2x10^{-19}$ | $2.7x10^{-19}$ |
| $\varepsilon^{Nn}$($mg^{-1}$) | $4.2x10^{13}$ | $4.2x10^{13}$ | $4.2x10^{13}$ | $4.2x10^{13}$ | $1.5x10^{14}$ |
| $t_{1/2}$(mins) | 31.746 | 31.746 | 31.746 | 31.746 | 23.809 |

**Table 4.24: Functional parameter for second order kinetics at pH 2 and varying dosages for TF coagulant**

| Parameter | 100 mg/L | 200 mg/L | 300 mg/L | 400 mg/L | 500 mg/L |
|---|---|---|---|---|---|
| $R^2$ | 0.856 | 0.946 | 0.962 | 0.990 | 0.962 |
| k($Lmg^{-1}mins^{-1}$) | $4.0x10^{-6}$ | $1.0x10^{-5}$ | $4.0x10^{-5}$ | $3.0x10^{-5}$ | $3.0x10^{-5}$ |
| $\beta_{BR}$ ($Lmg^{-1}min^{-1}$) | $8.0x10^{-5}$ | $2.0x10^{-5}$ | $8.0x10^{-5}$ | $6.0x10^{-5}$ | $6.0x10^{-5}$ |
| $k_R^{Nn}$($Lmin^{-1}$) | $2.7x10^{-19}$ | $2.1x10^{-19}$ | $2.6x10^{-19}$ | $3.7\ x10^{-19}$ | $3.6\ x10^{-19}$ |
| $\varepsilon^{Nn}$($mg^{-1}$) | $1.5\ x10^{13}$ | $4.8\ x10^{13}$ | $1.5\ x10^{14}$ | $8.1\ x10^{13}$ | $8.3\ x10^{13}$ |
| $t_{1/2}$ (mins) | 238.095 | 95.238 | 20.233 | 31.746 | 31.746 |

Equation (2.15), (2.18), (2.19) and (2.5c) were solved to obtain kinetics parameters and they are presented in Tables 4.12-4.14. Table 4.12 is the functional parameter for second order kinetics at pH of 2 and varying dosages for MM coagulant, Table 4.13 for AM and Table 4.14 is for TF coagulants. In these Tables, k which is the coagulation-flocculation rate constant was derived from the slope of equation 2.5b. k takes into

account the coagulation and flocculation process involved in the aggregation for second-order predominated process. $\beta_{BR,}$ $k_R^{Nn}$, $\varepsilon^{Nn}$ and $t_{1/2}$ are particle coagulation effectiveness factors, known to be responsible for the coagulation efficiency before particle aggregation (Menkiti *et al.*, 2011; Ugonabo *et al*., 2012). When variation in $k_R^{Nn}$ is negligible, $\varepsilon^{Nn}$ directly relates to $2k = \beta_{BR}$. Low $k_R^{Nn}$ is a condition for high $\varepsilon^{Nn}$, which is particle collision efficiency and is proportional to the kinetic energy acquired by the colliding particles. As observed in the Tables 4.12-4.14 all $k_R^{Nn}$ were low compared with $\varepsilon^{Nn}$ which are very high. High $\varepsilon^{Nn}$, results in high kinetic energy required to overcome additional repulsive forces caused, for instance by electrostatic interactions, that hinders particles from aggregating (Ugonabo *et al.*, 2012). High $\varepsilon^{Nn}$ can equally results in high kinetic energy to overcome the zeta potential. Which will ensures recession or total double-layer collapse to actualize low $t_{1/2}$ in favor of high rate of coagulation. The values posted in Tables 4.12- 4.14 were observed to be moving in this trend. $t_{1/2}$ is coagulation-flocculation period or half life, it indicates the time taken for the initial concentration of the coagulants to reduce by half and also serves as a measure for the rate of coagulation-flocculation process. Low period is a condition for fast rate of aggregation, which is desirable in process design (Okolo *et al.*, 2014; Hunter, 1993). $k_R^{Nn}$ is related to Boltzmann constant $K_B$, temperature T, and viscosity of the fluid $\eta_o$, also one of the pillars in calculation of $\varepsilon^{Nn}$, Inspection of the Tables 4.12-4.14 revealed the $t_{1/2}$ at the optimal dosage 100 mg/L for MM, 500 mg/L for AM and

300 mg/L for TF are 95.238 mins, 23.809 mins and 20.233 mins respectively. This result is in agreement with (Menkiti *et al*., 2011 and 2016, Ugonabo *et al*., 2012).

### 4.24 Coagulation-flocculation kinetics of modified coagulants in the treatment of paint industry effluent

The results of this coagulation-flocculation kinetics are shown in (Appendices 20, 21, Tables 4.24b-d). The first order and second order rate equations were used to test the experimental data (Appendices 20, 21, Table 4.24b-d) to determine the one that adequately fit the data. Figures 4.25a-c are the first order reaction for (a) MMM (b) MAM and (c) MTF coagulants. The Figures are plots of ln $C_t$ against time which give negative slopes indicating first order reaction. Figures 4.26a-c are plots for second order reaction for (a) MMM (b) MAM (c) MTF coagulants. A closer look at the Figures shows the plots of $1/C_t$ against time with a positive slope, which indicated second order reaction. Comparing Figures 4.25a-c and 4.26a-c, it is seen that the values of $R^2$ in Figures 4.26a-c are higher than those in Figures 4.25a-c. High values of $R^2$ suggest great level of linearity, accuracy of the fit of a graph and effectiveness of equation 2.19b in describing the coagulation-flocculation processes (Ani *et al*., 2012; Okolo *et al*., 2015). This suggests that the data fit second order reaction better.

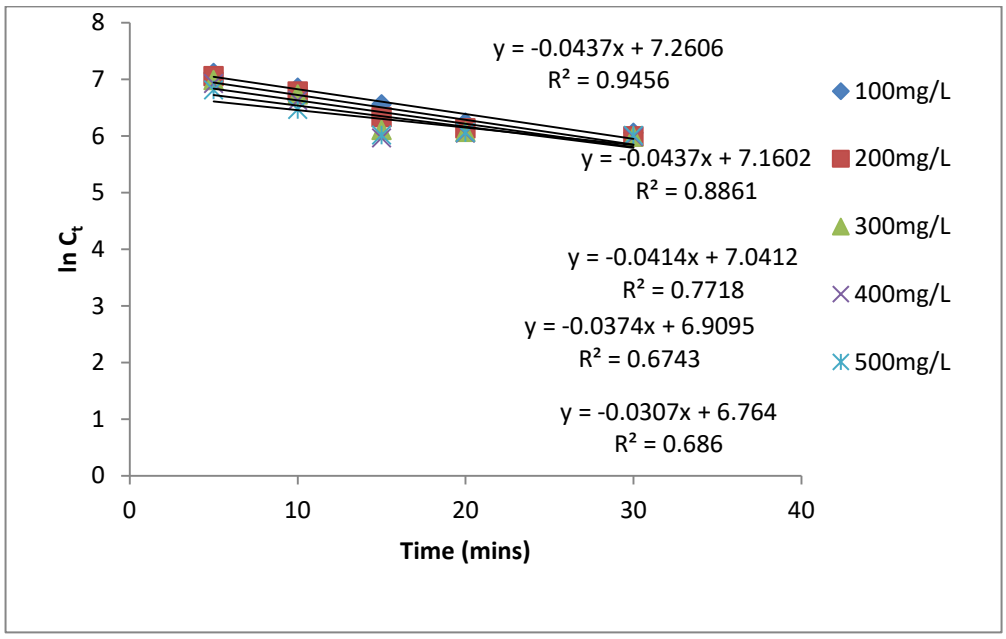


(a)

**Figure 4.25a: First order reaction for MMM coagulant**

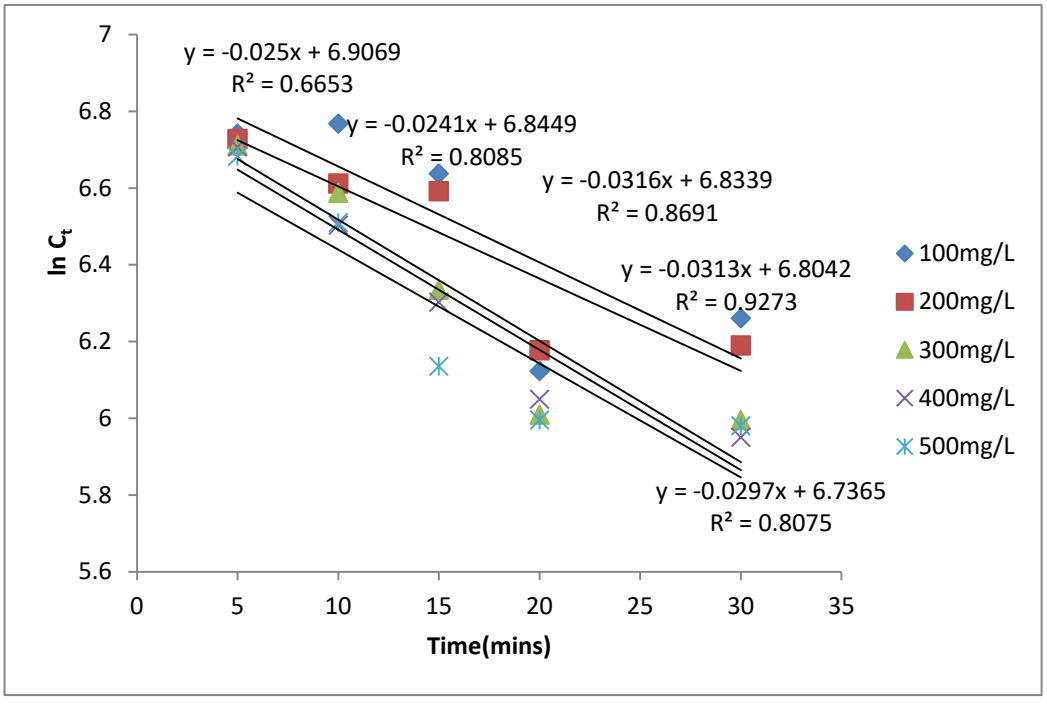


(b)

**Figure 4.25b: First order reaction for MAM coagulant**

(c)

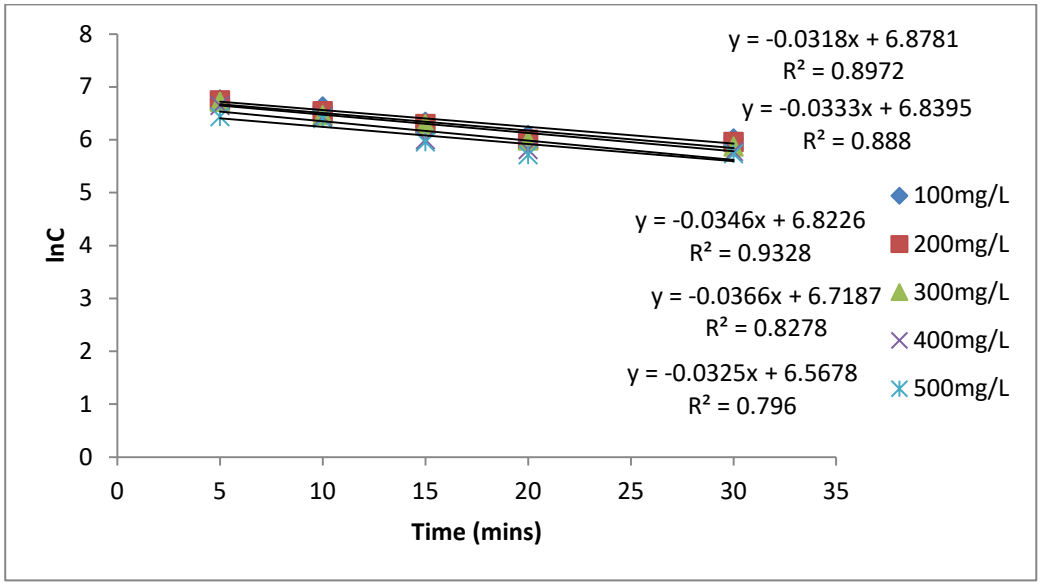


**Figure 4.25c: First order reaction for MTF coagulant**

(a)

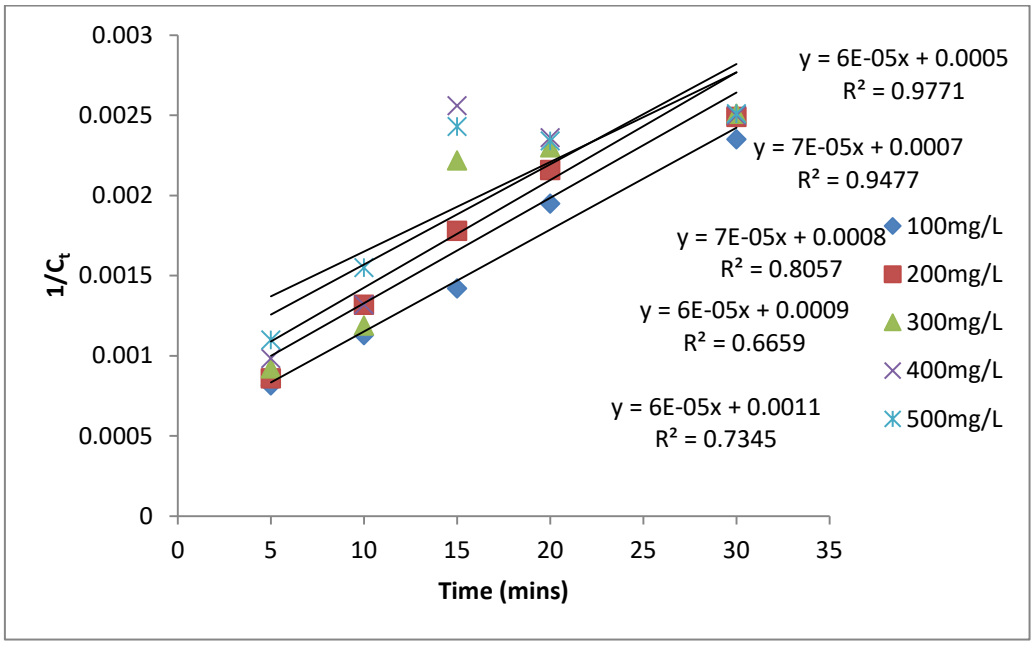


**Figure 4.26c: Second order reaction of MMM coagulant**

(b)

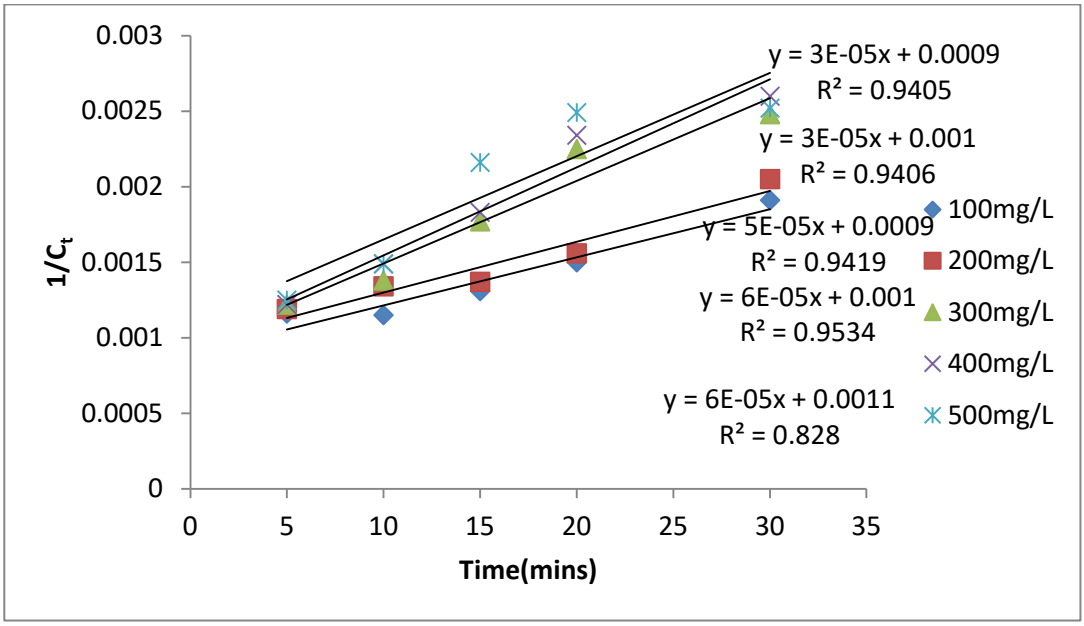


**Figure 4.26b: Second order reaction of MAM coagulant**

(c)

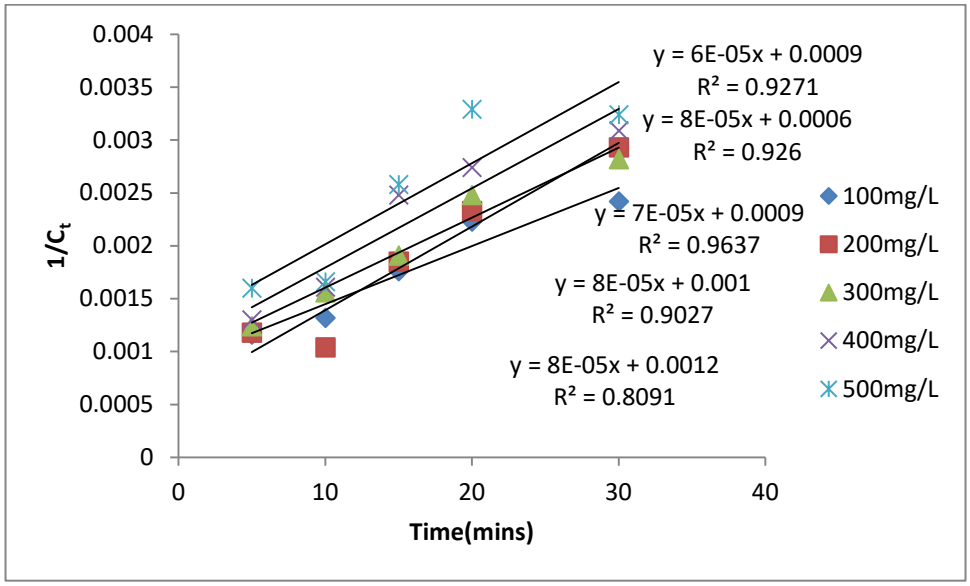


**Figure 4.26c: Second order reaction of MTF coagulant**

Since experimental data fitted better in second order, it means that the rate of reaction increases as the square of the concentration. The mechanism of coagulation-flocculation reaction between the colloid particles of the paint effluent (P) and B for MMM, R for

MAM and S for MTF coagulants are shown in equation (4.19-4.21), where $k_2$ is the rate constant;

For MMM coagulant $P + B \xrightarrow[\text{slow}]{k_2} PB$ 4.19

For MAM coagulant $P + R \xrightarrow[\text{slow}]{k_2} PR$ 4.20

For MTF coagulant $P + S \xrightarrow[\text{slow}]{k_2} PS$ 4.21

From the above mechanism a second order rate law expression can be written as equations (4.16-4.18)

$$\text{Rate} = k_2[P][B] \quad 4.22$$

$$\text{Rate} = k_2[P][R] \quad 4.23$$

$$\text{Rate} = k_2[P][S] \quad 4.24$$

**Table 4.25: Functional parameter for second order kinetics at pH of 6 at varying dosages for MMM coagulant**

| **parameter** | **100 mg/L** | **200 mg/L** | **300 mg/L** | **400 mg/L** | **500 mg/L** |
|---|---|---|---|---|---|
| $R^2$ | 0.977 | 0.947 | 0.805 | 0.665 | 0.734 |
| k($Lmg^{-1}mins^{-1}$) | $6.0x10^{-5}$ | $7.0x10^{-5}$ | $7.0 x10^{-5}$ | $6.0 x10^{-5}$ | $6.0 x10^{-5}$ |
| $\beta_{BR}$ ($Lmg^{-1}min^{-1}$) | $1.2.0 x10^{-4}$ | $1.4.0 x10^{-4}$ | $1.4.0 x10^{-4}$ | $1.2.0 x10^{-4}$ | $1.2.0 x10^{-4}$ |
| $k_R^{Nn}$($Lmin^{-1}$) | $5.5x10^{-19}$ | $4.7 x10^{-19}$ | $4.7 x10^{-19}$ | $5.5 x10^{-19}$ | $5.5 x10^{-19}$ |
| $\varepsilon^{Nn}$($mg^{-1}$) | $1.1x10^{14}$ | $1.5 x10^{14}$ | $1.5 x10^{14}$ | $1.1 x10^{14}$ | $1.1 x10^{14}$ |
| $t_{1/2}$ (mins) | 15.873 | 13.605 | 13.605 | 15.873 | 15.873 |

**Table 4.26: Functional parameter for second order kinetics at pH of 2 at varying dosages for MAM coagulant**

| parameter | 100 mg/L | 200 mg/L | 300 mg/L | 400 mg/L | 500 mg/L |
|---|---|---|---|---|---|
| $R^2$ | 0.940 | 0.940 | 0.941 | 0.953 | 0.828 |
| k($Lmg^{-1}mins^{-1}$) | $3.0x10^{-5}$ | $3.0x10^{-5}$ | $5.0x10^{-5}$ | $6.0x10^{-5}$ | $6.0x10^{-5}$ |
| $\beta_{BR}$ ($Lmg^{-1}min^{-1}$) | $6.0x10^{-5}$ | $6.0x10^{-5}$ | $1.0x10^{-4}$ | $1.2.0x10^{-4}$ | $1.2.0x10^{-4}$ |
| $k_R^{Nn}$($Lmin^{-1}$) | $9.1x10^{-19}$ | $9.1x10^{-19}$ | $4.1x10^{-19}$ | $4.5x10^{-19}$ | $4.5x10^{-19}$ |
| $\varepsilon^{Nn}$($mg^{-1}$) | $3.3x10^{13}$ | $3.3\ x10^{13}$ | $1.2\ x10^{14}$ | $1.3\ x10^{14}$ | $1.3\ x10^{14}$ |
| $t_{1/2}$ (mins) | 31.750 | 31.750 | 19.050 | 15.873 | 15.873 |

**Table 4.27: Functional parameter for second order kinetics at pH of 6 at varying dosages for MTF coagulant**

| parameter | 100 mg/L | 200 mg/L | 300 mg/L | 400 mg/L | 500 mg/L |
|---|---|---|---|---|---|
| $R^2$ | 0.927 | 0.926 | 0.963 | 0.902 | 0.809 |
| k($Lmg^{-1}mins^{-1}$) | $6x10^{-5}$ | $8\ x10^{-5}$ | $7\ x10^{-5}$ | $8\ x10^{-5}$ | $8\ x10^{-5}$ |
| $\beta_{BR}$ ($Lmg^{-1}min^{-1}$) | $1.2\ x10^{-4}$ | $1.6\ x10^{-4}$ | $1.4\ x10^{-4}$ | $1.6\ x10^{-4}$ | $1.6\ x10^{-4}$ |
| $k_R^{Nn}$($Lmin^{-1}$) | $3.6x10^{-19}$ | $8.2\ x10^{-20}$ | $3.1\ x10^{-19}$ | $8.2\ x10^{-20}$ | $8.2\ x10^{-20}$ |
| $\varepsilon^{Nn}$($mg^{-1}$) | $1.7x10^{14}$ | $9.8\ x10^{14}$ | $2.3\ x10^{14}$ | $9.8\ x10^{14}$ | $9.8\ x10^{14}$ |
| $t_{1/2}$ (mins) | 15.870 | 11.900 | 13.610 | 11.900 | 11.900 |

Equation (2.15), (2.18), (2.19) and (2.5c) were solved to obtain kinetics parameters and they are presented in Tables 4.25-4.27. k is the coagulation- flocculation rate constant, was derived from the slope of equation (2.5b). k takes into account the coagulation and flocculation regimes involved in the aggregation for second-order predominated process. $\beta_{BR,}$ $k_R^{Nn}$, $\varepsilon^{Nn}$ and $t_{1/2}$ are particle coagulation effectiveness factors, known to be responsible for the coagulation efficiency before particle aggregation (Menkiti *et al*.,

2011). When variation in $k_R^{Nn}$ is negligible, $\varepsilon^{Nn}$ directly relates to 2k = $\beta_{BR}$. Low $k_R^{Nn}$is a condition for high $\varepsilon^{Nn}$, which is particle collision efficiency and is proportional to the kinetic energy acquired by the colliding particles. High $\varepsilon^{Nn}$, results in high kinetic energy required to overcome additional repulsive forces caused, for instance by electrostatic interactions, that hinders particles from aggregating (Ugonabo *et al*., 2012). High $\varepsilon^{Nn}$ can equally results in high kinetic energy to overcome the zeta potential. Low zeta potential ensures recession or total double-layer collapse to actualize low $t_{1/2}$ in favour of high rate of coagulation. The values in Tables 4.25- 4.27 were observed to be moving in this rate. Low $t_{1/2}$ is a condition for fast rate of aggregation, which is desirable in process design (Okolo *et al*., 2014; Hunter, 1993). $k_R^{Nn}$, is related to Boltzmann constant $K_B$, temperature T, and viscosity of the fluid, $\eta_o$, also one of the bases in calculation of $\varepsilon^{Nn}$, inspection of the Tables 4.25-4.27 portrayed that the $t_{1/2}$ at the optimal dosage for MMM, MAM and MTF are 13.605 mins, 15.873 mins and 11.900 mins respectively.

# CHAPTER FIVE

# CONCLUSION AND RECOMMENDATION

## 5.1 Summary

Pollution has become a challenge in this modern world because of Science and Technology which the world cannot do without and it gave birth to industrialization. In an effort to curb this menace of pollution using green chemistry this research came to limelight. In this research unmodified and modified three species of snail shells namely *Mercenaria mercenaria, Archachatina marginata, and Tympanotonos fuscatus* have been used as coagulants to treat paint industry effluent. This study is justified because it a way of converting waste to wealth and the efficient way of treating paint effluent without addition of pollutant to the already existing ones. The method used in treating this paint industry effluent is coagulation-flocculaton. Response to Surface Methodolody by Box Behnken design (BBD) is used in optimization of the colour removal efficiency because the design summarizes the number of the experiment to be done and gave the model that was used to interpret the data. The BBD design also saves time, money and labour in the laboratory work. Coagulation-flocculation experiment was conducted to treat the paint industry effluent using design matrix of Box Behnken design. The physicochemical analyses were carried out to determine the level of pollution in the paint effluent before treatment and after treatment. Some of the physical characteristics such as tap density, bulk density, true density, Carr's index,

Hausner ratio, and Surface area help to determine whether these coagulants can pass the test as coagulant. The proximate analysis was analyzed to find and quantify the classes of food and mineral contents in the coagulants.

Characterization of the coagulants was done using FTIR, SEM, XRD and XRF. FTIR to determine the functional groups present in the coagulants, SEM to determine the surface morphology of the coagulants, XRD to analyze the crystalinity of the coagulants and XRF to evaluate the elements present in the coagulants. Finally, kinetics study was carried out to determine the rate constant, order of reaction and some functional parameter.

## 5.2 Conclusion

From experimental results and findings in this research, the following conclusion can be drawn;

Physical parameters tested like Bulk and Tap densities, Carr's index, Porosity, Hausner ratio, and Surface area of these six coagulants show that these coagulants can be considered as suitable precursors.

Proximate composition of the six coagulant demonstrated that these six coagulants contain much of carbohydrate.

Physicochemical analyses of the paint industry effluent before treatment showed that this effluent is highly polluted and after treatment the result showed an appreciable decrease in the values of the pollutants studied.

Response Surface Methodology by Box Behnken model has proved to be efficient in investigating the effect of three variables (dosage, pH, and settling time) by coagulation-flocculation process.

Second order polynomial regression model interpreted the experimental data with coefficient of determination $R^2$ close to unity.

ANOVA of the quadratic model demonstrated that the model is highly significant.

There was significant interaction of the three variables according to the 3D surface plot.

The most favourable pH for colour removal efficiency is acid medium.

Coagulation-flocculation was optimized using a desirability function in all the coagulants and the order of coagulant optimal colour removal efficiency is as follows; MM<AM<TF and MMM<MAM<MTF.

The kinetics of coagulation-flocculation model fitted better in $2^{nd}$ order in all the six coagulants and the rate of coagulation-flocculation reaction is dependent function of k and half life.

All the coagulants contained 90% of calcium and other element appeared in small quantity.

All the coagulants have amorphous structure except MTF which has crystalline structure.

Finally, what promoted colour removal efficiency using coagulation-flocculation method is the surface chemistry of these coagulants.

## 5.3 Recommendations

More research should be geared on the use of these coagulants in the treatment of other effluent apart from paint industry effluent. Again, experiments should also be conducted on the removal of the physicochemical parameters using the same coagulants with different dosages, time, pH and temperature.

## 5.4 Contribution to Knowledge

The discovery of green bio-coagulants in removal of colour and other pollutants from paint industry effluent which is an alternative to the conventional coagulants.

# REFERENCES

Abdullah Al-Mamun and Ahmad Tsaqif A. Basir (2016). White Popinac as Potential Phyto-Coagulant to Reduce Turbidity of River Water. Journal of Engineering and Applied Sciences 11(11):7180-7183.

Abel, J.S., Stangle, G.C., Schilling, C.H., and Aksay, I.A. (1994). Sedimentation in Flocculation. Journal Material Research, 9(2):451-461.

Ademoroti, C.M.A (1996). Standard methods for water and effluents analysis. Foludex press ltd, Ibadan, Nigeria. Pp 102-104. 159-161.

Ahlafi, Hammou, Hamou Moussout, Fatima Boukhlifi, Mostafa Echetna, Mohamed Naciri Bennani and Slimani My Slimane (2013). Kinetics of N-Deacetylation of Chitin Extracted from Shrimp Shells Collected from Coastal Area of Morocco. Mediterranean Journal of Chemistry, 2(3), 503-513.

Ahmadi, N., Chaibakhsh, N. and Zanjanchi, M. A. (2016). Use of *D*escurainia sophia*L*. As a natural coagulant for the treatment of dye-containing wastewater. Environ. Prog. Sustainable Energy, 35: 996–1001.

Ajayi Olubunmi Bolanle, Akomolafe Seun Funmilola, Adefioye Adedayo (2014). Proximate Analysis, Mineral Contents, Amino Acid Composition, Anti-Nutrients and Phytochemical Screening of *Brachystegia Eurycoma* Harms and *Pipper Guineense Schum and Thonn*. American Journal of Food and Nutrition, 2014 (2); 11- 17.

Ajiboye, A.A., Agboola, D.A, Fadimu, O.Y. and Afolabi, A.O.(2013). Antibacterial, Phytochemical and Proximate Analysis of *Prosopis Africana* (Linn) Seed and Pod Extract. FUTA, Journal of Research in Sciences, 2013 (1): 101-109.

Alabama Department of Environmental Management (ADEM) (1989). Water Works Operator Manual, p. 24.

Alex Cruden (2015). Article on Coagulation and Flocculation in Water and Wastewater Treatment. pp. 1-20.

Altaher, H., Tarek, E. Khalil and Abubeah, R. (2016). An Agricultural waste as a novel coagulant aid to treat high turbid water containing humic acids. *Global NEST Journal*, 18(2), 279-290.

American Public Health Association (1995) 3112B, Cold – Vapour Atomic Absorption Spectrometric Method, Standard Methods for the Examination of Water and Wastewater,20th Edition, APHA, AWWA,WEF. pp.16-21.

American Public Health Association (1998) 3111B, Direct Air-Acetelyne Flame Method, Standard Methods for the Examination of Water and Wastewater, 20th Edition, APHA, AWWWA, WEF. pp. 23-28.

Amirtharajah, A. and O'Melia, C. R. (1999). In water quality and treatment AWWA, 5th ed. American Water Works Association. Denver Co. p. 35.

Ani, J.U., Menkiti, M.C., and Onukwuli O.D. (2010). Coagulation and flocculation behaviour of snail shell coagulant in fibre- cement plant effluent. Journal of Engineering and Applied Sciences 5: 1-8.

Ani, J.U., Menkiti, M.C., and Onukwuli, O.D. (2011). Coagulation-flocculation performance of Snail shell biomass for waste water purification. New York Science Journal, 4(2):81-90.

Ani, T.U., Nnaji, N.J.N., Onukwuli, O.D., and Okoye, C.O.B. (2012). Nephelometric and functional parameter response of coagulation for the purification of Industrial waste water using *Detarium microcarpum*. Journal of Hazardous Materials, 243:59-66.

Anteneh, W., and Sahu, O. P. (2014). Natural coagulant for the treatment of food Industry waste water. International Letters of Natural Sciences, 4: 27-35.

Asrafuzzaman, Md., Fakhruddin, A. N. M., and Alamgir Hossain Md. (2011). Reduction of Turbidity of Water Using Locally Available Natural Coagulants. International Scholarly Research,2(3):1-6.

Association of Analytical Chemistry, Methods for proximate Analysis (AOAC, 1990). 2217-2280.

Bandela, N.N. and Puniya, P.N. (2008).Treatment of Paint content in Effluents of Automobile Industries. Journal of Environmental Research and Development, 2(3): 426-43.

Belbahloul Mounir , Anouar Abdellah, Zouhri Abdeljalil (2014). Low Technology Water Treatment: Investigation of the Performance of Cactus Extracts as a Natural Flocculant for Flocculation of Local Clay Suspensions. International Journal of Engineering Research & Technology, 3(3):2440-2445.

Belcher, A. M., Wu, X. H., Christensen, R. J., Hansma, P. K., Stucky, G. D., Morse, D. E. (1996). Control of crystal phase switching and orientation by soluble mollusc-shell proteins. Nature 381 (6577): 56–58.

Beltran-Heredia, J., Rodriguez-Sanchez, M. Sanchez-Martin, T. J. (2011). Textile wastewater purification through natural coagulants. Appl. Water Sci., 1:25–33.

Billuri Manognya, Bonner James S., Fuller Christopher B., and Islam Mohammad S. (2015). Impact of Natural Cationic Polymers on Charge and Clarification of Microalgae Suspensions.Environmental Engineering Science, 32(3): 212-221.

Bingol, D., Tekin, N., Alkan M. (2010). Brillant yellow dye adsorption onto Sepiolite using a full factorial design. Appl. Clay Sci., 50: 315-321.

Bolto, B., and Gregory, J., (2007). Review: Organic Polyelectrolytes in water treatment, Water Research, 41, 2301-2324.

Bratby John (2006). Coagulation and flocculation with an emphasis on water and waste water treatment. Upland Press ltd, Croydon pp 10, 11, 33, 34, 35, 37, 54, 55, 56, 187, 188, 189 and 193 .

Braul, L., Viraraghavan, T. and Corkal, D. (2001). Cold Water Effects on Enhanced Coagulation of High DOC, Low Turbidity Water. Water Quality Research Journal Canada, 36(4), 701-717.

Chi Fung Hwa, and Cheng Wen Po (2006). Use of Chitosan as Coagulant to Treat Waste water from Milk Processing Plant. Journal of Polymers and the Environment, 14(4): 411-421.

Chichuan, K., Huang C., and Pan, J. R. (2002). Time requirements for rapid mixing in coagulation: Colloids Surf. A Physicochemical Engineering Aspect, 204(1-3): 1-9.

Copley, Mark (2008). A test of quality. Manufacturing chemist bulletin, 31-33.

Crittenden, J.C., Trussel, R.R., Hand, D. W., Howe, K. J., and Tchobanoglous, G. (2005). “Coagulation, mixing and flocculation”, in Water Treatment: Principles and Design. 2nd edition, John Wiley & Son, New Jersey, p. 60.

De Campos Milene Minniti and Ferreira Maria do Carmo (2013). A Comparative Analysis of the Flow Properties between Two Alumina-Based Dry Powders. Advances in Materials Science and Engineering, 1- 7.

Dong-Su Kim (2003).Measurement of point of zero charge of Benonite by solubility technique and its dependence of the surface of the surface potential on pH. Environ. Eng. Res., 8(4):222-227.

Duan, J., and Gregory, J., (2003).Coagulation by hydrolysing metal salts, Advances in Colloid & Interface Science, 100(101): 475-502.

Dutta, P.K., Ravluman, M.N.V., and Dutta, J., (2002). Chitin and Chitosan for versatile application. J.M. S. Poly. Rev., 42:304-312.

Edokpayi Joshua N., Odiyo John O. , Odiyo Elizabeth O., Oluwagbemiga S. Alayande and Titus A. M. Msagati (2015). Synthesis and Characterization of Biopolymeric Chitosan Derived from Land Snail Shells and Its Potential for $Pb^{2+}$ Removal from Aqueous Solution. Materials 8: 8630–8640.

Fakhi, Ali (2013). Application of Response Surface methodology to optimize the process variables for fluoride ion removal using Maghemite nanoparticles. Journal of Saudi Chemical Society, 18: 340-347.

Fakhri, Ali (2014). Application of response surface methodology to optimize the process variables for fluoride ion removal using maghemite nanoparticles. Journal of Saudi Chemical Society. 18: 340–347.

Faust, S.D. and Aly, O.M. (1983). Chemistry of Water Treatment, Butterworth publishers, Stoneham, pp. 277-363.

Freitas , T.K.F.S., Oliveira V.M., de Souza, M.T.F., Geraldino, H.C.L., Almeida, V.C., Fávaro, S.L., and Garcia, J.C. (2015). Optimization of coagulation-flocculation process for treatment of industrial textile wastewater using okra (*A. esculentus*) mucilage as natural coagulant. Industrial Crops and Products, Elsevier 76: 538-544.

Ganesan, V., Rosentrater K. A., Muthukumarappan, K. (2008). Flowability and handling characteristics of bulk solids and powders – a review with implications for DDGS. Bio systems e n g i n e e r i n g, 1 0 1: 4 2 5 – 4 3 5.

Gotliv, B.; Addadi, L., and Weiner, S. (2003). "Mollusc shell acidic proteins: in search of individual functions.".Chembiochem : a European Journal of Chemical Biology 4 (6): 522–529.

Griffiths, P. and de Hasseth, J.A. (2007). Fourier Transform Infrared Spectrometry.2nd ed. John wiley and sons Inc, New Jersey, USA. pp. 51-55.

Harendra, S., Oryshchyn, D., Ochs, T., Gerdemann, S., Clark, J., and Summers, C. (2011). Coagulation-flocculation treatments for flue-gas-derived water from oxyfuel power production with $CO_2$ capture. Industrial & Engineering Chemistry Research, 50(17), 10335–10343.

Harish Kumar and Renu Rani (2013). Structural Characterization of Silver Nanoparticles Synthesized by Micro emulsion Route. International Journal of Engineering and Innovative Technology, (IJEIT), 3(3): 344-348.

Hendrawati Indra Rani Yuliastri, Nurhasni Eti Rohaeti, Hefni Effendi, and Latifah K Darusman (2016).The use of Moringa Oleifera Seed Powder as Coagulant to Improve the Quality of Wastewater and Ground Water. Earth and Environmental Science, 31:1-11.

Hunter, R. J. (1993). Introduction to Modern Colloid Science," 4th Edition, University Press, New York, pp. 67-71.

Jabasingh S.A., and Pavithra G.(2010). Response Surface approach for biosorption of $Cr^{6+}$ ion by mucor racemosus, Clean-Soil, Air, Water 38: 492-497.

Jatto, O.E., Asia, I.O., and Medjor, W.E.. **(**2010**)**. "Proximate and Mineral Composition of Different Species of Snail Shell". Pacific Journal of Science and Technology. 11(1):416-419.

Kaushik, P. and Malik, A. (2011). Process Optimization for efficient dye removal by *Aspergillius lentulus*. Journal of Hazard Material, 185: 837-843.

Kawamura, S., (1996). Optimization of Basic Water Treatment Processes - Design and Operation: Coagulation and Flocculation. Journal Water Supply Research and Technology, AQUA 45(1), 35-47.

Kaya Murat, Talat Baran, Sevil ErDogan, Ayler Mentes, Meltem Asan Ozusaglm, and Yavuz Selim Cakmak (2014). Physiochemical Comparism of Chitin and Chitosan

obtained from larvae and adult Colorado patoto beetle (Leptinotarsa decemlineata). Materials Science and Engimeering, 45: 72-81.

Kaya Murat, Talat Baran, Sevil ErDogan, Ayler Mentes, Meltem Asan Ozusaglm, and Yavuz Selim Cakmak (2014). Physiochemical Comparism of Chitin and Chitosan obtained from larvae and adult Colorado patoto beetle (Leptinotarsa decemlineata). Materials Science and Engimeering, 45: 72-81.

Kazi Tasneembano and Virupakshi Arjun (2013).Treatment of Tannery Wastewater Using Natural Coagulants. International Journal of Innovative Research in Science, Engineering and Technology, 2(8):4061-4068.

Kean Thomas, Roth Susanne, and Thanou Maya (2005). "Trimethylated chitosans as non-viral gene delivery vectors: Cytotoxicity and transfection efficiency". Journal of Controlled Release.103 (3): 643–53.

Kerri, K.D. (2002). Water Treatment Plant Operation. California State University, Sacramento, p,18.

Kolawole, M.Y., Aweda, J.O., and Abdulkareem,S. (2017). Archachatina marginata bio-shells as reinforcement material in metal matrix composites. International Journal of Automotive and Mechanical Engineering, 14 (1) 406:8-4079.

Körbahti, B.K. and Tanyolac¸ A. (2009).Electrochemical treatment of simulated industrial paint wastewater in a continuous tubular reactor. Chemical Engineering J. (148) 444–451.

Kraeuter, J.N. and M. Castagna (2001). The Biology of the Hard Clam. Elsevier Science, Amsterdam. p. 772.

Lee D. Wilson (2014). An overview of Coagulation-Flocculation technology. Water condition and purification, 1-4.

Lim Chanoong, Dong Woog Lee, Jacob N. Isrealachvili, YongSeok Jho, and Dong Soo Hwang, (2015). Contact time- and pH-dependent adhesion and cohesion of low molecular weight Chitosan coated surfaces. Carbohydrate Polymers, Elsevier, 117 (6): 887–894.

Luis G. Torres, Sandra Carpinteyro-Urban and Luis J. Corzo-Rios (2013). Use of *Annona Diversifolia and A. Muricata* Seeds as Source of Natural Coagulant- Flocculant Aids for the Treatment of Wastewaters. European Journal of Biotechnology and Bioscience, 1(2): 16-22.

Manahan, S.E. (2010). Environmental Chemistry, 9th Edition, CRC Press, p. 5.

McMullan, D. (2006). "Scanning electron microscopy 1928–1965".Scanning.17 (3): 175–185.

Menkiti M.C., Onyechi,C.A. D.O. Onukwuli, (2011). Evaluation of perikinetics compliance for the coag-flocculation of Brewery Effluent by *Branchystegia enrycoma* seed Extract. International Journal of Multi disciplinary sciences and Engineering, 2(6): 2011, 73 – 80.

Menkiti, M. C., Ezemagu I. G., Nwoye, C. I., and Ejimofor, M. I. (2016). Post-treatment sludge analyses and purification of paint effluent by coag-flocculation method. International Journal of Energy Enviromental Engineering, 7:69–83.

Menkiti, M.C. and Ezemagu, I. G. (2015). Sludge characterization and treatment of produced water (PW) using *Tympanotonos fuscatus* coagulant (TFC). Advancing research evolving sciences, 1:51-62.

Menkiti, M.C., and Onukwuli, O.D. (2011). Coag-Flocculation studies of Afzelia belia coagulant (ABC) in coal effluent using single and stimulated multiangle nephelometry. J.Miner. Mater. Charact. Eng., 10(3):279-298.

Menkiti, M.C., Nnaji, P.C., and Onukwuli, O.P. (2009).Coag-flocculation kinetics and functional parameters response of periwinkle shell coagulant to pH variation in organic rich coal effluent medium. Nataural Sciences., 7(6):1-18.

Meredith, M. White, Michael Chejlava, Bernard Fried, and Joseph Sherma (2007). The concentration of calcium carbonate in shells of freshwater snails. American Malacological Bulletin, 22, (1): 139- 142.

Mohammed Awad, Fengting Li and Wang Hongtao (2013). Application of Natural Clays And Poly Aluminium Chloride (Pac) For Wastewater Treatment. IJRRAS, 15 (2): 287-291.

Moshen, A. EL Shazly, Ezzat A. Hasanin and Kamel M.M., (2010).Appropriate Technology for Industrial Wastewater Treatment of Paint Industry. American-Eurasian J. Agric. & Environ. Sci., 8 (5): 597-601.

Mourabet, M., A. El Rhilassi, H. El Boujaady, M. Bennani-Ziatni, A. Taitai (2013). Use of Response Surface Methodology for optimization of fluoride adsorption in an aqueous solution by Brushite. Arabian Journal of Chemistry, 12: 765–774.

Nharingo Tichaona and Moyo Mambo (2015).Application of *Opuntia ficus-indica* in bioremediation of wastewater.A critical review. Journal of Environmental Management, 166:55-72.

Nnaji, N.J.N., Ani, J.U., Aneke, L.E., Onukwuli, O.D., Okoro, U.C., and Ume, J.I. (2013). Modeling the Coag-flocculation kinetics of cashew nuts testa tannins in an Industrial Effluent. Journal of Industrial and Engineerng Chemistry, 20: 1930-1935.

O' Melia Charles R., Kimberly A. Gray and Chonghua Yao (1999).Polymeric inorganic coagulants. AWWA Research foundation and American water works Association, 1-112.

O'Connor, J.T., and Brazos, B.J., (1990). An Assessment of the Use of Direct Microscopic Counts in Evaluating Drinking Water Treatment Processes, ASTM Special Technical Pubilcation: Monitoring Water in the 1990s: Meeting New Challenges. P. 1102.

Obiora –Okafor, I.A. and Onukwuli, O.D. (2015). Optimization of coagulation-flocculation process for colour removal from synthetic dye wastewater using natural organic polymers: Response surface methodology applied. International Journal of scientific and Engineering Research, 6(12):693-700.

Okolo Bernard Ibezimako, Nnaji Patrick Chukwudi, Menkiti Matthew Chukwudi, Ugonabo Victor Ifeanyi, Onukwuli Okechukwu Dominic (2014). Parametric Response Evaluation for *Xanthosoma* spp. Induced Coag-Flocculation of Brewery Effluent. Green and Sustainable Chemistry, 4: 7-14.

Okolo, B. I.,P. C. Nnaji, Menkiti, M. C. Onukwuli, O. D. (2015). A Kinetic Investigation of the Pulverized Okra Pod Induced Coag-Flocculation in Treatment of Paint Wastewater. American Journal of Analytical Chemistry, 6: 610-622.

Onuegbu, T.U., Umoh, E. T. and Onwuekwe, I.T. (2013). Physico-Chemical Analysis of Effluents from Jacbon Chemical Industries Limited, Makers of Bonalux Emulsion and Gloss Paints. International Journal of Science and Technology, 2(2):169-179.

Orange and Grapefruit Peels under Different Conditions. PLoS ONE 11(9): 1-16

Osobamiro M.T., and Atewolara-Odule O.C. (2015). Determination of Physicochemical Parameters and Levels Of Some Heavy Metals In Industrial Waste Water. International Journal of Scientific & Engineering Research, 6(7): 1910-1918.

Pamila Ramesh, Abdur Rahman B. S., Vasanthi Padmanaban, and Sivacoumar R. (2015). Influence of Homemade Coagulants on the Characteristics of Surface Water Treatment: Experimental Study. International Journal of Engineering Research & Technology (IJERT), 4(12):342-345.

Patale Varsha and Pandya Jay (2012). Mucilage extract of *Coccinia indica* fruit as coagulant-flocculant for turbid water treatment. Asian Journal of Plant Science and Research, 2 (4):442-445.

Pernitsky, David J., (2003). Coagulation, Associated Engineering, Calgary, Alberta, pp. 28- 45.

Pinhua Rau, Zhaowei Sun, Wengi Zhang, Wei Yao, Luanjiao Wamg and Guoyu Ding (2015). Preparation and application of Amorphous Fe-Ti bimetal oxide for arsenic removal. The Journal of Royal Society of Chemistry, 5:89545-89551

Polasek, P. and Mutl, S. (2002). Cationic polymers in water treatment Part 1: Treatability of water with cationic polymers, Water SA., 28: 69-82

Prabhakar,Misra and Dubinskii, Mark, eds. (2002). Ultraviolet Spectroscopy and UV Lasers. New York: Marcel Dekker pp. 34-36.

Pradip Kumar Dutta, Joydeep Dutta and Tripathi (2004). Chitin and chitosan: Chemistry, properties and application. Journal of scientific and Industrial Research, 63: 20-31

Prasad Sudamalla, Pichiah Saravanan and Manickam Matheswaran (2012). Optimization of operating parameters using response surface methodology for adsorption of crystal violet by activated carbon prepared from mango kernel. Sustain. Environ. Res., 22(1):1-7

Raed S. Al-Wasify1, Al-Sayed A. Al-Sayed, Sahar M. Saleh, and Ahmed M. Aboelwafa (2015). Bacterial Exopolysaccharides as New Natural Coagulants for Surface Water Treatment. International Journal of PharmTech Research, 8 (9):198-207

Rahbar, M.S., Alipour, E. and Sedighi, R.E. (2006). Colour removal from industrial wastewater with a novel coagulant formulation. Int. J. Environ. Sci. Tech., 3, 79-88

Ram Krishna, and SahuOmprakash (2013). Reduction of COD and Colour by polymeric Coagulant (chitosan). Journal of Ploymer and Biopolymer Physics chemistry, 1(1): 22-31

Ria Bhaumik, Naba Kumar Mondal, Soumya Chattoraj, Jayanta Kumar Datta (2013).Application of Response Surface Methodology for Optimization of Fluoride Removal Mechanism by Newely Developed Biomaterial. American Journal of Analytical Chemistry, 4:404-419.

Robinson, J. (2001). Water, Industrial Water Treatment in 'Kirk-Othmer Encyclopedia of Chemical Technology'. John Wiley & Sons, Inc, New Jersey, p. 45

Sahu, O.P. and ChaudharI, P.K., (2013). Review on Chemical treatment of Industrial Waste Water. J. Appl. Sci. Environ. Manage.,17 (2): 241-257

Sawyer, C. N., McCarty, P.L. and Parkin, G. E. (1994). Chemistry for Environmental Engineering 4th ed. McGraw-Hill, New York, P. 67

Scintag Inc (1999). Basic of X-rays diffraction, Cupertino CA , USA, pp. 72-78.

Shafad, M. R., Ahamad, I. S., Idris, A., and Zainal Abidin Z. (2013). A preliminary Study on Dragon Fruit Foliage as Natural Coagulant for Water Treatment. International Journal of Engineering Research & Technology (IJERT), 2(12):1057-1063.

Shangkun Li, Xiaofeng Lu, Yanpeng Xue, Junyu Lei, Tian Zheng, Ce Wang (2012). Fabrication of Polypyrrole/Graphene Oxide Composite Nanosheets and Their Applications for Cr(VI) Removal in Aqueous Solution. PLOS ONE 7(8):1-7

Shaukat Mahmud, Ghazala H. Rizwani, Huma Shareef, Shahnaz Gauhar, Sumaira Ishaq,Rehana Perve (2013). Development of Standardized Formulation of mono herbal (250mg) Capsule. International Journal of Herbal Medicine, 1(4): 44-49.

Shukla, S. K., Mishra, A. K.; Arotiba, O. A., and Mamba, B. B. (2013). Chitosan-based nanomaterials: A state-of-the-art review. International Journal of Biological Macromolecules, 59: 46–58.

Sincero Arcadia P. and Sincero Gregoria A. (2003). Physical-chemical treatment of water and water treatment.IWA Publishing House, Washinton D.C. p.559.

Sincero, Arcadio, P. and Sincero, Gregoria, A. (2003). Physical –chemical treatment of water and waste water. CRC press Washington DC, p. 564.

Siyanbola, T.O., Ajanaku K.O., James O.O., Olugbuyiro, J.A.O., Adekoya, J.O. (2011). Physico-Chemical Characteristics Of Industrial Effluents In Lagos State, Nigeria. G. J. P & A Sc. and Tech., 01:49-54

Sudo, S., Fujikawa, T., Nagakura, T., Ohkubo, T., Sakaguchi, K., Tanaka, M., Nakashima, K., and Takahashi, T. (1997). Structures of mollusc shell framework proteins.. Nature, 387(34):43-52.

Syafalni, Rohana Abdullah, Ismail Abustan, and Aimi Nadiah Mohd Ibrahim (2013).Wastewater treatment using bentonite, the combinations of bentonite- zeolite, bentonite-alum, and bentonite-limestone as adsorbent and coagulant. International Journal of Environmental Sciences, 4 (3): 376-391.

Thakur Sunita Singh and Choubey Sonal (2014). Use of Tannin based natural coagulants for water treatment: An alternative to inorganic chemicals. International Journal of ChemTech Research, 6 (7): 3628-3634.

Theodoro Joseane Debora Peruço, Guilherme Felipe Lenz, Ricardo Fiori Zara, and Rosangela Bergamasco (2013). Coagulants and Natural Polymers: Perspectives for the Treatment of Water. Plastic and Polymer Technology (PAPT), 2 (3): 55-62.

Thuy, K.T. and Lim, S.K. (2011). Response Surface Methodological approach to optimize the coagulation–flocculation process in drinking water treatment. Chemical engineering research and design, 89:1126–1135.

Tripathy Tridib and Bhudeh Ranjan De (2006). Flocculation: A new way to treat the waste water. Journal of Physical Sciences, 10: 93-127.

*TympanotonusFuscatus*,. Retrieved through wikipedia on 9th June 2016

Ugonabo, V. I, Menkiti, M .C, Atuanya, C.U. and Onukwuli, D. O. (2013). Comparative Studies On Coag-flocculation Kinetics of Pharmaceutical Industry Effluent by Achatina Maginata Shell Biomass and Aluminum Sulphate. International Journal of Engineering & Technology, 13(2):134-147.

Ugonabo, V.I., Menkiti, M.C., and Onukwuli, O.D. (2012). Kinetics and coagulation performance of snail shell biomass in pharmaceutical Effluent. IOSR Journal of Engineering (IOSRJEN), 2(7): 38-49.

Ugonabo, V.I., Menkiti, M.C., and Onukwuli, O.D. (2012b). Coagulation Kinetics and Performance Evaluation of *Corchorus Olitorus* Seed in Pharmaceutical effluent. International Journal of Multidisciplinary Sciences and Engineering, 3(7):20-32

Unabonah, E.I., Adebowale, B.I., Olu-Owolabi, Yang, L. X .Kong (2008). Adsorption of Pb(11) and Cd (11) from aqueous solution onto sodium tetraborate-modified kaolinite clay. Equilibrium and thermodynamic studies Hydrometallurgy, 93:1-9. Unabonah, E.I., Adie, G.U., Onah, L.O., and Adeyemi, O.G. (2009).Multistage Optimization of the adsorption of methlene blue dye onto defatted Carica papaya seeds. Chemical Engineering Journal, 155:567-579.

Usman Ameh. (2006**)**. "Standard Operating Procedure National Agency for Food and Drug Administration and Control (NAFDAC) Boriki Port Hacourt, Nigeria. Heinemann Medical Books Ltd.: New York, NY. 122, 184.

Vanerkar A. P., Sanjeev Satyanarayan, Shanta Satyanarayan (2013). Treatment of Food Processing Industry Wastewater by a Coagulation/ Flocculation Process. International Journal of Chemical and Physical Sciences, 2:63-72

Vijayaraghavan, G. and Shanthakumar, S. (2015). Performance study on algal alginate as natural coagulant for the removal of Congo red dye. Journal of Desalination and Waste Water Treatment, 57(14):6385-6392.

Vishali, S. and Karthikeyan, R. (2014).*Cactus opuntia* (*ficus-indica*): An eco-friendly alternative coagulant in the treatment of paint effluent. Journal of Desalination and Water treatment, 56(6):1489-1497.

Wang K.Lawarence, Yung-Tse Hung and Nazih, K. Shammas (2005). Physiochemical Treatment Processes; Hand book of Environmental Engineering, Human Press Inc, Totowa, 3:103-139.

Warren Viessman (Jr). Water Encylopedia ; Wastewater Treatment and Management., Science and Issue. http://www.waterencyclopedia.com/Tw-Z/Wastewater-Treatment-(2009and-Management.html#ixzz3vGJfY1LW retrieved on 24/12/15

Water soluble polymers: flocculation-coagulation. SNF FLOERGER, pp. 1-5

Witold Brostow,Haley, E. Hagg Lobland,Sagar Paland Ram, P. Singh (2009).Polymeric Flocculants for Wastewater and Industrial Effluent Treatment. Journal of Materials Education, 31 (3-4): 157 – 166.

World Health Organisation, (2012). Bulk Density and Tapped Density of Powders; Final Text for Addition to the International Pharmacopoeia, pp. 1-6.

Yusuf, Olabode Raji, Lawal Abubakar, Saidat Olanipekun Giwa, Abdulwahab Giwa, (2015). Assessment of Coagulation Efficiency of Okra Seed Extract for Surface Water Treatment. International Journal of Scientific & Engineering Research, 6 (2):719-725.

# Appendix 1

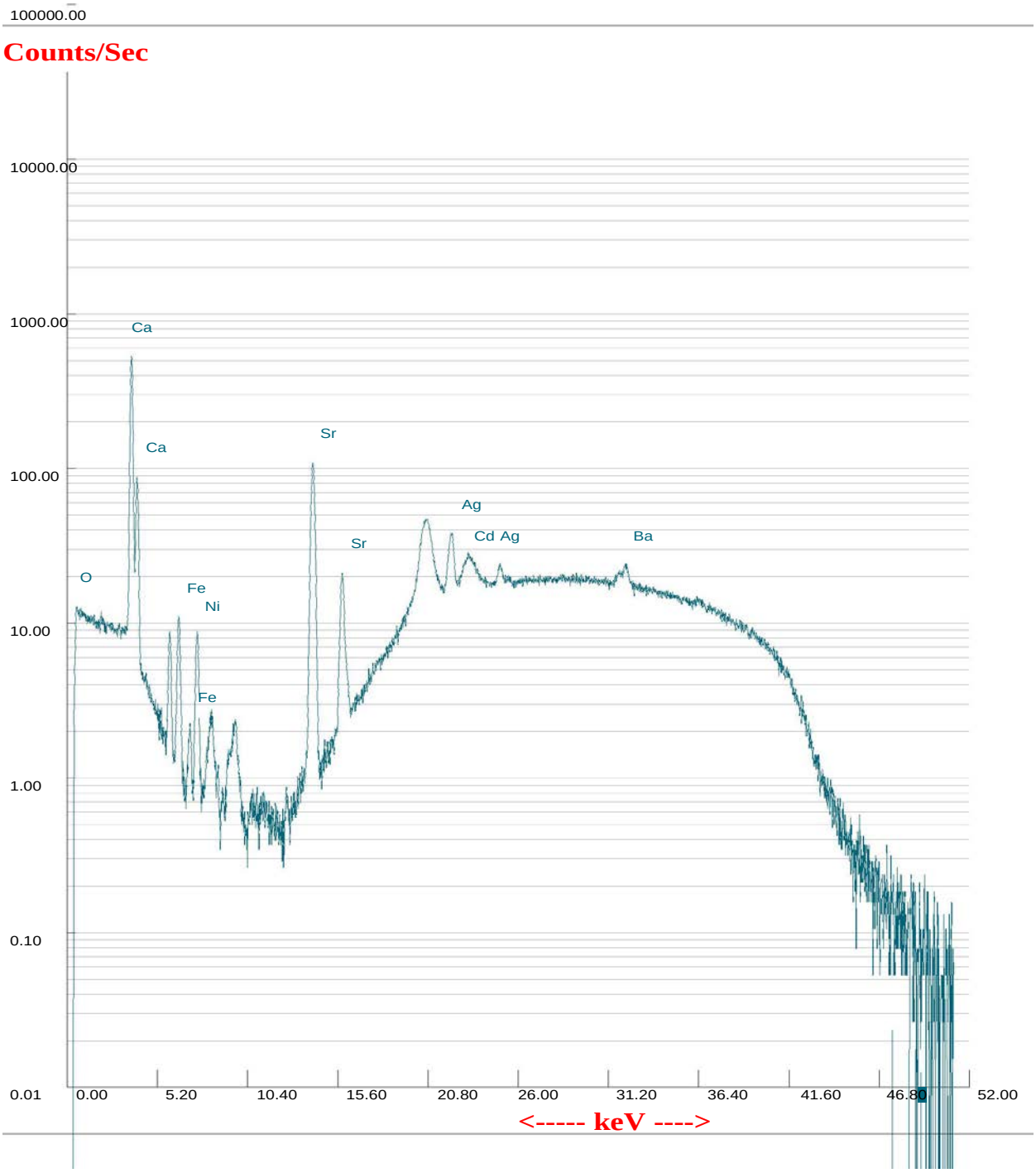


# Appendix 2

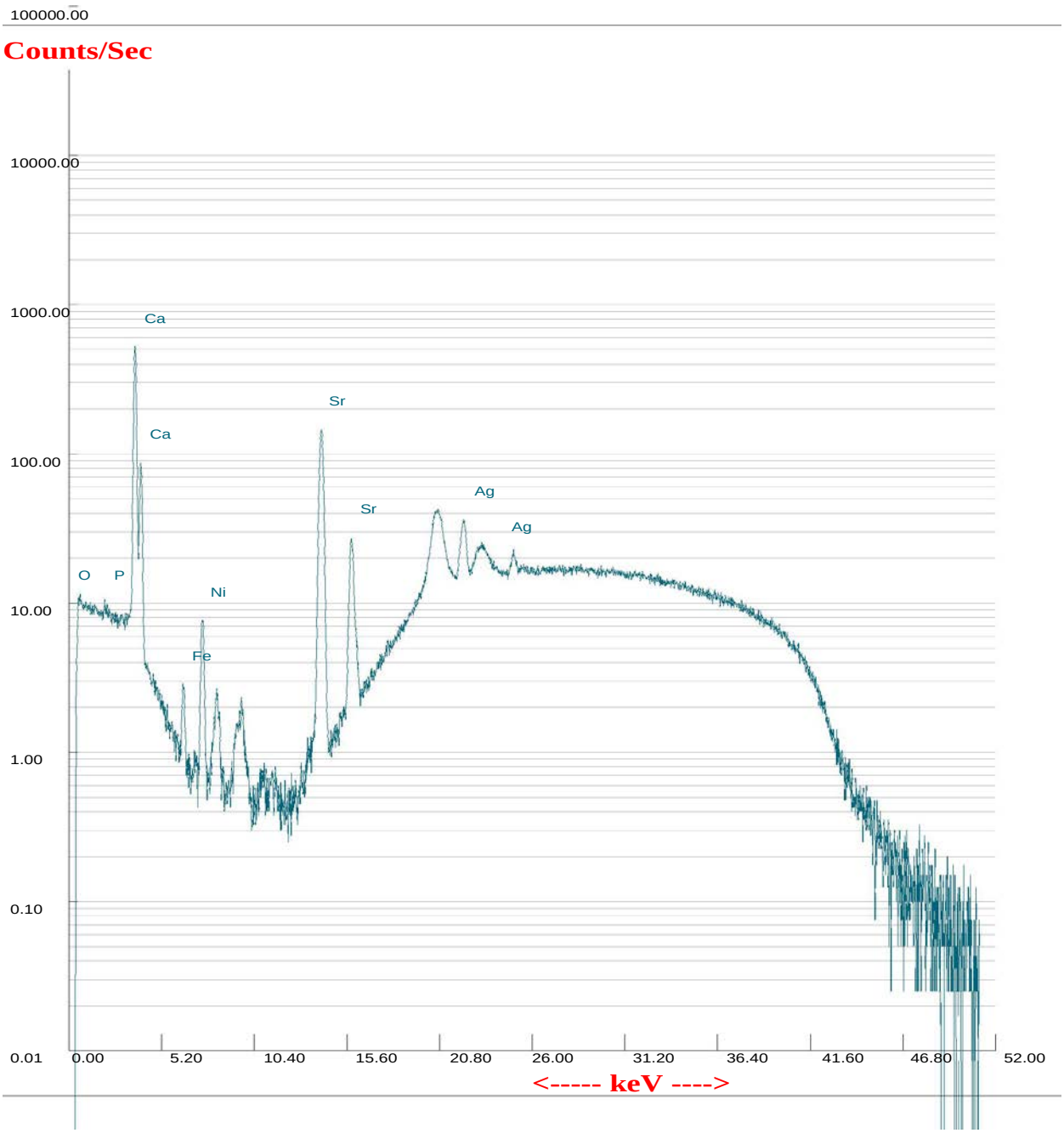
100000.00
Counts/Sec
10000.00
1000.00
100.00
10.00
1.00
0.10
0.01
Ca
Ca
Sr
Sr
Ag
Ag
O
P
Ni
Fe
0.00
5.20
10.40
15.60
20.80
26.00
31.20
36.40
41.60
46.80
52.00
<----- keV ---->
XRF of AM coagulant

# Appendix 3

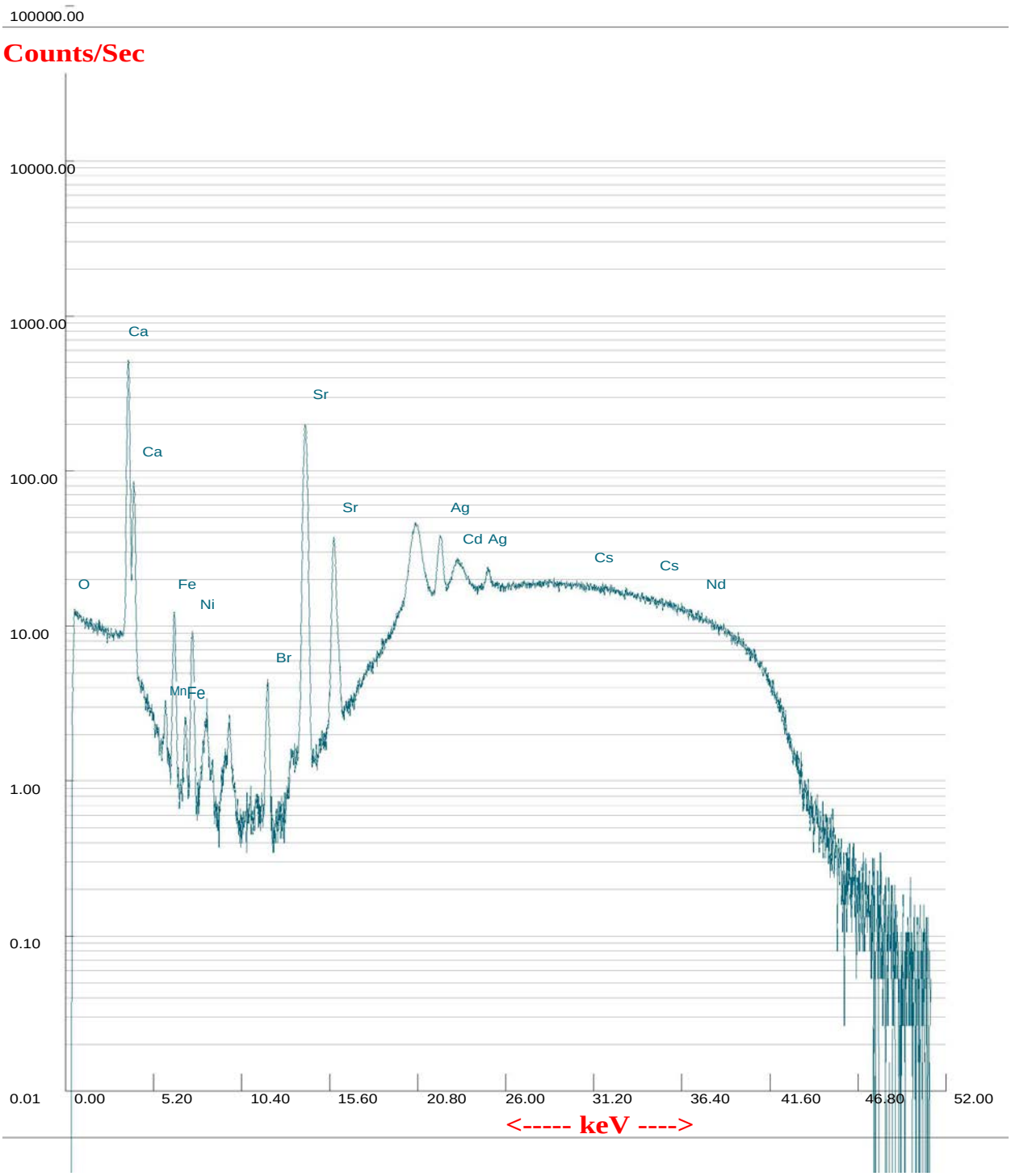
100000.00
Counts/Sec
10000.00
1000.00
100.00
10.00
1.00
0.10
0.01
Ca
Ca
Sr
Sr
Ag
Cd Ag
Cs
Cs
Nd
O
Fe
Ni
Br
Mn
Fe
0.00
5.20
10.40
15.60
20.80
26.00
31.20
36.40
41.60
46.80
52.00
<----- keV ---->
XRF of TF coagulant

# Appendix 4

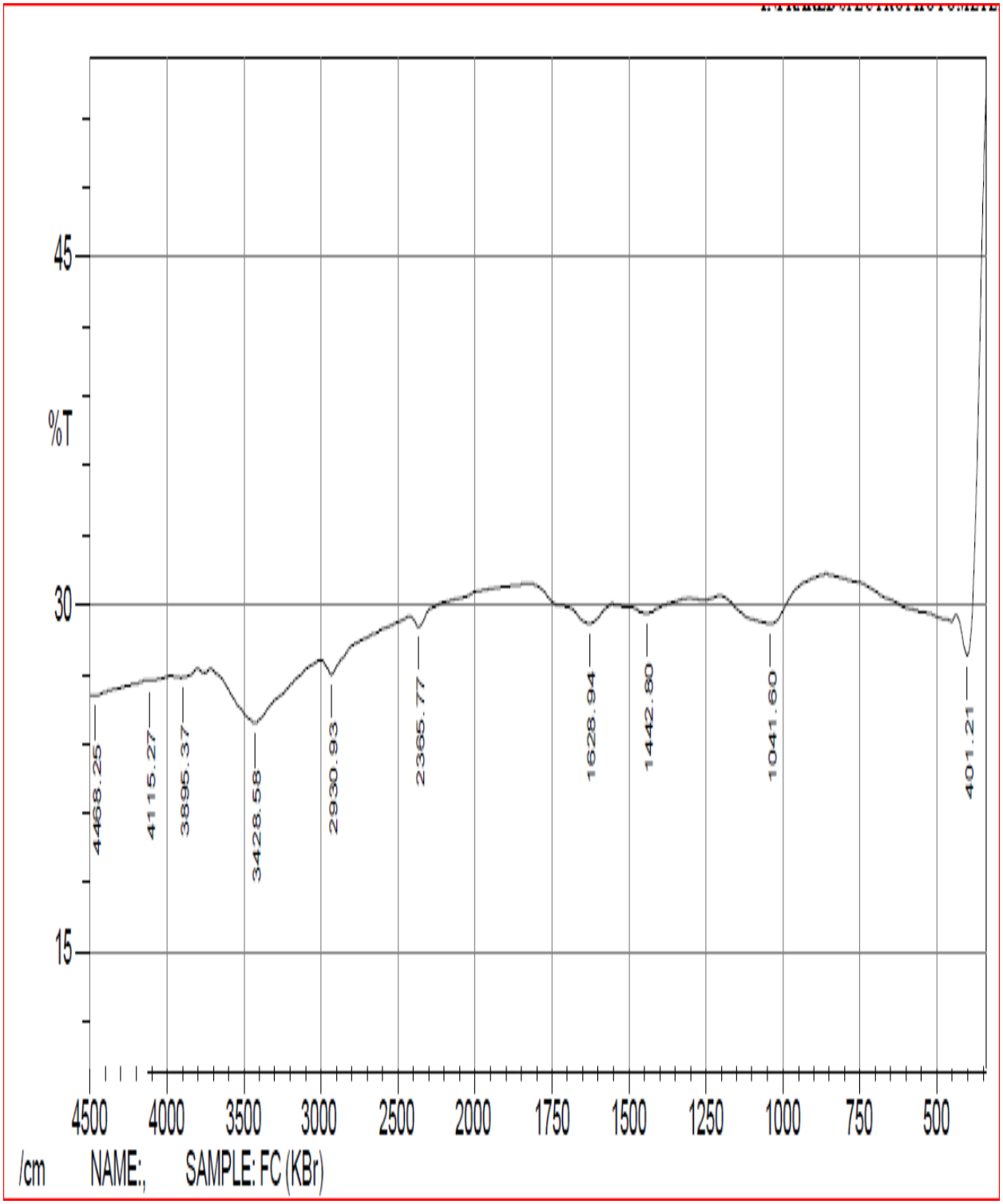


**FTIR result of MM coagulant**

## Appendix 5

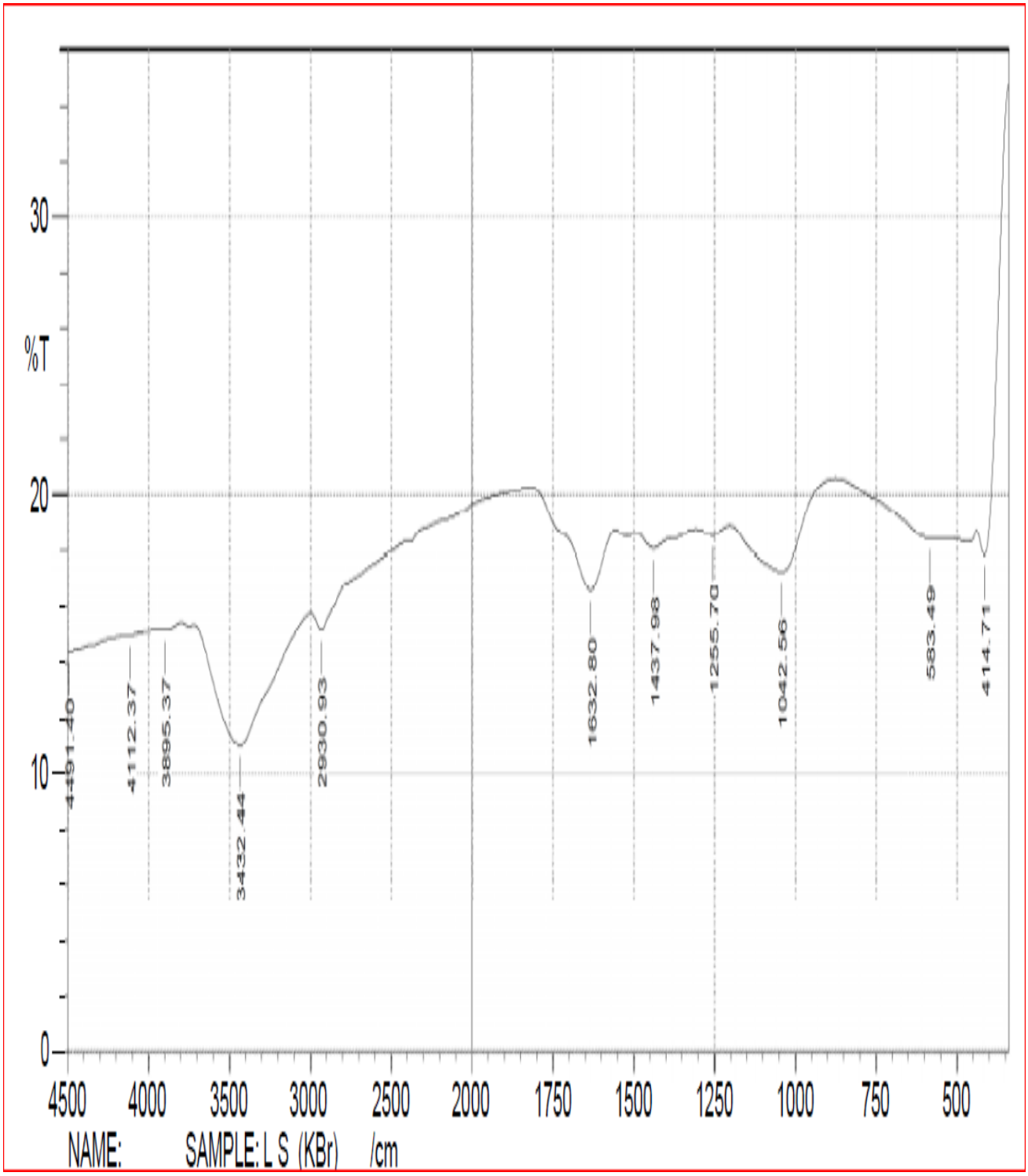


**FTIR result of AM coagulant**

## Appendix 6

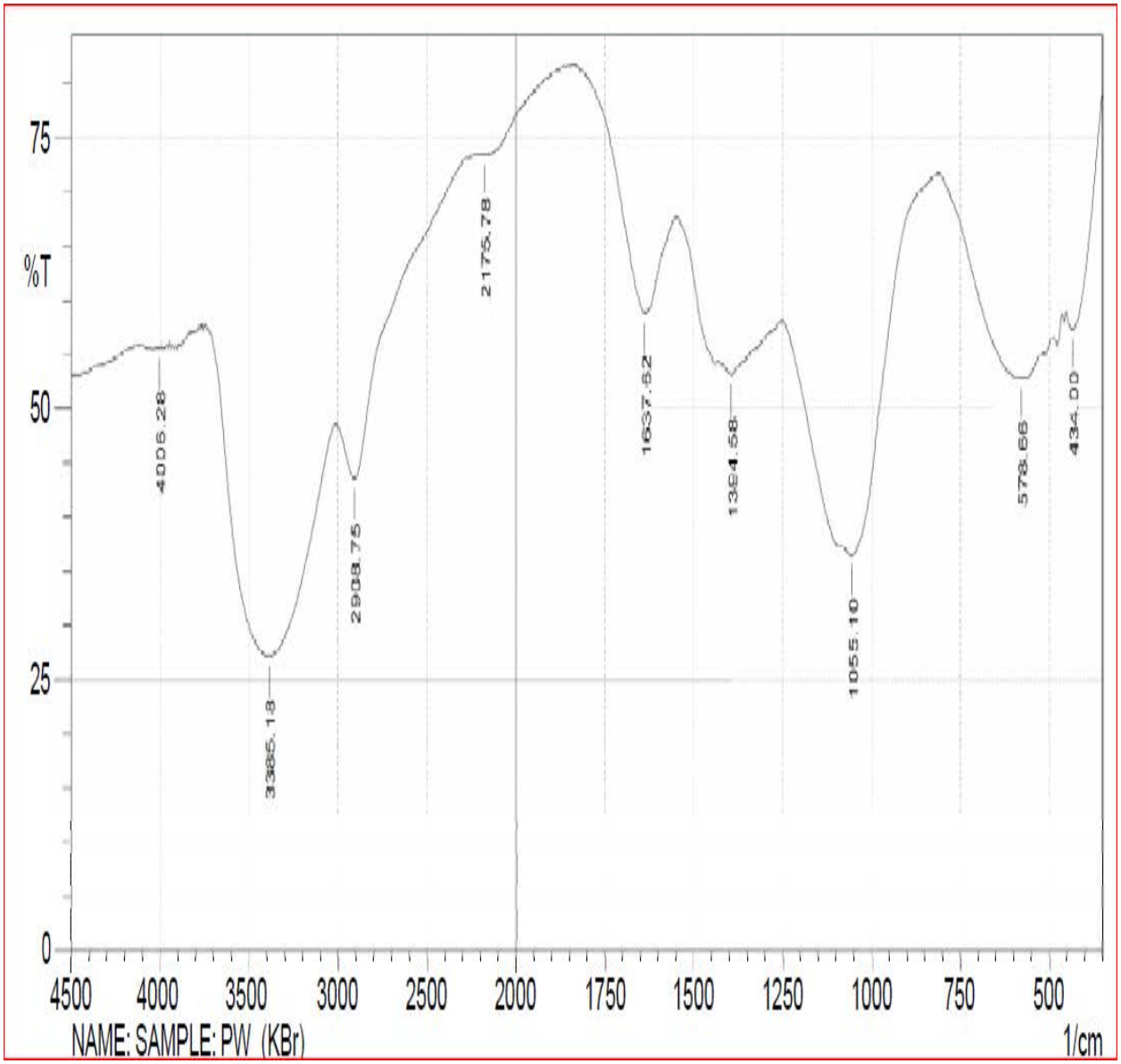


**FTIR result of TF coagulant**

## Appendix 7

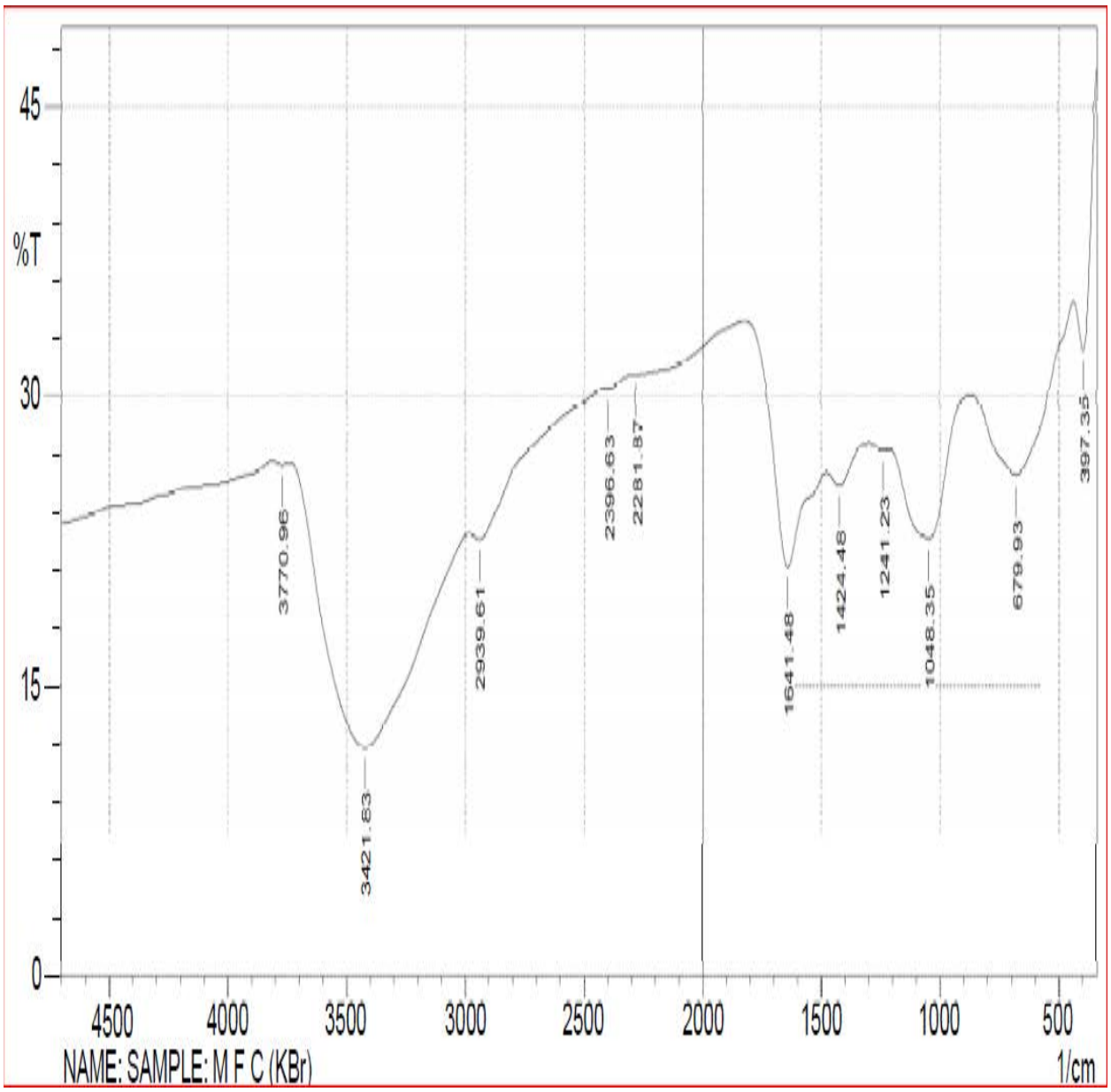


**FTIR result of MM sludge**

## Appendix 8

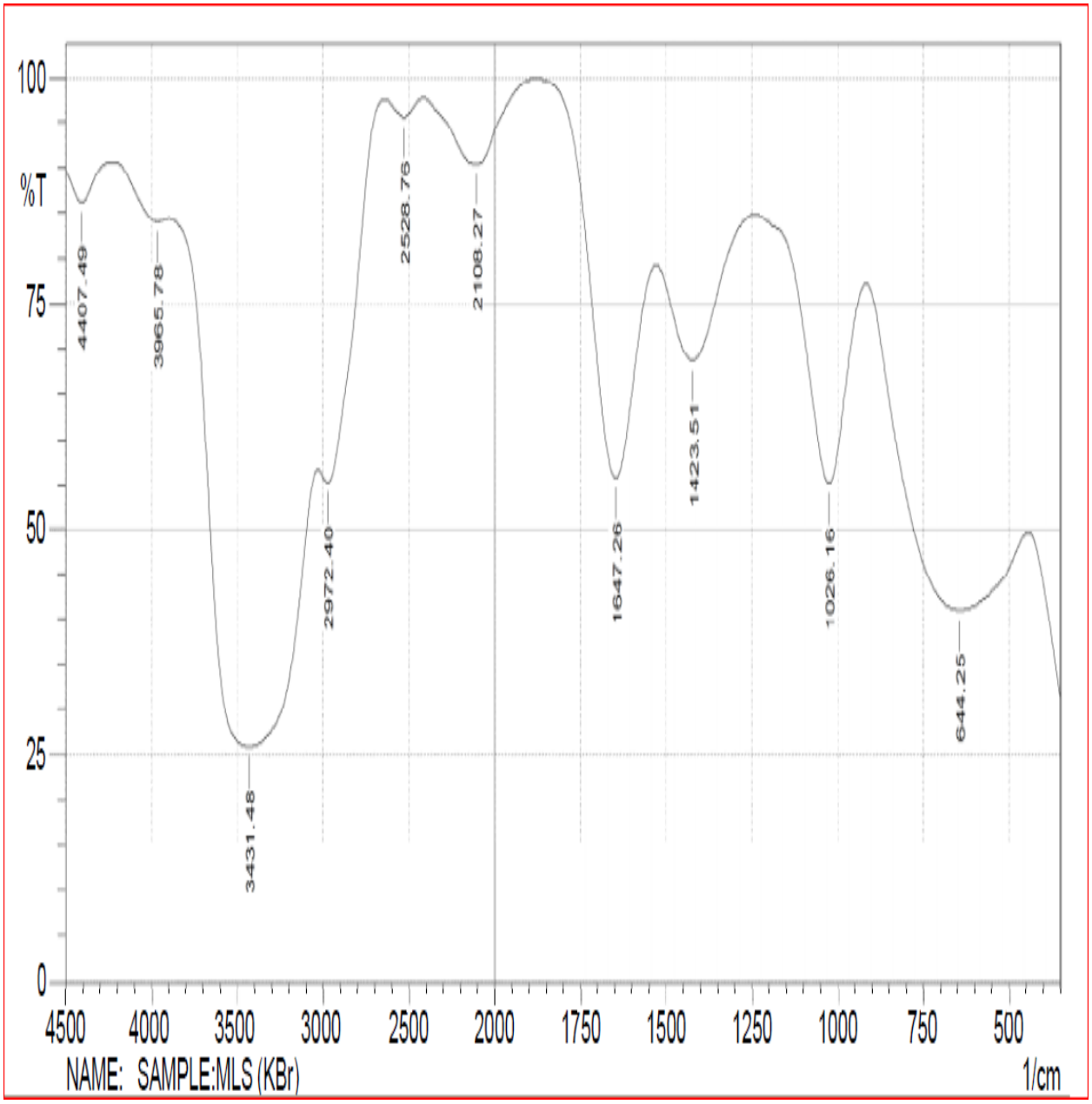


**FTIR result of AM sludge**

## Appendix 9

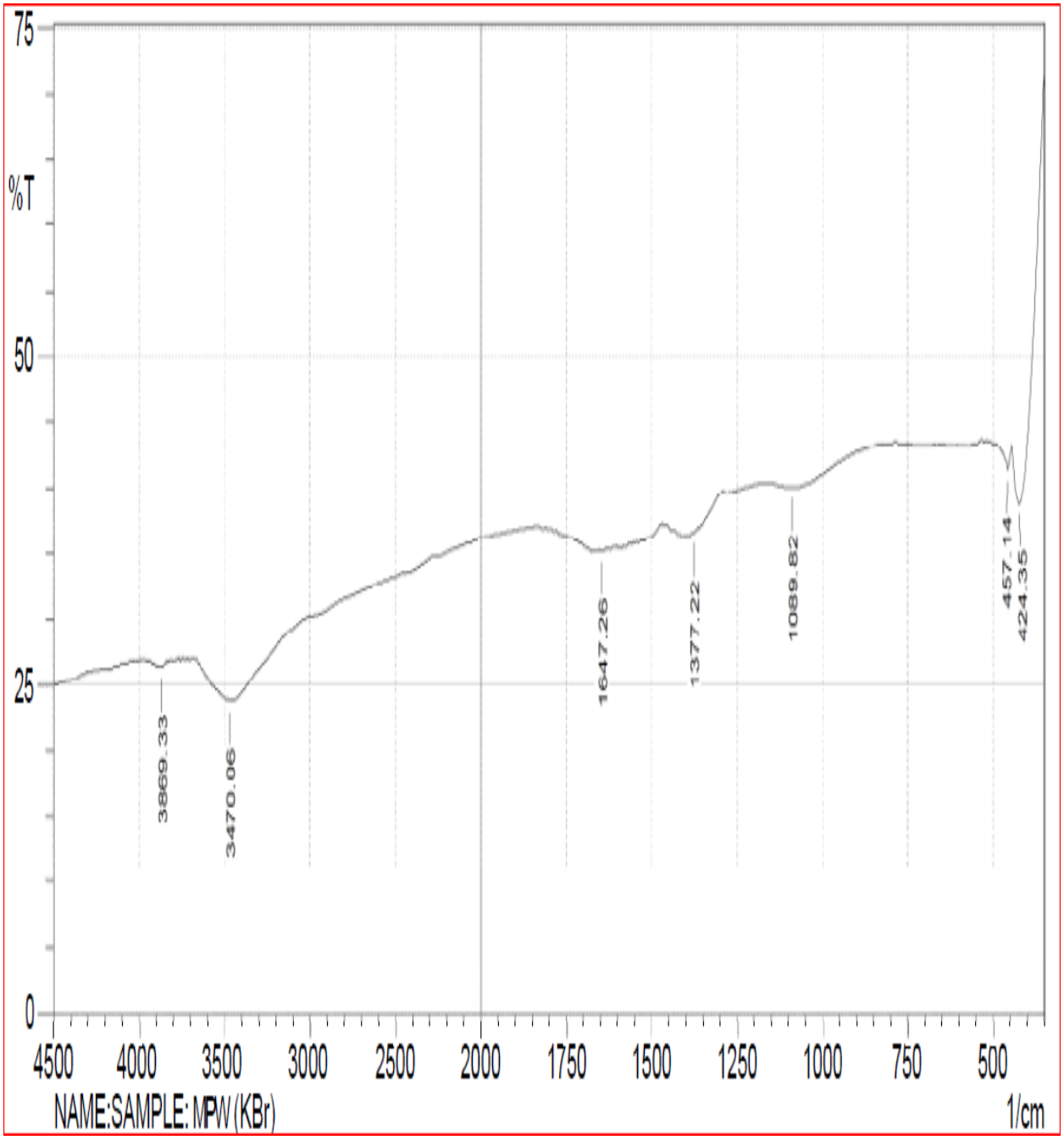


**FTIR result of TF Sludge**

## Appendix 10

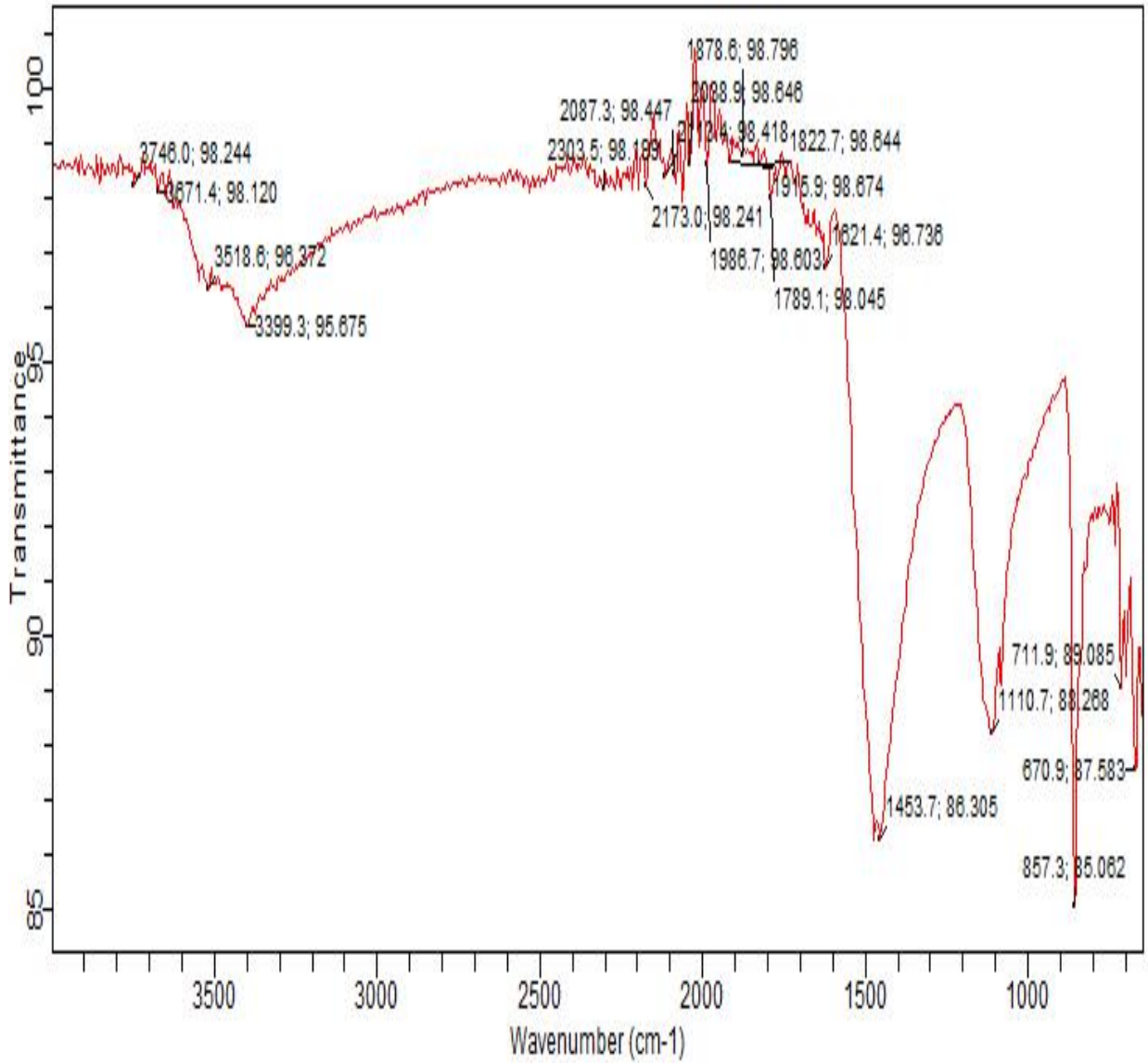


**FTIR result of MMM coagulant**

## Appendix 11

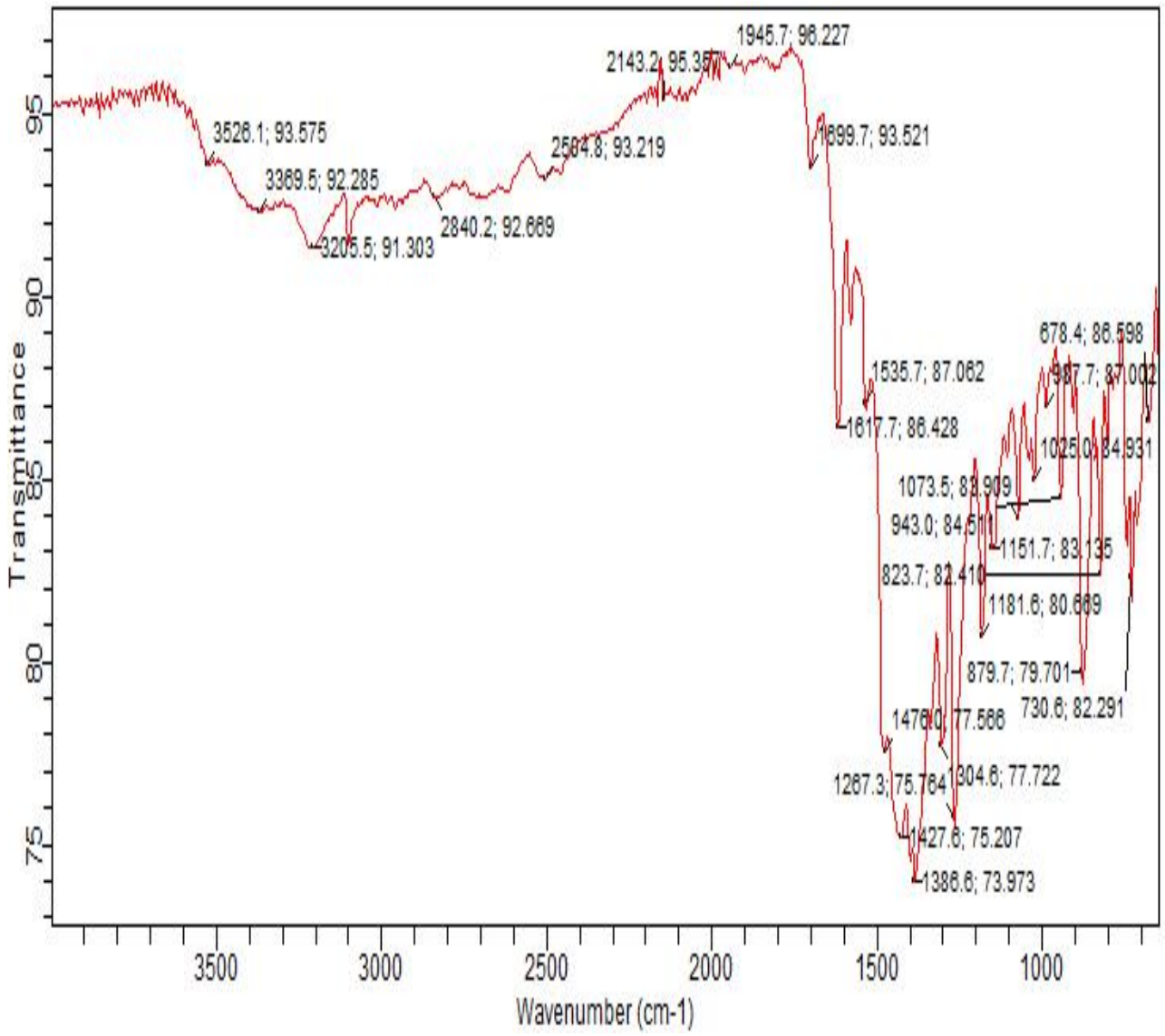


**FTIR result of MAM coagulant**

## Appendix 12

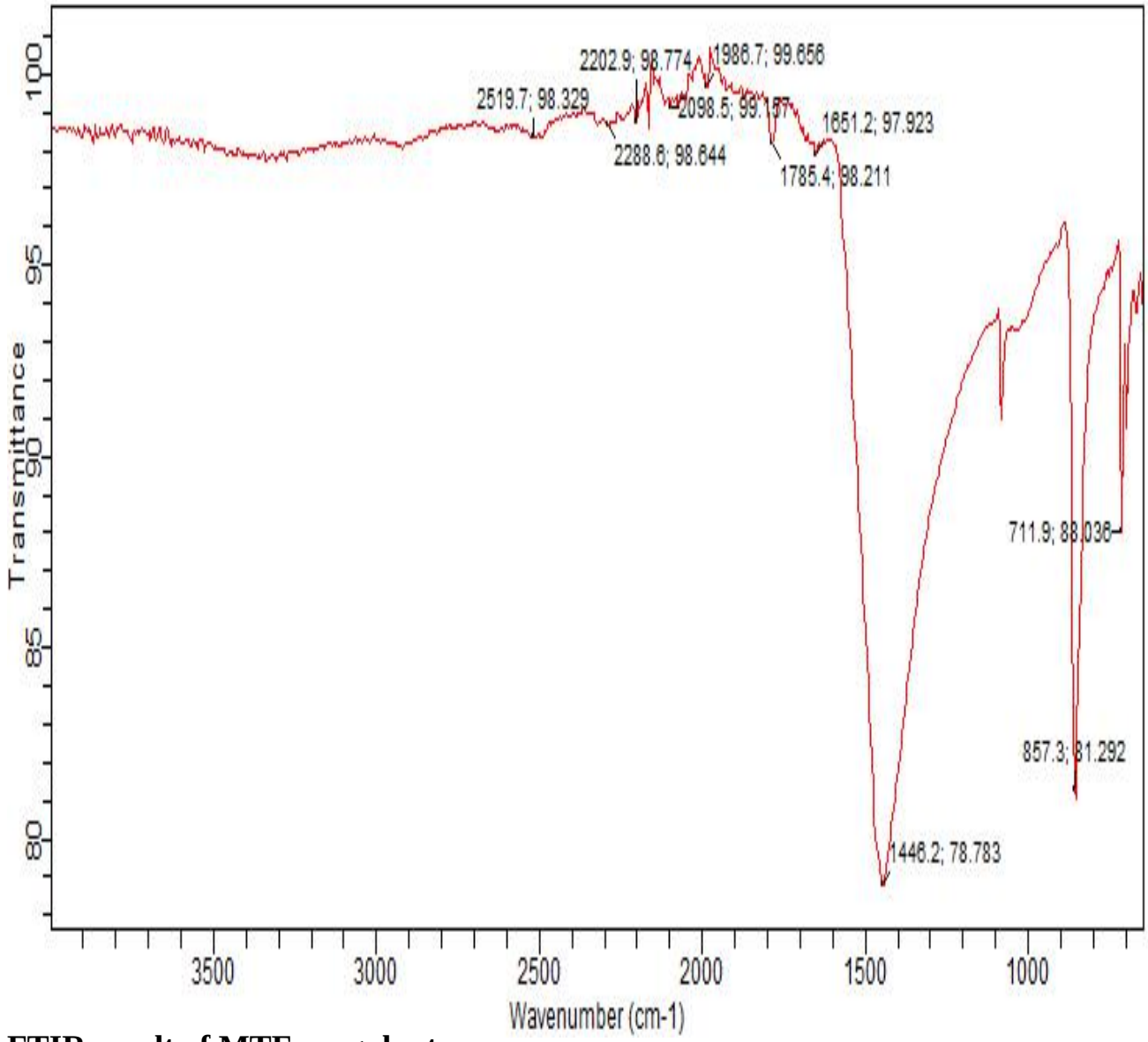


**FTIR result of MTF coagulant**

## Appendix 13

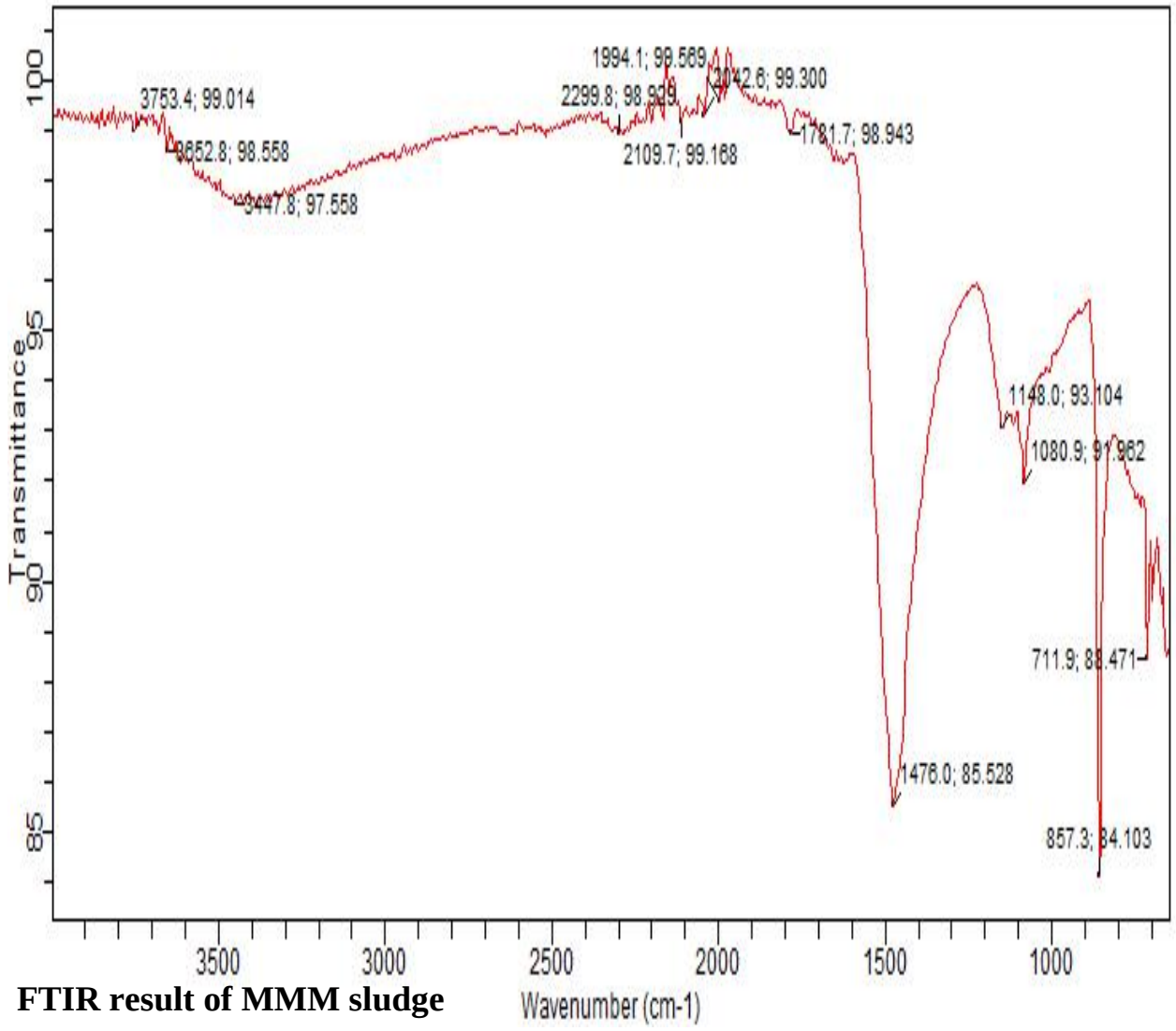


**FTIR result of MMM sludge**

## Appendix 14

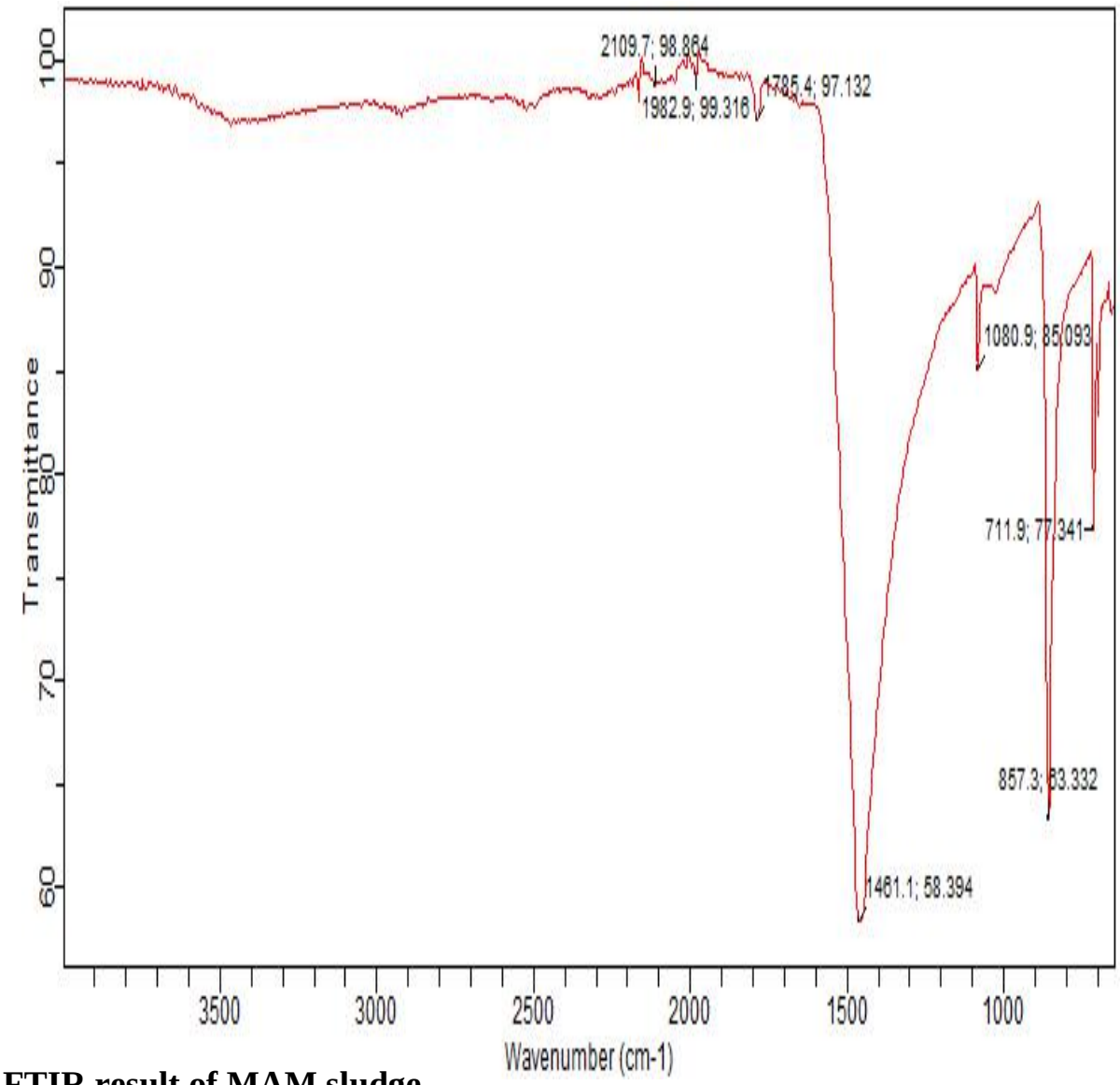


**FTIR result of MAM sludge**

## Appendix 15

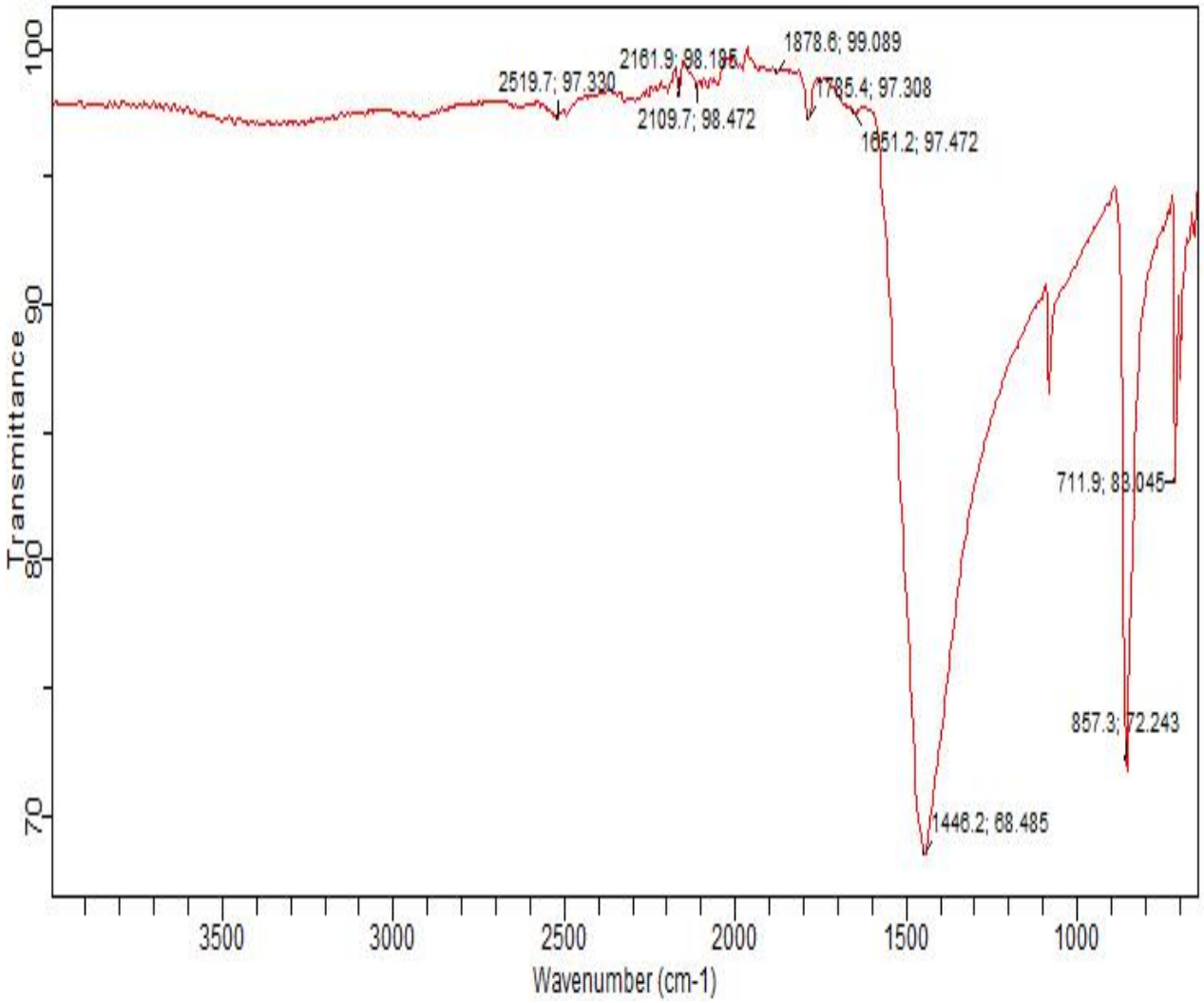


**FTIR result of MTF coagulant**

## Appendix 16

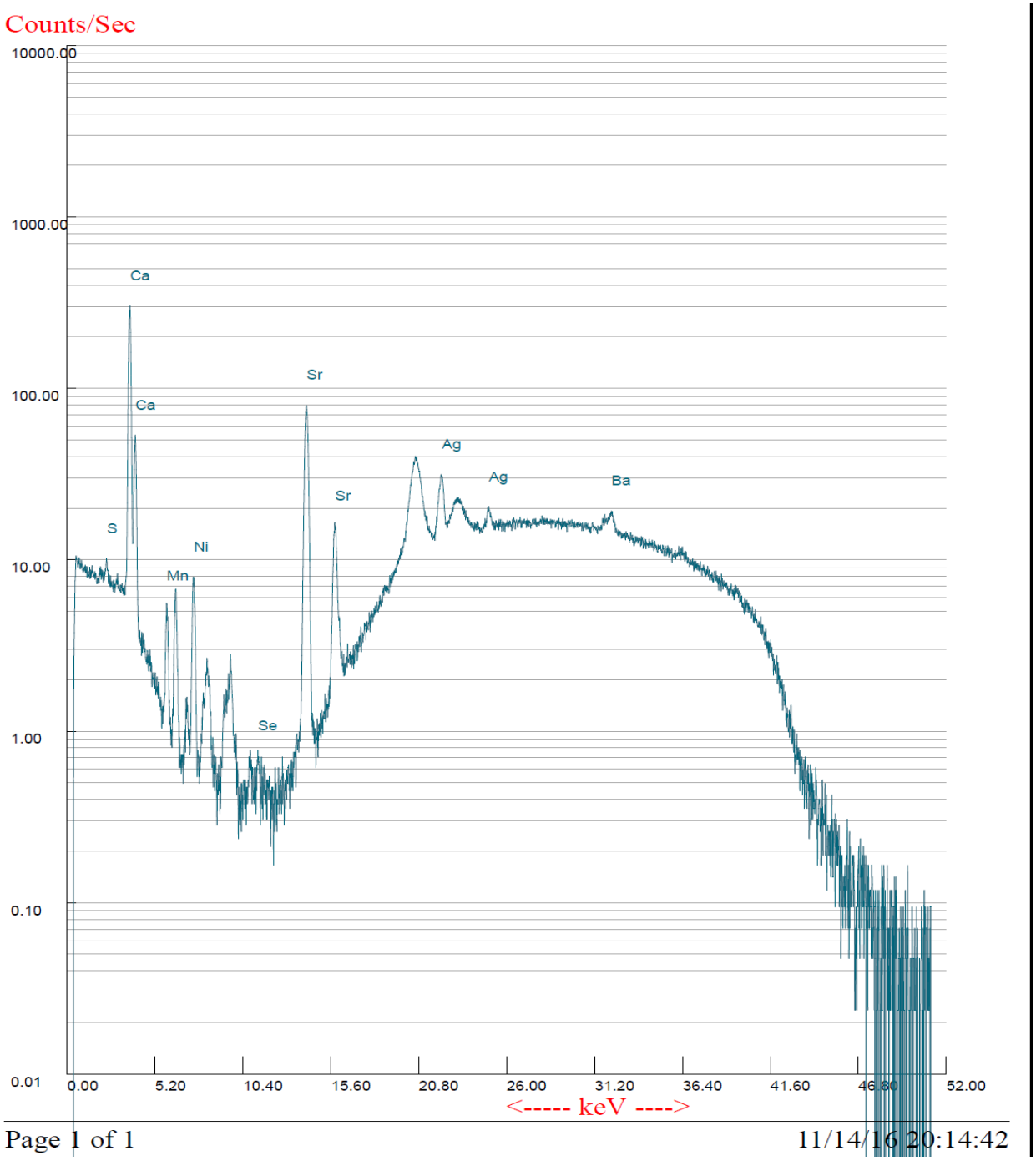


**XRF result of MMM coagulant**

## Appendix 17

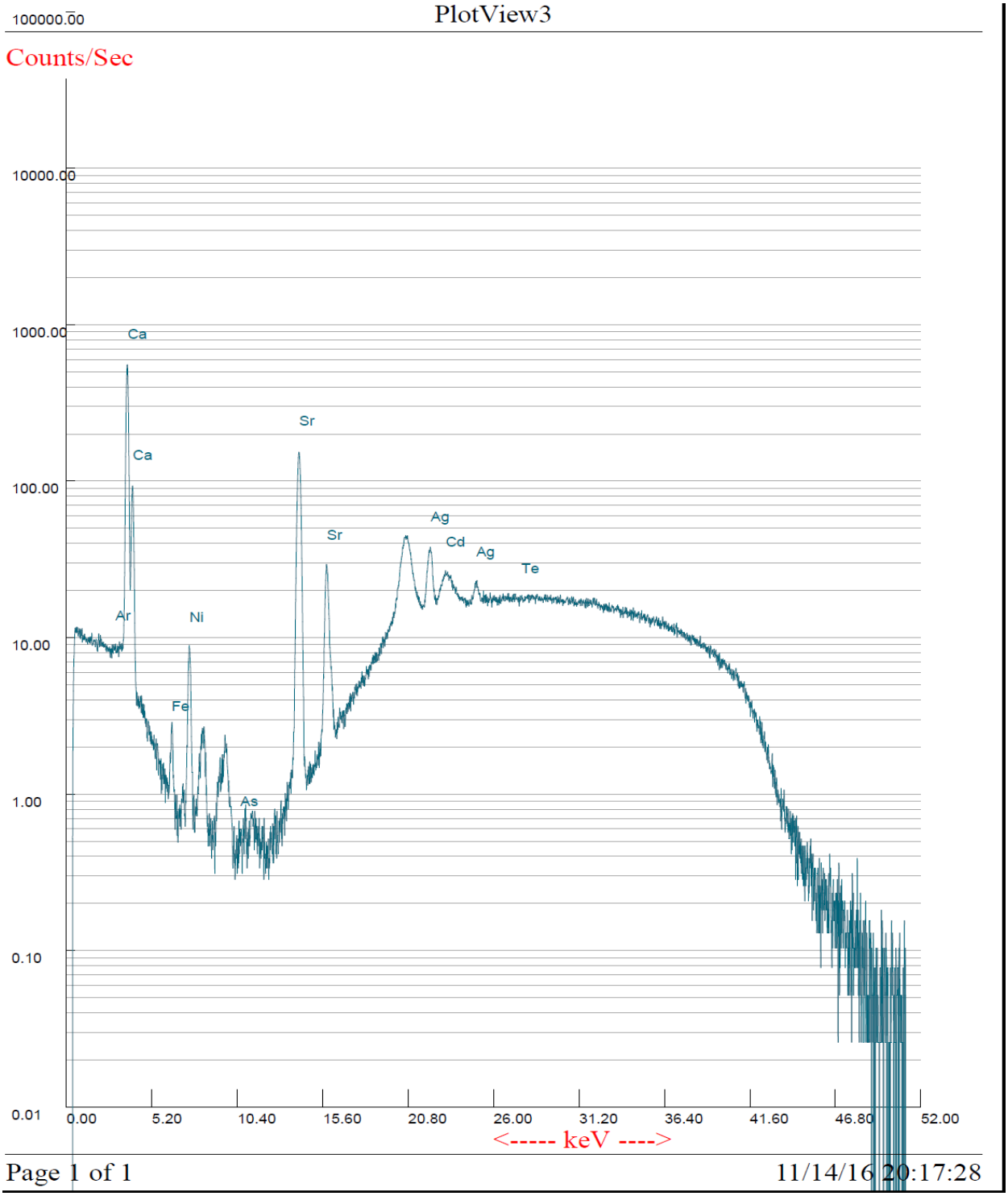


**XRF result of MAM coagulant**

## Appendix 18

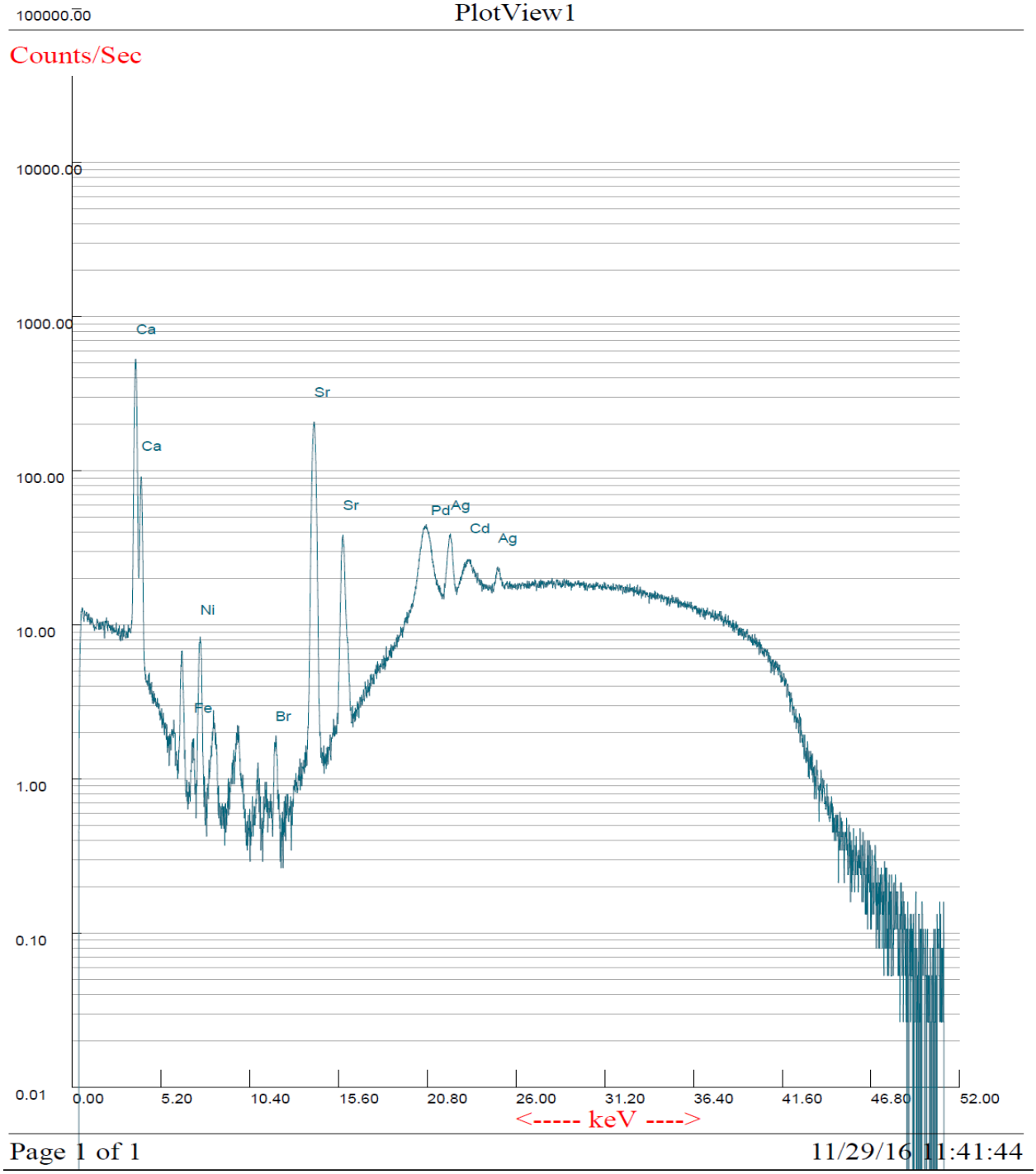


**XRF result of MTF coagulant**

**Appendix 19**

**Table 4.11b: Result of coagulation-flocculation kinetics of MM coagulant at pH 2, varying dosages, time and 27ºC**

| Time (mins) | 100 mg/L | 200 mg/L | 300 mg/L | 400 mg/L | 500 mg/L |
|---|---|---|---|---|---|
| 5 | 596 | 662 | 796 | 804 | 860 |
| 10 | 560 | 644 | 742 | 800 | 840 |
| 15 | 550 | 636 | 724 | 774 | 822 |
| 20 | 502 | 620 | 702 | 746 | 788 |
| 30 | 515 | 616 | 684 | 740 | 800 |

**Table 4.11c: Result of coagulation-flocculation kinetics of AM coagulant at pH 2, varying dosages, time and 27ºC**

| Time(mins) | 100 mg/L | 200 mg/L | 300 mg/L | 400 mg/L | 500 mg/L |
|---|---|---|---|---|---|
| 5 | 842 | 833 | 802 | 826 | 768 |
| 10 | 822 | 796 | 774 | 754 | 719 |
| 15 | 762 | 744 | 722 | 704 | 671 |
| 20 | 582 | 560 | 558 | 544 | 459 |
| 30 | 542 | 509 | 524 | 505 | 472 |

**Appendix 20**

**Table 4.11d: Result of coagulation-flocculation kinetics of TF coagulant at pH 2, varying dosages, time and 27ºC**

| Time(mins) | 100 mg/L | 200 mg/L | 300 mg/L | 400 mg/L | 500 mg/L |
|---|---|---|---|---|---|
| 5 | 972 | 836 | 602 | 590 | 522 |
| 10 | 960 | 778 | 562 | 554 | 484 |
| 15 | 928 | 736 | 528 | 530 | 448 |
| 20 | 919 | 704 | 442 | 490 | 396 |
| 30 | 911 | 674 | 334 | 422 | 370 |

**Table 4.24b: Result of coagulation-flocculation kinetics for MMM coagulant at pH 6, varying dosages, time and 27ºC**

| Time (mins) | 100 mg/L | 200 mg/L | 300 mg/L | 400 mg/L | 500 mg/L |
|---|---|---|---|---|---|
| 5 | 1224 | 1162 | 1086 | 1016 | 908 |
| 10 | 944 | 882 | 842 | 756 | 644 |
| 15 | 704 | 562 | 450 | 390 | 410 |
| 20 | 512 | 462 | 434 | 424 | 428 |
| 30 | 426 | 402 | 381 | 400 | 398 |

**Appendix 21**

**Table 4.24c: Result of coagulation-flocculation kinetics for MAM coagulant at pH 2, varying dosages, time and temperature 27ºC**

| Time (mins) | 100 mg/L | 200 mg/L | 300 mg/L | 400 mg/L | 500 mg/L |
|---|---|---|---|---|---|
| 5 | 847 | 836 | 822 | 818 | 798 |
| 10 | 870 | 744 | 726 | 668 | 672 |
| 15 | 763 | 729 | 564 | 546 | 462 |
| 20 | 456 | 482 | 444 | 424 | 402 |
| 30 | 524 | 436 | 402 | 384 | 396 |

**Table 4.24d: Result of coagulation-flocculation kinetics for MTF coagulant at pH of 6, varying dosages, time and temperature 27ºC**

| Time (mins) | 100 mg/L | 200 mg/L | 300 mg/L | 400 mg/L | 500 mg/L |
|---|---|---|---|---|---|
| 5 | 864 | 848 | 827 | 770 | 624 |
| 10 | 752 | 693 | 643 | 620 | 601 |
| 15 | 567 | 542 | 521 | 403 | 387 |
| 20 | 443 | 428 | 403 | 365 | 304 |
| 30 | 414 | 386 | 355 | 323 | 309 |